The effects of nanomaterials in the physiology and ecology of the freshwater crustacean *Daphnia magna*

Kai Benjamin Paul

Submitted for the degree of Doctor of Philosophy

Heriot-Watt University

School of Life Sciences

November 2015

Abstract

This research studied 3 differently coated silver nanomaterials (Ag NMs) and their ionic counterpart, dissolved Ag, focussing on their fate and toxicity in the aquatic environment. Silver is one of the most used nanomaterials with Ag NMs degradation potentially resulting in ionic silver release, which is well known to be highly toxic to aquatic organisms. The organism studied here was the aquatic model species, *Daphnia magna*, chosen for their non-selective particle feeding behaviour, sensitivity and importance in the aquatic food chain (Chapter 1).

In Chapter 3 the Ag NMs physicochemical properties were characterised within the appropriate aquatic matrices (i.e. Mill-Q water and environmental medium) using DLS, TEM-EDX, hyperspectral imaging, UV/Vis spectroscopy, centrifugal filtration and ICP-MS. Hyperspectral imaging was a novel technique but, highlighted is its potential usefulness within this discipline.

Chapter 4 explores the acute and chronic toxicity of Ag NMs and dissolved Ag to *D. magna*. The research here is one of the first to demonstrate that direct conversions of acute data for chronic predictions of hazard in *D. magna* may not be possible and that Ag NM toxicity cannot be fully explained by Ag^{+} release.

Critical modelling values were derived (biotic ligand modelling, BLM and biodynamic model, BDM) and the best predictors of toxicity established for use *in silico* models (Chapter 5).

Using biochemical techniques (Chapter 6) it was shown that Ag^{+} and Ag NM toxicity differed in their modes of action (MOA). The study is the first to derive possible schematic Ag NM MOA using multiple biochemical endpoints, with Ag^{+} affecting body cations and all Ag NMs causing perturbations to mitochondrial function and oxidative stress levels.

Within this thesis there are the first SEM images of Ag NMs trapped within the organism filtering apparatus. The study is the first to take an in depth look at ligand binding characteristics as they concern to Ag NMs and highlight any differences with Ag^{+}. In conclusion; Ag NMs are currently still one of the most toxic of all studied NMs current levels in the environment may not cause immediate impact on *D. magna* populations. However sub-lethal and long term effects under continuous exposure may still be of concern.

Acknowledgements

I would like to thank my supervisors Prof. Teresa Fernandes and Prof. Vicki Stone firstly for giving me the opportunity to partake in the project and Ph.D, and secondly for their ongoing support, kind words and encouragement as well as the invaluable insights and expertise they gave. Not only this, but also creating opportunities and experiences which I will never forget, and those which were key to my success. I would truly not have been the researcher and scientist I am today without you help and guidance.

I would also like to thank the two post-docs I was lucky enough to have on the project toward the latter stages of my Ph.D. Dr. Farhan Khan was indispensable to my development within the body burden of toxicants and modelling arena, and my Ph.D. Thanks for being there to listen, being a friend and accelerating what I thought was possible. Dr. Judit Kalman thank you for your patience, expertise (particularly, again in the modelling of body burdens) and unparalleled hard work, I know the project would not have been able to get through such a body of work at our institute without you over the last 6 months.

It would be remise of me to not finally thank the others within Heriot-Watt University and the NanoSafety Group. Dr. David Brown and Dr. Birgit Gaiser thank you for your help and guidance throughout my PhD, and all our "quick chats". Dr. John Kinross for always making sure we had a sound working environment and making sure I always had what I needed. Finally thanks to the entire group and those people within DB 2.65 who made my working days what they were, and the friends I have made on the way.

Thank you Clemson University ENTOX and thank you Prof. Stephen Klaine for letting me be part of your group, for your expertise and providing exactly what I needed without a second thought. I also have to thank those colleagues and friends I made in my time in the United States of America. You guys were great, and I can't thank you enough for your time, the rides to work and help. I feel lucky to have met you all.

I would like to thank everyone for listening to my incessant ramblings and your patience during such times and keeping me straight; it has been a pleasure.

Thank you to Penicuik rugby club for making me feel like I had a home from home, and providing me with a "creative outlet".

Thanks to my now fiancé Kerry for giving me the support, love and belief I needed when times were tough, when I was stressed or down, and pulling me out the other side.

Thanks to Jack for keeping me young and sane. I am lucky to have not only studied for my Ph.D but also found my own little loving family along the way.

Finally thanks to my caring and loving family, for whom it doesn't matter how far away I get I can always feel their support. I would not have been where I am today, let alone able to complete a Ph.D, without you all. Thanks for believing in me and always telling me everything is possible, thanks for always being proud and being there for me no matter what path I chose. Thank you, Mum, Dad, Karina, Senara and my Grandparents for always believing in me, loving and caring.

To all, my achievements and successes are yours as well as my own.

Ehaz ha sowenath whath tho why ha tho goz henath, Onen hag Oll.

ACADEMIC REGISTRY
Research Thesis Submission

Name*:*	Kai Benjamin Paul		
School/PGI:	School of Life Sciences		
Version: *(i.e. First, Resubmission, Final)*	Final	Degree Sought (Award **and** Subject area)	Ph.D

Declaration

In accordance with the appropriate regulations I hereby submit my thesis and I declare that:

1) the thesis embodies the results of my own work and has been composed by myself
2) where appropriate, I have made acknowledgement of the work of others and have made reference to work carried out in collaboration with other persons
3) the thesis is the correct version of the thesis for submission and is the same version as any electronic versions submitted*.
4) my thesis for the award referred to, deposited in the Heriot-Watt University Library, should be made available for loan or photocopying and be available via the Institutional Repository, subject to such conditions as the Librarian may require
5) I understand that as a student of the University I am required to abide by the Regulations of the University and to conform to its discipline.

* *Please note that it is the responsibility of the candidate to ensure that the correct version of the thesis is submitted.*

Signature of Candidate*:*		Date:	10/2015

Submission

Submitted By *(name in capitals):*	KAI B. PAUL
Signature of Individual Submitting:	
Date Submitted:	

For Completion in the Student Service Centre (SSC)

Received in the SSC by *(name in capitals):*			
Method of Submission *(Handed in to SSC; posted through internal/external mail):*			
*E-thesis Submitted (**mandatory for final theses)***			
Signature:		Date:	

Table of contents

List of Tables:

List of Figures

Abbreviations

95% CI; 95% Confidence interval

γ; Surface tension

ζ-potential; Zeta potential

AE; Assimilation efficiency

Ag^{+}; Ionic silver

Ag NMs; Silver nanomaterials

$AgNO_3$; Silver nitrate

Ag NPs; Silver nanoparticles

Au NPs; Gold nanoparticles

A_m; Molar surface concentration

aM7; Adapted Elendt M7 medium

ANOVA; Analysis of variance

ATP; Adenosine triphosphate

BDM; Biodynamic model

BLM; Biotic ligand model

B_{max}; Maximal biological ligand saturation

BSA; Bovine serum albumin

BSI; British standards institute

Ca^{2+}; Calcium ion

CAT; Catalase

Cd^{2+}; Cadmium ion

C_f; Concentration of contaminant in food

Cit-Ag NPs; Citrate coated silver nanoparticles

Cl^{2-}; Chloride

CO_3^{2-} Carbonate

C_{ss}; Steady state body burden concentration

Cu^{2+}; Ionic copper

CuO NPs; Copper oxide nanoparticles

C_w; Concentration of contaminant in water

d^{-1}; Per day

d.f.; Degrees of freedom

DPNH; 2,4-dinitrophenylhydrazine

DVLO; Derjaguin, Verwey, Landau and Overbeek

DW; Dry weight

DLS; Dynamic Light Scattering

EC; European Commission

EC_{50}; Median Effective concentration 50

EDTA; Ethylenediaminetetraacetic acid

EDX; Energy Dispersive X-ray Spectroscopy

ETC; Electron Transport Chain

EU; European Union

FFF; Field flow fractionation

GPX; Glutathione peroxidase

GST; Glutathione-S-transferase

H_2O_2; Hydrogen peroxide

HCl; Hydrochloric acid

HDD; Hydrodynamic diameter

HWU; Heriot Watt University

HMDS; Hexamethyldisilazane

HNO_3; Nitric acid

ICP-MS; Inductively Coupled Plasma Mass Spectrometry

IR; Ingestion rate

K^+; Potassium ion

K_2HPO_4; Dibasic potassium phosphate

K_d; Ligand binding affinity constant

k_e; Efflux rate constant

k_{ef}; Efflux rate constant from food

k_{ew}; Efflux rate constant from water

KH_2PO_4; Monobasic potassium phosphate ()

K_{sp}; Solubility product

k_u; Uptake rate constant

k_{uf}; Uptake rate constant from food

k_{uw}; Uptake rate constant from water

LA_{50}; Lethal accumulation 50

LDH; Lactate dehydrogenase

L g^{-1} d^{-1}; Litres per gram per day

LOEC; Lowest observed effect concentration ()

Log *K*; Strength of binding between chemical and biological ligand constant

MMP; Mitochondrial membrane potential

MOA; Mode of action

Na^+; Sodium ion

NADPH; Nicotinamide adenine dinucleotide phosphate

NanoBEE; The consortium of Nanoparticle Bioavailability and Environmental Exposure

NERC; Natural Environment Research Council

NMs; Nanomaterials

NOEC; No observed effect concentration

NPs; Nanoparticles

NTA; Nanoparticle tracking analysis

O_2^-; Super oxide

OECD; Organisation for Economic Co-operation and Development

·OH; Hydroxyl radical

PEG-Ag NPs; Polyethylene glycol coated silver nanoparticles ()

PVP-Ag NPs; Polyvinyl pyrrolidone coated silver nanoparticles ()

ROS; Reactive oxygen species

S.D.; Standard deviation

S.E.; Standard Error

SEM; Scanning Electron Microscopy

SOD; Super oxide dismutase

t; Time

TEM; Transmission Electron Microscopy

TiO_2 NPs; Titanium oxide nanoparticles

Tukey's HSD; Tukey's honestly significant difference test

UoB; University of Birmingham

USEPA; United States Environmental Protection Agency

UV/ Vis; Ultraviolet/ visible light spectroscopy

WW; Wet weight

WWP; Wastewater treatment plants

YCT; Yeast, chlorophyll and trout chow extract

ZnO NPs; Zinc oxide nanoparticles

List of Publications and Conference Presentations from this research

Kalman J., Paul K.B., Khan F.R. Stone V., and Fernandes T.F., (2015). Characterisation of bioaccumulation dynamics of three differently coated silver nanoparticles and aqueous silver in a simple freshwater food chain. *Environmental Chemistry*, Just accepted.

Khan F.R., Paul K.B., Dybowska A.D., Valsami-Jones E., Lead J.R., Stone V. and Fernandes T.F. (2015). Accumulation Dynamics and Acute Toxicity of Silver Nanoparticles to *Daphnia magna* and *Lumbriculus variegatus*: Implications for Metal Modeling Approaches. *Environmental Science and Toxicology*, 49(7), 4389-4397.

Correia Carreira S., Walker L., Paul K. and Saunders M. (2015). The toxicity, transport and uptake of nanoparticles in the in vitro BeWo b30 placental cell barrier model used within NanoTEST. *Nanotoxicology*, 9(S1), 66-78.

SETAC Europe Barcelona 2015 (platform presentation) Accumulation Dynamics and Acute Toxicity of Silver Nanoparticles to *Daphnia magna* and *Lumbriculus variegatus*: Implications for Metal Modeling Approaches. Khan F.R., Paul K.B., Dybowska A.D., Valsami-Jones E., Lead J.R., Stone V. and Fernandes T.F.

2014 – SETAC Europe, Basel (platform presentation) – A comparison of toxicity and accumulation kinetics of *D. magna* and *L. variegatus* exposed to differently coated silver nanoparticles. Kai Paul, Farhan Khan, Laura- Jane Ellis, Vicki Stone, Teresa F. Fernandes.

SETAC Europe Basel 2014 (poster) "A comparison of Acute and Chronic Ag NPs in *D. magna*: implications for regulation and wide-level screening." Kai Paul, Farhan Khan, Vicki Stone, Teresa F. Fernandes.

2014 – Carolina's SETAC, USA (platform presentation) "Toxicity, biokinetics and accumulation of Ag NPs in Aquatic invertabrates"

2014 – Heriot-Watt University Post-graduate conference (Platform Presentation). Toxicity and bioavailability of silver nanoparticles to *Daphnia magna*. Kai Paul, Farhan Khan, Vicki Stone, Teresa F. Fernandes.

2013 – ERIC-SETAC UK/Local Plymouth University UK (Platform Presentation): Toxicity and bioavailability of silver nanoparticles to *Daphnia magna*. Kai Paul, Farhan Khan, Vicki Stone, Teresa F. Fernandes.

Chapter 1. Introduction

Due to recent technological advances and understanding at the nanoscale there has been a surge of research and production within the field of nanotechnology in the latter half of the 20th century and beginning of the 21st century. In 2006 the global worth of nanotechnologies was estimated to be $10.5 billion (Farré *et al*., 2008). It was predicted that nanotechnology would exceed the impact of the industrial revolution by 2015 leading to a $1 trillion market (Farré *et al*., 2008 and Nel *et al.*, 2006). The predictions were not erroneous due to the adaptability of products at the nanoscale and their wide variety of applications. Most attribute the movement's inaugural steps to the Feynman 1959 Lecture 'There's plenty of room at the bottom: Invitation to enter a new field of physics' (Nature Nanotechnology, 2009), but even Feynman appreciated "nanotechnologies" (although he did not use this term) predated far before the 1950s, even if the technology was implemented unwittingly and the term not coined till later. Feynman was one of the first to appreciate the wide range of applications in the nano-field. He professed, "…a point that is most important is that it would have an enormous number of technical applications", even "writing the Encyclopaedia Britannica on the head of a pin…I am telling you what could be done if the laws [of physics] are what we think" (Feynman, 1960). Even in 1959 Feynman appreciated that as we manipulate technologies at this size "interesting problems" arise, partly due to these components acting within the laws of quantum mechanics. As such there were concerns as well as promise in the area. Herein the "interesting problem" (Feynman, 1960) of the potential toxicity of nanomaterials (NM) to the aquatic environment is explored .

The interest in NMs now of course goes far beyond writing tiny "volumes of interest" on pinheads. The interest in manipulation at this scale is further down to scientific evidence, such as size-specific novel physicochemical properties and the revolutionary potential "nano" holds for many areas. The ensuing pages present and discuss the work carried out during this research project, namely the analysis of NM physical and chemical properties within an aqueous phase followed by their aquatic toxicity, in particular to the freshwater water flea, *Daphnia magna*.

This Ph.D was conducted under the consortium for Nanomaterial Bioavailability and Environmental Exposure (NanoBEE, 2010). The work of the consortium was funded by the USA EPA and UK NERC. This PhD was funded by NERC.

1.1 The NanoBEE project aims and vision

In order to widely and sustainably apply NM innovations, it is crucial to minimise their potential unwanted impacts and implement appropriate risk mitigation strategies. Industry, policymakers and regulating bodies must base risk management decisions on NM information about: i) their environmental fate, ii) their bioavailability, and iii) any resultant biological effects (e.g. organismal toxicity). Through the creation and use of existing models and, the realisation of an NM profile database (known within NanoBEE as the Nanoparticle Information File (NIF)), the project aims to give decision-makers the tools for wide level high throughput assessment to enable successful and rapid implementation of nanotechnologies (NanoBEE 2010; Core Project Description of the Consortium for Manufactured Nanomaterial Bioavailability and Environmental Exposure). The goals of the NanoBEE project are:

i) To produce highly characterised NM libraries for environmental assessment;

ii) Show NM environmental modification can be classified by the extent of aggregation, dissolution and surface modification;

iii) Test and develop modified and/ or new biodynamic models (BDM) for NM bioavailability from both water and food (i.e. uptake from the background environment or via direct ingestion) quantifying influx – efflux;

iv) Produce and validate appropriate biotic ligand models (BLM) to predict exposure and any associated effects of NMs whilst identifying the mechanisms of such effects (e.g. signal cascades or gene effects);

These steps will enable NMs successful, safe and responsible incorporation into nanoproducts and technologies (NanoBEE, 2010).

The Ph.D addresses some of the NanoBEE goals as they pertain to silver nanomaterials and *D. magna*, namely goals iii and iv, by researching accumulation, accumulation kinetics (Chapter 4), and studying particle physicochemical characteristics in environmental medium whilst comparing these to the same particles suspended in Milli-Q water (Chapter 3). The other goals of the project were addressed by partners within the consortium and were not the responsibility of this project. Aspects novel from the project included in this thesis were, the research of toxicological effects, both acutely and chronically of silver nanoparticles, and the study of silver nanoparticles mode of

action, and adverse outcome pathways therein. Throughout the research also tries to determine differences and similarities between silver nanoparticles and its ionic counterpart for all the aforementioned.

1.2 Nanomaterials and manufactured nanomaterials in the environment

Nano is a prefix for many words which have precise definitions. The definition in relation to measure means $1x10^{-9}$ of the specific unit in question. Throughout the thesis the nanotechnology terminologies used will be as defined by the British Standards Institute (BSI, 2007). Here the focus is on the definitions based on material structure and these are given as written by BSI (2007). Nanoscale is a size range of approximately 1-100 nanometres (nm). A nanomaterial (NM) is a material having one or more external dimension(s) in the nanoscale or which is nanostructured (i.e. a structure in the nanoscale). However this definition has been expanded to further define NMs as "natural, incidental or manufactured materials containing particles, in an unbound, aggregated or agglomerated state for which 50 % or more of the particles size distribution has one or more external dimensions in the nanoscale" (European Commission (EC), 2011). This definition becomes important when assessing NMs in an environmental setting due to the behaviours they display. For example NMs will often agglomerate and aggregate forming a large bulk material which is made of discrete particulate matter. This will be expanded upon in Chapter 2. However, there are issues with this proposed EC definition, mainly to do with technical issues, such as measurements and analytical equipment, as well as considerations of life cycle of the material. A nano-object is a discrete piece of material with one or more external dimensions in the nanoscale (BSI, 2007). Nanoparticles (NPs) are nano-objects with all three external dimensions in the nanoscale (BSI, 2007). Nanorods and nanotubes are nano-objects with two similar external dimensions in the nanoscale and the third dimension significantly larger (often not in nanoscale) than the other two external dimensions, with the latter being hollow - a nanofibre is simply a flexible nanorod. Finally a nanoplate is a nano-object with one external dimension in the nanoscale and the two other significantly larger external dimensions (BSI, 2007).

NMs often have an unusually high reactivity when compared to their bulk material counterpart. At the nano-scale a higher percentage of atoms are available on the surface of the particle caused by the large surface area to volume ratio and high surface tension

which afford greater potential for reactive processes (Lowry *et al.,* 2012). Manipulations at the nano-scale, such as chemical composition (crystallinity, surface structure, surface groups, inorganic or organic coatings, etc.), solubility, and shape can dramatically change the behaviour and effect of the NM. Many of these characteristics and properties are important for the final product or the effects it may have outside the original intended purpose.

Throughout the thesis both the term nanomaterial and nanoparticle (NP) will be used. The term NP will be used when discussing results generated in this research project as the materials used are, by definition, NPs and where studies specifically state their particles have all 3 external dimensions within the nanoscale. The term NM will be used when the studiesdo not use NPs and thus the accepted definition of NP has been violated; such as with nanosheets or nanotubes.

Currently more than 1,628 NM-based materials and products are on the market, which is a 24% increase since 2010 (www.nanotechproject.org). NMs have been used for, and in; cosmetics, electronic goods, fuels, medical applications, sun screens and much more (Bystrzejewska-Piotrowska *et al.*, 2009, Geranio, Heuberger and Nowack, 2009, Kvitek *et al.*, 2008 and Sun *et al.*, 2008).

Silver NMs (Ag NMs) are diverse and relatively cheap to manufacture. As a consequence Ag NMs are currently one of the most used NMs within medical and commercial products, and industry (Fabrega *et al.*, 2011). Ag NMs now account for over ~50% of commercial nanoproducts (Asghari *et al.,* 2012 and McLaughlin and Bonzongo, 2012). Like silver in bulk or ionic form one use of Ag NMs is their antimicrobial and anti-viral properties; in fact silver has been used in health care since the 17th century (Marambio-Jones and Hoek 2010). Furthermore silver has the highest electrical and thermal conductivity and the lowest contact resistance of all metals and thus is highly favoured for electronics (Liu, Qi and Wang, 2012, Li, Wu and Ong 2005, Tzing, Holt and Ely, 1988, Parker *et al.*, 1961). Ag NMs are used in: imaging, catalysts, food packaging, odour resistant socks and underwear, room sprays, laundry detergents, washing machines, fridges, soaps, toothpaste, bone cements, wound dressings (and other medical applications e.g. anti-cancer drugs) and anti-soiling paints (Fabrega *et al.*, 2011, Allen *et al.*, 2010, Lee *et al.*, 2010, Marambio-Jones and Hoek 2010, AshaRani *et al.*, 2009a and Trop *et al.*, 2006). Despite the beneficial use of Ag NMs, and NMs, in a variety of new technologies, they may still have adverse biological

effects, to some degree in many forms of life, and this has been noted. Most notably a usually irreversible silver discolouration to the skin/ pigment (argyria) has been noted from chronic use and ingestion of silver colloids in humans (Asghari *et al.*, 2012 and Trop *et al.*, 2006), although this condition does not seem to lead to acute effects (Demling and Desanti, 2001). In general the potential risks of NMs, and Ag NMs, to human health and the environment in a setting representative of actual exposure at realistic doses/ concentrations are ambiguous, and as such NM risk has been the focus of many reviews and studies (Handy *et al.*, 2012, Handy *et al.*, 2008, Tiede *et al.*, 2008 Nowack and Bucheli 2007, and Moore, 2006).

The increased use and production of Ag NMs inevitably leads to their increased release into the environment. In 2010 it was estimated that Ag NMs would account for 15% of all silver released and this included intentional or incidental (Nowack and Bucheli 2007, and Tolaymat *et al.*, 2010). Intentional NM release could be during such processes as contaminated soil or ground water remediation (Zhang, 2003). Incidental release is often through spillage from factories, as well as release from nanoproducts such as fabrics, cosmetics, paints, washing machines and medical products (Nowack and Bucheli, 2007). Due to this increased release there is concern about Ag NM impact and potential risk to human health and the environment. Therefore it is important to consider the impact Ag NMs may have in these areas. Much research is now directed towards understanding NM fate and behaviour in the environment as well as the toxicological risk (Levard *et al.*, 2012, von der Kammer *et al.*, 2012, Zhao and Wang, 2012, Farkas *et al.*, 2010, Park *et al.*, 2010, Tolaymat *et al.*, 2010, and Nowack and Bucheli 2007). Current reviews have highlighted a lack of: i) research, ii) standardised testing methods (e.g. for regulation), iii) coalition between industry and academic bodies to move research and research methodologies forward, and, iv) more specifically to this project, tests to assess the environmental hazards of NMs (Handy *et al.*, 2012, von der Kammer *et al.*, 2012, Fabrega *et al.*, 2011, Handy *et al.*, 2008 and Nowack and Bucheli 2007). At present it is suggested that regulatory controls and testing strategies are likely to be inadequate with gaps remaining in our knowledge with regard to the best ways to treat and categorise these potential contaminants (Stone *et al.*, 2014). These highlighted challenges and knowledge gaps are essential to direct future research (Johnston *et al.*, 2013, Handy *et al.*, 2012, Baun *et al.*, 2008 and Handy *et al.*, 2008). It is of utmost importance to understand how to implement NM technologies in a sustainable and safe way due to their potential to revolutionise many key industries i.e.

remediation, waste water treatment, medical and renewable energies. For Ag NMs some research has addressed these knowledge gaps however some still persist, research and current gaps can be seen in Table 1.1. Some gaps will be addressed by the research conducted for the thesis.

The aquatic environment is likely to be a major compartment for the release and eventual fate of Ag NMs (Figure 1.1). These aquatic systems essentially act as the ultimate sink for many chemicals, including NMs, due to their many inputs e.g. rain, run-off and waste discharge (van der Oost *et al.,* 2003). Therefore it is particularly crucial to minimise potential unwanted impacts to this compartment. This can be achieved by researching the potential risks and behaviours of NMs within this environmental compartment. Successful use of Ag NMs is reliant upon appropriate risk mitigation and regulation strategies based on "sound science". An important, often used, model organism which allows the assessment of impact of contaminants in freshwater systems, and that which is used for this research, is the water flea *Daphnia magna*.. .

Table 1.1. Current studies conducted on the toxicity of Ag NPs to *Daphnia magna* and persisting knowledge gaps.

Endpoint type	Author	Findings	Conclusion	Knowledge gaps
Acute toxicity	Allen *et al.*, 2010	*D. magna*	Toxicity of Ag NPs is dependent on coating and presence of food. $AgNO_3$ and Ag NPs are of similar toxicity LC_{50}: ~1 µg L^{-1}, but commercially coated Ag NPs were less toxic (LC_{50}: 16-30 µg L^{-1}).	Coating and size varied so that level of toxicity cannot be entirely attributed to coating. No measure of dissolution. Main driver of toxicity unknown i.e. Ag^+ or nanospecific.
	Asghari *et al.*, 2012	*D. magna*	Toxicity of Ag NPs varied with commercial source (LC_{50}: 0.004-0.187 mg L^{-1}). $AgNO_3$ showed a similar level of toxicity.	Dissolution was not tested. Main driver of toxicity unknown i.e. Ag^+ or nanospecific. Too many variables to find main physicochemical characteristic that may relate to toxicity.
	Das *et al.*, 2013	*D. magna*	Ag NP 48 hour toxicity, LC_{50}: 2.75 µg L^{-1} .	Main driver of toxicity unknown i.e. Ag^+ or nanospecific. Differences between varying Ag NPs not established.
	Gaiser *et al.*, 2011	*D. magna*	Comparison between micro and nano-sized Ag. Ag NP: < 25 % mortality – 1 mg L^{-1}. Micro-Ag: 20-80 % mortality at 1 mg L^{-1}. No comparison with $AgNO_3$.	Main driver of toxicity unknown i.e. Ag^+ or nanospecific. No in depth analysis or discussion of physicochemical characteristics and their relationship with toxicity
	McLaughlin *et al.*, 2012	*Ceriodaphnia. dubia* & *Pseudokirchneriella subcapitata*	Smaller size NP in natural waters led to less toxicity to *Daphnia magna* and algae. For *Daphnia* LC_{50}: 221 ppb vs. 0.433 ppb for 73 nm compared to 192 nm Ag NP aggregates.	$AgNO_3$ was not compared to the toxicity levels.
	Seitz et al., 2015	*D. magna*	Particle characteristics and environmental scenario trigger toxicity of Ag NPs, and their degree of toxicity.	
	Volker *et al.*, 2013	*D. magna*	Smaller *Daphnia* are more susceptible to smaller Ag NPs. The filtering apparatus are smaller with higher propensity to filter small particles.	

Endpoint type	Author	Findings	Conclusion	Knowledge gaps
	Zhao and Wang, 2010		Size dependent uptake and toxicity of Ag NPs. Smaller particles led to higher toxicity due to higher aggregation, which led to easier uptake.	Size tested but not coating.
Chronic toxicity	Gaiser *et al.*, 2011	*D. magna*	Chronic effects at 0.001 mg L^{-1}. More toxic than micro-sized Ag	No comparison with $AgNO_3$. No comparison with other Ag NPs
	Mackevica *et al.*, 2015	*D. magna*	Chronic toxicity varied under different feeding conditions. High food treatment resulted in higher animal survival, growth and reproduction compared to result found for low food treatment. $AgNO_3$ showed greater toxicity than Ag NPs.	Only one Ag NP tested. Main driver of toxicity unknown i.e. Ag^+ or nanospecific.
	Volker *et al.*, 2013	*D. magna*	Multi-generation tests showed that Ag NPs are able to impact first and second generations even after the removal of the Ag NPs. Smaller *Daphnia* are more susceptible to smaller Ag NPs. Physicochemical characteristics were not attributable to effects due to insufficient evidence. High levels of Ag NP led to brown discolouration which could be accumulation of Ag NP.	Not confirmed that Ag NPs caused the brown discolouration.
	Zhao and Wang, 2011a	*D. magna*	Dissolution was tested and was said to be main driver for toxicity in acute toxicity tests. However chronic toxicity was still	
Risk assessment				
• Suitability	-			Currently unknown
• Current risk	-			Current presented risk unknown
Uptake	Zhao and Wang, 2010	*D. magna*	Ag^+ taken up more rapidly than Ag NPs. Larger aggregates caused by smaller particles leads to increased toxicity. Uptake rates were lower than those reported for Ag^+. Uptake rate 1.44 L g^{-1} d^{-1}.	No information on more than 1 Ag NP, only uptake rate but no other biodynamics were determined.

Endpoint type	Author	Findings	Conclusion	Knowledge gaps
BDM	-			None exist for *Daphnia* spp. exposed to silver nanoparticles.
BLM	-			None exist for *Daphnia* spp. exposed to silver nanoparticles.
NP physicochemical relationships with biological interaction	Newton *et al.*, 2013	*D. magna*	Toxicity of 3 differently sized and coated Ag NPs.	Toxicity changed with coating and size. It was concluded that toxicity was driven by Ag^{+}.
	Allen et al., 2010	*D. magna*	Smaller size NP in natural waters led to less toxicity in *Daphnia magna* and algae. For *Daphnia* LC_{50}: 221 ppb vs. 0.433 ppb for 73 nm compared to 192 nm Ag NP aggregates.	Dissolution was not tested. Main driver of toxicity unknown i.e. Ag^{+} or nanospecific. Too many variables to find main physicochemical characteristic that may relate to toxicity.
	Zhao and Wang, 2011b	*D. magna*	Coating dependent toxicity was shown for Ag NPs (1.1-29 µg L^{-1}). Toxicity was said to also be due to Ag^{+} release.	Needs to be further confirmed that no other parameters can effect toxicity. Size also changed not only coating and this effect may have been because of the smaller size not just a coating dependent effect.
Mode of action	Asghari et al., 2012	*D. magna*	Toxicity of Ag NPs varied with commercial source (LC_{50}: 0.004-0.187 mg L^{-1}). $AgNO_3$ showed a similar level of toxicity.	
	Stensberg et al.,	*D. magna*	Toxicity of Ag NPs was caused by mitochondrial perturbations. $AgNO_3$ toxicity was caused by perturbations in body cations.	Requires further elucidation.
	Newton et al., 2013	*D. magna*	Ag^{+} was concluded to be the main driver of toxicity.	No biochemical/ omic evidence to substantiate the claim.
	Zhao and Wang, 2013	*D. magna*	Ag NPs and Ag^{+} →Decrease in Sodium and potassium whole body homogenates. Ag+ for acute exposures was concluded to be the main driver of toxicity	Only 1 Ag NP was studied, and this requires further verification.
	Poynton et al., 2012		Upregulated: DNA repair gene REV1, metallothionein and heat shock protein genes	No physiological perturbations caused by these gene upregulations were studied.

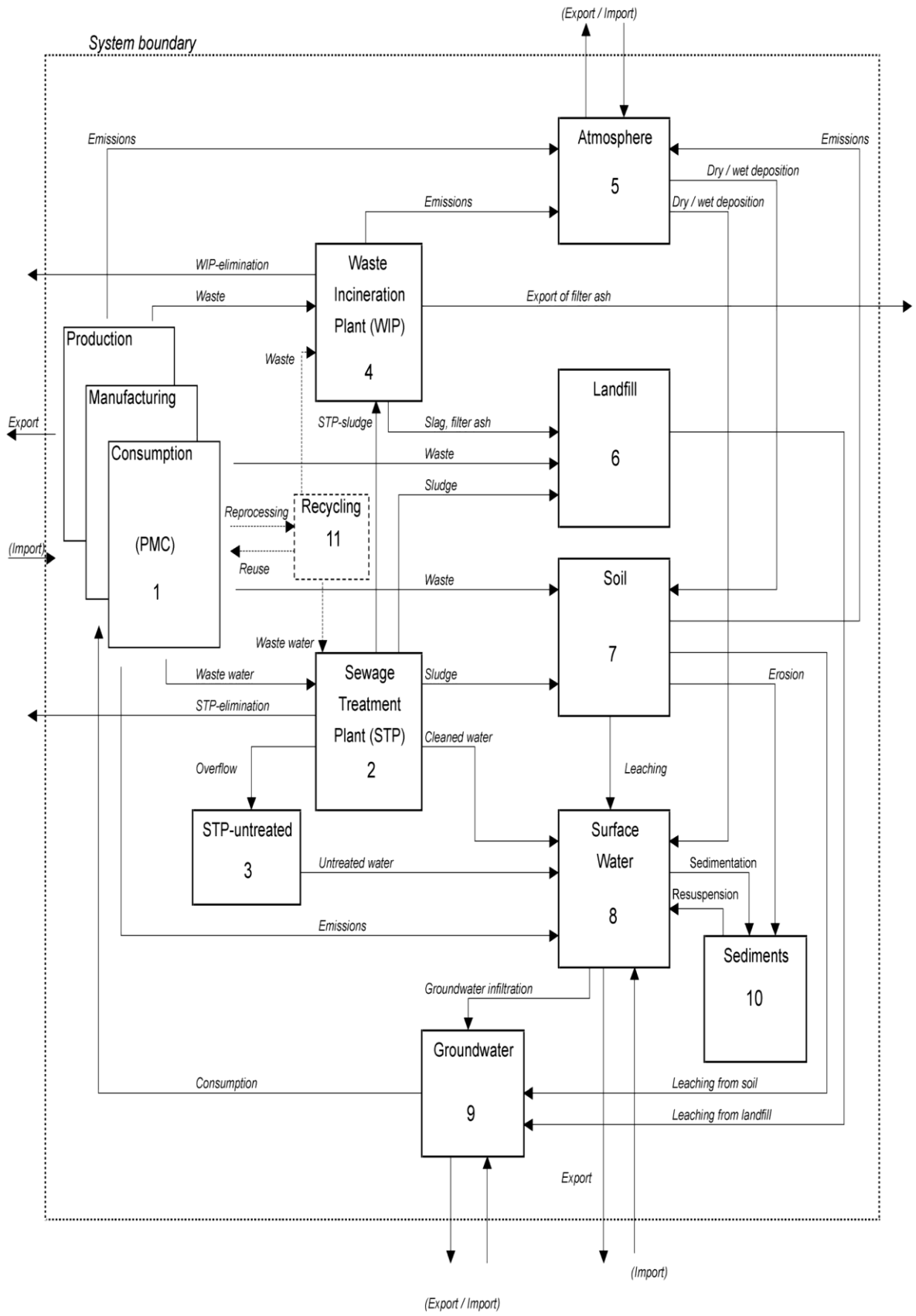

Figure 1.1 NM potential life cycle through environmental compartments and the flows between them – particularly those which are associated with run-off into the aquatic environment (2, 3, 7, 8, 9, 10) (Gottschalk, Sholz and Nowack, 2010).

1.3 *Daphnia magna*

Daphnia magna belongs to the phylum, subphylum and Super-Order of Anthropoda and Crustacea and Cladocera, respectively. *Daphnia magna* is adapted to living in freshwater environments. *D. magna* are native to northern and western North America, Eurasia and some regions of Africa. Unlike crabs and fish *Daphnia magna* do not have gills, as such, and so ion exchange (ionoregulation) and respiration occurs at specialised organs on the neck, nuchal organ (usually only found on juveniles), and thoracic limbs known as epipodites (Fig 1.2, Smirnov, 2013).

In their testing guidelines for daphnids (Tests 202 and 211), the Organization for Economic Cooperation and Development (OECD) state that individuals should be maintained in an environment with a pH of 6-9, dissolved oxygen content of $\geq$ 3mg L^{-1}, and a hardness of 140 and 250 mg L^{-1} (as $CaCO_3$), at a temperature of 18-22 ºC (OECD 2004 and OECD 2008). *Daphnia magna* are able to survive in temperatures ranging from 4-30 ºC (Lamkemeyer, Zeis and Paul, 2003). The temperature of their environment dictates their metabolic rate, life span, brood frequency and moulting frequency (Lamkemeyer, Zeis and Paul, 2003). Life span at optimal conditions is generally considered to be 52-days (Ebert, 2005). At 20 ºC moulting occurs every 2 days (Clare, 2009). Each moult is classed as an instar and coincides with growth, instars 1 to approximately 5 are juvenile instars, which are followed by a single adolescent instar and then the adult instars 6-26 (Clare, 2009). It is during the adolescent and adult instars that maturation and reproduction occurs (Clare, 2009). Reproduction usually coincides with each successive instar from the 5th instar onwards (i.e. per moult released during moulting after around 5 moults). At 20 ºC the first brood will occur when the *D. mag*na is 8-12 days old. *Daphnia magna* grow in length from juvenile to adult from around 0.5 to 5 mm (Smirnov, 2013).

The exterior of the *Daphnia magna* is a hard reticulated chitinous shell, which has antennae as swimming appendages, an apical spine and a rostrum with an antennule and sensory setae (Fig 1.2). The main physiological features internally and externally of *Daphnia magna* are: musculature; the compound eye which is sensitive to light and UV-light; filtering/ thoracic limbs with setae and setulae which act to catch food and are inseparably linked to respiration; food groove which transports food after filtration to the mandible; gastrointestinal tract; the epipodites (associated with the thoracic); postabdominal claw; the shell gland used for sequestration of unwanted products and

reactive oxygen species; a brain and a heart. The general physiological features of the *Daphnia magna* can be seen in Figure 1.2; these features are important when assessing exposure, metabolic pathways and effects, and as such as integral when setting hypotheses, assumptions and conclusions within this text.

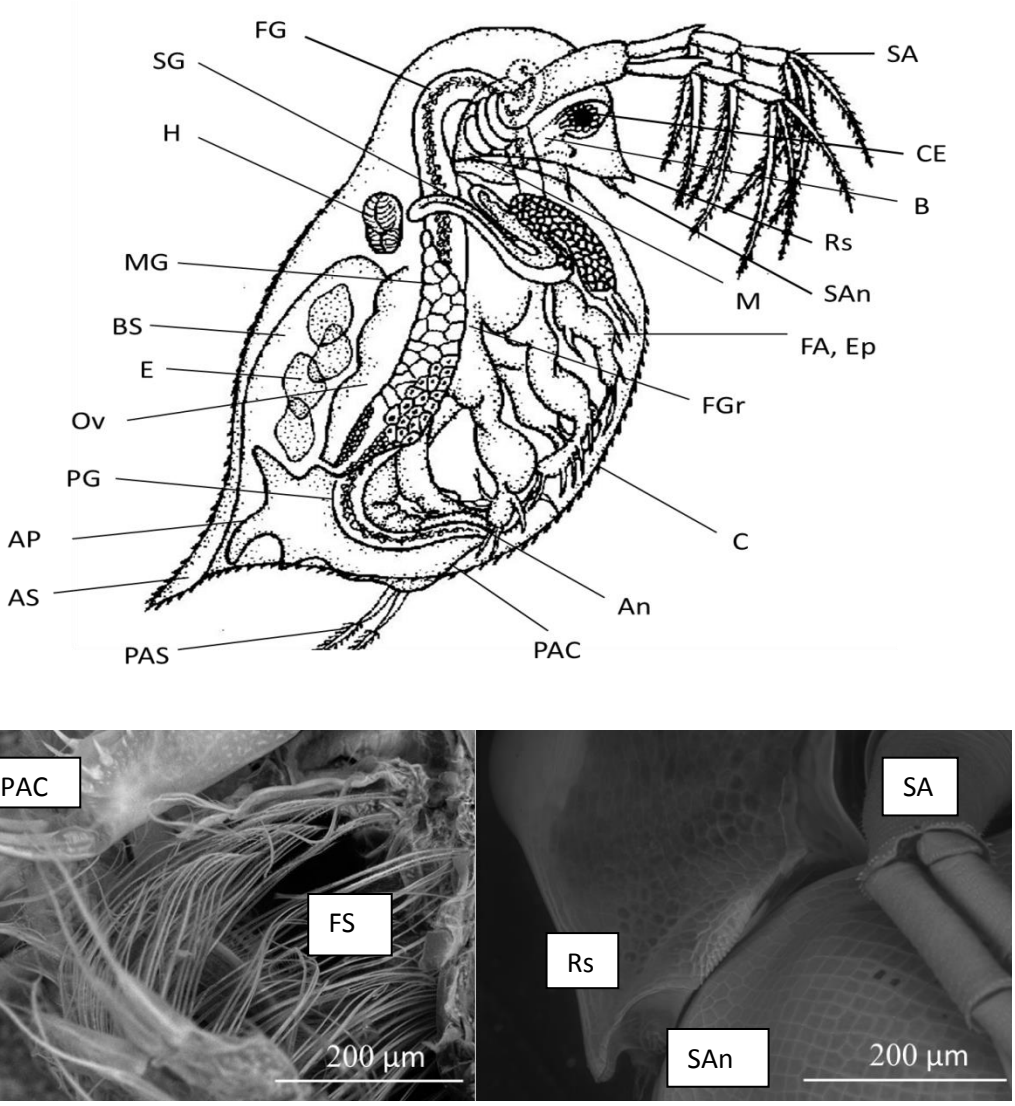

Figure 1.2. (Top) Diagrammatic of a *Daphnia magna* showing main physiological features; swimming antennae, SA; foregut/ stomodaeum, FG; compound eye, CE; shell gland, SG; brain, B; heart, H; rostrum, Rs; sensory setae of antennule, SAn; mandible, M; orientation of filtering apparatus/ thoracic limbs including epipodite, FA and Ep respectively; midgut/ mesenteron, MG; brood sack, BS; food groove, FGr; embryos, E; ovary, Ov; hindgut/ proctodaeum, PG; carapace, C; abdominal process, AP; anus, An; apical spine, AS; postabdominal claw, PAC; and postabdominal setae, PAS. Bottom left SEM image of postabdominal claw (PAC) and filtering setae/ apparatus (FS) and bottom right SEM image of head showing reticulated carapace, rostrum (Rs), sensory setae of antennule (SAn) and swimming appendage (SA). Diagram sourced from www.imagearcade.com, labelling by Kai B. Paul compiled from Smirnov (2013) and Ebert (2005). SEM images and labels Kai B. Paul.

Daphnia magna is one of the most sensitive organisms used in aquatic ecotoxicology and has been a model organism in toxicity testing for many years (Persoone *et al.*, 2009, OECD, 2008, OECD, 2004 and USEPA, 2002). Being in the middle of the aquatic food web, any change in *Daphnia magna* population can result in changes in the populations of other aquatic organisms. For instance lower numbers of *Daphnia magna* may result in food deprivation for higher organisms and result in uncontrolled algal blooms which may adversely change water chemistry. *Daphnia* are powerful model organisms as they: i) have few ethical challenges; ii) are easy to culture; iii) are non-selective filter-feeders; iv) are sensitive to contaminants; v) have conserved physiology through phyla; vi) have a predictable and short life-cycle; vii) reproduce mainly via parthenogenesis; viii) give rise to large broods; and ix) are important within the food chain (Lyu *et al.*, 2013, Zhao and Wang, 2012, Colbourne *et al.*, 2011, Lampert, 2011 and USEPA 2002).

As *Daphnia magna* mainly reproduces via parthenogenesis it is possible to have clonal stocks. This affords more comparable and reliable intra-laboratory results (USEPA 2002). Typically during reproduction *Daphnia magna* give rise to 2-20 neonates per brood dependent on environmental conditions, population dynamics and food availability (Smirnov 2013). For example, during good health and favourable conditions *D. magna* will usually have 12-20 progeny in one clutch (Ebert, 2003).

Importantly within Cladocera many enzymes have been previously found and assessed in order to establish either the mode of action of a contaminant or to explore suborder, population and species variability. Just a few of the found or assessed enzymes from whole body tissue homogenates are: lactate dehydrogenase (LDH), catalase, super oxide dismutase and Na^+ K^+ ATPase (Smirnov 2013). More recently, the closely related *Daphnia pulex* genome has been sequenced and the *Daphnia magna* genome is near completion (Colbourne *et al.*, 2011). Results from previous research on Cladocera physiology, biochemistry and their genome helped in the appropriate selection of toxicological endpoints for the chemical substances in question and further cement *D. magna* as a key ecotoxicological model.

1.4 Toxicity of Silver Nanomaterials with a focus on the Aquatic Environment

With the increased usage of Ag NPs environmental release is expected to rise and nano forms of silver are now calculated to account for 5-25% of all silver released into the environment from anthropogenic sources (Asghari *et al.*, 2012), with predicted

environmental concentrations as high as 0.32 μg L^{-1} (Fabrega *et al.*, 2011 and Prathna *et al.*, 2011). Currently, however, the level of risk, acutely or otherwise, that Ag NPs present to the environment is somewhat ambiguous and knowledge in critical areas are lacking despite a recent surge in research activities. The importance of assessing Ag NP risk is highlighted by the observations of their relatively high toxicity and the effects already noted for ionic silver (Ag^{+}) in aquatic environments (Asghari *et al.*, 2012, Wijnhoven *et al.*, 2009, and Bianchini and Wood, 2003). Furthermore they may pose higher risk to freshwater organisms than organisms in other compartments due to the low ionic strength of this environment in comparison to marine waters, for example. Therefore these environments are often more susceptible to contaminants' deleterious effects as they do not bind with medium ligands and other debris to the same degree as within higher ionic and more complex environments, meaning Ag NPs may remain more bioactive.

As mentioned Ag NMs have been shown to be toxic to many forms of life and this includes the aquatic environment. Toxicity has been seen in bacteria, algae, crustaceans and fish (Fabrega *et al.*, 2011). Due to the plethora of Ag NM types there is also a wide range of toxicity levels displayed between, and within, species when exposed to these NMs – some varying in orders of magnitude (Fabrega *et. al.*, 2011). For example within the same study Newton *et al.* (2013) showed that gum arabic-Ag NPs had a 48 hour median lethal concentration (LC_{50}, concentration that causes 50% lethality to the studied population) of 3.16 μg L^{-1} and PVP-Ag NPs had an LC_{50} of 14.81 μg L^{-1} in *D. magna* in USEPA reconstituted moderately hard water. Asghari *et al.*, 2012 tested the acute toxicity of several commercial nanosilver powders (ABC Nanotech Co., Ltd. Korea; Xuzhou Hongwu Nanometer Material Co., Ltd, China and Nano Nasb Pars Co., Ltd, Iran) they showed that in Elendt M4 medium these particles had different 48 hour LC_{50}'s which ranged from 6-275 μg L^{-1}. Ag NMs may display toxicity at low doses (i.e. low μg L^{-1} range) over chronic (longer) time scales. They have been shown to affect development, life-cycle events and reproduction of certain species. There are currently a few studies in the literature assessing Ag NM chronic toxicity to *Daphnia magna* (Mackevica *et al.*, 2015, Reibero *et al.*, 2014, Arndt *et al.*, 2014, Völker *et al.*, 2013and Zhao and Wang 2011a) but far fewer which compare toxicological results between different forms of Ag NP (Mackevica *et al.*, 2015) and none which assess the appropriate of the processes in risk assessment measures. The research within this thesis will address both.

The toxicity of ionic Ag (Ag^+) to aquatic species has been known for several decades and within fish and Cladocera the mode of action is well established, causing the disturbance of ionoregulation and mitochondrial function (Stensberg *et al.*, 2014 and Adams *et al.*, 2011). Ag^+ is highly toxic to freshwater organisms, competitively inhibiting Na^+, K^+, ATPase enzyme activity at the sight of animal ionoregulation; for example the gills in fish or the epipodite of some Cladocera, the disturbance eventually leads to cardiovascular collapse and mortality (Stensberg *et al.*, 2014 and Bianchini and Wood, 2003, Bury *et al.*, 2002).

Knowing that Ag NMs are prone to dissolution, to a certain extent (Fabrega *et al.*, 2011), it has been proposed that the toxicity of Ag NMs to aquatic species is attributable to Ag^+ release; that is, their dissolution into the aqueous phase (Newton *et al.*, 2013 and Kittler *et al.*, 2010). Here the main effects are the aforementioned disturbance of ionoregulatory processes (Biachini and Wood, 2003 and Bury *et al.*, 2002). At ambient temperatures the dissolution of silver to Ag^+ in an aqueous phase is a thermodynamically favourable outcome (Levard *et al.*, 2012). This temperature is similar to those found within water bodies in moderate climates and the temperature of suggested test conditions of several model testing species (OECD 2004, OECD 2008 and USEPA 2002). Much of the literature seems to support Ag^+ release hypothesis for Ag NM toxicity to several aquatic species (Golovina and Kustov, 2013) and Ag NM dissolution can also create reactive oxygen species which cause oxidative stress to the organism further causing detrimental effects to waterborne species (Li *et al.*, 2013). Newton *et al.* (2013) concluded that Ag^+ was solely responsible for the toxicity observed in *Daphnia magna* when exposed to 3 differently coated Ag NPs. Similarly Yang *et al.* (2012) showed that toxicity of Ag NPs to *Caenorhabditis elegans* was caused by the release of Ag^+ which was dependent on the Ag NP coating. However there are also contradictory publications and research. Results from these have demonstrated that there are nano-specific causes for toxicity and that toxicity can be linked to certain Ag NM physicochemical characteristics and behaviours within the aquatic environment.

Zhao and Wang (2012) showed size dependent uptake and toxicity of Ag NPs to *Daphnia magna* with smaller particles exerting greater toxic effect. Völker *et al.* (2013) showed *Daphnia* spp. had size dependent sensitivity with smaller *Daphnia* species' more susceptible to smaller particles and agglomerates/ aggregates. A previous *in vitro* cell line (rat alveolar macrophages) study has also shown Ag NMs cause a size-

dependent toxicity with smaller NMs exhibiting greater toxic effect, and the same correlation has been seen within bacteria (rat alveolar macrophages, Carlson *et al.*, 2008 and; *Escherichia coli* PHL628-gfp, Choi *et al*., 2008). It has also been found that charge and surface modification can alter toxicity, uptake, bioaccumulation and biodistribution of Ag NMs in many test models (Khan *et al.*, 2014, Carreira *et al.*, 2013, Zhu, Chang and Chen, 2010 and Lockman *et al.*, 2004).

Recently Stensberg *et al.* (2014) have shown Ag NP specific mitochondrial toxicity to *Daphnia magna*. Mitochondrial toxicity has previously been implicated as an Ag NM mode of action (MOA) to other species, within cell lines and isolated mitochondrial cultures. Costa *et al.* (2010) showed Ag NPs can cause inhibition of all 4 respiratory chain complexes in brain, skeletal, heart and liver homogenates of male Wistar rats. Ag NMs can also alter cell membrane permeability of bacteria, mouse germline stem cells human lung fibroblast cells and human glioblastoma cells, and have been shown to cross into the cytoplasm and thus can interact with varying cellular organelles such as the mitochondria (Teodoro *et al.*, 2011, AshaRani *et al.*, 2009 and Braydich-Stolle *et al.*, 2005).

One of the main routes for toxicity of Ag NMs may be that they act as a vessel or "Trojan-horse" to carry particulate Ag across the cell membrane which can then dissolve releasing Ag^+ within the cell leading to toxic effects (Park *et al.*, 2010). Ag^+ is detrimental to mitochondria and energy production. AshaRani *et al.* (2009) showed Ag NMs can reduce cellular ATP which led to mitochondrial damage and increased production of reactive oxygen species in fibroblast and glioblastoma cells. DNA damage and lipid peroxidation have also been demonstrated and these may be due to: ATP reduction, oxidative stress, mitochondrial dysfunction and/ or a direct effect of the Ag NM (AshaRani *et al.*, 2009 and Yu, Yin and Liu 2012). These effects are often accompanied by the increase in cellular apoptosis and necrosis factors such as TNF-alpha (Carlson *et al.*, 2008 and Gaiser *et al.*, 2011). Effects on mitochondrial and energy systems can lead to a series of signal cascades and effects within the cell causing excessive oxidative stress and eventually cell death. Indeed upon uptake and translocation into bacteria and various cell lines Ag NMs have been shown to cause an increase of ROS and/ or hydroxyl radicals leading to oxidative stress and this is a common theme of toxicity across many phyla (*E. coli*, Choi *et al.*, 2010; mouse macrophage RAW264.7, Park *et al.*, 2010; BRL 3A rat liver cells Hussain *et al.*, 2005 and A549 human type II alveolar epithelial cells, Stone *et al.*, 1998). The upregulation

of genes and enzymes associated with oxidative stress have been shown after organisms and cells have been exposed to Ag NMs. Among these enzymes catalase, super oxide dismutase, glutathione peroxidase and glutathione-s-tranferase have been shown to upregulate in classical biochemical testing as well as their respective genes (Yu, Yin and Liu 2012 and Kim *et al.*, 2010).

For the previous research, however, it is important to note that the relevance of the presented data in relation to the amount eventually released into the environmental compartment are still under debate. The problem is partly caused by a lack of techniques available for the analyses of *in situ* concentrations of Ag NMs and to separate these from natural sources. Further to this a weakness of many of the earlier studies was the lack of direct comparison to the ionic silver effects and the extent to which the Ag NMs dissolved (Reibero *et al.*, 2014). These concepts and the associated research will be explored further within the appropriate chapters. The current knowledge and knowledge gaps have been summarised in Table 1.1. Many of the knowledge gaps for *Daphnia magna* will be addressed within this doctoral research and thesis. Some of the research is novel compared to the original goals NanoBEE (2010) but no less pertinent.

1.5 Toxicological Modelling within the Environment

Based on assumptions arising from sound scientific data the development and application of predictive models for any potential toxicant may take place, and this is an important step in the understanding of pathways and prediction of potential toxicity. Within an environmental context two models have been extensively used by regulators and industry bodies to assess chemical hazard with some success. These are the biodynamic model (BDM) and the biotic ligand model (BLM) which assess and evaluate behaviour of chemicals in relation to their toxicity, body burdens and interactions with the organism (Luoma and Rainbow 2005 and Di Toro *et al.*, 2001). It has been proposed that by using the basic framework of these models, with appropriate adaptation, a nano-BDM and nano-BLM may be developed (NanoBEE, 2010). The research presented here takes the first steps, as directed by NanoBEE (2010), to create such models.

For a chemical to be toxic to an organism uptake must exceed its excretion, and in some instances, its detoxification (Adams *et al.*, 2011). Most BDMs assess accumulation as a simple unidirectional process i.e. **in** *vs*. **out**. BDMs breakdown accumulation processes

into discrete analyses of uptake and elimination from food-bound and waterborne contaminants. It is then possible to mathematically calculate whole body tissue/ organ burdens. The BDM predicts organism accumulation at biological ligands, such as the gill in fish or within the whole body in *D. magna*. BDMs allow accumulation kinetics to be compared among different environmental conditions such as different water chemistries (i.e. pH and hardness), and contaminants; and help highlight differences in bioavailability of such contaminants. Use of the BDM may help answer the following questions: i) is bioavailability dependent on contaminant properties and environmental modifications, ii) do contaminants persist after uptake and iii) are interactions between biological ligands and contaminant (i.e. do they lead to biological perturbation), or association at the surface of the animal's body of significance (e.g. in particulate form can mechanical load or irritation be sufficiently large to lead to reduced and/or harder motility, respectively) (Gaiser *et al.*, 2011 and NanoBEE, 2010). The same approach has now been discussed in terms of the application of the BDM approach to NM exposure and how it can be used to predict NM interactions with exposed organisms (NanoBEE, 2010). The thesis is one of the first to fully explore both waterborne and foodborne contributions of this model in any species.

BLMs model contextualises bioaccumulation of contaminants at an organism's biological site of uptake (e.g. gill, epipodite, gut or whole body) in relation to its toxicological responses. Traditionally this approach was used in aquatic toxicology to assess the bioavailability of metals in the aquatic environment and the likelihood of these metals to accumulate at the gill surface of the organism; now, however, BLMs are also used to assess whole body burdens (i.e. *Daphnia magna*) (Adams *et al.*, 2011). The BLMs strength is that it recognises the importance of *in situ* water quality parameters such as pH, hardness and dissolved organic carbon in the outcome of such interactions (i.e. toxicity and accumulation; Niyogi and Wood 2004 and Paquin *et al.*, 2002).

The model development was based on the assumption that animal-ligand interaction will occur when a contaminant's affinity for the ligand is greater than its affinity for other waterborne ligands (i.e. Cl^-, SO_4^-), or the affinity of the contaminant to the ligand is greater than the ligand's affinity with other medium cations (Na^+, K^+, Ca^+). The BLM framework is therefore founded on the principle that metal accumulation can be a predictor of acute toxicity when water body ion interaction is accounted for. Using

water chemistry and ligand binding constants, the BLM can relate short term accumulation (the LA_{50}, the lethal accumulation of metal on the biotic ligand that results in 50% mortality in short-term acute toxicity scenarios) at the site of uptake (the "biotic ligand", whole body accumulation in the case of invertebrate models) to acute toxicity (48 or 96 h LC_{50}, the exposure concentration that results in 50% mortality; Paquin *et al.*, 2002 and Di Torro *et al.*, 2001). Uptake and consequently short-term accumulation from solution are influenced by water chemistry, which affects the bioavailability of the metal ion to the biotic ligand. Moreover, the strength of binding between the biotic ligand and the metal of interest (the log *K* value) is correlated to acute toxicity (Niyogi and Wood 2004). One highlighted mechanism in the aquatic environment is competitive inhibition of Na^+, K^+ ATPase activity by the attachment of Ag^+ ions at the biological ligand which leads to ionic imbalances and mortality (Bianchini and Wood 2003). The same approach is now being tested for exposures to metal NMs. The research presented here is the first to fully explore all facets of an acute BLM for Ag NMs, and try to correlate BLM and BDM determined values with toxicological response in *D. magna.* The combination of models and how they link into NM risk management can be seen in Figure 1.3.

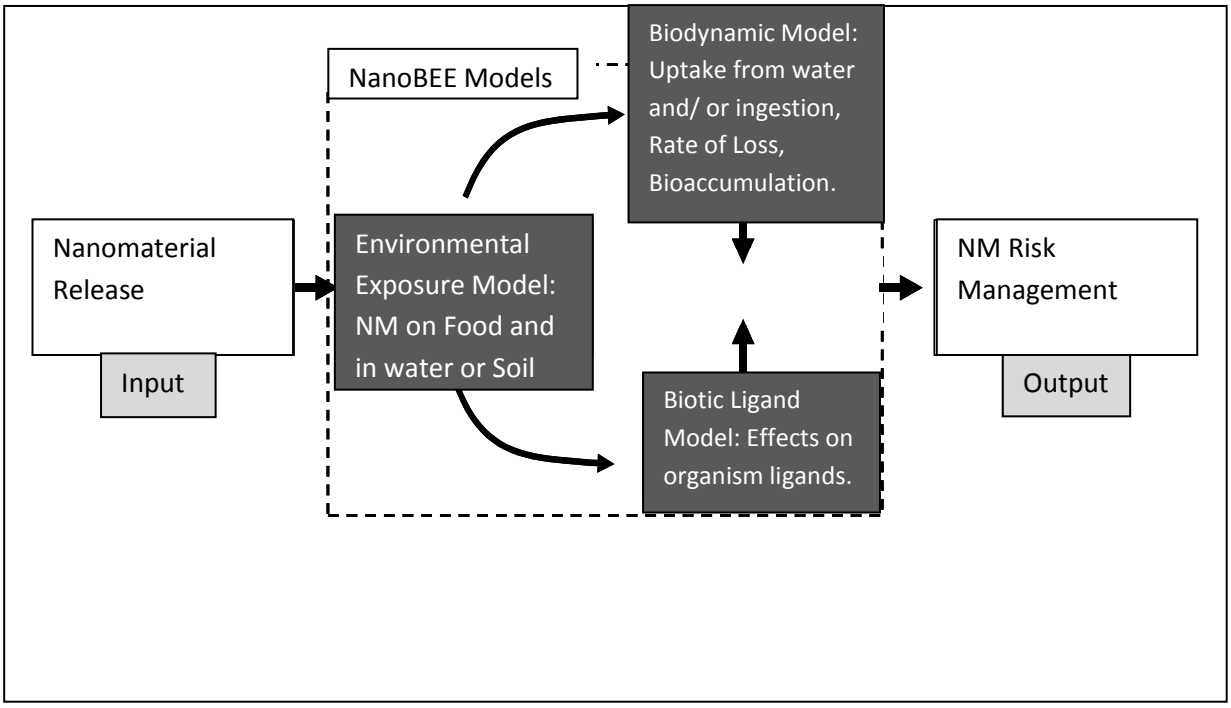

Figure 1.3 NM bioavailability and effects shown by using the combination of NanoBEE models derived from existing risk management strategies. (Adapted from NanoBEE Core document; NanoBEE, 2010).

1.6 Aims

This research was conducted in line with the aims of the UK-US project NanoBEE (NanoBEE 2010). The focus was on the model organism *Daphnia magna*. The main aims targeted here as directed by, and for, NanoBEE were to explore differences between Ag NPs and Ag^{+} acute toxicities, biodynamics and the biotic ligand interactions within the aquatic environment. Novel from the NanoBEE framework further research was conducted on chronic toxicities between Ag NPs and Ag^{+}. . Further novel research into biochemical response were conducted. The aim was to study endpoints to derive nano-specific modes of action and/ or adverse outcome pathways, or similarities between these and Ag^{+}. Based on previous research, e.g. the recently sequenced *Daphnia pulex* genome, and omics data provided by the University of Birmingham (UoB), we explored the energetic systems, and any detrimental effects caused by their disturbance when *Daphnia magna* were exposed to Ag NPs and dissolved Ag (as $AgNO_3$).

A major aim was to separate nano-effects from traditional effects of dissolved Ag in the aquatic environment. In order to do this the hypothesis that ionoregulation would be

disturbed at similar degree during equa-toxic (i.e. of equal toxicity) exposures of dissolved and nanoparticulate Ag was tested, since it has been shown that the major toxicological mode of action of dissolved Ag is to cause ionoregulatory disturbance (Bianchini and Wood 2003).

Again, Table 1.1 shows current literature and the endpoints derived, as well as highlighting data gaps.

These aims were achieved using pre-existing and adapted bioassays (OECD 202, 2004 and OECD 211, 2008), biodynamic and biotic ligand principles, and biochemical assays. The experiments included: i) lethality and reproduction tests, ii) uptake, excretion and bioaccumulation experiments, iii) biochemical assays and iv) varying microscopy techniques used to visualise NM distribution and potential translocation within the organism and to visualise any NMs attached to its surface and v) NM characterisation; via dynamic light scattering, dissolution experiments and microscopy in order to find correlations with physicochemical characteristics with toxicity and/ or accumulation kinetics.

Chapter 2.

Generic methodologies for nanomaterial testing, and organism testing, culturing and maintenance

2.1. *Daphnia magna* culturing, testing conditions and standard measured endpoints

All culturing of organisms and exposure tests were carried out in borosilicate glass or polypropylene beakers. *Daphnia magna* were purchased from Blades Biological (Kent, UK) and clones were established in an adapted Elendt M7 OECD medium with ethylenediaminetetraacetic acid (EDTA) removed (aM7; medium constituents and concentrations can be found in the Appendix, Table A2.1). EDTA was removed in order to negate the possibility of silver chelation with EDTA which can affect the toxicity silver displays and as directed per OECD guidelines for this purpose (OECD 202, 2004 and OECD 211, 2008). Culturing and testing in the same medium meant no pre-test acclimation period was required. The adapted medium was also seen as the optimal medium for *Daphnia magna* health in culturing and testing, and more environmentally relevant than other media that could be used (Elendt, 1990). The medium has also been shown to give rise to more consistent results during toxicity testing (Baer *et al.*, 1999). Culture medium was renewed 3 times weekly (Monday, Wednesday and Friday). During chronic tests, or tests exceeding four days, medium was also renewed every 3 days. A 5 mL non-toxic inert plastic wide mouth Pasteur pipette (VWR®, UK) was used to transfer the *Daphnia magna* into new culture or testing medium.

Daphnia magna were kept in large Belkin incubators. The organisms were maintained and tested at 20 ºC with a 16:8 hour light:dark photoperiod with ≥ 2 mL medium daphnid^{-1}. Hardness, dissolved oxygen (DO) and pH remained optimum during maintenance and testing at ≥ 3 mg L^{-1} (as $CaCO_3$), pH 6-9 and140 and 250 mg L^{-1} , respectively; as per OECD guidelines (OECD Test 211 2004, OECD Test 202, 2008). Hardness was calculated from the chemicals added to deionized water in order to make the medium as $CaCO_3$ and is also noted in OECD guidance (202, 2004). Dissolved oxygen and pH were measured with a HQ30D (Hach®, Loveland, USA) and an Orion 2-star benchtop pH metre (Thermo Scientific®, Massachusetts, USA), respectively. No

significant differences were observed in medium parameters during culturing, exposures or after testing.

Daphnia magna cultures were fed on an algal diet of *Chlorella vulgaris* (CCAP 211/12 from Heriot-Watt University Stock cultures) at a level of ≥ 2 mg carbon daphnid^{-1} day^{-1}, here we used a *C. vulgaris* cell density of 5 x 10^5 mL. Algae stocks were grown at 10 °C in a climate control roomed under continuous aeration in JM medium (Appendix Table 2.2) held in a 2 L glass Bijou bottle. The culture was harvested and taken back to a density to allow optimum growth (i.e. cells not too dense) *ad libitum*. When harvesting algae was centrifuged and the supernatant was discarded and replaced with Elendt aM7 these stocks were kept in sterile centrifuge tubes (Corning, Tewksbury, USA). *C. vulgaris* was checked for contamination at least once every few weeks months by plating a small amount of algal stock onto a petri dish with agar for substrate using aseptic technique, this was followed by assessing growth of bacterial colonies, if any, over several days. *C. vulgaris* was used immediately (and kept for no more than 2 weeks at 4 C in the fridge) or was frozen for later use. Optical density was used as an indicator of algal stock suspension cell density from which feeding volume was derived. Additionally the *D. magna* diet was supplemented with yeast (Allinson, London, UK), alfalfa powder (Now Nutrition, USA) and trout chow (Blades Biological, Kent, UK), these were mixed to make YCT at a 1:1:1 ratio and fed to the *D. magna* at 0.25 mL daphnid^{-1} three times per week (OECD Test 202, 2008 and USEPA, 2002). YCT was made by mixing 5 g of each component in 1 L of Milli-Q water. Before combining the three constituents trout chow was aerated for 7 days in Milli-Q water, alfalfa powder was stirred overnight in Milli-Q and yeast was immediately mixed with Milli-Q prior to use, all stocks were left to settle before filtering through muslin cloth to create the final preparation. Stocks were frozen in sterile centrifuge tubes and kept for no more than 2 month, or 2 weeks once defrosted open (Corning, Tewksbury, USA). During testing and the establishment of adolescent and adult *Daphnia magna* for testing, organisms were only fed *C. vulgaris* at a level of 5 x 10^5 cells mL^{-1} at the same frequency as husbandry feeding in order to remove the chelating properties of YCT. This food provision is also acceptable for optimal health (Stephenson and Watts, 1984). On Fridays culturing stocks were given a double dose of *C. vulgaris* to ensure sufficient food provision over the weekend. Animals requiring feed during tests were continued to be fed daily at the stated doses, inclusive of weekends.

The main studied endpoints as per OECD guidance can be seen in Table 2.1.

Table 2.1. Standard endpoints measured during OECD *D. magna* toxicological assessment (OECD, 2004 and 2008).

Measure:	Context	Acute or chronic endpoint
Immobility	A daphnid is considered immobile when, after 15 seconds of gentle agitation, no movement off the bottom of the testing vessel can be seen.	Acute and chronic
Deformations	Deformed Daphnia are checked for under a dissection microscope, either at the end or during toxicity testing.	Acute and Chronic
Number of moults	Daily vessels are checked for shed carapace which can be seen at the bottom of testing vessels and removed by a Pasteur pipette.	Chronic
Number of juveniles	Juvenilles are checked for and removed daily, the cumulative number and number per brood over 21 days are determined.	Chronic
Number of Broods	One brood equals one successful release event of juvenilles (dead or alive) from the brood sack and is counted daily. A brood is considered complete when juveniles are visible in the text vessel.	Chronic
Mean Length	The length of *Daphnia* is assessed at the end of the 21 day chronic exposure period under a dissection microscope.	Chronic

For each measured parameter it is possible to estimate the EC_{50} and determine NOEC and LOEC values.

2.2 Nanomaterials used

The NMs used throughout this Ph.D were obtained from UoB (UK) and were polyhedral (i.e. almost 'spherical') and by definition, nanoparticles (NPs), since they all had 3 external dimensions in the nanoscale. The NPs were: citrate coated silver nanoparticles (Cit-Ag NPs), polyethylene glycol coated silver nanoparticles (PEG-Ag NPs) and polyvinyl pyrrolidone coated silver nanoparticles (PVP-Ag NPs). Core size for each NP was measured via TEM at Birmingham University and these were 11.5 ± 3.3, 10.3 ± 3.2 and 10.8 ± 3.3 nm, for Cit-Ag NPs, PVP-Ag NPs and PEG-Ag NPs,

respectively. Cit-Ag NPs and PEG-Ag NPs were supplied at a concentration of ~10mg L^{-1} and PVP-Ag NPs were supplied at ~19mg L^{-1}.

PVP and PEG were both bound sterically to the Ag NP core. The binding is stronger (covalent bond) than found in charge bound coatings and as a result there is usually less degradation of the core material, loss of coating from the surface and complexation with media ligands (Tejamaya *et al.*, 2012). Citrate was charge bound to the Ag NP core relying on electrostatic attraction (van der Waals force) between Ag^{+} and negatively charged citrate. This type of binding is quick and relatively cheap to perform but the coating is usually only bound weakly in comparison to sterically bound coatings (Tejamaya *et al.*, 2012 and Römer *et al.*, 2011). All of these NPs are commercially and industrially relevant – e.g. PVP-Ag NPs , PEG-Ag NPs and Cit-Ag NPs and can be used in electronics, consumer products (i.e. toothpaste), for water clean-up in sewage treatment plants and for *in vivo* drug delivery systems (Kaegi *et al.*, 2011, Liong *et al.*, 2008, Li, Wu and Ong, 2005 and www.nanotechproject.org).

2.3 Nanoparticle synthesis and stocks

All Ag NPs tested were synthesised and suspended in Milli-Q water at Birmingham University and the methods of synthesis and characterisation have been previously described (Tejamaya *et al.*, 2012 and Römer *et al.*, 2011) and a brief description of their synthesis can be found in the Appendix (Text A2.1). All stocks were kept at 4 ºC in the dark at Heriot-Watt University. Silver nitrate (Ag NO_3, Sigma Aldrich, UK) was kept in the dark in powder form at room temperature; stock solutions were prepared in Milli-Q water and kept for a maximum of 2 weeks.

Silver nanoparticle stock suspension concentrations were checked using atomic absorbance spectroscopy (AAS) with an acetylene flame (Perkin Elmer, AAnalyst 200 Atomic Absorption Spectrometer, USA) in triplicate at Heriot-Watt University to confirm nominal concentrations. Original stocks were diluted by a factor of 10 with Milli-Q water in 20mL borosilicate vials (1 mL stock to 9 mL Milli-Q) before AAS analysis. Stock suspension concentrations were confirmed as correct (i.e. 95% of nominal stated concentrations, Appendix Table A2.3). Working stock suspensions were prepared by the addition of the Milli-Q water-NP suspension or $AgNO_3$-Milli-Q water solution, to aM7 medium of the correct strength immediately prior to testing. Particle addition was followed by gentle agitation (~15 seconds by hand) in all instances to avoid any unwanted ablation or interactions that may occur with more intensive mixing

processes (e.g. sonication and vortexing). $AgNO_3$ addition to any aqueous phase was followed by vortexing. In all instances the addition of *Daphnia magna* via a wide mouth pipette further mixed the test suspensions and/ or solutions. Expected nominal concentrations did not vary in medium or Milli-Q water by more than 10%; as such nominal concentrations are reported throughout for testing concentrations (Appendix, Table A2.3).

2.4 Statistical analyses

EC_{50} values were established using the trimmed Spearman-Karber method (USEPA 2002). Using R, general linear models were used to determine the best fit for mortality, uptake and depuration. Significant differences in mortality, uptake and depuration were then assessed using a contrast of fit for each plot. Sigma-plot v12 (Systat Software, San Jose, CA) was used to derive BLM parameters. All other statistical analyses were carried out in Microsoft Office Excel 2010 (Redmond, Washington: Microsoft) and SPSS v20 (Armonk, NY: IBM Corp). Normality was assessed using either the *z*-statistic or *W*-statistic from the Kolmogorov-Smirnov distribution test (data sets exceeding ~50) or Shapiro-Wilks distribution test (data sets under ~50), respectively, using SPSS. Acute no observed effect concentrations and lowest observed effect concentrations were established using either the Mann-Whitney U test or Dunnett's test for non-parametric and parametric data, respectively, using SPSS. Chronic no observed effect concentrations and lowest observed effect concentrations were established by the highest concentration preceding a significant effect and the lowest concentration at which a significant effect was seen, respectively, with significance determined by the Mann-Whitney U test or Dunnett's test for non-parametric and parametric data, respectively, using SPSS. Determination of significant differences in all other bioassay or biochemical tests were established by the Kruskal-Wallis test or one-way ANOVA for non-parametric and parametric data, respectively, unless otherwise stated, using SPSS. Should significance be found post-hoc tests used for each test were the Mann-Whitney U test or Dunnett's test both were used to test differences in comparison with the control, neither test relies upon homoscedasticity of the data set. If pairwise comparisons of the whole data set were required either the Tukey's honestly significant difference (Tukey's HSD), or Tamhane's post-hoc tests were conducted. Tukey's HSD relies on homoscedasticity of the data set whereas Tamhane's test does not, therefore when these tests are used Levene's test for homogeneity of variance was conducted with

significance level set at $p < 0.05$. Or, again, the Mann-Whitney U test was used for pairwise differences in the whole data set as the non-parametric method.

When a single data set was used in several statistical comparisons a Bonferroni correction was applied. Non-parametric data were not transformed as it was consistently not possible to transform the data sets to a normal distribution. Other mathematical and statistical methods will be described in the appropriate chapters. Differences were considered significant at $p < 0.05$. Throughout the thesis error bars on bar charts are one sided when the data is normally distributed and deviation is symmetrical as with the use of a confidence interval. Error bars are two-sided when the interquartile range was used as the measure of deviation due to the violation of normality, such devaitions are not symmetrical.

Chapter 3.

Characterisation of manufactured silver nanoparticles

3.1 Introduction

When placing an NP into environmental matrices, synthetic or otherwise, several changes to the original material are expected to occur. These changes have been documented within the current literature even if not at relevant exposure or environmental concentrations. Measuring NP characteristics is treated in the same manner as any other colloidal dispersion. However when colloids are within the nanoscale (i.e. NPs and NMs) these parameters become increasingly difficult to measure. The most frequently studied physicochemical characteristics for NPs are the hydrodynamic diameter (HDD, a diameter of a colloid in an aqueous suspension), diameter (measured out of suspension), zeta-potential (ζ-potential), agglomeration, aggregation, degree of dispersity (e.g. monodispersity/ polydispersity) and for dissolvable particles, dissolution. HDD is the diameter of a colloid in a solvent or aqueous phase (Baalousha *et al.*, 2012a). Diameter is often measured via transmission electron microscopy, and measurements of over 100 individual/ aggregated/ agglomerated particle counts are considered appropriate in order to give a statistically satisfactory mean diameter in a particle distribution (Baalousha *et al.*, 2012). What you measure under TEM depends on the point of interest of the particles, i.e. individual measures would give a size distribution of a NPs core diameter, whereas agglomerate/ aggregate measures would give an idea of stability and size distribution of these NP clusters. ζ-Potential is a charge measured in volts (often millivolts (mV)) and is measured at the slipping plane of the Debye layer of a colloid/ NP in suspension (Hunter, 1981). The Debye layer is formed by one layer of ions absorbed to the surface of the particle and a second layer of ions attracted to the first layer or surface charge dictated by Coulombs law. The second layer is a diffuse layer and is mobile over the first layer, the slipping plane occurs between these layers which gives rise to a charge and this is where ζ-potential is derived. ζ-Potential is therefore defined as the difference in charge between the medium and the stationary layer of fluid attached to the colloid or NP, and is related to surface charge (Hunter, 1981). Agglomerates are defined by the BSI (2007) as a collection of loosely bound particles or aggregates or mixtures of the two. Therefore agglomeration is the active process to form these agglomerates. The forces causing agglomeration are weak such as physical entanglement (nanotubes or

fibres may do this most frequently) and van der Waals forces (i.e. electrostatic forces). Aggregates are defined by the BSI (2007) as clusters of particles comprising strongly bonded or fused particles. Thus aggregation is the active process forming aggregates. The forces holding an aggregate together are strong forces, for example covalent bonds, or those resulting from sintering or complex physical entanglement. Both agglomerates and aggregates can be homo- or hetero- agglomerates and aggregates. The *homo* prefix simply means that the agglomerate or aggregate is made of the same particle material (chemical substance). The *hetero* prefix means that the agglomerate or aggregate consists of various particles composed of different materials (chemical substances). Monodispersity is the state of a dispersion in which the particle size distribution, hydrodynamic or otherwise, is uniform. Polydispersity is the state of a dispersion in which the particle size distribution, hydrodynamic or otherwise, is not uniform and instead has a wider size distribution (Kurshid *et al.*, 2014 and Jillavenkatesa, Dapkunas and Lum, 2001).

There is a suite of characterisation instruments and techniques available, ranging from those which use inherent particle properties such as Brownian motion, or atomic mass, to those more qualitative imaging techniques. Some of the most popular methods are listed in Table 3.1:

Table 3.1 Popular methods used in the physicochemical characteristic determination of nanomaterials.

Method:	Measure:
Dynamic Light Scattering (DLS)	Hydrodynamic diameter
Flow field fractionation (FFF)	Hydrodynamic diameter
Inductively couple plasmon mass spectrometry (ICP-MS)	NM concentration
Ultraviolet/ visible light spectroscopy (UV/Vis)	Dispersity and dissolution
Transmission electron microscopy (TEM)	Size and hetero-/ homo- aggregation/ agglomeration
Energy dispersive x-ray (EDX)	Confirmation of chemical composition
Ultrafiltration/ centrifugation	Separates solid phase from dissolved phase for those particles with a propensity for dissolution i.e. transition metals such as silver

*References used that highlight physicochemical characteristic determination methods are von der Kammer *et al.*, 2012, Zook *et al.*, 2011 and Domingos *et al.*, 2009.

Although there have recently been advances in each, when toxicological, environmental or exposure relevant NP concentrations are within the low milligram to microgram per litre range many of these methods remain inappropriate (Baalousha *et al.*, 2012a, Baalousha *et al.*, 2012b, Fabrega *et al.*, 2011, Prathna *et al.*, 2011, Tiede *et al.*, 2008). Another shortcoming is the ability to monitor such NP fate during *in situ* exposures

either *in vivo* or *in vitro*, and this is particularly important since these measurements would reflect the real exposure conditions of the organism or cell.

In order to fully understand the environmental impact of NPs it is important to understand the fate and behaviour of these particles (i.e. any changes in their physicochemical characteristics) within relevant environmental matrices. How, and where, an NP is released will likely determine what ligands and organisms it will eventually come into contact with and ultimately their behaviour and fate during the NP life-cycle. The importance of fully understanding the life-cycle of an NP cannot be overstated. Some highlighted NP environmental inputs are: sewers; wastewater treatment plants (WWP) effluents; biosolids from WWP applied to agricultural lands or landfills; pesticides applied on agricultural fields or residential yards; accidental spills of materials or waste streams discharged during manufacturing; usage of consumer products (e.g. sun screen or cosmetics) which may then dissociate from the skin into the environment, such as sunscreen off the skin whilst swimming, and direct infiltration or runoff of excreta from humans or livestock of NPs taken up via the diet (Figure 1.1, Chapter 1). The main life-cycle and release scenarios of NPs in the environment are: incidental release (e.g., emission from vehicles) and release from industrial and commercial products, and/ or processes during production or intended use (e.g., using nanosilver soap; remediation of contaminated soils/groundwater; use on buildings façades). The varying processes and 'aging' (fate in the environment over time) the NPs are subject to will eventually dictate not only their toxicity but also their environmental persistence. There is still lack of knowledge regarding fate and behaviour of Ag NPs in environmentally relevant scenarios and concentrations. These knowledge limitations are due to an unavailability of appropriate equipment and techniques able to assess and differentiate NPs within such dynamic and complex environmental matrices. Highlighting the difficulties of such an endeavour is the fact these limitations still exist in spite of known requirement in the nano-field for some time (Johnston *et al.,* 2012, Levard *et al.,* 2012, Farre *et al.,* 2009, Wijnhoven *et al.,* 2009 and Handy *et al.,* 2008). For example DLS is reliant on Brownian motion and is only applicable in fairly simple homogeneous systems at particle concentrations typically exceeding 1 mg L^{-1}, this is likely orders of magnitude higher than those environmentally relevant (von der Kammer *et al.,* 2012).

The prediction of Ag NP behaviour within the environment can be based on 3 major factors, their likely fate after release, dissolution and basic ligand affinities dictated by

their surrounding environment (Levard *et al.*, 2012, Levard *et al.*, 2011 and Zhang *et al.*, 2009). For instance adsorption/ complexation are a heterogeneous process that consists of a combination of physical, chemical, and electrostatic interactions dictated by fate and environmental ligand affinities (Zhang *et al.*, 2009). Ag^{+} released from Ag NPs due to dissolution will likely form nano- and micro-complexes with sulphur and/ or chloride (N.B. it is also possible, although unlikely, that silver can form complexes with carbonate (CO_3^{2-}); Levard *et al.*, 2012) in natural environments and this will dictate what remains in the nano-form, what is bioavailable and what becomes part of the dissolved aqueous phase (Levard *et al.*, 2012). Many Ag NPs are termed as spherical but are usually polyhedrons (i.e. shapes which vertices fit evenly into a sphere) and thus have a multi-faceted surface (Figure 3.1). Due to this and their high reactivity dissolution is not always required for complexation with inorganic and organic ligands to occur, these have been previously reported for both Cl^{2-} and S^{-}. Here the number of facets and corners present at the NP surface dictates the availability for particle reactions (Levard *et al.*, 2012 and Levard *et al.*, 2011).

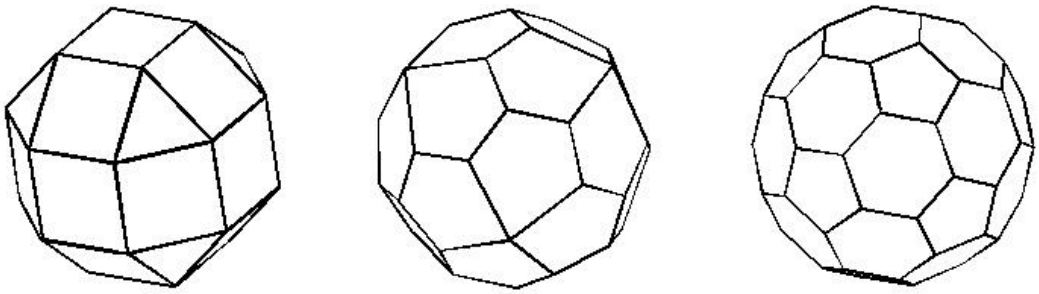

Figure 3.1 Varying types of spherical polyhedra which are common shapes for Ag NPs (image obtained from http://facweb.cs.depaul.edu/sgrais/mass_and_void.htm).

At room temperature the dissolution of silver to silver ions (Ag^{+}) is a thermodynamically favourable outcome (Levard *et al.*, 2012). Several studies have shown that in general reducing the size (usually based on diameter) of Ag NPs will tend to increase dissolution as there are higher surface areas and tensions (Allen *et al.*, 2010 and Carlson *et al.*, 2008).

Understanding NP transformations and behaviours under relevant exposure conditions, such as within environmental waters or environmentally relevant synthetic medium (i.e. Elendt M7), and after biological interaction, becomes important as varying processes such as agglomeration and/ or aggregation, complexation and dissolution may

dramatically change the eventual impact upon the environment and organism/ human health (Levard *et al.*, 2011 and Zhao and Wang 2010). Furthermore many of these parameters are closely related to physicochemical characteristics such as size and charge. Ultimately these transformations will affect the NPs fate, transport and toxic properties within the organism. These transformations have been shown to be particle, media, environment and organism dependent, thus changes in release scenarios can change NP behaviour (Zhao and Wang 2012, Croteau *et al.*, 2011, Prathna *et al.*, 2011, Zhao and Wang 2011b and Tolaymat *et al.*, 2010). By studying these properties in relation to toxicity or environmental impact it may be possible to derive certain NP physicochemical properties which are the main drivers of the seen response. Deriving these common themes or predictors of NP toxicity, will help to understand the key pathways of exposure and toxicity and, as such, will aid the development of appropriate regulatory and risk mitigation frameworks.

By focusing on relevant environmental physicochemical characteristics some advances are being made. Studies have previously noted that within freshwater systems organic matter and sulphides have a chemical affinity with silver and most likely dominate Ag speciation within this compartment. More recent research has confirmed this transformation in a study of Ag NPs within sewage sludge and the washing of varying nanotextiles (Lorenz *et al.*, 2012, Levard *et al.*, 2012, Levard *et al.*, 2011 and Liu, Pennell and Hurt, 2011). In seawater systems chloride silver complexes have been shown to predominate speciation and this Ag form is now generally accepted as being bioavailable (Levard *et al.*, 2012). However these findings were based on levels of Ag NP magnitudes higher than current predicted environmental concentrations (Levard *et al.*, 2012 and Zook *et al.*, 2011). That said, such data will still be useful to elucidate common behaviours and traits of NPs within these environmentally relevant matrices and how this may change their biological impact. By furthering the knowledge base in this area it may be possible to build appropriate, accurate and reliable data-based predictive models that can be used in risk mitigation strategies, risk assessment, wide level screening, regulation and the safe implementation of nanotechnologies.

3.2 Aims

This study aims to analyse the behaviour of 3 different Ag NPs within a highly complex synthetic medium and the changes in NP physicochemical properties in comparison to

pristine suspensions in Milli-Q water. When possible we aim to assess the differences in the NPs behaviour between particles, if any, and relate these back to their 'as manufactured'/ pristine characteristics, and assess if those characteristics can act as predictors of their behaviour in synthetic environmental medium. The data will be used, where possible, in ensuing chapters to derive any common themes or correlations between these behaviours and physicochemical characteristics and the chapters' respective endpoints (i.e. toxicity, uptake and elimination) within this thesis.

3.3 Methods

3.3.1 Nanoparticles, nanoparticle synthesis and stocks

As reported in Chapter 1 and the Appendix Text 2.1 the NPs are spherical/ polyhedra PVP-Ag NPs, PEG-Ag NPs and Cit-Ag NPs with a nominal diameter measured by TEM of ~10 nm (measured at University of Birmingham). All coatings are used extensively in nanotechnology products for varying purposes, and this highlights the importance for testing their fate, behaviour and toxicological impact within the environment. Ultimately, all coatings are used to create a more robust (i.e. an NP that does not degrade rapidly) and stable NP suspension.

3.3.2 Characterisation

Characterisation was performed in OECD Elendt aM7 medium suspended Ag NPs. For medium suspended particles characteristics were taken at 1, 24, 48, 96, and 168 hours after suspension, to reflect laboratory exposure scenarios, medium changes and to derive particle behaviour in the medium over extended periods.

Mean HDD and mean ζ-potential in aM7 medium were analysed using dynamic light scattering (DLS) (Zetasizer Nano, Malvern Instruments, Malvern UK) with a ~pH of 8 at 20 °C. At least five consecutive measurements per replicate were recorded to calculate z-average HDD and ζ-potential, three replicates were measured at each time-point. Each replicate consisted of a 10 mL medium-NP suspension at 4 mg L^{-1} Ag contained in a 20 mL borosilicate glass vial. Medium-NP suspensions were removed using a syringe and placed into a disposable capillary zeta-cell (Malvern Instruments, UK).

Dissolution was determined by centrifugal ultrafiltration method (Khan *et al.*, 2015, Croteau *et al.*, 2014a, Hadioui, Leclerc and Wilkinson 2013 and Misra *et al.*, 2012) using an Ag NP dispersion of 1 mg L^{-1} in the medium. This concentration was higher than those used within the exposure studies. Previously, Croteau *et al.* (2014a) tested the dissolution of citrate-Ag NPs at varying starting concentrations (10, 100, 1000 µg L^{-1}) and found reduced recovery (10-fold decline) of the total Ag at the lower concentrations after 24 h which was attributed to sorption of Ag forms (dissolved and particulate) to the container walls. No such losses were reported when using the higher starting concentration. Croteau *et al.*, (2014a) also validated the ultrafiltration method in synthetic freshwater (comparable to the freshwater medium used in the present study) with samples of dissolved Ag (added as $AgNO_3$). Recovery following centrifugation was 93% (measured at time 0, 24 and 72 h, *n*=3). In the present study, dissolution experiments were performed at 20 °C and sampled at 24, 48, 72 and 168 hours. At each time point, samples were removed and placed in centrifugal ultrafiltration tubes (3 kDa membrane, Millipore Amicon Ultra-4 3K, Billerica, MA, USA) and centrifuged at 4190 g (30 min, HERMLE Z200A centrifuge, HERMLE Labortechnik GmBH, Germay) to separate the dissolved and NP forms of silver based on size and molecular weight. Dissolved and particulate silver fractions were then measured using inductively coupled plasma mass spectrometry (ICP-MS; 7500ce ICP-MS, Agilent Technologies, Santa Clara, CA) in triplicate. A rhodium internal standard was used for quality control. Release of dissolved ions was expressed as a percentage of the total retrievable silver.

TEM images and energy dispersive x-ray spectra were acquired at Leeds University by Judit Kalman. Ten millilitre particle suspensions were made in aM7 medium and left for 48 hours at 20 °C under 16:8 hour light:dark cycle in borosilicate glass vials. The TEM grids were prepared at Heriot-Watt University (by Kai B. Paul) by dropping 20 µL of a 4 mg L^{-1} particle-aM7 medium suspension onto a 300 µm copper TEM grid (Agar Scientific) with the excess liquid absorbed onto an absorbent tissue. These grids were then allowed to dry for 24 hours dry at room temperature (~20 ºC). Additional TEM images were acquired by similar processes conducted by Laura-Jayne Ellis at Birmingham University.

The pilot study of hyper-spectral imaging (CytoViva, USA) analysis was conducted at Clemson University (SC, USA) at the Electron Microscopy Facility within the Department of Biological Science. Help analysing and obtaining the images was given by Rhonda Reigers Powell. Particles were taken directly from transported stocks

suspended in Milli-Q water. These suspensions were dropped (20 μL) onto a borosilicate glass microscopy slide and left to dry at room temperature (~24 ºC) for ~4 hours before the images were acquired at 40x magnification. Post analysis a UV/ vis spectrum was achieved by creating bins at wavelengths every 10 nm between ~450-~790 absorbance. Each measured peak was presented as percentage of the total distribution measured.

3.3.3 Statistical Analysis

All data were parametric as established by Shapiro-Wilks and Kolmogorov-Smirnov tests for data sets under and over ~50 respectively ($p > 0.05$). Within this Chapter 3 replicates for each Ag NP were used. A repeated measures experimental design for sampling at each time point (i.e. the samples for each time point were taken from the same replicates) was used. Therefore, a repeated measures ANOVA test was used to assess overall differences, followed by least significant difference (LSD) pairwise post-hoc comparisons with a Bonferroni correction to establish where the significant differences between the endpoint occurred. Tests were conducted in SPSS v20 (Armonk, NY: IBM Corp). All other statistical methods have previously been stated in Chapter 2.

3.4 Results

Table 3.2 shows the previously reported pristine particle physicochemical properties of the Ag NPs studied within this thesis which were manufactured at Birmingham University by Mila Tejamaya (Tejamaya *et al*., 2012). Here it can be seen all Ag NP core sizes are ~10-11 nm with hydrodynamic sizes in the 20-30 nm range. All ζ-potentials were measured at Heriot-Watt University at a concentration of 4 mg L^{-1} to mimic the conditions previously used to obtain the pristine Ag NPs ζ-potentials. ζ-potentials were all below -20 but above -40 mV.

Table 3.2 Mean Physicochemical characteristics of pristine (as manufactured) Ag NPs in Milli-Q water adapted from Tejemaya *et al.* (2012) with the addition of ζ -potential obtained at Heriot-Watt University (Kai B. Paul) (*n* = 3).

Particle	Birmingham University TEM (nm)	Birmingham University HDD (nm)	Heriot-Watt University ζ -potential (mV)
PVP-Ag NP	11.5 ± 3.3	22.0 ± 1.0	- 31.6 ± 2.5
PEG-Ag NP	10.3 ± 3.2	22.0 ± 1.0	- 21.0 ± 0.5
Cit-Ag NP	10.8 ± 3.3	28.3 ± 0.8	- 31.5 ± 5.4

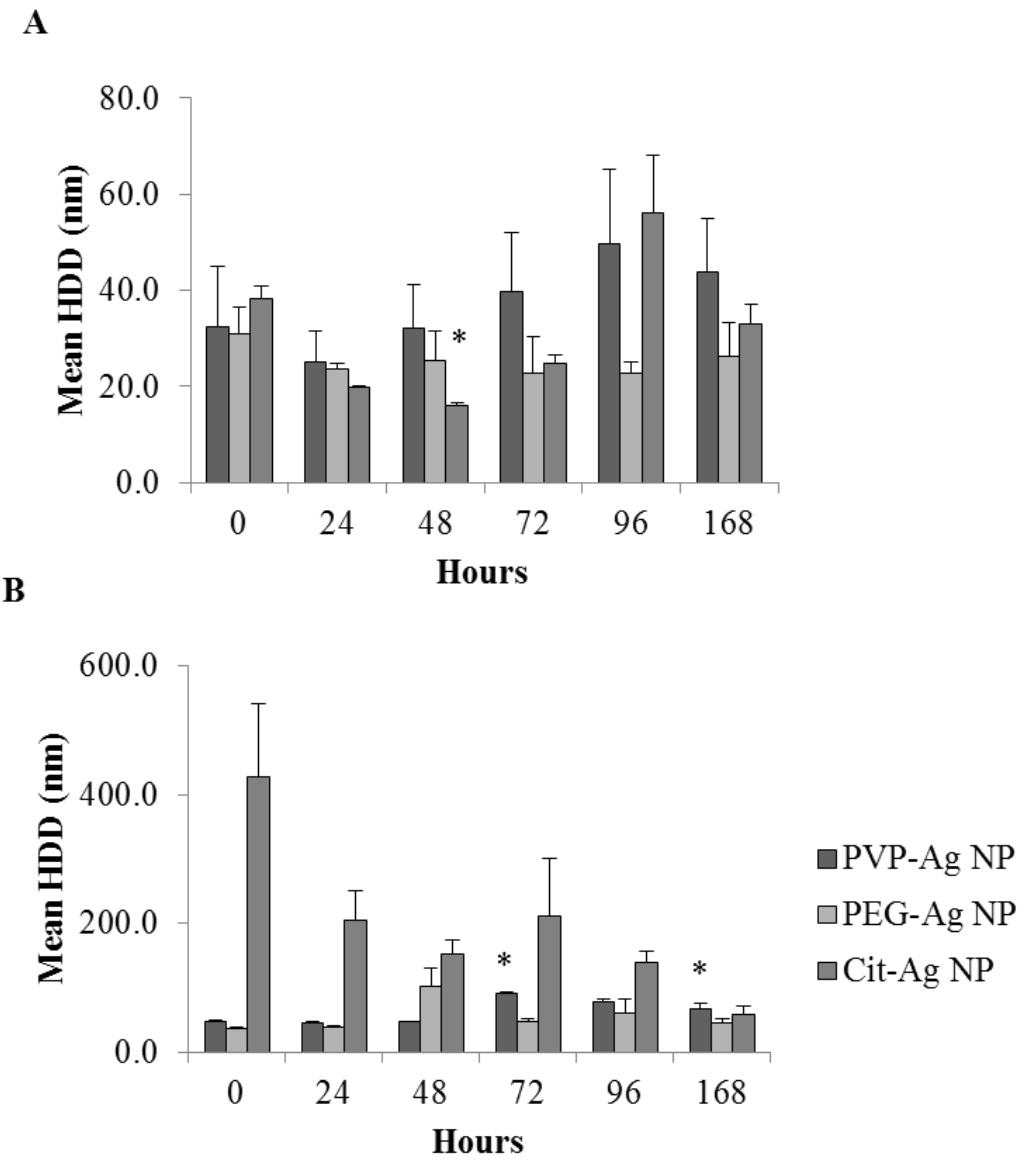

Figure 3.2 Mean hydrodynamic diameter (nm) (*n* = 3) as obtained by DLS at 0, 24, 48, 72, 96 and 168 hours in Milli-Q water (A) and aM7 medium (B). Error bars are 95% confidence intervals (95% CI). * denotes significant difference from 24 hours at $p < 0.05$.

Figure 3.2 shows the mean HDD of each Ag NP suspended in either aM7 medium or Milli-Q water. The mean HDD of PVP-Ag NPs exposed to aM7 medium differed significantly over time (37.7-92.3 nm; F = 58.88, d.f. = 17, $p < 0.05$; Figure 3.2 B) however these differences were only found at 72 (92.3 ± 0.5 nm) and 168 (68.5 ± 6.1 nm) hours in comparison to 24 hours (44.8 ± 1.8 nm) where they were significantly higher than the 24 hour mean HDD (Figure 3.2 B). Measurements taken at 96 hours (37.7 ± 3.6 nm) showed no significant difference in HDD when compared to all time points in a LSD pairwise comparison with Bonferroni correction ($p > 0.05$; Figure 3.2 B). However, no consistent increases or decreases in HDD were found over time for PVP-Ag NPs. Although there was an overall significant difference between HDD over time when PVP-Ag NPs were suspended in Milli-Q water (25.1-49.7 nm; F = 7.007, d.f. = 17, $p < 0.05$) there was no pairwise significance after LSD post-hoc testing with Bonferroni correction ($p > 0.05$). Within aM7 medium PEG-Ag NPs HDD significantly changed over time when taken as an overall (37.9-101.5 nm; F = 11.885, d.f. = 17, $p < 0.05$), however LSD post-hoc pairwise comparisons with Bonferroni correction showed no significant differences ($p > 0.05$) between each time point. In Milli-Q water PEG-Ag NPs HDD did not significantly change over time (22.8-31.1 nm; F = 6.765, d.f. = 17, $p > 0.05$). Cit-Ag NPs suspended in aM7 significantly changed over time with an apparent continual decrease in HDD (59.6-427.5 nm; F=13.28, d.f. = 17, $p < 0.05$), again after LSD post-hoc pairwise comparisons with Bonferroni correction significance could not be determined between isolated time points. In Milli-Q water Cit-Ag NPs also had significant differences in HDD when analysed globally, this time with no obvious pattern, (16.0-56.2 nm; F = 56.492, d.f. = 17, $p < 0.05$), after LSD post-hoc pairwise comparisons with Bonferroni correction only 48 hours when compared to 0 hours had a significantly smaller HDD (16 ± 6 and 38.3 ± 2.7, respectively; $p < 0.05$), all other time points during the exposure period did not significantly differ ($p > 0.05$) and the 48 hour measurements could be an anomaly.

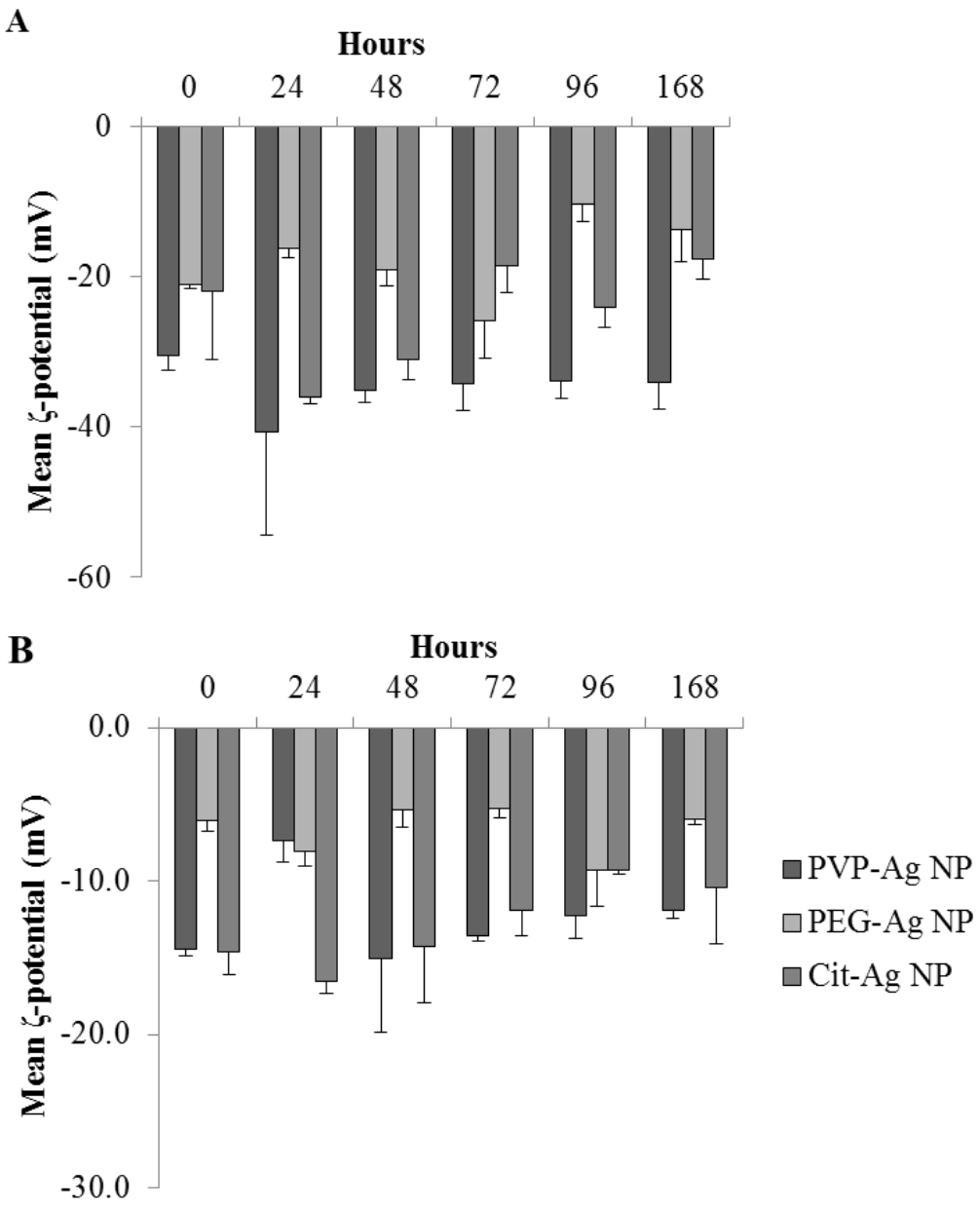

Figure 3.3 Mean ζ-potential (mV) (n = 3) as obtained by DLS at 0, 24, 48, 72, 96 and 168 hours in Milli-Q water (A) and aM7 medium (B). Error bars are 95% CI.

PVP-Ag NP, PEG Ag NP and Cit-Ag NP ζ-potentials in Milli-Q water and aM7 medium over time did not significantly vary. In Milli-Q water Ag NP ζ-potentials ranged between -30.5 to -40.6, -10.3 to -25.8 and -17.6 to -36.0, for PVP-Ag NP, PEG Ag NP and Cit-Ag NP respectively (F = 4.464, d.f. = 17, p > 0.05 for PVP-Ag NPs; F = 16.056, d.f. = 17, p > 0.05 for PEG-Ag NPs in Milli-Q water; F = 28.866, d.f. = 17, p > 0.05 for Cit-Ag NPs in Milli-Q water; Figure 3.3). In aM7 medium Ag NP ζ-potentials was lower than the Ag NP ζ-potential in Milli-Q water and ranged between -7.4 to -15.1, -5.3 to -9.3 and -9.3 to -16.5 mV for PVP-Ag NP, PEG Ag NP and Cit-Ag NP

respectively (F = 12.31, d.f. = 17, p > 0.05 for PVP-Ag NPs in aM7 medium; F = 16.056, d.f. = 17, p > 0.05 for PEG-Ag NPs in aM7 medium; F = 14.918, d.f. = 17, p > 0.05 for Cit-Ag NPs in aM7 medium; Figure 3.3).

As there were generally no consistent significant changes over time up to 96 hours in most pairwise comparisons (e.g. only 2 within the PVP-Ag NP group 72 and 168 hours which when viewed overall showed no pattern for aggregation/ agglomeration or dissociation) geometric means for HDD and ζ-potential in Milli-Q water and aM7 were taken using time points up to 96 hours (Table 3.3). The geometric means were used to assess any differences between the Ag NPs behaviours in Milli-Q water and aM7 medium. The geometric mean HDD and ζ-potential of the 3 Ag NPs in aM7 medium will be used to assess if changes in NP characteristics may be used to derive common themes in toxicity or experimental end-points in later chapters, should any occur. Furthermore this reflects all testing conditions as no test exceeded 96 hours without medium change.

When the Ag NPs were suspended in aM7 *Daphnia magna* medium at 20 ºC with a 16:8 hour light:dark cycle physicochemical characteristics changed, with increases in mean HDD and decreases in mean ζ-potetial, in comparison with those suspended in Milli-Q water at 20 ºC with a 16:8 hour light:dark cycle (Figures 3.2 and 3.3, respectively).

Comparing HDD between aM7 medium suspended particles and Milli-Q suspended particles incubated in the same manner (i.e. at 20 ºC with a 16:8 hour light:dark cycle) Ag NPs were all significantly larger in aM7 medium (Table 3.3; F = 12.505, d.f. = 29, p = 0.001 PVP-Ag NPs; F = 21.09, d.f. = 29, p < 0.001 PEG-Ag NPs; and F = 21.09, d.f. = 29, p < 0.001, Cit-Ag NPs, respectively). ζ-Potential measurements between Milli-Q water and aM7 medium suspended Ag NPs also significantly differed for each particle, and were all significantly lower in aM7 medium (Table 3.3; F = 93.227, d.f. = 29, p < 0.001; F = 127.967, d.f. = 29, p < 0.001, F = 52.3, d.f. = 29, p < 0.001, for PVP-Ag NPs, PEG-Ag NPs and Cit-Ag NPs, respectively). Ag NPs in Milli-Q water at 20 ºC exposed to a 16:8 hour light:dark cycle only one physicochemical characteristic between particles (not medium) was found to be significantly different (F = 6.220, d.f. = 44, p < 0.01) via Tukey's HSD post-hoc test (p < 0.01), this was the significantly lower ζ-potential found for PVP-Ag NPs (-35.2 ± 3.5 mV) in comparison to both other particles (PEG-Ag NPs -19.5 ± 4.2 mV and Cit-Ag NPs -25.1 ± 2.7 mV; Table 3.3). No significance was found between Ag NP size within Milli-Q water (25.2-35.8 nm; F =

2.800, d.f. = 44, $p > 0.05$). In aM7 medium size significantly differed between Ag NPs (56.2-249.2 nm; $F = 31.824$, d.f. = 44, $p < 0.001$; Table 3.3). Tamhane post-hoc analysis showed that Cit-Ag NPs (249.2 ± 70.5nm) had a significantly larger HDD than both PVP-Ag NPs (56.2 ± 9.5 nm) and PEG-Ag NPs (56.4 ± 17 nm) ($p < 0.001$; Table 3.3). ζ-Potential also significantly differed between particles within this medium (-6.2 to -13.6 mV; $F = 27.074$, d.f. = 44, $p < 0.001$; Table 3.3). However ζ-potential did not correlate with the difference in size seen nor the difference between particles in Mill-Q water, as here via Tamhane's post-hoc analysis only PEG-Ag NPs were found to have a significantly lower ζ-potential (-6.2 ± 0.8; $p < 0.001$) than both PVP-Ag NPs (-12.5 ± 2.0 mV) and Cit-Ag NPs (-13.6 ± 1.5 mV), but HDD between PEG-Ag NPs and PVP-Ag NPs did not differ significantly (Table 3.3).

Table 3.3 Physicochemical characteristics of Ag NPs in aM7 medium and Milli-Q water physicochemical characteristics. Values are ± 95% confidence interval (CI). Values are mean HDD (nm) and ζ -potential (mV) over 96 hours ($n = 12$). Dissolution values were obtained from collective means over 72 hours ($n = 9$). † Dissolution for PVP-Ag NP in aM7 was derived from the mean over 48 hours ($n = 6$) due to the significance seen between 24 and 72 hours. †† dissolution values obtained from manufacturer. *, **, *** denotes significant difference of the same particle between dispersion water (Milli-Q) and aM7 medium * $p < 0.05$ ** $p < 0.01$ *** $p < 0.001$. ‡, ‡‡, ‡‡‡ denotes significant differences between particles physicochemical characteristics within the same dispersion water (Milli-Q) or aM7 medium ‡ $p < 0.05$ ‡‡ $p < 0.01$ ‡‡‡ $p < 0.001$.

Particle	Medium	Dissolution (%)	Mean HDD (nm)	Mean ζ -potential (mV)
PVP-Ag NP	Milli-Q	<2%††	35.8 ± 7.4	-35.2 ± 3.5‡
PEG-Ag NP	Milli-Q	<2%††	25.2 ± 2.2	-19.5 ± 2.7
Cit-Ag NP	Milli-Q	<2%††	31.7 ± 9.4	-25.1 ± 4.2
PVP-Ag NP	aM7	16.1 ± 1.9†‡‡	56.2 ± 9.5***	-12.5 ± 2.0***
PEG-Ag NP	aM7	28.9 ± 1.7‡‡	56.4 ± 17.0***	-6.2 ± 0.8***‡‡‡
Cit-Ag NP	aM7	21.5 ± 0.8‡‡	249.2 ± 70.5***‡‡‡	-13.6 ± 1.5***

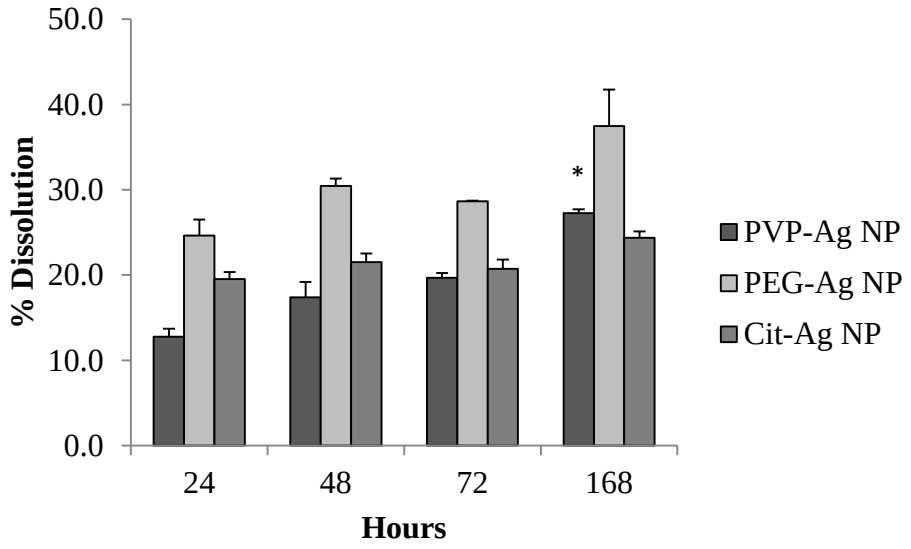

Figure 3.4 Total percentage of dissolution of PVP-Ag NPs, PEG-Ag NPs and Cit-Ag NPs at 24, 48, 72 and 168 hours from an aM7 medium particle suspension (n = 3). Values are expressed as a percentage of total retrieved silver at the end of the exposure. Error bars are 95% CI. *denotes significance from 24 hours within particles.

During dissolution studies in aM7 medium PEG-Ag NPs and Cit-Ag NPs varied significantly over time and ranged between 24.6-37.5% and 19.5-24.4%, respectively (F = 15.036, d.f. = 11, $p < 0.05$ and F = 12.781, d.f. = 11, $p < 0.05$, respectively; Figure 3.4). However after LSD post-hoc pairwise comparisons with Bonferroni correction for Cit-Ag NPs this significance was only seen as a significant increase when comparing 24 hours (24.6 ± 1.9%) to 168 hours (37.5 ± 4.3%; Figure 3.4, $p < 0.05$). No significance was found in the LSD post-hoc pairwise comparisons with Bonferroni correction for PEG-Ag NPs ($p > 0.05$). Again, as few tests throughout the thesis exceeded 72 hours without a particle/ medium change the geometric mean between 24 hours to 72 hours will be used and can be seen in (Table 3.3), these data again will be used to derive differences or commonalities in toxicity of the Ag NPs. PVP-Ag NPs dissolution significantly increased over time and this was reflected in the LSD post-hoc pairwise comparisons with Bonferroni correction (12.8-27.3%; F = 168.993, d.f. 11, $p < 0.05$ and $p < 0.05$, respectively; Figure 3.4). However there was no significant increase found between 24 and 48 hours (12.8 ± 0.9 and 17.4 ± 1.8% respectively), therefore in tests that do not extend past 48 hours the collective mean of 24 and 48 hours will be used (Table 3.3 and Figure 3.4). Seventy-two hour dissolution (19.7 ± 0.6%) was significantly higher from 24 hours (12.8 ± 0.9%) and significantly lower from 168 hours (27.3 ± 0.5%) but no significance could be found between 72 hours and 48 hours (19.7

± 0.6% vs. 17.4 ± 0.5%, respectively) indicative of the gradual increase in ionic silver over each successive 24 hours (Figure 3.4). Due to the significant differences in dissolution of the PVP-Ag NPs over time, any tests exceeding 48 hours (i.e. chronic toxicity tests which had medium changes every 72 hours) will consider solubility differences in time by comparing data from ensuing tests with the appropriate time-point for PVP-Ag NP dissolution, i.e. a 48 hour bioassay result will be compared to 48 hour PVP-Ag NP dissolution measures, however a 72 hour bioassay will be measured with 72 hour dissolution measurements. Dissolution was significantly different between particles within aM7 medium (F = 54.644, d.f. 26, $p < 0.001$; Table 3.3). Tamhane's post-hoc test showed each particle was significantly different from the other ($p < 0.01$) with the rank order from highest to lowest dissolution seen as PEG-Ag NP>Cit-Ag NPs>PVP-Ag NPs (28.9 ± 1.7, 16.1 ± 1.9 and 21.5 ± 0.8, respectively; Table 3.3).

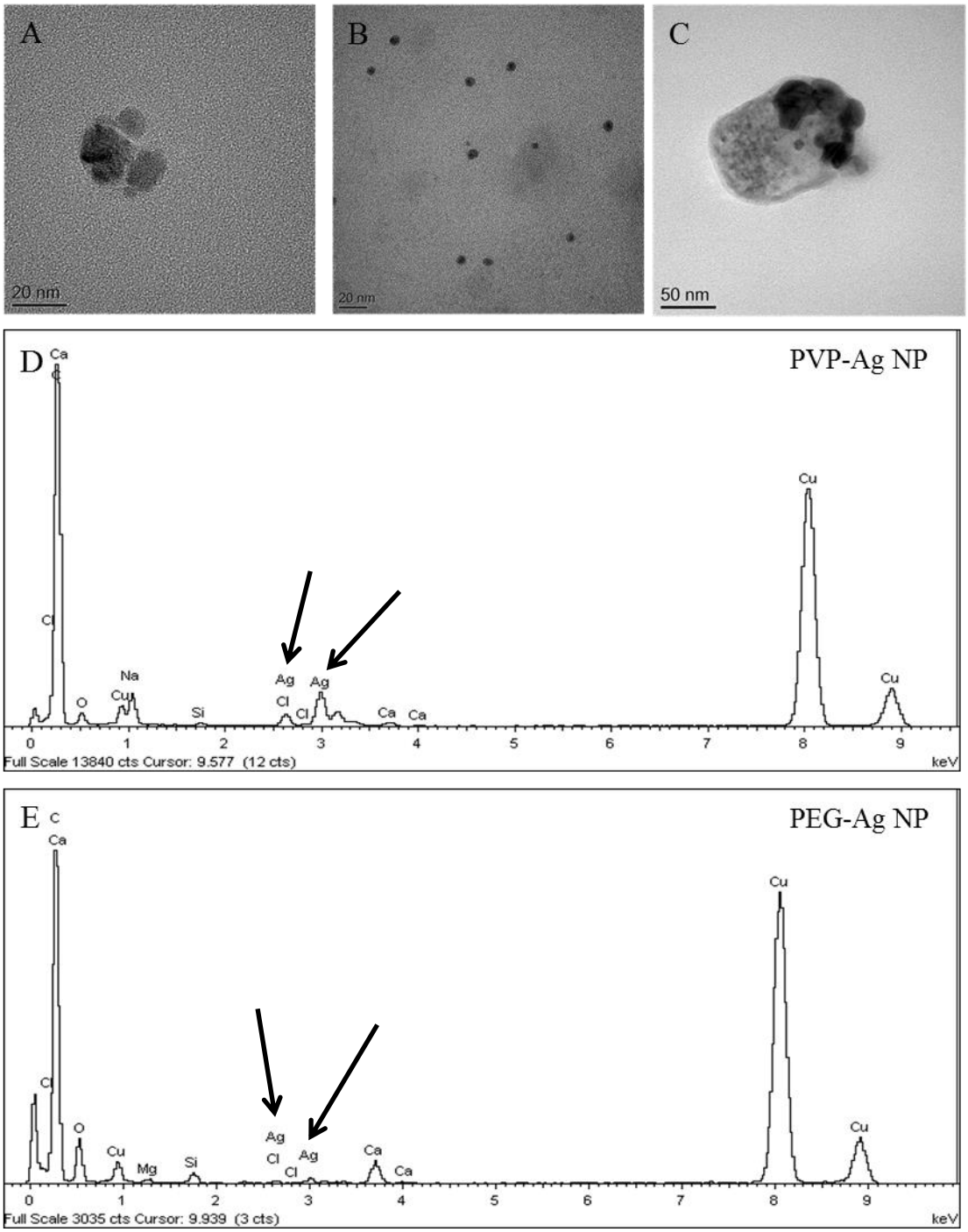

Figure 3.5 TEM images obtained from Leeds University by Judit Kalman after 48 hour exposure to aM7 medium; from left to right Cit-Ag NP (A), PEG-AG NP (B) and PVP-Ag NP (C). PVP-Ag NPs and PEG-Ag NPs were confirmed as silver via energy dispersive x-ray (EDX) D, and E of the figure respectively, arrows point to Ag peaks. No EDX confirmation was possible for Cit-Ag NPs possibly due to interference from medium ligands that had complexed to this Ag NP.

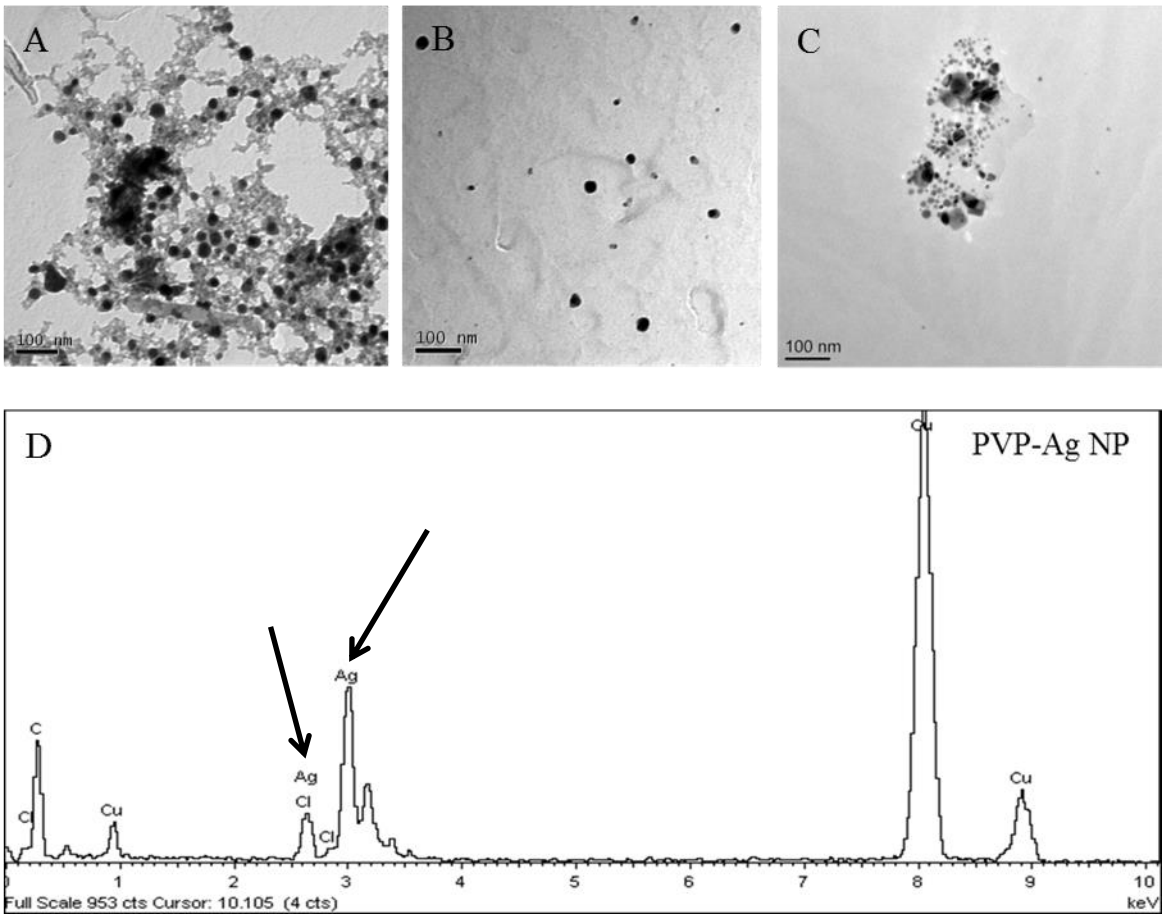

Figure 3.6 TEM images of Cit-Ag NP (A), PEG-Ag NP (B), and PVP-Ag NP (C) at 4 mg L^{-1} at 1 hour post exposure in aM7 medium obtained from Birmingham University and Leeds University by Laura-Jane Ellis and Rachel Wallace, respectively. Only PVP-Ag NPs were confirmed as being silver via energy dispersive x-ray (D), arrows point to Ag peaks. However the other particles were not attempted to be confirmed.

For the TEM images those peaks from EDX analysis which are not associated with Ag come from medium ligand salts (Ca^{2+}) or the composition of the TEM grid (Cu^{2+}).

In both TEM images of PVP-Ag NPs they appear bound to medium ligands which could be indicative of hetero-agglomeration/ aggregation (Figure 3.5 and 3.6), the same can be seen for Cit-Ag NPs (Figure 3.6) however there are far more ligand bridges connecting this particle. The complexation with other ligands could also cause the drop in ζ-potential seen. In all instances PEG-Ag NPs appeared as discrete particles and this could mean that any increase in HDD may be due to homo-agglomeration/ aggregation or the properties of the medium creating a larger hydrated diameter than pure water on the NP surface (i.e. larger Debye layer caused by higher ionic strength in the medium).

Interestingly these properties and patterns can also be seen after hyper-spectral imagery despite suspension of the NP in Milli-Q water (Figures 3.7, 3.10 and 3.12 for PVP-Ag NPs, PEG-Ag NPs and Cit-Ag NPs respectively). Again, PVP-Ag NPs (Figure 3.7) seem moderately complexed, PEG-Ag NPs (Figure 3.10) seem to remain discrete and Cit-Ag NPs (Figure 3.12) appear to complex to the highest degree. Although EDX was not obtained for all TEM images, the hyperspectral imagery supported the presence of silver in all instances with UV/ Vis absorbance wavelengths between 400-500 nm.

Table 3.4 UV/ Vis Spectra of three Ag NPs from traditional methods (i.e. UV/ vis spectrophotometer; abosorbance λ) at 0 and 24 hours in aM7 medium at 0 and 24 hours (n = 3).

	Milli-Q Suspension (absorbance λ)	
Particle Type	1 hour	24 hours
PVP-Ag NP	400	400
PEG-Ag NP	400	404
Cit-Ag NP	398	400

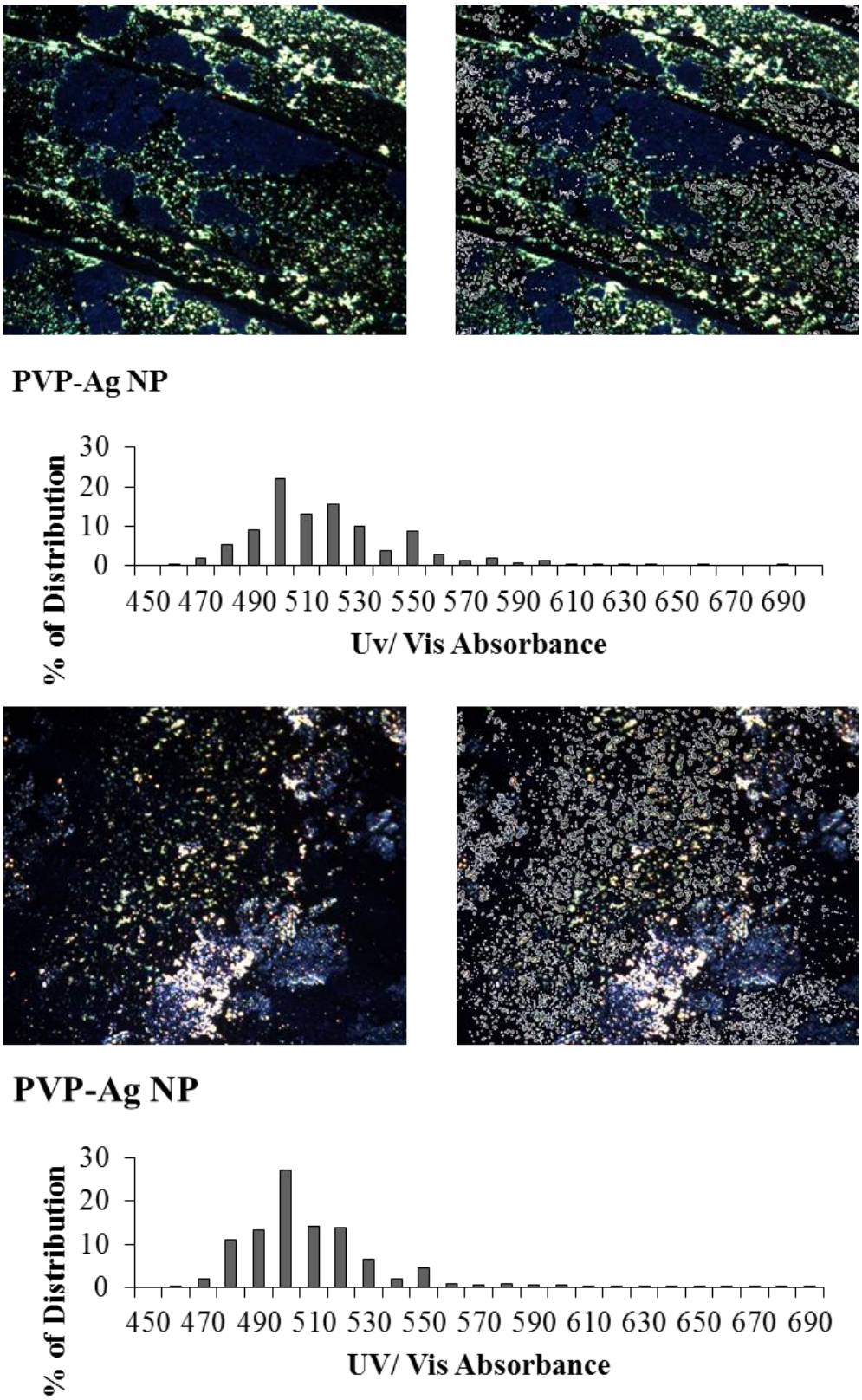

Figure 3.7 Two areas of PVP-Ag NPs from the prepared sample visualised on hyper-spectral images at 40x magnification dried from a Milli-Q water suspension. The left of each image shows original image before "binning wavelengths" to establish a UV/ Vis wavelength distribution. Top right shows the image after "binning" from which the wavelength distribution was derived (bottom of each image) (n = 1).

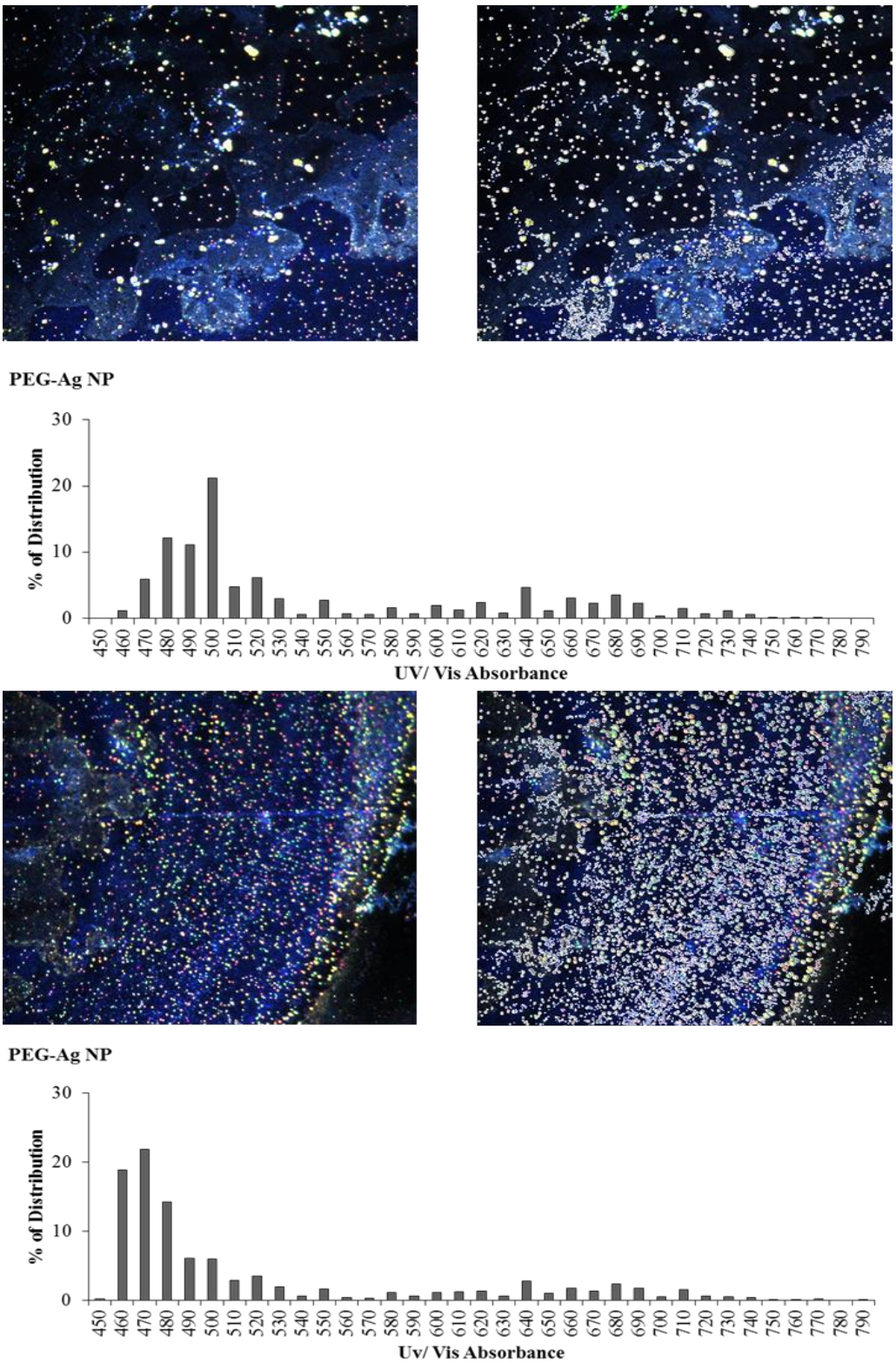

Figure 3.8 Two areas of Cit-Ag NP from the prepared sample visualised on hyper-spectral images at 40x magnification dried from a Milli-Q water suspension. The left of each image shows original image before "binning wavelengths" to establish a UV/ Vis wavelength distribution. Top right shows the image after "binning" from which the wavelength distribution was derived (bottom of each image) (n = 1).

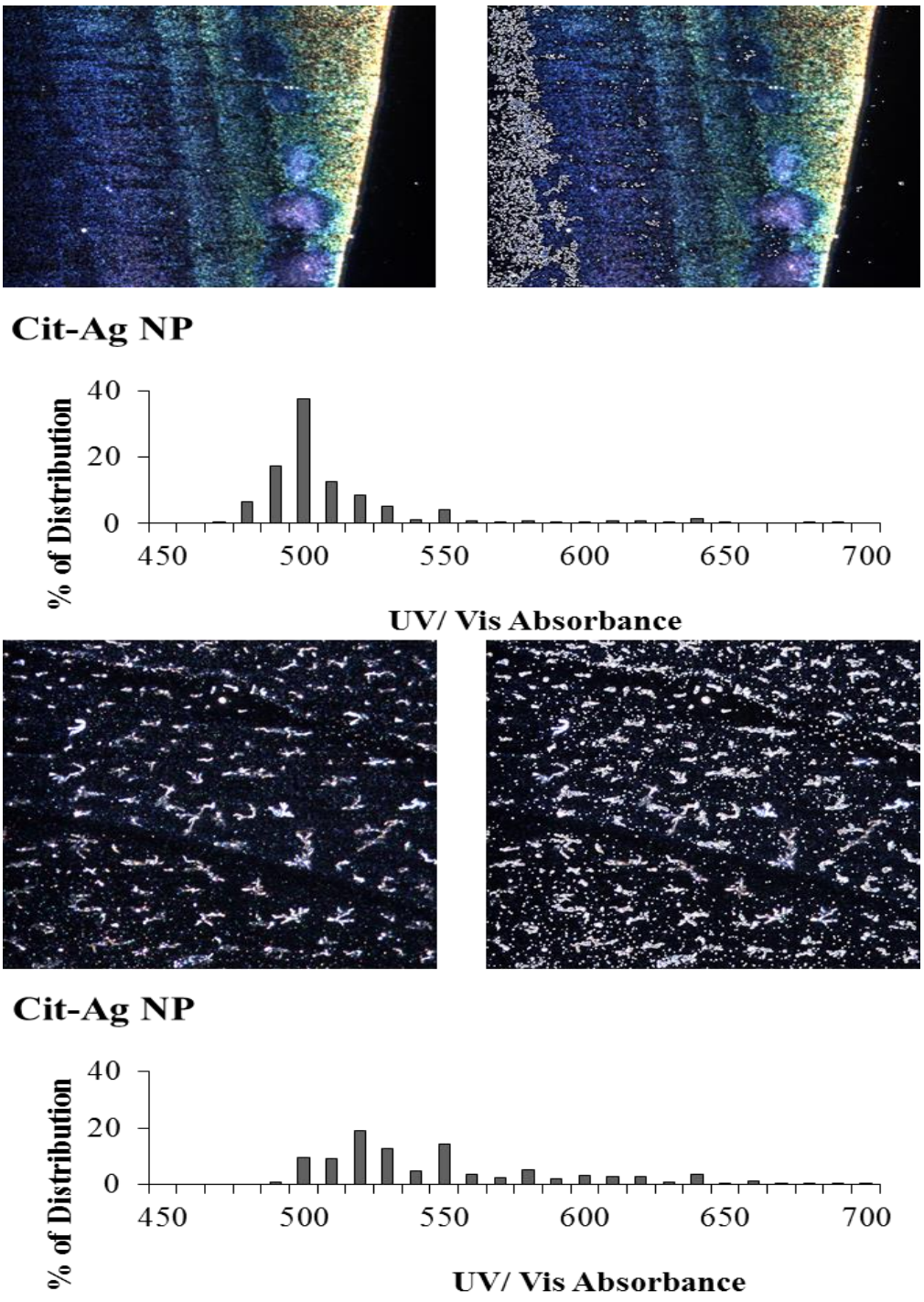

Figure 3.9. Two areas of Cit-Ag NP from the prepared sample visualised on hyper-spectral images at 40x magnification dried from a Milli-Q water suspension. The left of each image shows original image before "binning wavelengths" to establish a UV/ Vis wavelength distribution. Top right shows the image after "binning" from which the wavelength distribution was derived (bottom of each image) (n = 1). The top image also shows a shift from yellow to blue indicative of more agglomaertion of the particles at the edge of the sample.

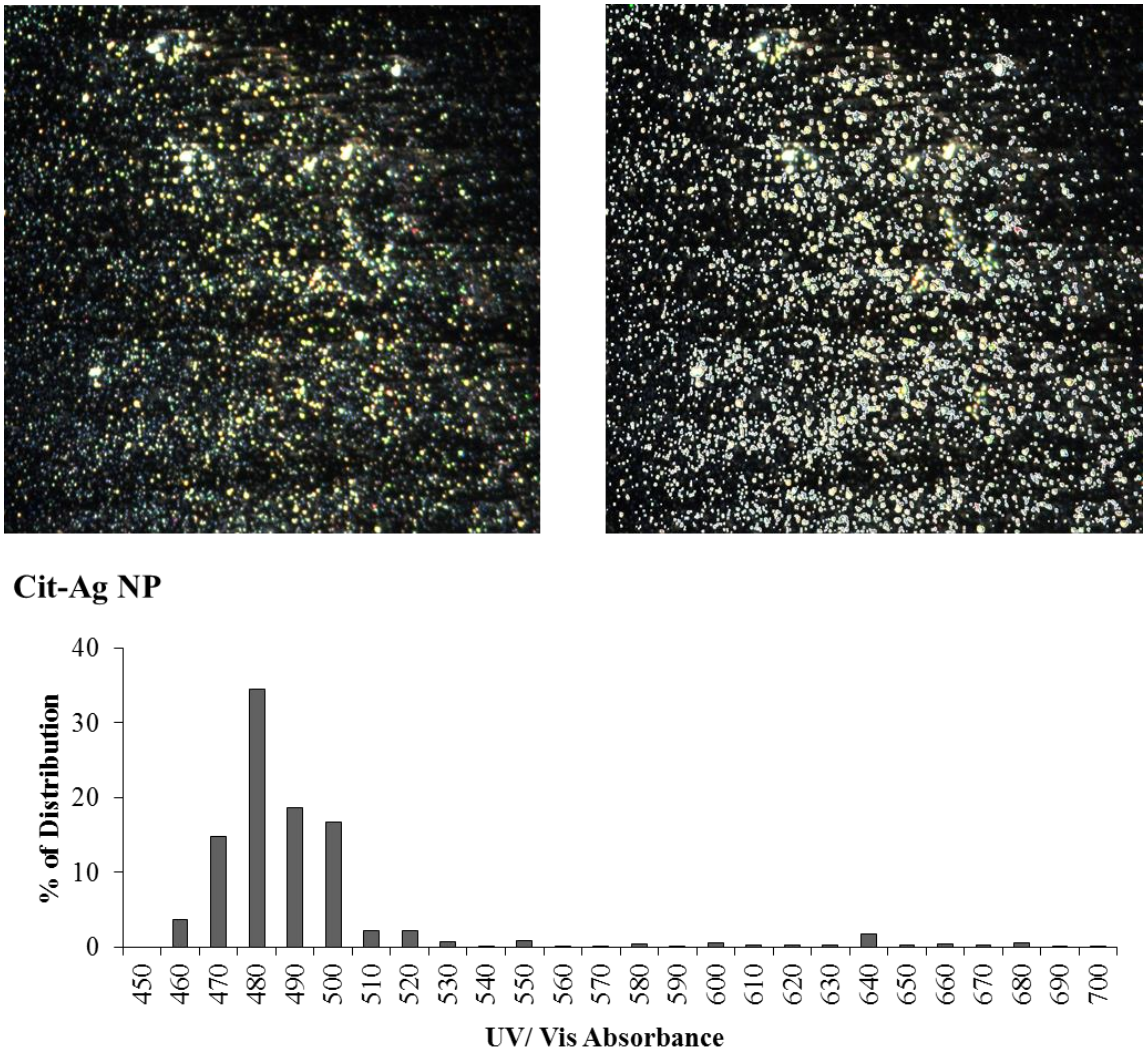

Figure 3.10. Final area from Cit-Ag NPs prepared sample analysed by hyper-spectral imaging, at 40x magnification dried from a Milli-Q water suspension. Top left shows original image before "binning wavelengths" to establish a UV/ Vis wavelength ditribution. Top right shows the image after "binning" from which the wavelength distribution was derived (bottom row) (n = 1).

It is well known that Ag NPs exhibit an UV/ Vis absorbance wavelength of ~400nm (Zook *et al.*, 2011). In Table 3.4 the mean (n = 3) absorbance is displayed for each Ag NP tested via UV/ Vis spectrophotometry. These values are in corroboration with literature reports (Zook *et al.*, 2011). The images and histograms thereafter, Figures 3.7 to 3.10, are UV/ vis absorbance taken from an emerging imagery technique, hyper-spectral imaging. Unlike traditional UV/ Vis spectroscopy where usually only one wavelength is used, or 2-wavelengths some distance apart, these images can be used to "bin" specific spectra within a 1 nm range and no masking of subtle differences in

spectra between particles, or the same particle in differing media, occurs. PVP-Ag NPs have 1 discrete spectral peak at 500nm (Figure 3.7). PEG-Ag NPs has discrete spectral peaks at 470 and 500nm (Figure 3.8). Cit-Ag NPs have 3 discrete peaks, or "bins" of absorbance with the peaks occurring at 500, 520 and 480 nm (Figures 3.9 and 3.10). These wavelengths during traditional measurements would likely fall under one gross peak and shifts in wavelengths could be missed between particles and medium, as seen in Table 3.4.

3.5 Discussion

The importance of physicochemical characteristics and NP behaviour has already been highlighted within Chapter 1. Furthermore many studies suggest that these characteristic may be implicated in the eventual toxicity of the NP, ranging from dissolution rates to the core material and size of the NP or its agglomerates/ aggregates (Newton *et al.*, 2013 and Zhao and Wang 2011b). Here the physicochemical characteristics of 3 differently coated Ag NPs that of polyvinylpyrolidone (PVP), polyethylene glycol (PEG) and citrate (Cit) coated Ag NPs within differing suspensions and suspension time, were studied. Within this study the core size of the NPs was similar, as well as the core material (silver), which enabled the examination of the effects of particle coating on the Ag NPs eventual physicochemical characteristics and behaviour in aM7 medium and pure water (as Milli-Q water). In later chapters results from the assessment of how these characteristics are, if at all, implicated in the eventual toxicological outcomes of the Ag NPs within the aquatic environment particularly *Daphnia magna*, will be presented. As aforementioned this is key to the sustainable application of nanotechnologies as this allows manipulations at the nanoscale to ensure product efficacy but avoid unwanted environmental impacts.

The size of the core and the HDD of these nanoparticles, "as manufactured", have been previously published: these are 10-11 nm and 22-30 nm, respectively with guidelines provided on dissolution in Milli-Q water (~2%) by the manufacturer (Table 3.1 and 3.2). However ζ-potentials were not described or reported. These were therefore firstly obtained for these particles as manufactured. However these measurements were taken on NPs that were held in Milli-Q water in the dark at ~4 ºC, as previously described by Tejamaya *et al*. (2012) so that all pristine characteristics could be related to each (i.e. they were subject to the same conditions).

In order to provide a control with only one variable to allow direct comparison we exposed "as manufactured" Ag NPs in Milli-Q water at the same concentration, to the same light cycle and temperature as those kept in *Daphnia magna* aM7 medium. These were kept at temperatures and light cycles as prescribed by the OECD tests 202 and 211 (2004, 2008) which ensure *Daphnia* health and uniform testing conditions across laboratories. The aim of this experiment was to identify whether physicochemical characteristics of Ag NPs varied in aM7 medium compared to Milli-Q water and what were their physicochemical properties in the *Daphnia magna* exposures. Furthermore, to check the stability in Milli-Q water and aM7 medium each parameter over a time course of 168 hours was measured (apart from dissolution which was only measured within aM7 medium over time). This time course was chosen firstly to encompass all test condition time-points (i.e. at cessation or just prior to medium change) and to see if an equilibrium could be reached within this time frame.

3.5.1 Size, agglomeration and aggregation

In all instances when the Ag NPs were suspended in aM7 medium there was an increase in HDD when compared to those suspended in Milli-Q water. Both PVP-Ag NPs and PEG-Ag NPs had similar HDD and this may be due to similar binding of the coating to the Ag NP core (i.e. both are sterically bound) and Cit-Ag NPs had the largest HDD, which may be indicative of the weakly charge bound coating which may be less protective and stable in complex medium (Fabrega *et al.*, 2009 and Tejemaya *et al.*, 2012). The increased HDD is likely due to agglomeration, aggregation or in the case of PEG-Ag NPs, a larger hydrated shell due to medium and coating characteristics and not the growth of the core material. PEG is well known to be highly hydrophilic and is able to sorb many water molecules. Levard *et al.* (2012) showed increased aggregation and the creation of sulphide bridges when Ag NPs were added to a sulphur rich medium. Similarly, Römer *et al.* (2011) showed Cit-Ag NPs agglomerate, aggregate and flocculate to a greater degree in more complex and higher ionic strength media. The TEM images for both Cit-Ag NPs and PVP-Ag NPs show them to be bound to medium ligands and in some instances the presence of Ag could not be confirmed by EDX (Cit-Ag NPs) and give an observable indication of why size characteristics may change in aM7 medium between each particle. This would suggest some form of hetero-agglomeration or aggregation whereby the particles increase in apparent size is due to complexation and interaction with components of the medium other than themselves. PEG-Ag NPs, however, seem to stay well dispersed within the medium and do not seem

to interact with medium ligands in the same way, and this has been previously noted within the literature (Tejemaya *et al.*, 2012 and Zook *et al.*, 2011). This may be due to the protective shell of water that the PEG creates, in this instance any increase in size may be due to either homo-aggregation (a strong binding with other Ag NPs in the medium leading to increases in several crystalline planes) or that the medium gives rise to a larger hydrated shell due to PEG's hydrophilicity (Veronese and Gianfranco, 2005). Furthermore this water shell seems to keep PEGylated particles well dispersed through mechanical means.

Interestingly hyperspectral imaging showed a somewhat similar pattern when compared to the TEMs despite the particles being suspended within Milli-Q water. However in the case of PVP-Ag NPs and Cit-Ag NPs the aggregation did not seem as aggregated in comparison to the TEM images of the NPs exposed to aM7 medium. Due to this it cannot be ruled out that some of the ligand bridges seen in the TEM images of Cit-Ag NPs and the complexes in the PVP-Ag NPs may well be formed by the coating itself, however the hyperspectral imaging did not show full bridging or complexes as large in comparison. These images may also support the presence of Ag in the TEM images due to a similarity in pattern and the wavelength of UV/ Vis absorbance given by hyperspectral imaging. These images also show how coating can radically change NP behaviour and properties even when suspended in simple matrices by looking at dehydrated Ag NP patterns and the differing UV/ Vis spectra exhibited by each NP. Ag NPs have a local plasmon resonance of ~400nm for unagglomerated/ unaggregated particles (Table 3.4), however a shift to longer wavelengths occurs when significant agglomeration/ aggregation occurs (Zook *et al*., 2011). Again, indicative of the type of coating and the inherent size stability of each (i.e. sterically bound coatings are more stable, charge bound coatings are less stable) Cit-Ag NPs show the largest shift in absorption away from 400 nm to 520 nm. Furthermore Cit-Ag NPs also showed 3 discrete peak wavelengths indicative of the more polydispersed distribution which may be expected of such particles in corroboration with the literature (Tejemeya *et al.*, 2012, Romer *et al.*, 2011 and Zook *et al.*, 2011). The lowest wavelengths and wavelength variation were seen for PEG-Ag NPs and this supports the DLS data that these particles remain the most well dispersed in Milli-Q water and that they are also less prone to agglomeration/ aggregation in environmental medium which has been previously stated within the literature (Zook *et al.*, 2011). PVP-Ag NPs exhibited a wavelength similar to Cit-Ag NPs but only showed one peak wavelength (~500nm), again indicative of

stability when suspended in Milli-Q water. This stability immediately after suspension in complex medium has been previously highlighted within the literature and is likely similar when suspended in Milli-Q water; again this is somewhat supported by our DLS data in aM7 medium (Zook *et al.*, 2011). Although the hyperspectral imaging data showed great promise, further investigations are required to fully understand the data obtained. For example when DLS shows increases in agglomeration/ aggregation over time will hyperspectral imaging UV/ Vis peaks continue to increase in wavelength indicative of this process (Zook *et al.*, 2011). Unlike traditional UV/ Vis spectrophotopic techniques, spectra in hyper-spectral imaging are not taken from samples suspended in water but from samples dehydrated on microscope slides thus shifts in absorbance strength (i.e. the height of the observed peak) and wavelength will not be due to flocculation as in suspensions, or in highly flocculating suspensions this shortcoming, will be forgone and assessment of agglomeration/ aggregation will be more accurate. However a limitation of hyper-spectral imaging of dehydrated samples is the fact that dissolution can likely not be measured using UV/ Vis like in traditional spectrophotometry using a liquid phase (Zook *et al*., 2011).

Over time (0-168 hours) it also becomes apparent that the different coatings give rise to significant differences in behaviours and characteristics of the Ag NPs. Cit-Ag NPs initially gave rise to a large HDD which decreases over time, likely due to some breakdown of the original Ag NP due to the fact charge bound coatings are less protective of the core material and as it is less stable in complex media which leads to greater agglomeration and aggregation, and due to flocculation. Both PVP-Ag NPs and PEG-Ag NPs HDDs appear to change little over time and remain within the range of 50-100 nm during 168 hours. Again this is likely coating-dependent behaviour. Sterically bound coatings allow greater protection and stability of the particles within complex medium; however even when there was significant differences (seen as increases and decreases) between HDD measures for any Ag NP there was no consistent significant pattern of increase or decrease in HDD over time. The significance may have occurred due to limitations of the DLS when measuring particle size of polydisperse NP suspensions. Here it is often the case that larger particles can mask smaller particles which can cause a skewed distribution. Furthermore as DLS is designed to measure monodispersed and well suspended NPs, any flocculation or sedimentation may cause changes to, or cessation of, Brownian motion and thus change the relationship this has with HDD of the NPs. This was also evident in the data reports

under the expert advice from the DLS technical outputs. The decrease in HDD of the Cit-Ag NPs over time may have occurred due to the larger particles flocculating from the original suspension and thus not being analysed in further DLS measurements. The data highlight how coating type and binding type may be used as predictors of physicochemical changes and behaviours within environmental matrices.

3.5.2 Zeta-potential

Zeta-potential dropped significantly when particles were suspended in aM7 medium in comparison to Milli-Q suspensions which is consistent with the literature (Tejamaya *et al.*, 2013 and Romer *et al.*, 2011). This is often indicative of agglomeration and/ or aggregation with medium cations which lead to a drop in electrical potential. Our TEM, hyperspectral imaging and DLS data showed that PEG-Ag NPs appeared to be the most stable and well dispersed in both Milli-Q water and aM7 medium. However this is direct opposition to the electrostatic repulsion theory, as PEG-Ag NPs were consistently shown to have the lowest ζ-potential. The theory suggests larger charges should result in more steric repulsion and a more disperse colloid. The stability may be due to some physical force allowing for a more stable suspension such as a large water layer around the particle caused by PEGs high hydropholicity. In aM7 medium Cit-Ag NPs had the ζ-potential furthest from zero but were still shown to agglomerate/ aggregate to the greatest degree. PVP-Ag NPs had a similar ζ-potential to Cit-Ag NPs but TEM, hyperspectral imaging and DLS showed them to be an intermediary in terms of agglomeration and aggregation between the particles. Within the literature it is suggested that those particles with ζ-potentials lower than -30 to -40mV or higher than 30 to 40 mV are most likely to be stable in suspension (Heurtault *et al.*, 2003 and Buyer, 1975). Again this is derived from the electro static repulsion theory (i.e. Coulombs Law). However our shows that ζ-potential in isolation may be a poor indicator of particle stability or monodispersity. These data again support that Ag NP coating and type of binding is far more important and likely consistent characteristic when trying to predict Ag NP behaviours and physicochemical characteristic changes within complex medium.

3.5.3 Dissolution

Dissolution of the Ag NPs ranked from highest to lowest was: PEG-Ag NPs > Cit-Ag NPs > PVP-Ag NPs and mean dissolution was found to significantly differ between particles. PEG-Ag NPs and Cit-Ag NPs dissolution appeared to be more constant over time only significantly changing at 168 hours from 24 hours, but did not reach a plateau indicative of a constant level of dissolved Ag that would not change over longer periods of time. PVP-Ag NPs did not reach a plateau indicative of a constant level of dissolved Ag which would not change over longer periods of time in 168 hours and unlike PEG-Ag NPs and Cit-Ag NPs had a more rapid dissolution increase over the time course with significant differences occurring at 72 hours not 168 hours. Interestingly the particle with the highest dissolved fraction was PEG-Ag NPs despite being the most stable in terms of agglomeration and/ or aggregation. This could be due to 2 reasons: i) PEG's affinity for water may cause increased interaction between water and the metal at the surface and ii) as they remain more monodisperse and less agglomerated and/ or aggregated there is more surface area thus higher reactivity and potential for dissolution (Zhao and Wang, 2012). Cit-Ag NPs dissolution occurred at the second highest rate, and this is likely due to disassociation of the coating which is likely to occur when competitive medium ligands have a higher affinity for Ag NP binding sites than the citrate (Tejamaya *et al.*, 2012). This disassociation would lead to more of the core metal exposed to the medium to allow dissolution processes to occur, however, as these were seen to aggregate/ agglomerate this may lead to some protection as less surface area would be available for reactions to occur. In the case of PVP-Ag NPs the lowest dissolution occurred over 24, 48 and 72 hours; this was reflected in the overall mean when these time points were combined. This is likely due to 2 main processes; i) agglomeration/ aggregation of the particles lead to a lower core particle surface area and thus lower reactivity than PEG-Ag NPs and ii) as the coating is sterically bound to the Ag NP core it afforded greater protection of the Ag NP core (Tejamaya *et al.*, 2012). No physicochemical characteristic in isolation consistently related to the dissolution observed. In order to predict dissolution the measurement of a combination of physicochemical characteristics is likely required and once again this parameter is far more reliant on coating and coating binding type than any other characteristic (Yang *et al.*, 2012).

3.6 Conclusion

The study has demonstrated here that although physicochemical characteristics change over time, for Ag NPs in Milli-Q water and aM7 medium, that in most instances these differences can be negligible and thus, after the initial immediate changes, geometric means can be reported. In most cases, the rank order of these characteristics does not change (i.e. smallest to largest HDD) when suspended in the same medium. This allows ease of analysis and correlations with future data sets to assess toxicity associations with physicochemical characteristics. If it is known that particles do not significantly change in physicochemical characteristics over time we are also able to expose organisms and be confident that these particles represent the interactions in an environmental/ experimental (i.e. bioassay) setting. However it is appreciated, an organism added to any exposure most likely will affect NP behaviour as they will add varying secretions such as mucus and faeces to the medium which may interact with the NPs; in addition, uptake and depuration through a biological system may also change the NP physicochemical characteristics. The data show that many physicochemical characteristics although highly related do not always work in a conventional manner. Prediction of one behaviour or characteristic based on another measurement is highly complex, if at all possible. This highlights that a suite of techniques and physicochemical measurements should be ensued to ensure full and appropriate characterisation and correct conclusions of the Ag NP fate and behaviour and the cause of their toxicity, if any. In addition, particle behaviours and physicochemical characteristics rely more upon core type and particle coating, and the manner in which they are bound than any other particle property. The study provides a base of physico-chemical characteristics for which to compare, or associate with, toxicological responses and toxicodynamics of an organism.

Chapter 4.

Silver nanoparticle and silver nitrate acute and chronic toxicity to *Daphnia magna*: implications for risk assessment and future research.

4.1 Introduction

Studies on the toxicity of Ag NP to varying aquatic organisms suggest that Ag NP toxicity can be directly related to Ag^+ release into the aqueous phase, as highlighted in Chapter 1. Ag^+ is highly toxic to freshwater organisms, competitively inhibiting Na^+, K^+, ATPase enzyme activity at the site of animal ionoregulation; for example the gills in fish or the epipodite within some Cladocera (Stensberg *et al.*, 2014 and Bianchini and Wood, 2003, Bury *et al.*, 2002,). Levard *et al.* (2012) and Zhao and Wang (2011a) have shown decreased acute toxicity of Ag NPs upon agglomeration/ aggregation and due to lower dissolution of the Ag NP, or chelation in sulphide rich freshwater environments. This reduced toxicity is likely due to precipitation and decreased bioactivity of Ag^+ and/ or Ag NP when Ag_xS_y is formed. The reports and data from the aforementioned literature suggest a main ionic effect for acute toxicity. Low levels of Ag^+ that are not acutely toxic can still lead to chronic life-cycle effects in aquatic organisms likely via the same mode of action (MOA) as for acute effects (Adams *et al.*, 2011). Chronic effects in several species have been noted, such as decreases in reproduction, viable progeny and growth (Atli and Canli 2013, Völker *et al.*, 2013, Zhao and Wang 2011a, Naddy *et. al.*, 2007 and Bianchini and Wood, 2002).

Further studies have shown NP physicochemical characteristics other than dissolution may be of importance other than dissolution. Zhao and Wang (2010) showed size specific Ag NP increases in toxicity to *Daphnia magna* with decreasing size, as smaller NP size led to larger agglomerate/ aggregate size. This is concluded to be due to the higher propensity of *D. magna* to filter larger particulate matter leading to greater and more rapid body burdens. Furthermore when Ag^+ produced from these Ag NPs is removed via precipitation methods (i.e. here cysteine was introduced into the system to form AgS complexes) the Ag NPs are still able to cause chronic effects, suggesting a particle effect separate from that of Ag^+ release and possible different modes of action (Zhao and Wang, 2011a). Importantly it is currently not well established if the differences in toxicological contribution of Ag NP or Ag^+, or a combination of both, are reliant on specific physicochemical characteristics such coating, and how these change

the organism and particle behaviours as well as the toxicological MOA. Such knowledge is key to the advancement of the safe implementation of nanotechnology to ensure the lowest, or no, toxicological responses can be observed after NP release.

At Ag NPs current predicted environmental concentrations (≤ 0.32 μg L^{-1}) scenarios which result in gross mortality of organisms are unlikely. Ag NPs current predicted levels may not lead to acute toxicity but they are highly likely to result in low level exposure over an organism's life-cycle due to their potential persistence within the environment. Therefore the impact on the organism and ecosystem during this exposure time, and thereafter, is of high interest and importance. Particularly for Ag NPs, many papers have focused on acute toxicological end points failing to report chronic life-cycle effects such as impact on fecundity (Baun *et al.*, 2008). Although, literature is now becoming available for Ag NP chronic toxicity in the environment and previous studies exist for silver in ionic form, but this still represents a large data gap particularly due to the plethora of Ag NP types (Mackevica *et al.*, 2015, Ribierio *et al.*, 2014 Völker *et al.*, 2013, Griffitt *et al.*, 2012 and Naddy *et al.*, 2007).

To date very few studies have addressed *D. magna* Ag NP chronic toxicity and often only in a limited range of concentrations and Ag NP types (Zhao and Wang 2011a, and Völker *et al.*, 2013). Zhao and Wang (2011a) have noted significant effects on the life-cycle of *Daphnia magna* at a limited range of concentrations – particularly on fecundity and, to a lesser degree, on growth. Such studies are critical to the advancement of our knowledge and so they warrant further investigation. For instance a greater range of concentrations are required by OECD testing standards (OECD Test 211, 2008) and knowledge about how different surface coatings or sizes of Ag NP affect toxicity would be highly valuable to advance current regulations, risk management frameworks and modelling efforts.

With the current knowledge-gaps difficulty arises when trying to create regulatory frameworks based on the most representative environmental scenarios. Furthermore within the European Union risk assessment and environmental quality criteria often chronic toxicity data are required (Adams *et al.*, 2011 and De Schamphelaere and Janssen, 2004). Ratios can be applied by risk assessors to acute toxicological datasets to establish chronic toxicity when limited chronic data are available (Hoff *et al.*, 2010). This predicts chronic effect levels to allow implementation of regulation in some form. Such strategies are implemented by the US Environmental Protection Agency where

known acute and chronic data for one species is used to gain an acute:chronic ratio for another, which is then corrected for often based on species sensitivity distributions. The ratio is then applied to other species acute data, when the species in question has limited data on the chronic toxicity of a chemical (Hoff *et al.*, 2010). However these may be under or over cautious and make the assumption that acute and chronic toxicity MOA and acute critical body residues (i.e. an accumulation/ residue which is significantly high enough to cause an adverse biological action) are directly related. However it has previously been highlighted in metal toxicity that this may not be the case (Adams *et al.*, 2011, Heijerick *et al*., 2005 and De Schamphelaere and Janssen, 2004).

4.2 Aims

The aim of this study is to address some of the key knowledge gaps within the literature by assessing the safety of nanoparticles in aquatic systems. The research aims to compare the acute and chronic toxicity of 3 differently coated silver nanoparticles of similar core size (~10nm) in parallel with $AgNO_3$, to the model organism *Daphnia magna*. From the data sets it is aimed to derive critical values such as median acute effective concentration (i.e. the water column concentration which causes 50% immobility to a population) and acute and chronic no-observed effect concentrations and lowest acute and chronic observed effect concentrations, while relating these back to particle physicochemical characteristics, and organism life-cycle effects, where possible. The study also aims to elucidate common themes and rationales for the toxicity presented as they relate to Ag NP physicochemical characteristics and establish if acute and chronic toxicity are related.

4.3 Methods

4.3.1 Organisms

Daphnia magna acquisition and husbandry has been presented in Chapter 2.

4.3.2 Nanoparticle synthesis and stocks

Nanoparticle synthesis and stock preparations were reported in the Appendix Text A2.1 and, Chapter 2 and 3, respectively.

4.3.3 Characterisation of Ag NPs

Physicochemical characteristics were reported in Chapter 3.

4.3.4 Toxicity Tests

For acute toxicity tests the OECD Test 202 (2004) guideline was followed. At the initiation of all tests organisms were <24 hour old or ~5-6 days old. Briefly, acute toxicity was derived in non-fed semi-static waterborne exposures and daphnids were seeded at a density of 1 daphnid/ 4 mL of medium or medium-particle suspension, with 10 organisms per replicate (i.e. 10 organisms in 40 mL per replicate). *Daphnia magna* were exposed to 7 concentrations per experimental exposure group (i.e. $AgNO_3$, PEG-Ag NP, PVP-Ag NP and Cit-Ag NP) in triplicate or quadruplicate in parallel with one control group. Concentration ranges for <24 hour old daphnids were 0-2 µg L^{-1} $AgNO_3$, 0-10 µg L^{-1} PVP-Ag NPs, 0-30 µg L^{-1} PEG-Ag NPs and 0-25 µg L^{-1} Cit-Ag NPs, based on pilot studies. For ~5-6 d old daphnids concentration ranges were 0-2 µg L^{-1} $AgNO_3$, 0-8 µg L^{-1} PVP-Ag NPs, 0-22.5 µg L^{-1} PEG Ag NPs, 0-14.5 µg L^{-1} Cit-Ag NPs. The concentration ranges for ~5-6 d old daphnids were selected after the acute toxicity test for *D. magna* neonates <24 hour old was conducted. The concentration ranges differed as this was a refinement of concentration ranges based on the acute toxicity tests for *D. magna* neonates (i.e. a less broad range was required). Therefore these exposures required a narrower range of concentrations as compared to the initial neonate exposures. Immobilization (%) was measured at 48 hours.

The testing on neonates was conducted as this is advised by OECD guidance. The testing on juveniles was conducted to establish if the relationships of toxicity between the different exposures (i.e. $AgNO_3$ PVP-Ag NPs etc.) were consistent over age. This was important for other experimental results within the thesis. To increase biological matter for biochemical testing (Chapter 6) and reduce number of *Daphnia* required older organisms were used. To ensure measurable Ag in biodynamic and biotic ligand analysis (Chapter 5) older organisms were also used. Therefore the juvenile endpoints were used to relate to the results of these experiments to their acute toxicity at the most relevant age.

For chronic toxicity tests OECD Test 211 (2008) guidelines were followed. Chronic toxicity was derived from semi-static waterborne exposures with a medium change every 3 days. Daphnids were seeded at a density of 1 daphnid/ 80 mL of medium or

medium-particle suspension, with 1 organism (<24 hour old) per replicate. The organism was fed a daily diet of green algae, in this instance *Chlorella vulgaris*, supplying ≥ 0.2 mg carbon daphnid^{-1} day^{-1}. To achieve this level of carbon availability 5 x 10^5 cells mL^{-1} *C. vulgaris* were used. Five to seven concentrations per experimental exposure group were used (i.e. $AgNO_3$, PEG-Ag NP, PVP-Ag NP and Cit-Ag NP) with 10 replicates per concentration in parallel with a control group. Concentrations ranges were 0-0.6 µg L^{-1} $AgNO_3$, 0-1.5 µg L^{-1} PVP-Ag NPs, 0-5 µg L^{-1} PEG-Ag NPs and 0-2 µg L^{-1} Cit-Ag NPs. *Daphnia magna* were also exposed to ½ food rations to test the hypothesis that Ag NPs may inhibit food uptake. The inhibition of food uptake may cause a starvation effect that is not specific to Ag NPs but non nutritious particulate matter in general. Mortality, reproduction, number of moults, number of broods and mean length per organism was noted either daily over a 21-day period or at the end of the exposure (i.e. length). Chronic exposure concentrations were based on acute 48 hour EC_{50} values where 25% of the EC_{50} was used as the highest dose and refined in subsequent experiments if no response or acute/ sub-chronic mortality was observed.

4.3.5 Imaging

Length and deformities were measured on a Leica dissection microscope (2.4x) and length was taken from the top of the compound eye to the base of the apical spine.

Figure 4.1. Dissection microscope image at 1.6x magnification and arrow which represents from which anatomical points length was consistently measured.

In all instances measures were made with Image J software (Rasband, 1997-20014). Scanning electron microscopy examination of *Daphnia magna* filtering apparatus after dissection was carried out on a Hitachi S3400 (Tokyo, Japan). Samples were loaded onto aluminium stubs topped with double sided carbon tape. Samples were not sputter coated and viewed at varying magnification at 20 kV. For SEM imaging *Daphnia magna* were exposed to 4 mg L^{-1} of PVP-Ag NPs and collected once immobilisation was observed. The organisms were then transferred to 24-well plates (VWR tissue culture plates) the medium was removed and then 400 µL of fixative, 2.5% glutaraldehyde (Sigma Aldrich) with 0.1 M of cacodylate buffer (Sigma Aldrich) was added to the wells, the organisms were left for 8 hours. The fixative was removed and replaced with 400 µL of ethanol, the *D. magna* were then sequentially dehydrated in 50%, 70%, 80%, 90% and 100% ethanol for 5 minutes at each ethanol concentration. After the initial dehydration with ethanol *Daphnia magna* were then completely dehydrated in 100% hexamethyldisilazane (HMDS) – an easy chemical alternative to critical point drying (Laforsch and Tollrian, 2000). Daphnids were completely submerged in HMDS and then the HMDS was immediately removed and the daphnids were placed in a desiccator and left to dry overnight. Within 24 hour *Daphnia* were placed on the aluminium stubs. The organisms were orientated under a dissection microscope at 1-10x magnification (Leica Microsystems©) and dissected in their dehydrated form.

4.3.6 Statistical analysis

Methods for statistical analysis have been reported in Chapter 2. Briefly, EC_{50} values were estimated using the trimmed Spearman-Karber model, NOEC and LOEC values as well as significant differences in the chronic test in comparison to the control were determined using ANOVA followed by Dunnett's post-hoc analysis. For chronic toxicity data was rejected for an animal if mortality occurred before cessation of the test as such *n* numbers (n = 3-10) of statistical analysis reflect this. This was in order to ensure that any noted effects were not only chronic but also sub-lethal and as per the revised OECD test guideline (2012).

4.4 Results

4.4.1 Toxicity tests

For <24 hour old neonates and ~5-6 day old juveniles the EC_{50} values significantly differed between $AgNO_3$ and all 3 particle types (n = 2, d.f. = 1, z < -11, p < 0.0001; Table 4.1, Figures 4.2 and 4.3). There was a consistent EC_{50} rank order for both neonates and juveniles which, from most to least toxic, were $AgNO_3$ > PVP-Ag NPs > Cit-Ag NPs > PEG-Ag NPs (Table 4.1, Figure 4.2 and 4.3). Regardless of age $AgNO_3$ was the most toxic form of silver and PVP-Ag NPs were the most toxic nanoparticle during the 48 hour acute toxicity tests (Figure 4.2, Table 4.1). Despite the relatively high dissolution (~29%, Chapter 3, Table 3.4), PEG-Ag NPs were the least toxic nanoparticle irrespective of age (Figure 4.2, Table 4.1). In Table 4.1 and Figure 4.3 ~5-6 day old daphnids were significantly more sensitive than <24 hour old daphnids to PEG-Ag NPs and Cit-Ag NPs (n = 1, d.f. 1, z < -2, p < 0.05; Table 4.1). However when looking at NOEC and LOEC values there is little variation between ~5-6 d old and <24 hour old daphnids. NOEC and LOEC values also differ between Ag exposure type and follow the same rank order as the EC_{50} values for both < 24 hour old neonates and ~5-6 day old juveniles (Table 4.2). $AgNO_3$ was significantly less toxic to older organisms (n = 1, d.f. 1, z < -2, p < 0.05) and this is also reflected in the difference between NOEC and LOEC values (Tables 4.1 and 4.2, and Figures 4.2 and 4.3).

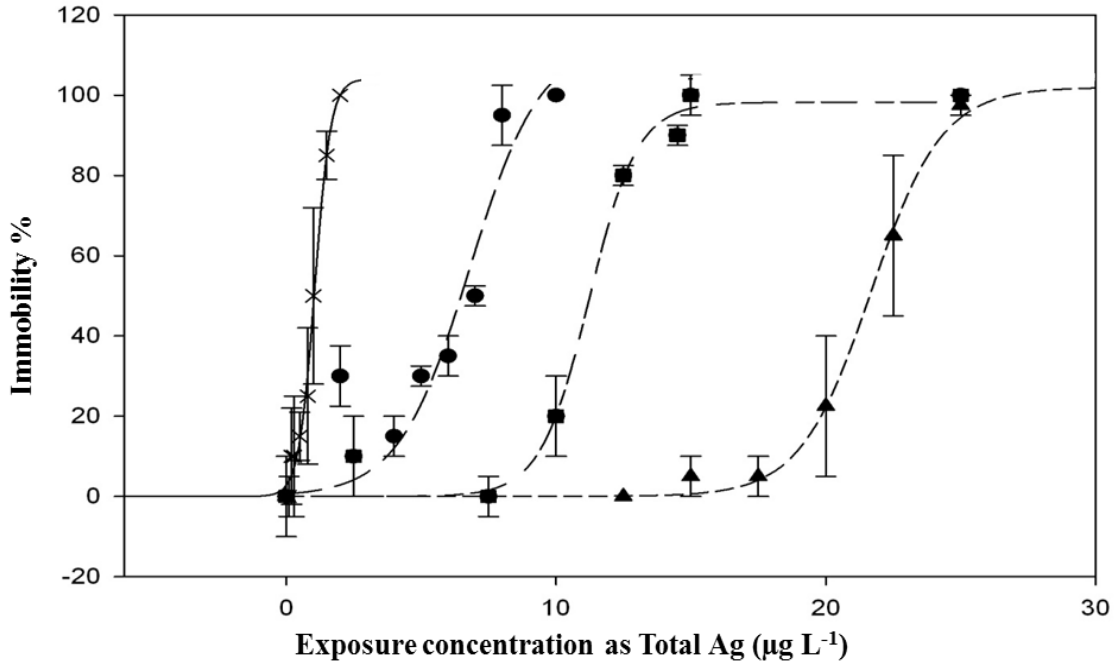

Figure 4.2. Acute toxicity dose response of *Daphnia magna* neonates (<24 hour old) exposed to $AgNO_3$ (**X**), PVP-Ag NPs (●), PEG-Ag NPs (▲) and Cit-Ag NPs (■) in 48 hr immobility test (n = 4). Error Bars: 95% CI.

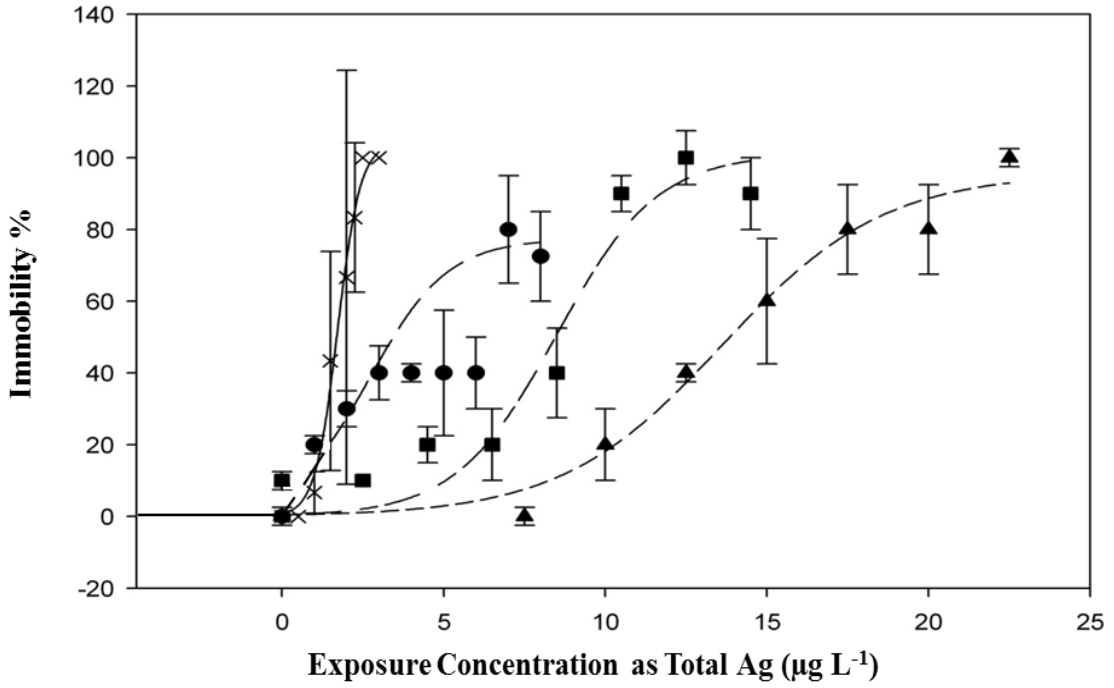

Figure 4.3 Acute ~5-6 day old *Daphnia magna* toxicity dose response of $AgNO_3$ (**X**), PVP-Ag NPs (●), PEG-Ag NPs (▲) and Cit-Ag NPs (■) in 48 hr immobility test (n = 3). Error Bars: 95% CI.

Table 4.1. Acute EC_{50} values of *Daphnia magna* in varying silver exposures conducted on < 24hour old neonates and 5-6 day old juveniles. *, **, *** denotes significant differences between particles during same age at exposure ($p < 0.05$, $p < 0.01$, $p < 0.001$, respectively). †, ††, ††† denotes significant differences between different ages with the same exposure ($p < 0.05$, $p < 0.01$, $p < 0.001$, respectively).

Exposure ($\mu g\ L^{-1}$)	<24 h old EC_{50}	~5-6 d old EC_{50}
$AgNO_3$	0.9 ± 0.1***	1.1 ± 0.1***†
PVP-Ag NP	6.8 ± 0.4***	5.9 ± 1.7***
Cit-Ag NP	11.7 ± 0.8***	8.5 ± 1.1***†
PEG-Ag NP	22.2 ± 0.5***	13.4 ± 1.5***†

Table 4.2 NOEC and LOEC of *Daphnia magna* in varying silver exposures conducted on < 24hour old neonates and 5-6 day old juveniles. The values were derived from Dunnett's post hoc test on the corresponding dose response (Figure 4.2 and 4.3).

Exposure ($\mu g\ L^{-1}$)	<24 h old NOEC	<24 h old LOEC	~5-6 d old NOEC	~5-6 d old LOEC
$AgNO_3$	0.5	0.8	1.5	2.0
PVP-Ag NP	2.0	3.0	6.0	7.0
Cit-Ag NP	10.5	12.5	8.5	10.5
PEG-Ag NP	12.5	15.0	10.0	12.5

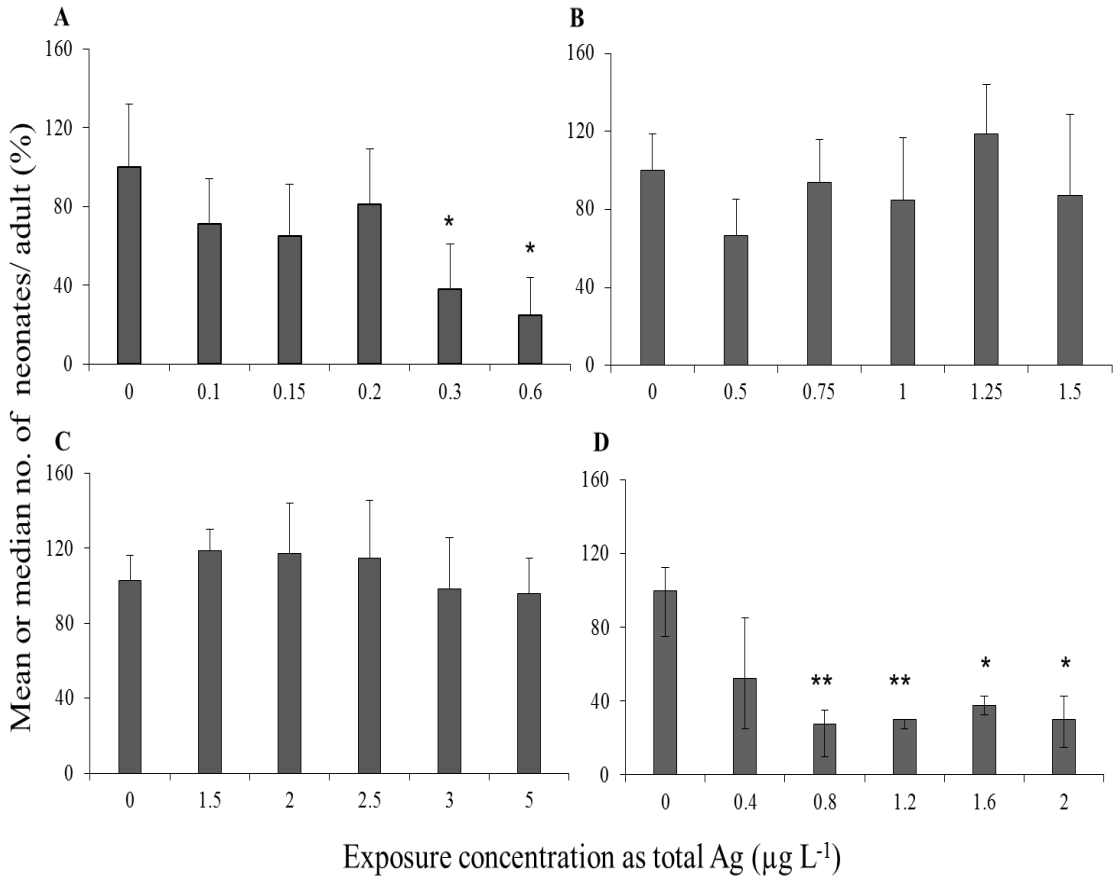

Figure 4.4 Mean and median cumulative number of neonates produced per *Daphnia magna* at differing Ag concentrations when *Daphnia magna* were exposed to $AgNO_3$ (A), PVP-Ag NPs (B), PEG-Ag NPs (C) and Cit-Ag NPs (D) (n = 3-10). Single sided error bars are 95% CI and double-sided error bars are interquartile ranges. *, ** denotes significant difference from control at $p < 0.05$ and $p < 0.01$, respectively.

Both Ag NPs and $AgNO_3$ were able to exert significant chronic effects on reproduction and growth of *D. magna* (Figure 4.4-4.8) with lowest observed effect concentrations for $AgNO_3$, Cit-Ag NPs, PEG-Ag NPs and PVP-Ag NPs being, 0.1, 0.8, 1.5 and 1.5 µg L^{-1}, respectively. *D. magna* started to produce neonates between days 9 and 12 (Figure A4.1). Only $AgNO_3$ and Cit-Ag NP treated organisms showed a dose dependent and significant reduction in the number of neonates produced over 21 days ($AgNO_3$ n = 3-10, d.f. = 2-9, F = 3.832, $p < 0.01$; Cit-Ag NPs n = 4-10, d.f. = 3-9, χ^2 = 16.451, $p <$ 0.01, Figure 4.4 A and D). PVP-Ag NPs and PEG-Ag NPs had no effect on total cumulative reproduction over 21 days (PVP-Ag NPs n = 6-10, d.f. 5-9, F = 0.454, $p >$ 0.05; PEG-Ag NPs n = 7-10, d.f. 6-9, F = 1.037, $p > 0.05$, Figure 4.4 B and C). $AgNO_3$ and Cit-Ag NPs were the most toxic silver forms and Ag NP, respectively, when

assessing the reproductive end point. No full ranking of the potential contaminants could be obtained from reproduction data alone due to this. Figure 4.5 shows the number of neonates per adult *Daphnia magna* brood, again a significant dose dependent decrease in reproduction was seen for $AgNO_3$ (n = 3-10, d.f. = 2-9, z < -2.315, $p < 0.05$; Figure 4.5 A), however no other silver exposure showed a decrease in reproduction using this parameter. PEG-Ag NPs had a significant hormetic effect on reproduction, seen as an increase in the number of neonates per brood at 2.0 and 2.5 µg L^{-1} (n = 7-10, d.f. 6-9, z < -2.300, $p < 0.05$; Figure 4.5 C). PVP-Ag NPs and Cit-Ag NPs showed no changes in neonates produced per brood.

The sequence of significant decreases to *D. magna* life-cycle events during chronic exposures appears to differ between $AgNO_3$ compared to PVP-NPs (Figure 4.4-4.8). Here growth, as measured by length over time was affected in PVP-Ag NP exposures, and the reproduction was decreased during $AgNO_3$ exposures.

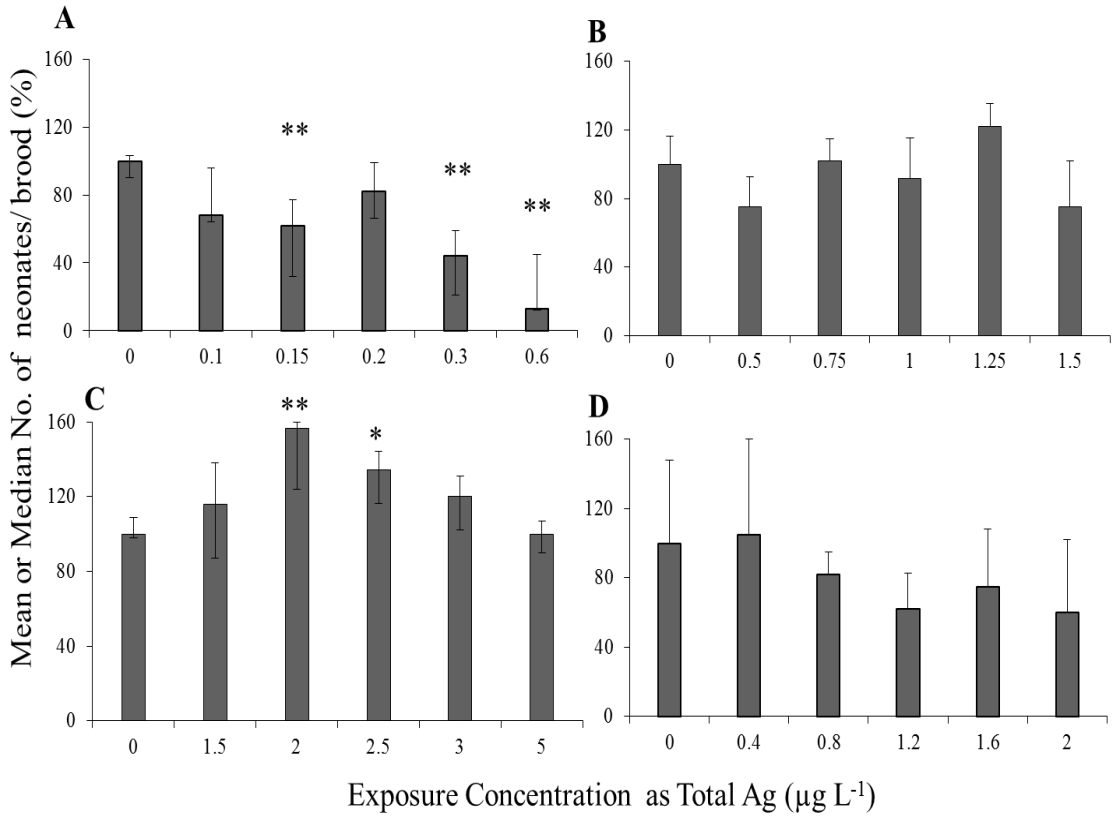

Figure 4.5 Mean or median total neonates per *Daphnia magna* brood when exposed to $AgNO_3$ (A), PVP-Ag NP (B), PEG-Ag NP (C) and Cit-Ag NP (D) expressed as a percentage of their respective controls. n = 3-10 dependent on survival. Error bars were chosen based on normality, one sided error bars denote parametric data and are 95% CI, 2-sided error bars denote non-parametric data and represent the interquartile range. For the Y-axis parametric data are expressed as a mean and non-parametric data are expressed as a median. * denotes significance at $p < 0.05$ and ** denotes significance at $p < 0.01$.

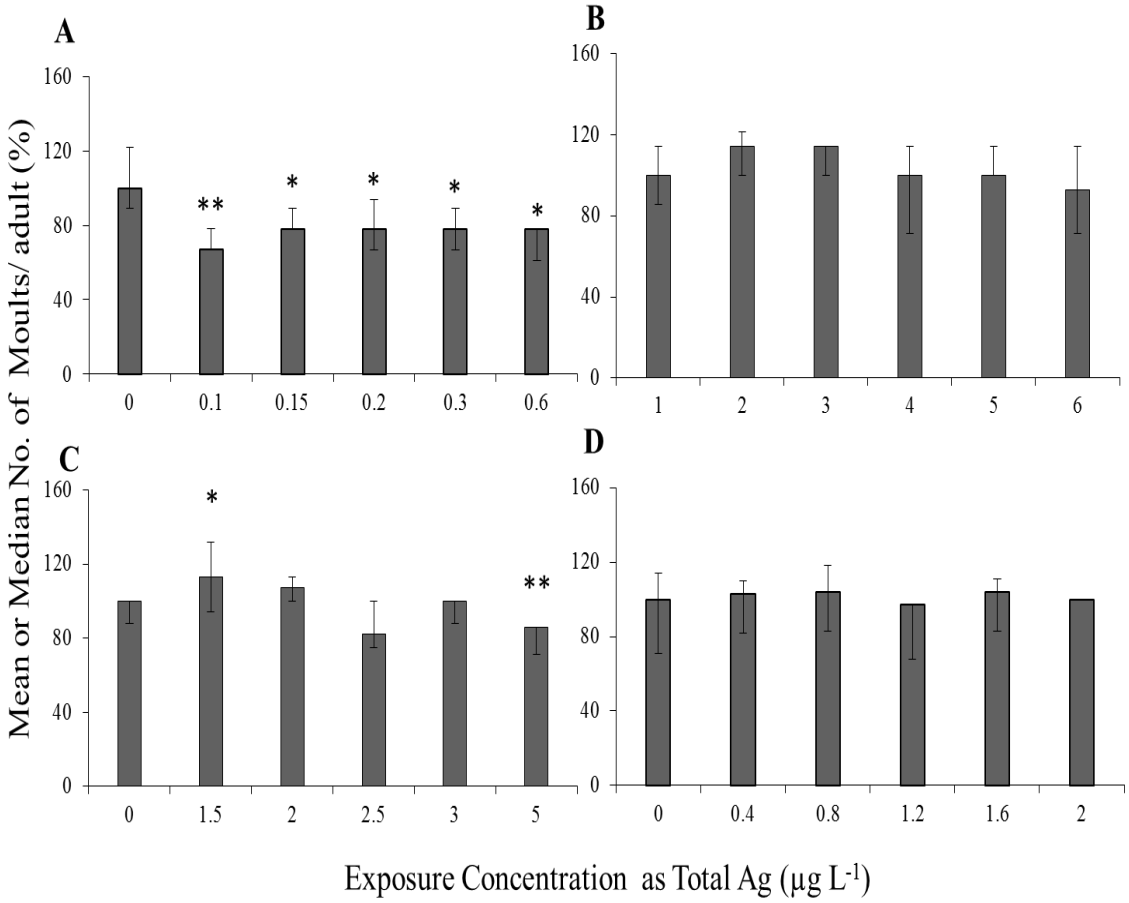

Figure 4.6 Mean/ median total moults per *Daphnia magna* when exposed to $AgNO_3$ (A), PVP-Ag NP (B), PEG-Ag NP (C) and Cit-Ag NP (D) expressed as a percentage of their respective controls. n = 3-10 dependent on survival. Error bars were chosen based on normality, one sided error bars denote parametric data and are 95% CI, 2-sided error bars denote non-parametric data and represent the interquartile range. For the Y-axis parametric data is expressed as a mean and non-parametric data is expressed as a median. * denotes significance at $p < 0.05$ and ** denotes significance at $p < 0.01$.

Only $AgNO_3$ and PEG-Ag NPs induced a significant reduction in carapace shedding at >0.1 and 5 µg L^{-1}, respectively (n = 3-10, d.f. = 2-9, z < -2.100 $p < 0.05$ and, n = 7-10, d.f. = 6-9, z = 2.707 $p < 0.05$, respectively; Figure 4.6 A and C). In contrast PEG-Ag NP induced a significant increase in the number of moults at 1.5 µg L^{-1} displaying a hormetic like effect (n = 7-10, d.f. = 6-9, z = -2.480, $p < 0.05$; Figure 4.6 C). Here PVP-Ag NPs and Cit-Ag NPs showed no effect on this chronic endpoint (PVP-Ag NPs n = 6-10, d.f. = 5-9, $\chi^2 = 4.474$, $p > 0.05$; Cit-Ag NPs n = 4-10, d.f. = 3-9, $\chi^2 = 3.924$, $p > 0.05$, Figure 4.6 B and D). Toxicity could not be ranked on this chronic endpoint.

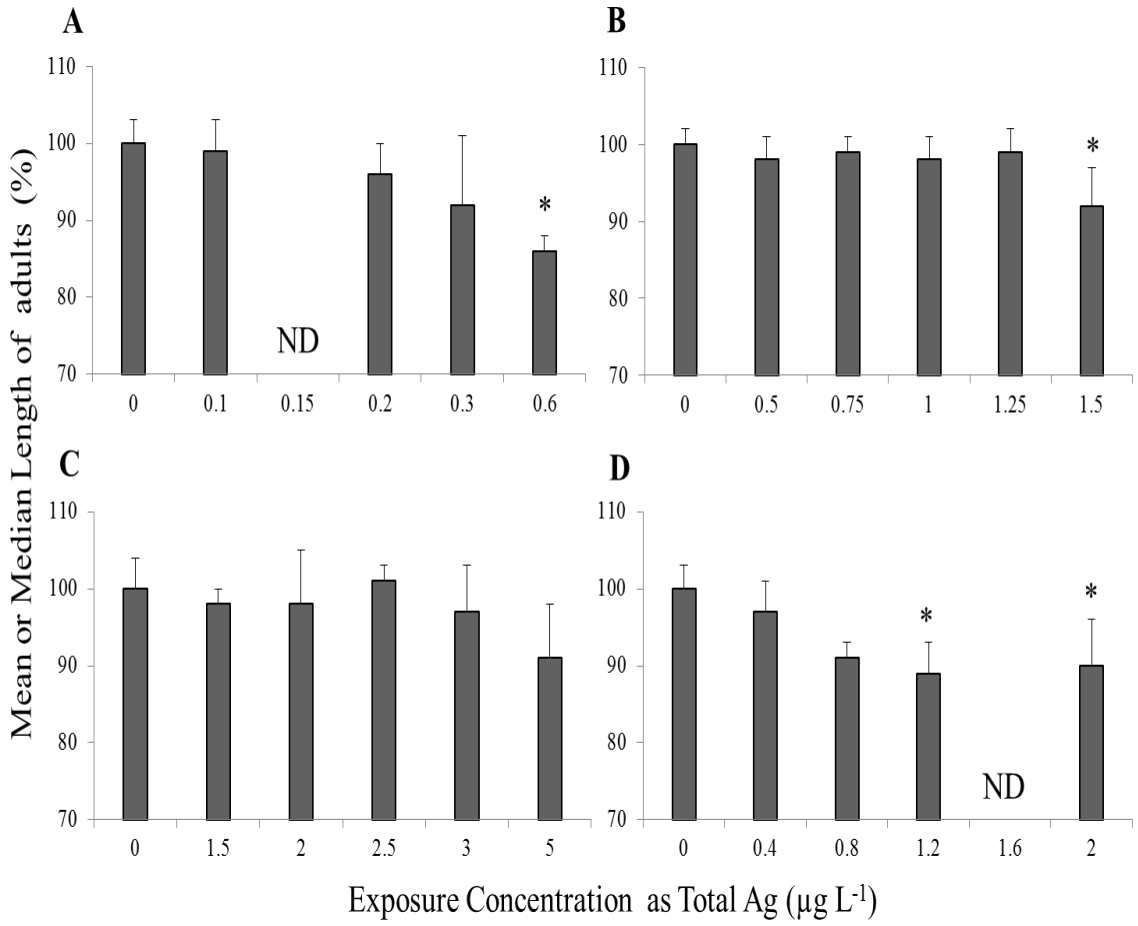

Figure 4.7 Mean/ median total *Daphnia magna* length when exposed to $AgNO_3$ (A), PVP-Ag NP (B), PEG-Ag NP (C) and Cit-Ag NP (D) expressed as a percentage of their respective controls. n = 3-10 dependent on survival. Error bars were chosen based on normality, one sided error bars denote parametric data and are 95% CI, 2-sided error bars denote non-parametric data and represent the interquartile range. For the Y-axis parametric data is expressed as a mean and non-parametric data is expressed as a median. * denotes significance at $p < 0.05$ and ** denotes significance at $p < 0.01$.

All Ag forms were able to decrease *Daphnia magna* length by 8-10%, measured at 21 days, however only PVP-Ag NPs, Cit-Ag NPs and $AgNO_3$ exposures showed significant differences when compared with the control group ($AgNO_3$ n =3-10, d.f. 2-9, $F > 6.059$, $p < 0.01$; PVP-Ag NPs n = 6-10, d.f. 5-9, $F = 3.322$, $p < 0.05$; Cit-Ag NPs n = 4-10, d.f. = 3-9, $F = 5.434$, $p < 0.05$; Figure 4.7 A, B and D). In contrast PEG-Ag NPs did not significantly affect this parameter (PEG-Ag NPs n = 7-10, d.f. 6-9, F =

1.594, $p > 0.05$), but there was still a decrease in length at the highest dose by 12 ± 7% (Figure 4.7 C). Rank order of toxicity for effects to *Daphnia magna* length were: $AgNO_3$ > Cit-Ag NP > PVP-Ag NP > PEG-Ag NPs. If the chronic toxicity rank was obtained from effects on fecundity, carapace shed and length, and not established from one endpoint in isolation (effect and level of effect can be seen in Table 4.3) chronic toxicity ranking would still corroborate with the ranking gained from length effect alone (i.e. $AgNO_3$ > Cit-Ag NP > PVP-Ag NP > PEG-Ag NPs).

The acute and chronic toxicity rankings vary for the Ag NPs which are PVP-Ag NP > Cit-Ag NP > PEG-Ag NP and Cit-Ag NP > PVP-Ag NP > PEG-Ag NP, respectively, meaning the proportional contribution of Ag NP or dissolved Ag release to toxicity as well as contribution of other modes of action may vary with exposure time. Starvation (i.e. ½ food ration) had an effect on all measured chronic end points (Table 4.3). Please note all chronic effects and results have been compiled in Table 4.3.

4.4.2 Imaging

A series of neonates were taken from exposure conditions due to an increasing occurrence of neonates found at the bottom of the $AgNO_3$ treatment vessel. Light microscopy revealed a higher frequency in deformed progeny of these exposures within each brood. $AgNO_3$ exposures resulted in more observed deformed progeny (Figure 4.8), where antennae (swimming antennae) were unable to fully form, there was pronounced curvature of the apical spine, a large nuchal cell protrusion at the head (indicative of possible issues with respiration and ionoregulation) and a reduced ability to feed as guts appeared empty. Figure 4.9 shows a failed moult and trapped neonate after PVP-Ag NP exposures (0.75 µg L^{-1} at day 15). Furthermore only random observations of deformities were seen in Ag NPs where most neonates were found to be healthy and well formed. Deformities and healthy neonates from control and the highest PEG-Ag NP exposure can be seen in Figure 4.8, as well as a failed moult from a PVP-Ag NP exposure (0.75 µg L^{-1}) in Figure 4.9. SEM imaging of the *Daphnia magna* filtering apparatus revealed space between setae and setulae of 10 µm and 400 nm, respectively (Figure 4.10). SEM imaging also showed Ag NP agglomerates/ aggregates could be caught by the *Daphnia magna* filtering apparatus and Ag chemical composition was confirmed by EDX (Figure 4.10).

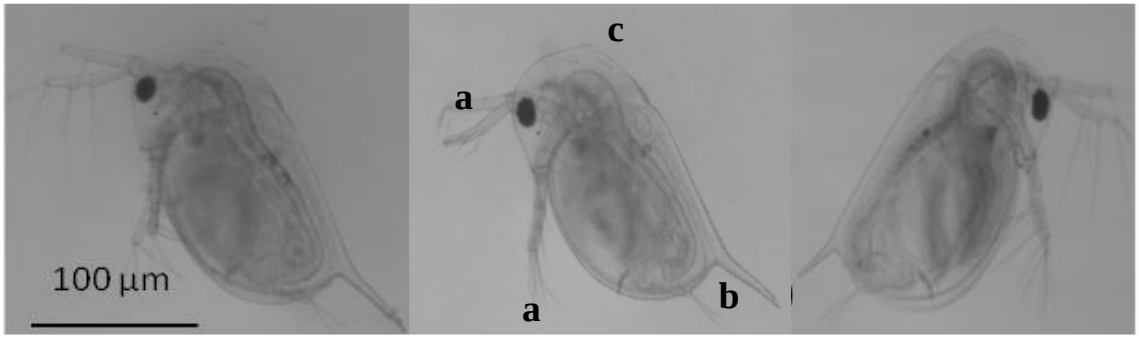

Figure 4.8 Left-Right Control, PEG-Ag NP, $AgNO_3$ exposed *Daphnia magna.* Deformed neonate from adult exposed to Ag^+; letters highlight comparative deformities; a) not fully formed swimming apparatus, b) pronounced curvature of the apical spine c) protrusion at the posterior of the head likely increased nuchal cell tissue.

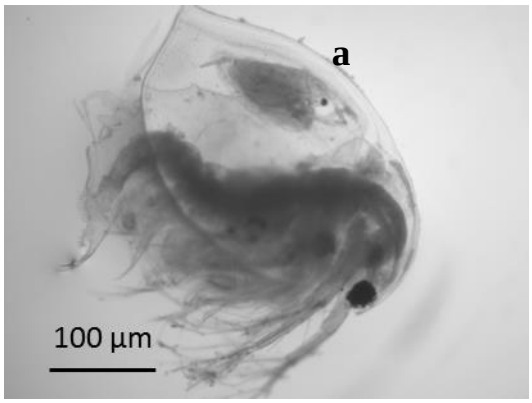

Figure 4.9 Failed moult of female adult *D. magna* after PVP-Ag NP chronic exposure which led to mortality and a trapped neonate in the brood chamber (a; 0.75 µg L^{-1} day 17)

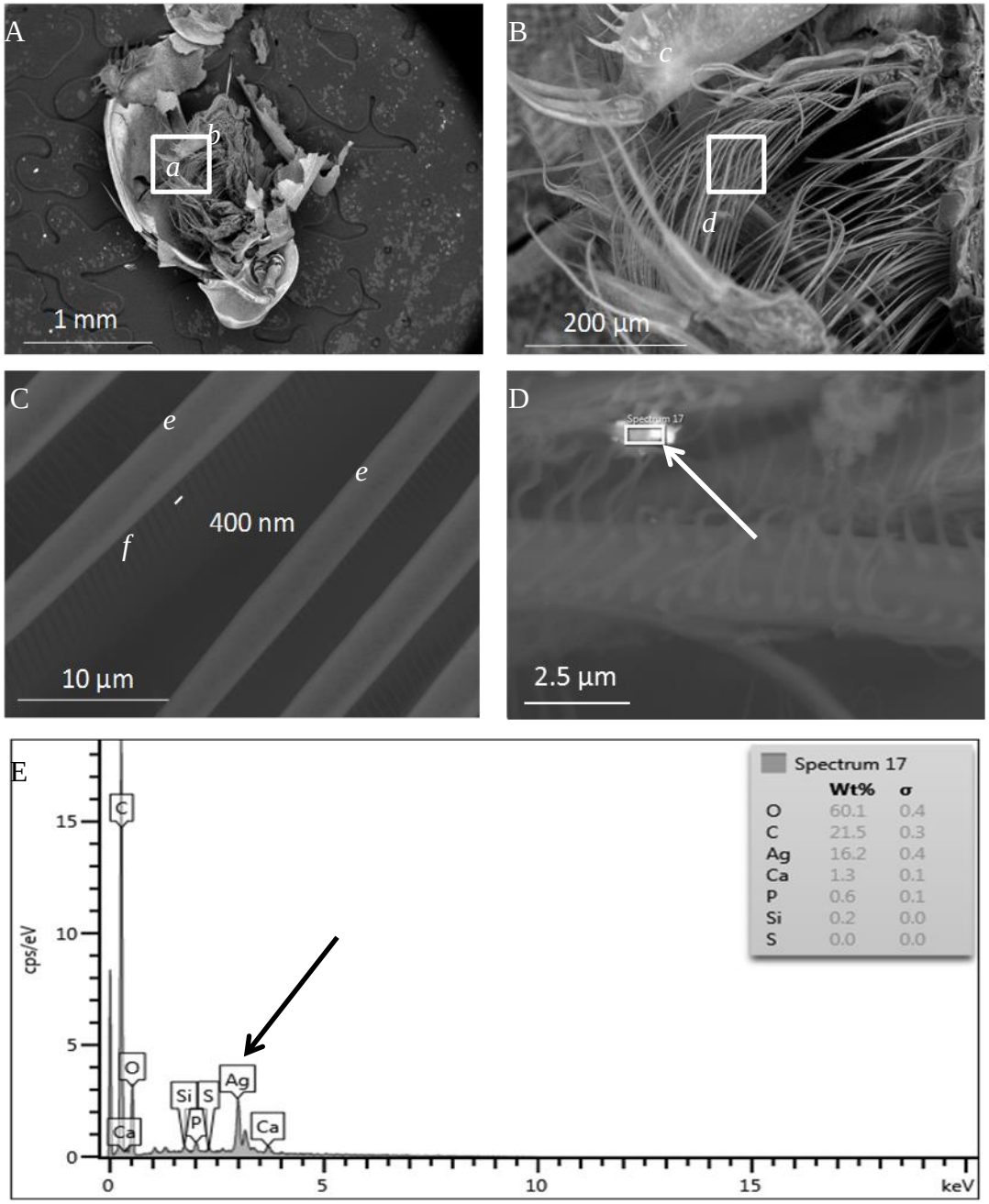

Figure 4.10 (A) A 32x magnification cavity of *Daphnia magna* showing filtering apparatus (*a*) and gut (*b*). (B) A 210x magnification of image A near post-abdominal claw (*c*) showing filtering apparatus (*d*). (C) Further magnification (4000x) of filtering apparatus (setae and setulae) showing space between *Daphnia magna* setae (*e*) (10 µm) and setulae (*f*) (~400nm) used for catching and filtering food. (D) A1.4 µm PVP-Ag NP aggregate (see arrow on image D) caught in filtering apparatus after 1 hour exposure at 4 mg L^{-1} and (E) EDX confirmation of Ag agglomerate/ aggregate with arrow pointing to Ag peak.

Table 4.3 Effects of $AgNO_3$, Ag NPs and food rationing to *D. magna* after the 21 day *D. magna* reproduction test (OECD test 211, 2008).

	Mean or median % of control of neonates per live female *Daphnia magna*					**Mean/ median % of control Neonates per Brood**				
Exposure Concentration µg Ag L^{-1}	$AgNO_3$	PVP-Ag NP	PEG-Ag NP	Cit-Ag NP	food ration	$AgNO_3$	PVP-Ag NP	PEG-Ag NP	Cit-Ag NP	food ration
0	100 ± 32	100 ± 19	100 ± 25	100 (75-113)	-	100 (90-103)	100 ± 16	100 (98-109)	100 ± 48	-
0.1	71 ± 38	-	-	-	-	68 (64-96)	-	-	-	-
0.15	65 ± 26	-	-	-	-	62 (32-77)**	-	-	-	-
0.2	81 ± 28	-	-	-	-	82 (66-99)	-	-	-	-
0.3	38 ± 23**	-	-	-	-	44 (21-59)**	-	-	-	-
0.4	-	-	-	53 (25-85)	-	-	-	-	105 ± 55	-
0.5	-	67 ± 19	-	-	-	-	75 ± 18	-	-	-
0.6	25 ± 19**	-	-	-	-	13 (12-45)*	-	-	-	-
0.75	-	94 ± 22	-	-	-	-	102 ± 12	-	-	-
0.8	-	-	-	28 (10-35)**	-	-	-	-	82 ± 13	-
1	-	85 ± 32	87 ± 30	-	-	-	91 ± 24	100 (63-106)	-	-
1.2	-	-	-	30 (25-30)**	-	-	-	-	62 ± 21	-
1.25	-	119 ± 25	-	-	-	-	122 ± 13	-	-	-
1.5	-	87 ± 42	119 ± 11	-	-	-	75 ± 27	116 (87-138)	-	-
1.6	-	-	-	38 (33-43)*	-	-	-	-	75 ± 33	-
2	-	-	117 ± 27	30 (15-43)*	-	-	-	157 (124-160)**	60 ± 42	-
2.5	-	-	115 ± 31	-	-	-	-	135 (117-145)*	-	-
3	-	-	98 ± 27	-	-	-	-	120 (102-131)	-	-
5	-	-	96 ± 10	-	-	-	-	100 (90-107)	-	-
100% food	-	-	-	-	100 ± 15	-	-	-	-	100 ± 5
50% food	-	-	-	-	40 ± 21*	-	-	-	-	66 ± 11*

Table 4.3 cont.

Concentration µg Ag L^{-1}	Mean or median % of control Broods per *Daphnia magna*					Mean/ median % of control Moults per *Daphnia magna*				
	$AgNO_3$	PVP-Ag NP	PEG-Ag NP	Cit-Ag NP	food ration	$AgNO_3$	PVP-Ag NP	PEG-Ag NP	Cit-Ag NP	food ration
0	100 (100-133)	100 (100-100)	100 (100-100)	100 (75-100)	-	100 (89-122)	100 (86-114)	100 (88-100)	100 (71-114)	-
0.1	100 (67-133)	-	-	-	-	67 (67-78)**	-	-	-	-
0.15	133 (100-133)	-	-	-	-	78 (78-89)*	-	-	-	-
0.2	100 (83-117)	-	-	-	-	78 (67-94)*	-	-	-	-
0.3	100 (83-133)	-	-	-	-	78 (67-89)*	-	-	-	-
0.4	-	-	-	96 (71-109)	-	-	-	-	103 (82-110)	-
0.5	-	100 (83-100)	-	-	-	-	114 (100-121)	-	-	-
0.6	67 (50-117)	-	-	-	-	78 (61-78)*	-	-	-	-
0.75	-	100 (100-100)	-	-	-	-	114 (100-114)	-	-	-
0.8	-	-	-	100 (75-100)	-	-	-	-	104 (83-118)	-
1	-	100 (67-100)	100 (84-117)	-	-	-	100 (71-114)	82 (75-100)	-	-
1.2	-	-	-	51 (51-51)	-	-	-	-	97 (68-97)	-
1.25	-	100 (100-100)	-	-	-	-	100 (100-114)	-	-	-
1.5	-	117 (67-133)	100 (100-133)	-	-	-	93 (71-114)	113 (94-132)*	-	-
1.6	-	-	-	93 (68-106)	-	-	-	-	104 (83-111)	-
2	-	-	100 (67-100)	77 (77-77)	-	-	-	107 (100-113)	100 (100-100)	-
2.5	-	-	100 (67-100)	-	-	-	-	82 (75-100)	-	-
3	-	-	100 (67-100)	-	-	-	-	100 (88-100)	-	-
5	-	-	100 (84-100)	-	-	-	-	86 (71-86)**	-	-
100% food	-	-	-	-	100 (100-100)	-	-	-	-	100 ± 8
50% food	-	-	-	-	66 (66-83)*	-	-	-	-	71 ± 26**

Table 4.3 cont.

	Mean % of control Length of *Daphnia magna*				
Concentration µg Ag L^{-1}	$AgNO_3$	PVP-Ag NP	PEG-Ag NP	Cit-Ag NP	food ration
0	100 ± 3	100 ± 2	100 ± 4	100 ± 3	-
0.1	99 ± 4	-	-	-	-
0.15	ND	-	-	-	-
0.2	96 ± 4	-	-	-	-
0.3	92 ± 9	-	-	-	-
0.4	-	-	-	97 ± 4	-
0.5	-	98 ± 3	-	-	-
0.6	86 ± 2**	-	-	-	-
0.75	-	99 ± 2	-	-	-
0.8	-	-	-	91 ± 2	-
1	-	98 ± 3	98 ± 2	-	-
1.2	-	-	-	89 ± 4*	-
1.25	-	99 ± 3	-	-	-
1.5	-	92 ± 5*	100 ± 7	-	-
1.6	-	-	-	-	-
2	-	-	101 ± 4	90 ± 6*	-
2.5	-	-	97 ± 6	-	-
3	-	-	97 ± 6	-	-
5	-	-	88 ± 7	-	-
100% food	-	-	-	-	100 ± 3
50% food	-	-	-	-	87 ± 5*

4.5 Discussion

$AgNO_3$ was the most toxic form of silver across all measured endpoints for acute and chronic toxicity. PVP-Ag NPs were the most acutely toxic NP, however Cit-Ag NPs were the most chronically toxic NP. PEG-Ag NPs were consistently the least toxic NP across all measured acute and chronic endpoints. Acute and chronic toxicity rank order therefore changed due to the difference in the most toxic NP between each exposure duration, these rankings were $AgNO_3$ > PVP-Ag NPs > Cit-Ag NPs > PEG-Ag NPs and $AgNO_3$ > Cit-Ag NPs > PVP-Ag NPs > PEG-Ag NPs, for acute and chronic exposures, respectively. $AgNO_3$ was seen as significantly less toxic to ~5-6 day old daphnids than it was to 24 hour old daphnids, reflected in the EC_{50}, NOEC and LOEC values. Ag NP 24 hour old and ~5-6 day old daphnid, NOEC and LOEC values were similar. Only $AgNO_3$ and Cit-Ag NPs were able to reduce reproduction over the chronic test. For Cit-Ag NPs this was not seen on a per brood basis, but it was with $AgNO_3$. The reduction caused by Cit-Ag NPs was due to an early cessation of reproduction (Appendix Figure A4.1). PVP-Ag NPs caused mortality before effects on fecundity could be observed. PEG-Ag NPs were able to exert a hormetic effect for both reproduction and number of moults, but it was the only particle which displayed such an effect. $AgNO_3$affected the number of moults which was seen as a significant decrease; however no other exposures even at their highest tested levels (i.e. PVP- and Cit-Ag NPs) were able to decrease number of moults over the 21 day period. A reduction in length was seen in all silver exposures apart from PEG-Ag NPs and the toxicity was able to be ranked using this endpoint and conformed to the aforementioned chronic toxicity ranking which was derived from the combined endpoints studied (Table 4.3). The sequence of significant effects on *Daphnia magna* life cycle events during chronic exposures appears to differ between $AgNO_3$ and PVP-Ag NPs. Here for $AgNO_3$ the number of moults was affected first, followed by reproduction and eventually length, whereas PVP-Ag NPs affected length first before reproduction or number of moults. This effect has been previously seen, where the impact on the *D. magna* life-cycle is different between silver forms (Zhao and Wang, 2011a). In $AgNO_3$ exposures more observations were made of deformed neonates compared to other treatments. The deformations made the neonates unable to swim and, were considered as unviable.

The study showed$AgNO_3$ was the most toxic of all Ag forms tested, and that Ag NP toxicity can be significantly impacted by Ag NP coating, and exposure time. PVP-Ag NPs were the most acutely toxic Ag NP but Cit-Ag NPs were the most chronically toxic

Ag NPs. This has implications for the use of acute:chronic ratios for Ag NPs, such values are commonly used for the risk assessment of chemicals (Hoff *et al.*, 2010). Use of such ratios based on the obtained data can be both under and overprotective. Moreover, regardless of form, Ag caused chronic effects below the current acceptable level as per Ag water quality criteria (3.2mg L^{-1}; USEPA, 2009). This has been highlighted for $AgNO_3$ within previous studies for chronic dietary borne silver but this research is one of the first to also show this with Ag NPs during chronic OECD tests (Zhao and Wang 2011a).

4.5.1 Particle Size and the potential relationship to toxicity

Recently nanoparticle size has been used to explain differences in *Daphnia* species' sensitivity to Ag NPs, as each species has different setae spacing and thus filtering capacities. Smaller daphnids have smaller setae and setulae spacing and are more sensitive to smaller particle or particle agglomerates/ aggregates (Völker *et al.*, 2013 and Zhao and Wang, 2011b).

Despite similar core size of the Ag NPs, mean particle HDD were all different between particle types, thus aqueous suspended physicochemical characteristics were more reliant on particle surface coating than particle core size. In *D. magna* aM7 medium Cit-Ag NPs were the least stable in terms of size and agglomeration/ aggregation characteristics. It was hypothesised this would likely relate to the toxicity presented, as *D. magna* rely on catchment of food between setae and setulae of the filtering apparatus. Similar relationships have been seen by Zhao and Wang (2011b) who showed greater toxicity and uptake with increasing Ag NP aggregate/ agglomerate size. Within this study the space between the setae and setulae was measured of the *D. magna* tested (via SEM) and the smallest particulate matter likely to be captured based on these measurements was ~400 nm (Figure 4.10), therefore a relationship between increasing size and toxicity is logical and to some degree the more big particles present in the medium the more rapid it may be for the *D. magna* to uptake the Ag NP Catchment was confirmed here, with aggregates/ agglomerates of PVP-Ag NP (~1.4µm) imaged trapped within this apparatus which could then be moved to the food groove and gut of the organism. In relation to acute toxicity in this study the more relatively size stable PVP-Ag NPs were the most toxic, not the most agglomerated/ aggregated Cit-Ag NPs which one may assume would be more easily trapped by the filtering apparatus; this observation is also in contrast with previous observations by Zhao and Wang, 2010, and

Völker *et al.,* 2013. This maybe because *Daphnia* are see large particles as undesirable sources of food, and are not digested but excreted. There may also be more than one uptake route aside from feeding such as; Ag NP epipodite binding and, translocation which do not rely on size but chemical binding constants. Völker *et al.* (2013) showed Ag NPs were able to bind to the epipodite on the thoracic limbs of *D. magna* causing a brownish discolouration at high Ag NP concentrations (>20 µg L^{-1}). However, they were unable to observe this at lower concentrations.

When assessing only the results from the chronic toxicity studies, there is some indication that size dynamics may predict the toxicological outcome. The Ag NP with the largest HDD (N.B. all Ag NPs HDDS were inside the *D. magna* feeding range so the largest is likely the easiest to be caught) (i.e. Cit-Ag NP), indicative of higher agglomeration/ aggregation, was also the most toxic. Here, the rank order of toxicity positively correlated to increasing particle size (i.e. size rank order was Cit-Ag NPs>PVP-Ag NPs~PEG-Ag NPs and chronic toxicity rank order was Cit-Ag NPs>PVP-Ag NPs~PEG-Ag NPs). In the current study PEG-Ag NPs were one of the least agglomerated/ aggregated of the 3 NP types, and therefore could likely be the least ingestible and toxic (toxicity often relates to bioavailability) which the data consistently supports. PEG-Ag NPs were also the least toxic in both exposure scenarios which corroborates with previous literature and the filtering capacity theory aforementioned (Völker *et al.*, 2013).

The data showed no consistent rank order of particle toxicity between acute and chronic exposures so consistent conclusions on how particle size relates to toxicity cannot be made. Volker *et al.* (2013) also concluded size and aggregation were not correlated with toxicity despite other studies showing this (Zhao and Wang, 2010). Based on the data to infer particle size in isolation for the prediction and modelling of toxicological events is likely unwise due to the discrepancies displayed between the acute and chronic tests. It is likely that toxicity is a function of a range of characteristics such as size, sedimentation and type of agglomeration/ aggregation. We are somewhat limited as a research community by the fact that we are not able to routinely analyse characteristics at exposure relevant concentrations and particle characteristics at this level may change. Therefore particle size dynamics and behaviour in environmental medium and how these relate to toxicological responses require further investigation at relevant concentrations in relevant matrices to fully understand NP toxicity to aquatic organisms. This has been previously highlighted within the literature (Handy *et al.,* 2012 and

Johnston *et al.,* 2012). Furthermore to understand if uptake is related to toxicity, and is dependent on size, biodynamic studies should proceed and these have been studied in Chapter 5.

4.5.2 Zeta-potential and the potential relationship to toxicity

Zeta-potential shows consistency with toxicity as the particles with zeta-potentials farthest from zero appear to be the 2 most toxic particles (PVP-Ag NPs and Cit-Ag NPs). However, despite similar zeta-potentials the EC_{50}'s are still significantly different between these 2 Ag NPs (2-fold; $n = 2$, d.f. = 1, z = -13.011, $p < 0.0001$). The chronic toxicity also differs between PVP- and Cit-Ag NPs with Cit-Ag NPs being the most toxic NP. Therefore this particle characteristic may also be unable to fully and consistently be related to particle toxicity. This may be due to differing behaviours of the particles after uptake, and their persistence within the organism. Should Ag NPs persist within the organism Ag NP physicochemical characteristics within physiologically relevant medium need to be explored in relation to their eventual toxicity.

4.5.3 Dissolution and the potential relationship to toxicity

Ag^+ is a well-known toxicant for aquatic life. Therefore many authors have hypothesised and shown that Ag^+ release from Ag NPs is responsible for the observed toxicity. However both the acute and chronic data presented here are antithetical to some previous assumptions and reports (Newton *et al.*, 2013, Levard *et al.*, 2012, and Zhao and Wang, 2011b). Newton *et al.* (2013) showed that particle dissolution could account for Ag NP acute toxicity using similar particles to those used here.

In the current study PVP-Ag NP Ag^+ release is relatively low in comparison to PEG-Ag NPs but is still shown to be the most acutely toxic of the Ag NP types tested. Cit-Ag NPs exhibit significantly less acute toxicity than PVP-Ag NPs ($p < 0.0001$), despite similar dissolution, while they are the most toxic in chronic exposures. In no instance were PEG-Ag NPs observed to be the most toxic despite ~10% greater dissolution of these particles compared with PVP-Ag NPs and Cit-Ag NPs. Therefore, Ag^+ release into the water-column could not be used to predict the degree of the Ag NP acute or chronic toxicity to *D. magna*. A few recent papers support this (Stensberg *et al.*, 2014 and Zhao and Wang, 2010) but our data are the first to show an inverse relationship between toxicity and Ag NP dissolution NPs.

The reduced toxicity of both Cit-Ag NPs and PEG-Ag NPs in comparison to PVP-Ag NPs may also be due to higher dissolved Ag re-precipitation at higher concentrations. Precipitation as $AgCl^{(n+)}$/ Ag_nS complexes may cause the dissolved Ag to be less bioavailable either via ingestion or, the epipodite (Levard *et al.*, 2012 and Zhao and Wang, 2010). Furthermore, citrate NP coatings have been shown to dissociate from the NP core and be released into the medium. Subsequently the citrate can bind dissolved Ag released from the NP, reducing its bioavailability (Yang *et al.*, 2012). Therefore NP solubility and interactions with the ligands released from the NP need to be considered. Total Ag^+ release from Ag NPs is currently likely to be a poor predictor of eventual toxicity for modelling purposes.

4.5.4 Potential toxicologcal modes of action (MOA)

As mentioned, the reduction in neonates caused by $AgNO_3$, was caused by a reduction of viable neonates per brood ($p < 0.01$, Figure 4.5). The reduction in daphnid fecundity seen in Cit-Ag NP exposures is due to a late maturation and an eventual early cessation of neonatal production at day 18 not on a neonate per brood basis (Appendix Figure A4.1). Similarly to $AgNO_3$ the hormetic effect caused by PEG-Ag NPs also had a significant effect on the number of neonates per brood but in contrast was an increase. PEG-Ag NPs at the lower tested concentrations appear to have a hormetic effect on reproduction and number of moults and was consistently the least toxic NPs.

The difference in acute and chronic toxicity rankings, as well as differences in observed effects chronically, suggest different MOA for each Ag NP or that complimentary MOA are present but at differing degrees. A change in metal MOA between short and long term exposures has been previously highlighted. Most notably Cu^{2+} acutely affects respiration and ionoregulation at high concentrations (i.e. high enough to cause acute toxic responses), and chronically it can effect endocrine function and block chemosensory function (Adams *et al.*, 2011). It is likely at the nano-scale and with differing coatings such changes in acute and chronic MOA of silver toxicity may also occur, although classically Ag^+ toxicity MOA acutely and chronically does not differ (Adams *et al.*, 2011). For example the acute toxicity of Ag NP may be due to epipodite interaction much the same as Ag^+ and Cu^{2+} (Adams *et al.*, 2011 and Bianchini and Wood, 2003).

Acutely, toxicity maybe due to the difference in bioavailability and binding affinity of the Ag form and Ag NP coating to the target ligand. Therefore acute toxicity may be

rather biased toward reaching a level of saturation at the water-epipodite interface and disturbing such biological ligands as Na^+, K^+-ATPase which causes eventual ionoregulatory or respiratory failure. For any Ag form with lower affinity for the ligand the Ag concentration within the water column would need to be higher to reach the same levels of saturation to cause the same effect. Previous studies support saturation at higher concentrations, where similar effects between dissolved Ag and Ag NP were seen on *D. magna* ionoregulatory capacity and mortality, but the latter effects were seen at higher concentrations (Völker *et al.*, 2013 and Zhao and Wang *et al.*, 2013). These high concentrations needed to cause critical levels of saturation would only occur at relatively high levels of Ag NPs and thus is a rather unlikely environmental scenerio. Knowing the MOA for acute toxicity may not suitably support regulatory or industrial decision making for chronic exposure periods. Instead further investigation into the MOA of both exposure periods is required for modelling purposes and the discovery of common themes or differences between particles and exposure duration.

Ag NP chronic toxicity may be due to a particular MOA which affects the organism at more than one level through varying biochemical perturbations much the same as Cu^{2+} (Adams *et al.*, 2011). Thus accumulation at other biotic ligands may become more important such as in the gut, which has previously been shown to accumulate Ag NPs (Zhao and Wang 2011a). In one previous study the same change in sequence of chronic toxicological events as shown in this study has also been seen between $AgNO_3$ and PVP-Ag NPs (Zhao and Wang, 2011a), where growth was significnatly reduced before reproduction for Ag NP exposures and the opposite was seen for $AgNO_3$ exposures. Studies of population dynamics show that under starvation energy stores are used to support maintenance, reproduction and growth, in this order of priority, similar to the sequence of events seen in the PVP-Ag NP exposures i.e. overall length is reduced before reproduction. This ensures survival of the population and species, and opportunity for adaptation to the new environmental stressors. Such reactions ensure fitness of the population over the individual. Although it is unknown whether the length directly impacts the *Daphnia*'s susecptibility to prey, or ability to feed. In both instances this will affect the ecological balance of the freshwater environment. Thus, this short term solution may have long term impacts that have not been assessed here. The balance change may cause increased algal blooms due to not predation of algae and increased acidity of the freshwater environment leading to an unlivable ecosystem for many species. Cit-Ag NPs early cessation of reproduction also suggests inadequate

energy stores. The current study has shown significant effects on all life-cycle parameters during starvation likely to ensure organism maintainance and survival. However, as only one ration level was used in this instance it was not possible to establish which parameter would be effected first during times of limited food resource.

Although several energy allocation models exist for daphnid species all models recognize the priority for reproduction over growth as the daphnid ages (Nisbet, McClauley and Johnson, 2010, and Kooijman, 1986). However, when interpreting such results and basing effects on population dynamics there needs to be an appreciation that this allocation of energy can be size, clone and age dependent. The energy allocation shift may again cause decreased reproduction and an imbalance in the food web, with ecological consequence as aforementioned. It is possible that after uptake Ag NPs may cause some form of nutrient inhibition at the gut lining causing a similar reaction to starved populations rather than that of disturbed ionoregulation, and this 'gut load' would increase over time should uptake rate surpass excretion of the Ag NP (Zhao and Wang 2011a). During waterborne only exposures Ag NPs may competively inhibit food uptake processes and this has been shown or suggested as a mechanism of action for both Ag NPs and TiO_2 NPs (Campos *et al.*, 2013 and Zhao and Wang 2011a). NPs may also reduce the function of nutrient uptake sites rather than block them (Heinlaan *et al*., 2011 and Zhao and Wang 2011a). Au NPs and CuO NPs have both been shown to bind to the peritrophic membrane and microvilli of the *Daphnia magna* midgut and in the latter case they have induced ultrastructural changes and increases in bacterial colonization which are implicated in there toxicity and exclusive to NPs (Khan *et al*., 2014 and Heinlaan *et al*., 2011). As Ag^{+} and Cu^{2+} work through a similar MOA the same may be true for there NP counterparts.

Another explaination – and one gaining popularity – for this decrease in energy reserves is that uptake may lead to Trojan-horse mechanisms (Park *et al.*, 2010). In this instance the Ag NP is taken into the cell/ organism where a bolus internal dose of Ag ions is released. These act differently after uptake in comparison to the uptake of ions alone and the Ag^{+} may localise in areas in which they are not usually found within the organism. For example recently published data have shown the possible effects of Ag NPs on mitochondrial health within *D. magna*. This effect can create an energy deficit within the *D. magna* and can cause damage to important cellular structures as well as other perturbations contraindicated to organism health. Such an effect would in turn cause a pseudo-starvation effect (Stensberg *et al.*, 2014 and Park *et al.*, 2010). Here

energy deficit is caused by the inability to undergo efficient resperation (i.e. produce energy via aerobic pathways) again causing similar organism effects as seen in the Ag NP exposures. MOA involving energy disturbance leading to mortality have been seen in the bacteria *Escherichia coli* (bacteria produce energy in a similar manor to mitochondria), human lung fibroblast cells (IMR-90) and human glioblastoma cells (U251) subjected to Ag NPs (Poynton *et al.*, 2010, AshaRani *et al.*, 2009a, AshaRani *et al.*, 2009b, Choi *et al.*, 2008). However biochemical studies would be needed to elucidate such a MOA in *D. magna* and in later chapters this will be explored (Chapter 6).

Chronically only PEG-Ag NPs and $AgNO_3$ were shown to significantly affect moulting, PVP-Ag NP exposures did induce some disturbance qualitatively by failure of the daphnids to properly moult. The regulation of moulting may be dependent on cations such as Ca^{2+} and thus its distrubance leads to effects on the shedding of the carapace (Zhao and Wang 2013). The effects on length, which are seen more consistently for Ag NP treatments than the reduction of reproduction, may also be as a result of calcium distrubances (Zhao and Wang 2013 and Hessen, Alstad and Skardal, 2000). Measures of Na^+, K^+ and Ca^{2+} in the organism may provide further detail on MOA and warrant investigation and are explored in Chapter 6.

An interesting effect seen during the chronic exposures was the hormetic effect that PEG-Ag NPs had. The increase in daphnids per brood may be in an attempt to ensure surivial of the population and species, and population dynamic theories support this (Nisbet, McClauley and Johnson, 2010, and Kooijman, 1986). Furthermore it is well known that PEG can act as a dense source of carbon and thus may have provided the daphnids with enough energy for increased reproduction (Arndt *et al.*, 2014). It may be that the small amount of Ag NP acted to decrease harmful bacteria or pathogens creating a more optimal environment for the *D. magna* (Marambio-Jones and Hoek., 2010). The increase in moulting may be due to attempts to increase depuration of the Ag NPs.

Although $AgNO_3$ was consistently ranked as the most toxic exposure condition with respect to all Ag NPs, Cit-Ag NP and PVP-Ag NPs rank orders differ between acute and chronic exposures, this would unlikely be the case if only one MOA was responsible for the toxicities shown, therefore each of the aforementioned theories must be given equal consideration in future studies. Furthermore the relative contributions of

these MOA may begin to explain how Ag NP toxicity differs from Ag^+ toxicity and why discrepencies sometimes appear in Ag NP toxicity testing. Ensuing chapters will explore these issues (Chapter 5 and 6).

4.6 Conclusion

The *D. magna* study is one of few to make an in-depth attempt to relate various Ag NP characteristics and behaviours, other than dissolution, to their eventual acute and chronic toxicity. It is also one of the first studies to consider implications of using acute toxicity data for predicting chronic effects for risk assessment processes. The data clearly demonstrates that using simple ratio conversions of acute data sets may lead to both over and under protection; within this study for PVP-Ag NPs and Cit-Ag NPs, respectively. The study is also one of only a few to observe chonic effects of Ag NPs (Mackevica *et al.*, 2015, Ribeiro *et al.*, 2014, Völker *et al.*, 2013 and Zhao and Wang 2011a).

To aid in well advised and informed nanotechnologies based on "good science" to reduce environmental impact, modelling based on nanoparticle toxicity assumptions must progress. If we look to base predictions of toxicity on physicochemical characteristics the best approach will likely be to assess a combination of these physicochemical characteristics as well as core material characteristics and their respective contribution toward the acute and chronic waterborne toxicity. In this way no direct physicochemical characteristic common themes with toxicity have been derived by this study but the paper has highlighted how important it remains to assess NPs on a case by case basis until a wide pool of data is available. However, it is appreciated assumptions based on physicochemical characteristics may eventually be possible by taking account for each property (e.g. coating, core size etc.) in much the same way Ag^+ models deal with varying levels of water hardness, for example. The study also showed that toxicity models and predictions should factor for physicochemical changes casued by NP coating; the issue again arises when extrapolating data from acute to chronic toxicity or vice versa as data can be inconsistent. Regardless, the importance of particle coating still seems to far outweigh any other characteristic. In terms of deriving common themes the field is somewhat limited by its ability to accurately assess NP behaviour and their physicochemical characteristics at relevant concentrations within relevant matrices. Furthermore should

mechanisms after uptake be responsible (i.e. Trojan-horse mechanisms) a more in-depth knowledge of particle behaviour physiologically would need to be established, such as within the gut or cellular environment. Research into NP behaviour within physiologically representative medium should be pursued to aid in this area (Stone *et al.*, 2014).

Although acute tests can provide a quick glance at the potential toxicity of any NP extrapolating these data to effects observed during chronic exposures is ill-advised due to the inconsistencies seen in rank order and the potential differing MOA. These limitations often make correlations difficult and cause inconsistencies in interpretations, therefore it is currently suggested commonalties should be derived from other more established and accurately measured ecotoxicological endpoints such as critical biodynamic values and biochemical analysis rather than focusing on the particle physicochemical characteristics themselves. The study further contributes to the generation of data for risk assessment and modelling purposes.

Chapter 5.

The Application and Suitability of Biodynamic and Biotic Ligand Modelling in Silver Nanoparticle Toxicity Assessment

5.1 Introduction

The biodynamic model (Luoma and Rainbow, 2005) allows the determination of individual unidirectional uptake and elimination (efflux) rate constants from food and water. Although this model is used to quantify these processes in tandem the BDM can be modified to assess unidirectional processes of each separately (Khan *et al.,* 2013). The sum of these uptake processes and their respective efflux rates allow steady state body burdens (at defined concentrations) and critical exposure levels (i.e. exposure level which leads to uptake outweighing efflux) to be quantified. Currently the main body of work on freshwater metal NP accumulation frameworks has been conducted on benthic invertebrates (Croteau *et al.*, 2014b, Oliver *et al.*, 2014, Khan *et al.*, 2012 and Croteau *et al.,* 2011) with little research done on their pelagic counterparts (Zhao and Wang, 2010). Previous literature has demonstrated that Ag^{+} uptake from the environment is consistently faster than that of Ag NPs irrespective of whether the metal is from waterborne or foodborne exposures; likely due to the Ag^{+} higher affinity for biological ligand(s) (Khan *et al.,* 2012, Croteau *et al.*, 2011 and, Zhao and Wang, 2010). One previous study has focused on *Daphnia magna* toxicity and accumulation and showed that Ag NP uptake was 4.3 times slower than Ag^{+} (Zhao and Wang, 2010). However, during diet-borne exposures Ag NPs assimilation efficiency (AE) was higher than that of Ag^{+}. AE is defined as the percentage component of a contaminant which has incorporated with the organism via cellular uptake or strong adsorption to a physiological surface. Using biokinetic modelling these authors suggested that dietary uptake of Ag NPs may be more important than the waterborne uptake accounting for 70 and 30% of the Ag NP ingestion, respectively (Zhao and Wang 2010). The dietary route of exposure is now generally accepted to be one of the most important uptake routes for trace metal accumulation in a many aquatic species, and thus this may also be the case for metal NPs and warrants further investigation (Croteau and Luoma 2009). During diet-borne exposures Croteau *et al*. (2011) showed that efflux (k_e) similarities between ZnO NPs and Zn^{+} may be indicative of a common physiological fate of both within *Lymnaea stagnalis* after uptake. Similarly slow phase efflux for Ag NPs was

found to be no different in comparison to Ag^+ slow phase efflux of *Lymnaea stagnalis* again possibly highlighting the same physiological fate (Croteau *et al*., 2011). The implications of diet-borne transfer (i.e. trophic transfer) and possible biomagnification cannot be overlooked when assessing overall impact of a contaminant on the health of the environment. After waterborne and diet-borne biodynamics are defined it becomes pertinent to establish their impacts both separately and together in order to best inform risk assessment. Furthermore defining the relative contribution from each environmental partition may allow for such models to be simplified when one uptake pathway prevails, thus is paramount to inform regulators for the simplest *in silico* model development to ensue (Croteau and Luoma 2009).

For trace metals, accumulation is said to be proportional to toxicity, such as short term accumulation at the site of uptake, as proposed by the biotic ligand model (BLM; Di Toro *et al*., 2001; Paquin *et al*., 2002). However a similar relationship between accumulation and toxicity has not been fully investigated for Ag NPs. Modelled values for Ag NPs such as the lethal accumulation 50 (LA_{50}; where the level of a toxicant within an organism causes 50% mortality of the population) and Log *K* (ligand binding strength) are not fully elucidated limiting advancements of regulatory and risk assessment frameworks. Although some studies have been key for investigating *D. magna* Ag NP accumulation they used a limited range of concentrations and particles meaning it is difficult to derive biological ligand saturation (B_{max}), and particle characteristics (e.g. core, coating and charge) which may change their accumulation and toxicity. If models such as the BLM are to aid risk assessment and regulation of Ag NPs, as they have for metals, then it is important that modelled relationships be verified whether it be accumulation, Log *K* or a combination of parameters.

The BLM frameworks are founded on the fundamental principle that metal accumulation can be the main predictor of toxicity. By using the BLM and BDM frameworks it is possible to hypothesise the physiological fate and behaviour of a toxicant in relation to another. Using ligand binding constants (i.e. k_d (binding affinity), B_{max} and Log *K*), the BLM relates short term accumulation (the LA_{50}) at the site of uptake/ interaction (i.e. the 'biotic ligand') to toxicity (usually acute toxicity where the exposure concentration results in 50% mortality) (Di Toro *et al*., 2001 and Paquin *et al*., 2002). The strength of BLM model is that it is able to account for local water

chemistries when assessing potential risks of a xenobiotic to the environment by using such chemical speciation models as WHAM V and CHEMQL+ (Paquin *et al.*, 2002 and Niyogi and Wood 2004). The BLM revolves around traditional pharmacokinetic principles (e.g. Michaelis-Menten Kinetics) that are inherently related to the toxic response of an organism, tissue and/ or cell. For instance, the fish gill Log *K* values of Ag^{+} and Cu^{+} are 10.0 and 7.4, respectively, and therefore Ag^{+} is regarded as the more toxic metal (Niyogi and Wood, 2004). It is well known that metal interaction with the biotic ligand, or organism as a whole, is influenced by water chemistries of the surrounding water bodies (e.g. alkalinity, water hardness, the presence of complexing waterborne ligands (such as anions and dissolved organic matter (DOM)); Niyogi and Wood, 2004) and these interactions can then impact their binding site constants and thus their level of toxicity. When a binding affinity of a biological ligand is stronger than the affinity for waterborne debris and water ligands then accumulation at this biological site can occur, further to this, in the case of *Daphnia magna*, should the contaminant bind to waterborne debris, DOM or food (i.e. algae) this solid may be easily filtered and ingested. Furthermore the smaller the species within a phyla or the lower the B_{max} the more sensitive the organism is likely to be as the limit of saturation is lower but the biological binding site and, thus binding constants, will be the same. An obvious caveat to any such approach is the internal detoxification of metals through sequestration into metallothionien complexes or metal rich granules which, although result in high tissue body burdens, renders the metals biologically inactive and incapable of causing adverse effects (Luoma *et al.*, 2009).

Studies have demonstrated Ag NP toxicity to both freshwater pelagic and benthic organisms; however, there is currently limited data on Ag NP biodynamics for *Daphnia magna*. To our knowledge only two studies address *Daphnia magna* biodynamics, however, although these studies report waterborne and dietborne accumulation neither study report critical values essential for *in silico* model development. Zhao and Wang (2010) have shown size specific increases in Ag NP accumulation with decreasing size of the Ag NPs to *Daphnia magna.* This is due to their increased propensity to aggregate/ agglomerate allowing easier catchment by the organism related to setae and setulae spacing size (spacing of these features can be seen in Chapter 1 Figure 1.2 and Chapter 3 Figure 3.9). Conversely Levard *et al.* (2012) have shown a decreased toxicity of Ag NPs upon hetero-aggregation/ complexation with sulphides in freshwater environments likely due to flocculation leading to less uptake or biological inactivation

of the Ag NP. Indeed the physicochemical properties of metals, and some NPs, and their behaviour within the aquatic environment are known to affect their toxicity and bioavailability (Khan *et al.*, 2012). Therefore these characteristics may be integral in predicting metal NP toxicity and accumulation dynamics in the same manner as trace metals.

5.2 Aims

Considering the success of the BDM and BLM models for trace metal aquatic organism toxicity and biological interaction prediction, and the possible similarities between trace metals and Ag NPs, this study aims to use these approaches for assessing and predicting Ag NP toxicity. Within this chapter the research aims to investigate the waterborne toxicity and accumulation, and diet-borne accumulation dynamics of $AgNO_3$ and 3 differently coated Ag NPs. Accumulation dynamics were determined in accordance with the principles of the previously mentioned biodynamic model (Luoma and Rainbow, 2005). Traditionally for trace metals uptake rate constants were derived from 2 partitions that of food and water. Here the study first aims to derive the BDM parameters in their own right separately before considering their impact together. Using experimentally derived rate constants of uptake and efflux, the study aims to model accumulated tissue burdens. For the waterborne Ag NP BDM model scenarios exposure concentration were set at, or close to, the *Daphnia magna* EC_{50} (described in the methods and in Chapter 4) and the research aimed to derive the relationship between calculated short-term tissue burdens, ligand binding constants and toxicity through the BLM framework. For the foodborne BDM the algae *Chlorella vulgaris* was used as the dietary vessel for *D. magna* exposed to Ag NPs through diet, and the organism was exposed to the spiked food for 40 minutes to 24 hours. The 40 minute time point was used to establish 100% possible burden before any defecation/ gut purging took place. After uptake a depuration period of the *D. magna* the study aimed to derive assimilation efficiency and efflux during spiked food exposures (k_{ef}). To establish body residues here rather than the traditional use of EC_{50} data to derive LA_{50} for waterborne toxicants the study aims to calculate the steady state burden in the context of predicted environmental exposures from this partition.

The main aims of the current study were to characterize the accumulation dynamics in *Daphnia magna* and the appropriateness of the current trace metal models in their original form for use with Ag NPs. The research presented herein is critical to the aforementioned knowledge gaps and begins to answer many pertinent questions such as, are there differences in toxicity and accumulation dynamics between exposures, does toxicity and accumulation dynamics relate to the dissolved fraction of Ag NPs and/ or a nano-specific effect, and finally can the BLM and BDM in part, or in full, be applied successfully for Ag NP assessment and regulation?

5.3 Methods

5.3.1 Organisms

Daphnia magna acquisition and husbandry has been discussed in Chapter 2.

5.3.2 Nanoparticle synthesis and stocks

Nanoparticle synthesis and stocks were reported in Appendix Text A2.1, Chapter 2 and 3. The tested Ag NPs were ~10 nm Cit-Ag NP, PVP-Ag NPs and PEG-Ag NPs, $AgNO_3$ was tested in parallel.

5.3.3 Characterisation

Physicochemical characteristics were reported in Chapter 3.

5.3.4 Toxicity tests

For acute toxicity tests ~5-6 day old *Daphnia magna* were used to represent the age of the organisms that were collected for metal analysis. Older organisms were used due to their larger size so metal recoveries would be greater allowing analysis of silver by ICP-MS. Acute toxicity was derived in non-fed semi-static waterborne exposures as per OECD guidelines (OECD, 2008). For the acute toxicity assessment daphnids were exposed to 7 concentrations per experimental exposure group (i.e. $AgNO_3$, PEG-Ag NP, PVP-Ag NP and Cit-Ag NP) in triplicates with one control group. *D. magna* were seeded at a density of 1 daphnid/ 4 mL of aM7 medium with 10 organisms per replicate. Immobilization (%) was measured at 48 hours. Please refer to Chapter 4 for detailed results (Section 4.4) and methods (Section 4.3).

5.3.5 Waterborne exposure: uptake and efflux

Exposures for establishing uptake rates in *Daphnia magna* lasted 24 hours. The organism was exposed to a range of Ag NP or Ag NO_3 concentrations. Maximal dose was set at, or around, the organisms 48 hour EC_{50}, to ensure the best chance of reaching ligand saturation over a 24 hour period. The concentration ranges were; 0-51.0 nmol L^{-1} (0-5.5 µg L^{-1}) PVP-Ag NPs, 0-167.0 nmol L^{-1} (0-18 µg L^{-1}) PEG-Ag NPs, and 0-68.6 nmol L^{-1} (0-7.5 µg L^{-1}) Cit-Ag NPs.

For efflux studies *Daphnia magna* were again exposed for 24 hours but only to a single dose set at, or around, the organisms 48 hour EC_{50} to ensure measurable Ag recovery (via ICP-MS) after exposure without causing mortality; 37.1 nmol L^{-1} (4 µg L^{-1}) PVP-Ag NPs, 162.3 nmol L^{-1} (17.5 µg L^{-1}) PEG-Ag NPs, 69.8 (7.5 µg L^{-1}) Cit-Ag NPs. This exposure was followed by a 5 day depuration period where remaining internal body burdens were measured at 0, 0.33, 1, 2, 3, 4, and 5 days; triplicate groups of 20 individual *D. magna* were collected at each sampling time-point. At each depuration time-point organisms were washed and transferred into clean medium to remove weakly bound Ag and stop re-ingestion or association of the NP from faecal matter. For both uptake and efflux exposures, immediately after removing the organism for analysis, the organisms were washed in Milli-Q water to remove any weakly associated Ag NPs or Ag from their surface and transferred into Eppendorf tubes. Wet weights were immediately taken once the organisms were placed in the Eppendorf tubes (Khan *et al.*, 2015). Dry weights were unobtainable as *D. magna* are only 5-10% dry weight and thus a dry to wet weight ratio of 8% was applied to the wet weight obtained (Smirnov 2013 and Peterson *et al.*, 2009). During the depuration daphnids were fed a diet of *C. vulgaris* at of 5 x 10^5 cells mL^{-1}.

Parallel to all Ag NP exposures, control exposures were conducted (i.e. 0 µg L^{-1} Ag) to ensure that there was no inadvertent contamination from the experimental conditions used. In addition, a sample of organisms was sacrificed to measure the initial background Ag burden. The background concentration was subtracted from the measured Ag concentration in each experimental sample. As waterborne Ag^+/ $AgNO_3$ BDM and BLM frameworks are already well established within the literature it was possible to obtain critical modelling values from published research (Lam and Wang 2006 and Bury *et al.*, 2002; see Table 5.1).

5.3.6 Foodborne exposure: assimilation efficiency and efflux

D. magna were exposed to silver through a foodborne diet of $AgNO_3$ and the 3 Ag NPs separately. The algae used were *Chlorella vulgaris*. The alga was exposed to $AgNO_3$ and the Ag NPs, separately for 4 hours at 250 µg L^{-1} and 2000 µg L^{-1} of silver, respectively, to create the spiked food stocks. To remove weakly bound Ag from the surface of the algae the *Chlorella vulgaris* was centrifuged to separate it from the silver containing medium. After the initial centrifugation the algae was then washed 3 times by the addition of Milli-Q water, and subsequent centrifugation (at 2,680 g; Jouan C3i centrifuge) which was followed by the removal of the supernatant and subsequent re-suspension. After the final wash the algae was suspended in aM7 medium and a ratio of non-spiked:spiked food was supplied to the organism at a cell density of 5 x 10^5 cells mL^{-1}. The spiked food was diluted with non-spiked food to ensure there was no organism mortality. A total of 60 organisms per replicate vessel were used at a density of 4 mL of medium per organism, each exposure were performed in triplicate. After 40 minutes of exposure to the spiked food the daphnids were collected to establish 100% uptake without the possibility of re-feeding or gut purging of the Ag for each exposure. For the AE and efflux rate of Ag consumed from food sources (k_{ef}) daphnids were exposed for 24 hours to; $AgNO_3$, PVP-Ag NPs, PEG-Ag NPs or Cit-AgNPs spiked food. The exposure was followed by a 4 day depuration period where remaining internal body burdens were measured at 0, 0.04, 0.08, 0.16, 0.24, 1, 2, 3 and 4 days; triplicate groups of 60 individual *D. magna* were collected at each sampling time-point. At each depuration time point organisms were washed and transferred into clean medium to remove weakly bound Ag and stop re-ingestion or association of the NP from faecal matter. For both uptake and efflux exposures, immediately after removing the organism for analysis, the organisms were washed in Milli-Q water to remove any weakly associated Ag NPs or Ag from their surface and transferred into Eppendorf tubes. Wet weights were immediately taken once the organisms were placed in the Eppendorf tubes. Dry weights were unobtainable as *D. magna* are only 5-10% dry weight and thus a dry to wet weight ratio of 8% was applied to the wet weight obtained (Peterson *et al.,* 2009 and Smirnov 2013).

5.3.7 Sample analysis

Tissue sample analysis was carried out at the Natural History Museum and Edinburgh University. Tissue samples from the uptake and elimination studies were dried until reaching a constant weight at 80 ˚C (~72 hours), weighed and subsequently digested in 100 µL concentrated analytical grade nitric acid (Aristar grade, VWR, UK) at 100 ˚C. Samples were made up to 5 mL with 2% nitric acid and the Ag concentration was determined by ICP-MS at the Natural History Museum (waterborne exposure samples) and Edinburgh University (diet-borne exposures) (Varian 810, Agilent Technologies, Santa Clara, CA). Procedural blanks were used (HNO_3 only digests) in both instances to account for any background Ag used within this method. A certified reference material NIST-1566b (oyster tissue, National Institute of Standards and Technology, US Department of Commerce; waterborne exposures) was also analysed alongside samples to ensure the ICP-MS was working correctly throughout (i.e. measuring the right chemical quantities). Furthermore 3 Ag standards were measured every 15 samples and an internal standard solution (indium for Ag NP waterborne exposures and rhodium for food-borne exposures; institution dependent) was added at 1% of the final solution volume to ensure the ICP-MS did not drift skewing the results. All Ag tissue concentrations are expressed as nmol g^{-1} (dw).

5.3.8 Biodynamic modelling and membrane transporter characteristics

Biodynamic models deconstruct bioaccumulation into singular unidirectional processes of uptake and loss from water and food (and growth where appropriate) which can be experimentally derived. The full model is described in detail by Luoma and Rainbow, 2005. The present study determined uptake (k_u) and efflux (k_e) rate following waterborne and foodborne exposures. Rate constants were used to model toxicologically relevant accumulated tissue concentrations at the LC_{50} i.e. the LA_{50}. In the biodynamic model, the uptake of Ag from solution/ suspension is expressed as a function of the unidirectional uptake rate constant k_u (in L g^{-1} d^{-1}), the exposure concentration (C_w in nmol l^{-1}) and exposure duration (t in d^{-1}).

$$Ag_{Influx} = C_w . k_u . t \qquad \text{(eq 5.1)}$$

The efflux rate constant, k_e, was calculated from the change in Ag tissue concentration over the depuration period following exposure (eq 5.2), where $[C]_{org}$ is the Ag concentration (nmol g^{-1}) at the time points during efflux, $[C]^0_{org}$ is the Ag concentration

(nmol g^{-1}) at the start of the efflux period (i.e. concentration at zero days depuration), k is the rate constant of loss per day (d^{-1}), and t is depuration time in days (d). The slope formed by the points of $[C]_{org}$ and $[C]^0_{org}e^{-ket}$ represents the rate constant for loss (k_e in d^{-1}), where $[C]^0_{org}e^{-ket}$ is the % depuration at time (t) expressed as its natural logirithm.

$$[C]_{org} = [C]^0_{org}e^{-ket} \quad \text{(eq 5.2)}$$

To calculate the LA_{50} used within the BLM as a predictor of the EC_{50} in this study eq. 5.3 was used where k_u, was the uptake rate constant for each Ag form, C_w the water concentration at the EC_{50} of each form and t was set to 48 h; i.e. the accumulation at the end of the acute toxicity test and thus its related burden. To fully model the tissue accumulation of Ag at this time (i.e. the Ag concentration in the organism at the EC_{50} at 48 hours) it is necessary to account for loss. Although metal accumulation for many species can be calculated using the one-component loss model, the physiological loss of accumulated Ag in *D. magna* is bi-phasic. This is defined by fast (high efflux rate over a short period) and slow (low efflux rate during longer depuration periods) elimination phases. To calculate accumulation of Ag following exposure at the EC_{50} using a one-component model, the loss term $1-k_e$ can be added to eq 1 (eq 5.3):

$$\text{Ag Accumulation at } EC_{50} = C_w.\ k_u.(1-k_e).t \quad \text{(eq 5.3)}$$

However to predict the Ag accumulation in daphnids exposed to dissolved Ag and Ag NPs, the single efflux component in equation 5.3 must be separated into 'fast' and 'slow' phases, where k_{e1} is the fast efflux rate constant for the proportional duration of the fast elimination phase (t_1), k_{e2} is the slow efflux rate constant for the proportional duration of the slow elimination phase (t_2). Here t is the total exposure time, and C_w and k_u remain as the EC_{50} and uptake rate constant, respectively (eq 5.4).

$$\text{Ag Accumulation at } EC_{50} = C_w.k_u.t.(1-((k_{e1}.t_1) + (k_{e2}.t_2))) \quad \text{(eq 5.4)}$$

Metal influx ($Influx_{org}$ in nmol g^{-1} d^{-1}) at the site of uptake (in this instance the whole *D. magna*) following waterborne exposure can also be interpreted in terms of membrane transporter characteristics (eq. 5.5) based on traditional pharmacokinetic principles. Here B_{max} is the binding site capacity for the metal (in nmol g^{-1}), k_d is the transporter affinity of the metal for each binding site (in nmol g^{-1}) from which the Log K is derived as an affinity constant which is the strength of this binding to the binding site, and $[M]_{exposure}$ is the exposure concentration (nmol l^{-1}) (Niyogi and Wood, 2004).

$$Influx_{org} = B_{max}.[M]_{exposure} / k_d + [M]_{exposure} \quad \text{(eq. 5.5)}$$

Foodborne biodynamics were also established for each Ag exposure using traditional BDM methods (eq 5.6). AE is the assimilation efficiency (%) of the metal from the ingested food, C_f is the metal concentration in food (nmol g^{-1}), IR is the ingestion rate of food (g g^{-1} d^{-1}), and k_{ef} is the efflux rate constants of foodborne particles (d^{-1}). In this study the ingested food is either non-spiked or $AgNO_3$/ Ag NP spiked *Chlorella vulgaris*.

$$\text{Accumulation from Food-borne Ag} = (AE.\ IR\ .C_f)/\ (k_{ef}) \quad \text{(eq 5.6)}$$

The complete equation to establish steady state body burdens (C_{ss}) based on Ag exposure concentrations then becomes the contribution of uptake, assimilation, ingestion and excretion from water and food exposure from each respective part of the model using BDM principles seen as eq 5.7.

$$C_{ss} = ((C_w.k_u)/\ k_{ew})) + ((AE.\ IR\ .C_f)/\ (k_{ef})) \quad \text{(eq 5.7)}$$

From this equation it is also possible to predict steady state tissue concentrations from predicted Ag NP environmental concentrations of the freshwater water-column (i.e. water exposure) and the suspended material (i.e. that which the daphnid feeds upon) as well as the relative contribution and importance of each to the overall body burden (Kalman *et al.*, 2010).

5.3.9 Statistical analysis

Statistical methods have been previously discussed (Chapter 2). To determine EC_{50} the trimmed Spearmen-Karber method was used.

To determine which of the waterborne modelled or derived parameters (i.e. short term accumulation (LA_{50}) and binding site affinity strength (Log *K*); and uptake rate constant (k_u), respectively) best explained toxicity a two-step analysis was undertaken. Firstly, Pearson's correlation was used to investigate the linear relationship between each parameter and toxicity. For this analysis data (except for Log *K* values) were Log_{10} transformed for linearity. Pearson's correlations were significant, but not meaningful as significance was typically dependant on clusters of data-points at either end of the regression rather than consistent correlations (described in the results). Therefore Kendall's tau-b test was instead used to determine the concordance between the rank

orders of toxicity and the aforementioned parameters. Kendall's tau-b coefficients range from -1 to 1 denoting perfect inverse and direct correlations (concordance) between ranked data. This rank test has been shown to be preferable to Spearman's rho particularly when analysis is conducted with smaller datasets (Field, 2009 and Broitman *et al.*, 2004). Here analysis was performed for both $AgNO_3$ and Ag NPs together and the Ag NP data alone. This allowed the investigation whether the rank orders of the modelled or derived parameters could be used as general predictors of toxicity and whether this was consistent across Ag form or if some of the relationships were more driven by one Ag form than another; possibly skewing interpretations. Kendall's tau-b analysis was conducted on untransformed data.

5.4 Results

5.4.1 Acute toxicity tests

Toxicity of all exposures to 5-6 day old juveniles has been mentioned previously (Chapter 4). Briefly; EC_{50}'s for each acute exposure were 1.1 ± 0.1, 5.9 ± 1.7, 8.5 ± 1.1, and 13.4 ± 1.5 μg L^{-1}, for $AgNO_3$, PVP-Ag NPs, Cit-Ag NPs and PEG-Ag NPs, respectively. Please visit Chapter 4 for more detailed analysis. These values will be used to obtain critical body burdens using BDM and BLM principles.

5.4.2 Waterborne uptake of $AgNO_3$ and Ag NPs by *D. magna*

The background Ag concentrations in laboratory cultured *D. magna* was 4.4 ± 0.95 nmol Ag g^{-1} (dry weight; dw) (0.48 ± 0.1 μg Ag g^{-1} (dw)), n = 3 pools of 20 individuals). The uptake rate constant from solution/ suspension (k_u ± 95% C.I.) for each Ag form was determined by the slope of the linear relationship between unidirectional (1 d) Ag influx into the organism and the exposure concentration. PVP-Ag NP exposure resulted in the highest uptake rate constant of the three NPs with *D. magna* (k_u 1.65 ± 0.56 L g^{-1} d^{-1}), which was approximately 2 and 6 fold faster than Cit-Ag NPs and PEG-Ag NPs, respectively (Figure 5.1, Table 5.1). A k_u value of 6.20 ± 0.07 L g^{-1} d^{-1} for dissolved Ag exposure (derived from Lam and Wang, 2006) indicated that $AgNO_3$ was the most bioavailable form.

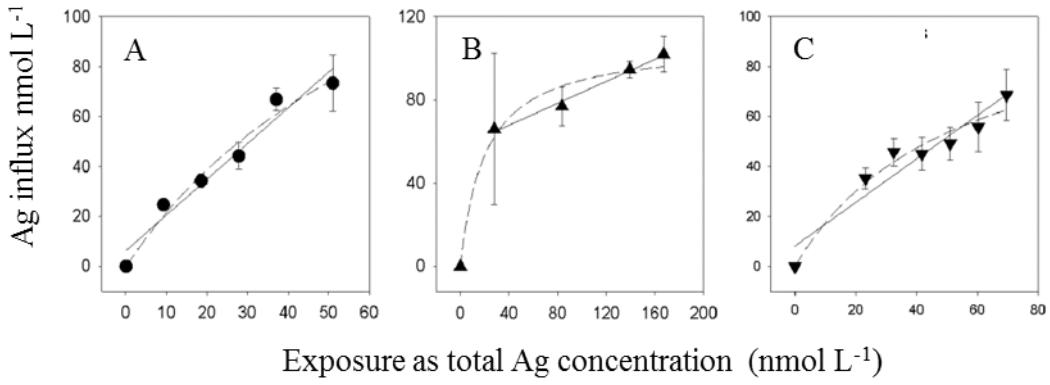

Figure 5.1 *Daphnia magna* uptake rates after 1 day of waterborne exposure to PVP-Ag NPs, PEG-Ag NPs and Cit-Ag NPs. Mean tissue concentrations (nmol g^{-1} (dry weight) d^{-1}) ± S.D., n = 3) are shown following the subtraction of background Ag concentration. Linear regression (solid line) was used to determine the uptake rate constants (L g^{-1} d^{-1}). Nonlinear regression (Michaelis−Menten) fits were used to derive metal binding characteristics.

Ag uptake generally demonstrated saturation at the higher exposure concentrations (Figure 5.1). Non-linear (Michaelis-Menten) regressions were used to determine the binding site density (B_{max}) and ligand binding affinity (k_d) from which the ligand binding strength constants (Log K) were derived (Table 5.1). B_{max} values (the biological maximal saturation of the ligand/ organism in question) were ~200 (Lam and Wang, 2006) 186 ± 67, 108 ± 9 and 111 ± 26 nmol g^{-1} for $AgNO_3$, PVP-Ag NPs, PEG-Ag NPs and Cit-Ag NPs, respectively (Table 5.1). The binding maximum can vary based on affinity and the binding sites available to the chemical or particle in question, hence these values are not the same. k_d (ligand binding affinity) values were 1.25 (Lam and Wang, 2006) 76 ± 41, 20 ± 8 and 54 ± 24 nmol L^{-1} for PVP-Ag NPs, PEG-Ag NPs and Cit-Ag NPs, respectively (Table 5.1). Rank orders of Log K values were $AgNO_3$ (8.9, Bury *et al*., 2002)) > PEG-Ag NPs (7.7 ±0.2) > Cit-Ag NPs (7.3 ± 0.2) > PVP-Ag NP (7.1 ± 0.2) (Table 5.1). k_u, B_{max}, and k_d all followed a similar rank order to toxicity (i.e. an inverse relationship with EC_{50}). However in a risk assessment and BLM context the most pertinent parameters are k_u and Log K and therefore further analysis will be conducted on these variables, this is because body burdens are usually a function of both these parameters (e.g. high Log K high binding strength lower rates of loss lead to higher burdens and more rapid k_u leads to more rapid accumulation).

5.4.3 Loss of waterborne accumulated silver nanoparticles and silver nitrate

During depuration *D. magna* showed a biphasic depuration curve indicative of ingestion of the Ag^{+} and Ag NPs. As discussed bi-phasic depuration is comprised of a slow elimination loss phase (k_{e2}) which was calculated as described above (eq. 2), and a fast elimination loss phase (k_{e1}) determined by mathematical stripping (Riggs, 1963 and Croteau *et al.*, 2004). Briefly, the difference between those data points at start of the depuration period where considerable losses occurred (i.e. k_{e1}) and the value predicted by the slow elimination slope were plotted against time and a linear regression fitted, once the slope of the slow phase had been derived this constant was stripped (i.e. subtracted) from the fast phase elimination constant (Figure 5.2 A-C, short-dashed line). The combination of k_{e1} and k_{e2} describe the overall loss dynamics of Ag accumulated from the different forms (Figure 5.2 A-C, solid line). For each of the different Ag NPs k_{e1} lasted for approximately 8 h, and the rate of loss was relatively consistent; the resulting fast phase efflux rates after mathematical stripping were 2.48 ± 0.78, 2.28 ± 0.11 and 2.40 ± 0.64 for PVP-Ag NPs, PEG-Ag NPs and Cit-Ag NPs, respectively (Table 5.1 and Figure 5.2). Slow phase efflux rates more indicative of depuration after stronger binding or incorporation of Ag NPs to specific ligands or the organism as a whole were 0.27 ± 0.35, 0.46 ± 0.28 and 0.51 ± 0.20 for $AgNO_3$, PVP-Ag NPs, PEG-Ag NPs and Cit-Ag NPs, respectively (Table 5.1 and Figure 5.2). For $AgNO_3$ uptake and depuration constants a biodynamic interpretation was made of the *D. magna* Ag elimination data presented by Glover and Wood (2005). k_{e1} and k_{e2} values of 4.27 ± 0.83 d^{-1} and 0.61 ± 0.26 d^{-1}, were derived from the exposure and subsequent elimination of Ag (added as radiolabelled $^{110m}AgNO_3$), with duration of the fast elimination phase estimated to be 6 h.

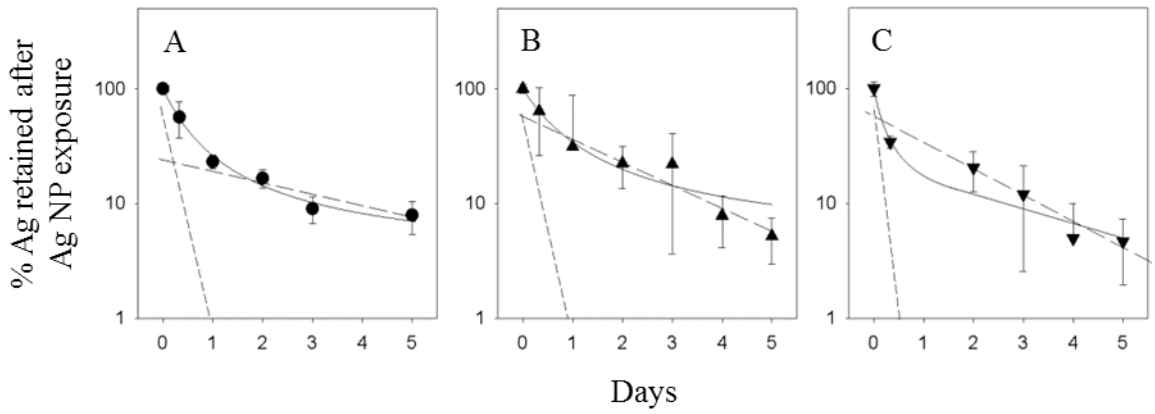

Figure 5.2 Proportional loss of Ag over time from *Daphnia magna* (A-C, closed symbols) following 1 day of waterborne exposures. *D. magna* were exposed to 37, 162 and 69 nmol L^{-1} for PVP-, PEG- and Cit-Ag NPs were, respectively. Each symbol represents the Ag tissue concentration (with background concentration subtracted) as a percentage of the tissue concentration at Day 0 (mean value ± S.D., n = 3). *D. magna* (A-C) loss of Ag over 5 d is described by a two-component efflux model where the dashed line represents the slow elimination phase and the dotted line the fast elimination phase, determined by mathematical stripping (see text). The solid line represents the sum of these two terms.

From the biodynamic constants of uptake and depuration, and using toxicity data of each exposure, it is possible to establish the LA_{50} using BDM and BLM principles (eq. 1). Table 5.1 shows the LA_{50} for each exposure based on toxicity data we collected on ~5-6 day old daphnids. LA_{50}'s for Ag NO_3, PVP-Ag NPs, PEG-Ag NPs and Cit-Ag NPs were 12.3, 63.7, 14.9 and 23.1 nmol g^{-1} dry weight, respectively (Figure 5.3).

5.4.4 Relationship between the waterborne modelled parameters and waterborne silver nanoparticle and silver nitrate toxicity

The strength of the linear relationship was ordered as k_u (R^2=0.91) > Log K (R^2=0.65) > LA_{50} (R^2=0.15) (Figure 5.3), plus Log K and uptake were shown to have significant correlation with EC_{50} when using Pearson's correlation coefficient. For Log K however the relationship resulted from clusters of data points at either end of the regression ($AgNO_3$ at one end and Ag NPs at the other) rather than consistent correlations across the regression line. Importantly, the regression formed by points within each cluster is not reflective of the overall correlation and therefore the overall regression model

overestimates fit. This has often been found to be the case when a dataset is composed of nested subsets (Khan *et al*., 2012 and Schielzeth *et al*., 2008). To delineate this effect the rank orders of each parameter were correlated to the rank order of toxicity. To achieve this, the Kendall's tau-b analyses were made.

Kendall's tau-b coefficients for the correspondence of rank orders of LA_{50} to acute toxicity did not demonstrate a significant relationship ($R^2 = 0.15$; *W*-statistic = -.333, $p > 0.05$; Table 5.2). There was also no relationship demonstrated between *D. magna* EC_{50} and Log *K*, however $AgNO_3$ had the lowest EC_{50} which was associated with the highest Log *K* value which is typical of such relationships (Paquin *et al.*, 2002; Table 5.2 and Figure 5.3, A). The rank order for experimentally derived uptake rate constants were $AgNO_3$> PVP-Ag NPs > Cit-Ag NPs > PEG-Ag NPs and these rates were inversely correlated to the rank order of toxicity in both species ($R^2 = 0.91$; *W*-statistic = -1.000, $p < 0.05$, Figure 5.3 C and Table 5.2). Thus the Ag form with the highest influx rate was the most toxic (i.e. lowest EC_{50}).

Although this study tested a limited set of data points for Ag NP exposures (i.e. only 3 different types of Ag NP) it is still worth determining Ag NP relationships in isolation from $AgNO_3$, to see if; i) $AgNO_3$ is skewing potentially nano-specific relationships and ii) if these relationships may differ; this may highlight areas of future research and points of interest which may explain other nano-related responses. If we treat Ag NPs separately from $AgNO_3$ as a toxicant in its own right we are able to improve the correlations EC_{50} has with the biodynamic and biotic ligand parameters and improve the R^2 of the regression line (Log *K* vs EC_{50}, $R^2 = 0.91$, $W = 1.00$, $p < 0.05$; k_u vs EC_{50}, $R^2 = 0.99$ $W = 1.00$, $p < 0.05$; LA_{50} vs. EC_{50}, $R^2 = 0.96$ $W = 1.00$, $p < 0.05$; Figure 5.3 A-C). Furthermore the distribution and correlations are not driven by 2 clustered populations. The adjustment also shows how the Ag NP relationships as they pertain to the model parameters can be skewed or driven by $AgNO_3$ and that these relationships may differ from the ionic form of Ag in a modelling context (Figure 5.3, A). For example as medium anions or sulphur increases within matrices Ag in ionic form often becomes less toxic due to complexation with these ligands, this is associated with a drop in Log *K* value and body burden, however here, dependent on coating, in the current study an opposite relationship is seen (i.e. higher Log *K* correlated with lower toxicity). Due to the limited dataset this warrants further investigation and any concrete conclusions are hard to determine.

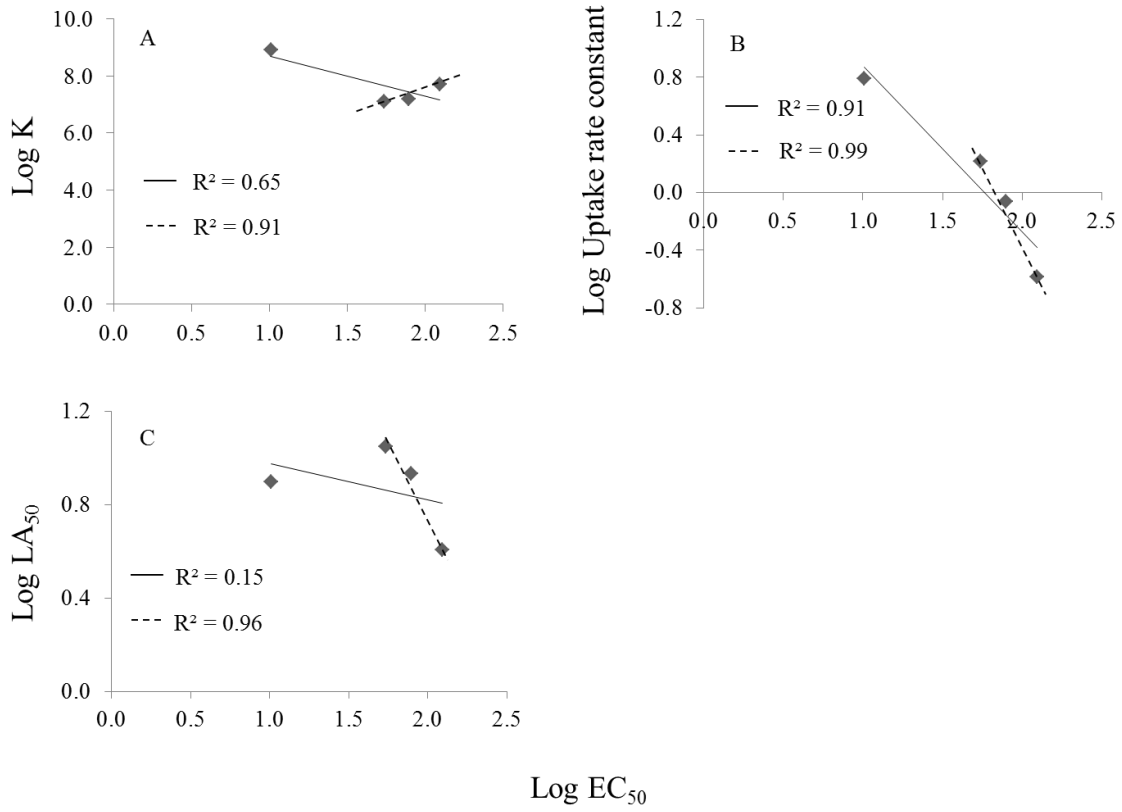

Figure 5.3 Correlations and relationships between, the Log of waterborne biodynamic (B, Log of uptake rate constant; L g^{-1} d^{-1}) and biotic ligand model (A, Log *K*; and C, LA_{50}; nmols g^{-1} dry weight) parameters with the Log of the EC_{50} of the Ag NPs and $AgNO_3$ (Solid lines), and the relationship of Ag NPs in isolation (dotted line). In this instance the strength of the relationship is shown as the R^2 value.

5.4.5 Foodborne silver nanoparticle and silver nitrate loss dynamics and assimilation efficiencies.

After foodborne exposures *D. magna* rapidly lost accumulated Ag between 0 and 24 hours due to gut purging. After this time the slow phase elimination was indicative of incorporated Ag from the diet. Therefore AE was derived from the percentage at the beginning of this rate constant, thus AE was the percentage of Ag remaining at 24 hours. AE for each exposure was 7.9 ± 0.8 % $AgNO_3$, 16 ± 1.4 % PVP-Ag NPs, 15.3 ± 1.1 % PEG-Ag NPs and 14.3 ± 0.02 % Cit-Ag NPs (Figure 5.4 and Table 5.1). k_{ef} derived from the slow phase efflux constant was similar for all exposures and was 0.53 ± 0.11, 0.32 ± 0.07, 0.28 ± 0.02 and 0.59 ± 0.04 for $AgNO_3$, PVP-Ag NPs, PEG-Ag NPs and Cit-Ag NPs, respectively (Figure 5.4 and Table 5.1).

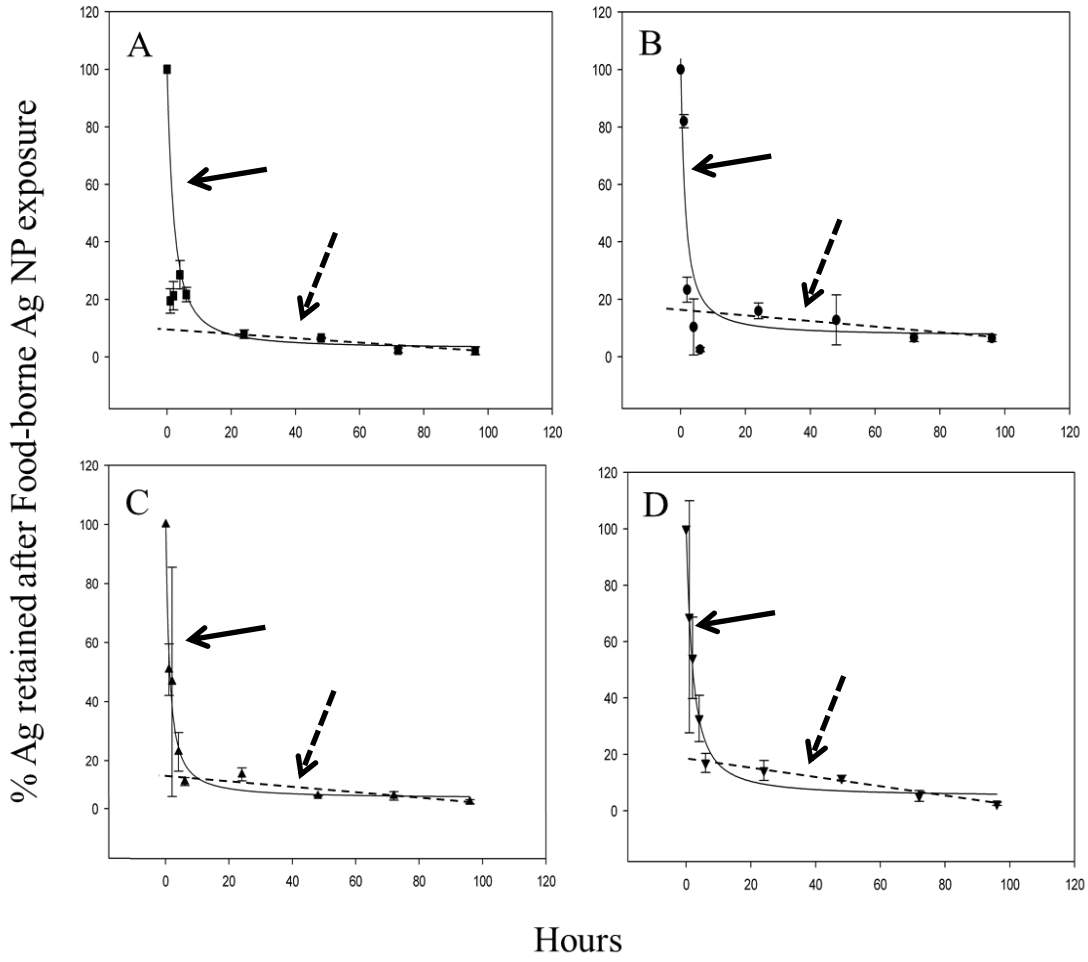

Figure 5.4 Proportional loss of Ag over time from *Daphnia magna* (A-C, closed symbols) following 1 day of foodborne exposures. *D. magna* were exposed to algae that had been pre-exposed to 18541 nmol L^{-1} of each NP or 2317 nmol L^{-1} for $AgNO_3$. Each data point represents the Ag tissue concentration (with background concentration subtracted) as a percentage of the tissue concentration at hour 0 (mean value ± S.D., n = 3). *D. magna* loss of Ag over 96 hours (4 days) for $AgNO_3$ (A), PVP-Ag NPs (B), PEG-Ag NPs (C) and Cit-Ag NPs (D), is described by a two-component efflux model where the dashed line represents the slow elimination (k_{ef}; dotted arrow) after rapid defecation (solid arrow). The solid line represents the sum of the fast and slow phase eliminations.

Table 5.1 Biodynamic parameters (± 95% C.I.) metal binding characteristics (± S.E.) and lethality for *D. magna* exposed to Ag NO_3, and PVP-, PEG- and Cit-Ag NPs.

	Ag NO_3	**PVP-Ag NPs**	**PEG-Ag NPs**	**Cit-Ag NPs**
Biodynamic parameters				
K_u (L g^{-1} d^{-1})	6.20 ± 0.07[a]	1.65 ± 0.56	0.26 ± 0.09	0.87 ± 0.31
K_{e1} (d^{-1})	4.27[b]	2.48 ± 0.78	2.28 ± 0.11	2.40 ± 0.64
K_{e2} (d^{-1})	0.61[b]	0.27 ± 0.35	0.46 ± 0.28	0.51 ± 0.20
K_{ef} (d^{-1})	0.53 ± 0.11	0.32 ± 0.07	0.28 ± 0.02	0.59 ± 0.04
AE (%)	7.9 ± 0.8	16.0 ± 1.4	15.3 ± 1.1	14.3 ± 0.1
Metal binding characteristics				
B_{max} (nmol g^{-1})	~200	186 ± 67	108 ± 9	111 ± 26
K_d (nmol L^{-1})	1.25	76 ± 41	20 ± 8	54 ± 24
Log *K*	8.9[c]	7.1 ± 0.2	7.7 ± 0.2	7.2 ± 0.2
Lethal Accumulation				
Waterborne LA_{50} (nmol g^{-1})	12.3	63.7	14.9	23.1

[a]The uptake rate constant per day (in L g^{-1} d^{-1}) was derived from the hourly rate constant of 6.14-6.24 L g^{-1} h^{-1} by Lam and Wang (2006) for *D. magna* adults exposed to dissolved silver in US EPA reconstituted moderately hard freshwater. [b]The Log *K* value for dissolved silver was taken from Bury *et al*., 2002. [c]Fast (k_{e1}) and slow (k_{e2}) efflux rate constants were calculated from the data presented by Glover and Wood (2005) for *D. magna* adults eliminating Ag in the absence of Aldrich humic acid.

Table 5.2 EC_{50} correlations (Kendall's Tau test (*W* statistic)) with biodynamic and biotic ligand model derived parameters.

EC_{50} correlations with:	***W*-statistic for $AgNO_3$ and Ag NPs (significance)**	***W*-statistic (significance) for Ag NPs only**
K_u	-1.00 ($p < 0.05$)	-1.00 ($p < 0.05$)
Log *K*	.000 ($p > 0.05$)	1.00 ($p < 0.05$)
LA_{50}	-.333 ($p = 0.497$)	-1.00 ($p < 0.05$)

5.4.6 Biodynamic modelling of Ag burdens from food and water in a representative freshwater environment

Dependent on Ag form, waterborne and foodborne Ag concentration scenario, the relative body burden contributions from each partition differs. $AgNO_3$ waterborne body burdens lead to 26 and 66% of the total body burden for the high and low Ag exposure concentration scenarios, respectively. High waterborne and foodborne concentrations lead to higher levels of uptake from food, and the converse can be said for the low exposures of Ag in the environment. This is in opposition with some trace metal literature for *Daphnia magna* and other species which consistently highlight foodborne exposure as the most important route for metal accumulation (Wang, 2013, Zhao and Wang, 2010 and Croteau and Luoma 2009). However it is a similar pattern to that observed by Kalman *et al.* (2010) when assessing Ag steady state burdens of a marine polychaete in different environments and demonstrates how dependent contributions to overall body burdens from each phase (i.e. aqueous or food) are on local environmental factors and Ag form/ Ag NP type. Steady state tissue concentrations were 0.03-0.27 nmol g^{-1} when assuming 75% of the total measured silver from the environment is in the ionic form or, 0.01-0.09 nmol g^{-1} when considering ionic and NP fraction concentrations to be at equal doses (i.e. 25% of total environmental Ag). Each Ag NP corroborated with the literature, PVP-Ag NPs, PEG-Ag NPs and Cit-Ag NPs consistently showed dietary uptake as the dominant source for Ag accumulation independent of exposure scenario. PVP-Ag NP dietary uptake contributed to 74-94% of total steady state body burdens, PEG-Ag NP dietary uptake contributed to 97-99% of total steady state body burdens and Cit-Ag NPs dietary uptake contributed to 83-96% of total steady state body burdens. Despite dissolved Ag being predicted as 3 times greater in the environment even at lower levels, all Ag NPs were able to accumulate to a similar degree. For all Ag NP types the conclusion is similar to that noted by Zhao and Wang (2010) who showed

Ag NP accumulation in the environment was mainly through the dietary route (>70%). The differences in contribution of each partition seen in $AgNO_3$ exposure scenarios, and the dominance of accumulation from Ag NP exposure in all scenarios, highlights how the importance of each partition is highly dependent on Ag form and environmental scenario, and that these variations must be accounted for within BDM models to further advance regulatory and risk assessment frameworks. When comparing total body burdens in each respective scenario Ag NPs consistently produced the lowest concentrations, however these were still similar to those observed in the $AgNO_3$ (0.03-0.276 $AgNO_3$vs. 0.007-0.250 nmol g^{-1} Ag NPs; Table 5.3). Assuming equal concentrations of both $AgNO_3$ and Ag NPs, Ag NPs accumulated to the highest degree (0.01-0.092 $AgNO_3$ vs. 0.007-0.250 nmol g^{-1} Ag NPs; Table 5.3). Currently these steady state burdens are highly unlikely to cause adverse acute or chronic effects i.e. waterborne LA_{50} values are all higher than steady state tissue concentrations (Table 5.1 and Table 5.3), furthermore during chronic exposure, organisms are usually able to cope with higher loads than seen during acute exposure as detoxification and sequestration mechanisms are able to upregulate to a greater degree (Adams *et al.*, 2011).

Table 5.3 Biodynamic modelling of body burdens based on environmentally relevant total silver concentrations obtained from San Francisco Bay and Monterey Bay (Griscom, Fisher and Luoma, 2002) and adapted to the predicted contribution from nano-silver complexes (i.e. 25% of all released Ag is nano-Ag the remaining fraction is dissolved Ag; 75% Gottschalk *et al.*, 2009). Food Ag was based on concentration ranges obtained from phytoplankton and water column concentrations were obtained from overlaying water measures.

		Body burden from C_w (nmol g^{-1})	**Body burden from C_f** (nmol g^{-1})	**Total Body burden** (nmol g^{-1})
$AgNO_3$	Min.	0.020	0.010	0.030
	Max.	0.073	0.203	0.276
PVP-Ag NP	Min.	0.004	0.011	0.015
	Max.	0.015	0.228	0.243
PEG-Ag NP	Min.	0.0002	0.012	0.012
	Max.	0.001	0.249	0.250
Cit-Ag NP	Min.	0.001	0.006	0.007
	Max.	0.004	0.110	0.114

Minimum values are based on C_w of 0.024 nmol L^{-1} and C_f 0.927 nmol g^{-1} of Ag. Maximum values are based on C_w of 0.089 nmol L^{-1} and C_f of 18.559 nmol g^{-1} of Ag (Griscom, Fisher and Luoma, 2002).

5.5 Discussion

Using traditional biodynamic and biotic ligand principles it was possible to define uptake rate constants (food, k_{uf}; waterborne exposures, k_{uw}), efflux rate constants (food, k_{ef}; waterborne exposures, k_{ew}), assimilation efficiencies (food, AE), biological binding maximum at the ligand(s) (water, B_{max}), binding affinity (water, k_d) and binding strength (water, Log *K*) values for all Ag NPs and $AgNO_3$. For Ag NPs these parameters did not appear to correlate with any nanoparticle physicochemical characteristics other than particle coating.

Using Ag levels obtained from a representative freshwater environment and the biodynamic parameters i.e., k_{uw}, k_{uf}, AE, IR, k_{ew} (slow phase efflux from water) and k_{ef} (slow phase efflux from food), it was possible to obtain steady state tissue burdens using biodynamic principles (Luoma and Rainbow, 2005). Ag NO_3 and Ag NPs were all able to cause steady state Ag burdens however in the scenarios presented here these burdens, currently, may not be of concern. However it is important to note the rapid and ongoing

growth of nanotechnology and these concentrations (both Ag NP and its dissolved products) are likely to rise, however for acute effects there would currently need to be 40-400 times greater environmental concentration of Ag^+ and 60-4000 fold greater Ag NP environmental concentrations. Currently therefore either increase use or accidental spill may be the only scenarios possible of gross acute toxicity, and Ag^+ may still be the most important Ag form in terms of ecological impact due to its current dominance in the environment. For risk assessment, chronic effects often need to be established and as such attempts to adapt these models based on acute data has been attempted, however due to differing physicochemical behaviours and organism fate over the long term the direct adaptation of these models has proved unsuccessful (Heijerick *et al.*, 2005 and De Schamphelaere and Janssen, 2004). The chronic implications of such tissue burdens as they relate to Ag^+ and Ag NPs are yet to be established in a BLM-construct and these burdens and Ag NP MOA may change in chronic scenarios..

All $AgNO_3$ values were consistent with the literature and k_u, k_{e1}, AE, Log *K* and LA_{50} all differed in comparison to each Ag NP suggesting different organism fate and, binding affinities and or sites, k_{e2} also corroborated with the literature as did k_{ef} but did not differ greatly from Ag NP exposures. Compared to Ag NPs k_u was more rapid for $AgNO_3$, B_{max} was higher (more sites for interaction), k_d was lower (higher affinity at lower concentrations) and Log *K* was higher (higher binding strength), which are all indicative of the higher toxicity presented by $AgNO_3$. For example, as mentioned, fish gill Log *K* values of Ag^+ and Cu^{2+} are 10.0 and 7.4, respectively, and therefore Ag^+ is regarded as the more toxic metal (Niyogi and Wood, 2004). Similarly Cu^{2+} and Zn^+ Log *K* values in moderately hard water are 8.0 and 5.3 for the freshwater invertebrate *Daphnia magna*, therefore copper is more toxic than zinc (Paquin *et al.*, 2002). Although higher B_{max} and k_u mean that there is higher potential for toxicant interaction this does not necessarily correlate with higher toxicity between metals, as this depends on the mode of action and the strength of the effect after binding; something which can only be established using critical accumulation factors linked to toxicological outcomes (i.e. LA_{50}). Croteau and Luoma (2007) showed a high rate of uptake for cadmium as well as a high B_{max}, which was higher than the more toxic Cu^{2+}, despite Cu^{2+} greater toxicity. However, when dealing with a contaminant which is constructed of a similar main composite (i.e. differently coated Ag NPs), or the same metal within different matrices, such values may correlate with toxicity; and this is where the strength of such models as the BDM and BLM lie. For instance Bury, Galvez and Wood (1999) showed

lower binding site constants and toxicities to rainbow trout exposed to Ag at different water chloride (Cl^-) concentrations (higher Cl^- lead to less toxicity). Zhao and Wang (2010) showed reduced uptake rates and toxicity of $AgNO_3$ to *Daphnia magna* in a cysteine rich environment (again more cysteine led to reduced toxicity). Furthermore the authors showed Ag NPs were less acutely toxic than $AgNO_3$ to *Daphnia magna* and this was also related to uptake rate, with Ag NP uptake rate (1.44 L g^{-1} d^{-1}) being lower than that of $AgNO_3$ (6.20 L g^{-1} d^{-1}) found within the literature (Zhao and Wang 2010, and Lam and Wang, 2006). Analysis of these studies as a whole highlight that when using the same metal but within differing scenarios (i.e. different matrices or metal forms) that Ag uptake and biotic ligand capacities may predict toxicological outcome. Therefore when using an NP of the same core type such values may help reliably predict their toxicity.

Here it was found that for $AgNO_3$ and each Ag NP k_u, Log *K* and LA_{50} values, which may each correlate to the different toxicity for each of the exposures to some degree. However, waterborne exposure LA_{50}, unlike what is found within the trace metal literature, showed a poor relationship with the combined values for $AgNO_3$ and Ag NP toxicity. The implication is that body burdens within the organism do not directly and consistently correlate with the toxicity observed. This is likely due to the interference the Ag NP coating has on the bioavailability and bioactivity of the toxicant as well as different or greater Ag sequestration (i.e. in metal rich granules, phagocytic cells or Ca^{2+}) in NP form. Therefore, using this parameter as a predictive tool for toxicity of any silver form would be ill advised. Furthermore such relationships can be skewed when there is more than one route of entry, or interaction. Interestingly Log *K* showed a poor correlation with toxicity for *D. magna*, again contrary to previous trace metal literature, but it did show a reasonable linear relationship with the EC_{50}. Log *K* values therefore show some promise within risk assessment, more data must be pooled from other NP types and organisms to solidify any relationships due to the poor correlations found using the Kendall's tau-b test. The strongest correlation and linear regression was found between the uptake rate and EC_{50} of the particles and $AgNO_3$. Again, as was previously highlighted, such rate constants may be the simplest and most reliable way to predict toxicity when using the same metal but in differing forms – and our data seems to confirm this. Another reason for the importance of uptake rates and the correlation with toxicity with *Daphnia magna* is due to their feeding and swimming behaviour. *Daphnia magna* are also able to interact with particulate matter not just through binding

at sites such as the epipodite, but also through capturing the particles as food within the setae (as previously demonstrated; Chapter 3 Figure 3.9) and in the food groove via interception, inertial impaction and diffusional deposition (Hou, Westerhoff and Posner 2013). Toxicity will largely be driven by uptake/ interaction not just at the toxicological site of interest but by ingestion of the Ag NPs as these organisms have no particular avoidance behaviour for these contaminants and thus these influx rates are not necessarily dependent on ligand binding constants but filtering rates of the species. Therefore the previous concept of one active site/ ligand is skewed by a proportional contribution from several possible interaction sites which will all have their own "ligand binding constants", which may affect the final BLM parameters – again our data seems to confirm this with the poor correlations seen between Log *K* and toxicity of the different Ag forms. After ingestion not only can ligand binding be responsible but also mechanical entrapment within physiological features such as the gut microvilli (Khan *et al.*, 2014 and Heinlaan *et al.*, 2011). Again this is not accounted for within such models and may skew final data analysis and interpretation when using single binding site saturation kinetics and models which rely on chemical speciation constants. Interestingly Croteau and Luoma (2009) have previously demonstrated metal influx was a better predictor of diet-borne metal toxicities (for Cu^{2+} Cd^{2+} and Ni^{+}) than tissue concentration in *L. stagnalis*. The same relationship has been found here (i.e. influx is a better predictor of toxicity) as *Daphnia magna* are technically feeding on the particulate matter (i.e. the Ag NPs). Furthermore influx rates do not depend on detoxification rates thus simplifying the model, as accumulation can often differ between acute and chronic toxicities due to these mechanisms (Croteau and Luoma 2009).

Although initial efflux (k_{e1}), uptake, AE, Log *K* and LA_{50} all differed, there were similarities thereafter (i.e. slow phase k_{ef} and k_{ew}), for Ag NPs and $AgNO_3$ which indicates they may have similar physiological fates. It is likely after the initial loss from defecation – which is largely proportional to the uptake rate of Ag – that all forms of Ag are bound strongly to a biological ligand(s), likely within the gut and at the surface of the epipodite and sequestering and depurative processes are likely the same. However it is still possible, dependent on silver exposure type (i.e. ionic or NP form), that the ratio between gut bound and epipodite bound Ag may differ which may lead to the differences seen here between toxicity and modelled characteristics compared to what is traditionally seen; such assumptions are in opposition for those made for other species (Croteau *et al.*, 2014b). It therefore becomes important to quantify or qualitatively

establish if differences exist between organism compartmentalisation of Ag in its different forms.

The AE for each NP was consistent (~15%). These AE's were higher than the AE established here for $AgNO_3$ and such a pattern has been previously observed within the literature (Zhao and Wang 2010). The higher AE for Ag NPs suggest that they are more likely to persist within *D. magna* than $AgNO_3$, for reasons aforementioned, thus establishing these differences, the route of NP toxicity (NPs releasing ions into the organism's internal environment which interact with the ligand, or direct interaction of the NP with the ligand) and particle characteristics within this physiological environment are likely of high importance.

Dealing with Ag NPs in isolation for waterborne exposures (i.e. excluding $AgNO_3$) we begin to see patterns opposite to those seen in the models for traditional metal BLM frameworks. For instance, Log *K* and LA_{50} show a positive and negative correlation and regression, respectively, with EC_{50}. For instance the less xenobiotic that is bound to the animal/ ligand for the same critical effect (LA_{50}) means the more potent the effect when dealing with a single contaminant between species or matrices. In contrast a higher Log *K* is usually indicative of a higher toxicity i.e. higher binding strength leads to a stronger toxic effect. However for Ag NPs we see the opposite relationship despite having the same core material, meaning they may need to be treated as separate entities from ionic Ag. Here the particles which accumulate to the greatest degree are the most toxic. The reason for this is likely down to how the toxic fraction becomes bioavailable, if Ag NPs are ingested or associated with the organism and act as a Trojan-horse (a carrier for silver ions) then the higher the burden the higher the release of silver ions within the organism, which leads to toxicity. This has been shown in literature, for example Park *et al.* (2010) showed Ag NPs caused toxicity to a RAW264.7 mouse peritoneal macrophage cell line by releasing silver ions after uptake into the cell. If this were the case we may not expect to see Ag NPs within the cell but we would expect greater intracellular disturbances caused by Ag NPs than its ionic form (which is poor at crossing the cell membrane), as Ag NPs would allow the cellular internalisation of Ag^+. However the elucidation of the differences in cellular response requires further investigation to establish such mechanisms, either by imagery (i.e. to study the interaction of the Ag NP within the organism) or biochemical analysis techniques (to study the effects thereafter). Furthermore if Ag NPs are acting as a Trojan-horse then the characteristics of these particles within the appropriate organism compartment (e.g.

gut or cell) will be of high importance and such characteristics as dissolution rate of the particles within the organism/ cell may be drivers for the toxicity seen.

The physicochemical characteristics after uptake are likely more important than those characteristics within environmental matrices as these are the ones directly acting at the site of action, particularly when ingestion is the likely route of exposure. Furthermore if these characteristics prove to have consistent correlation with toxicity it may in fact render particle physicochemical characteristics within environmental matrices moot, as internally the particles will end up having the same fate irrespective of the organism's external matrices. If similar MOA are seen across Ag NP type then such relationships may warrant further investigation as this demonstrates despite differing surface chemistries the particles eventually have similar physiological fate and impact.

An important caveat to the modelling approach is that more work is required. In order to make a fully predictive model for regulatory and risk assessment purposes such as the BLM we must not only establish relationships between these parameters and toxicity but how these may be affected in different matrices and if some are only relevant to particular species. The BLM's strength for trace metal assessment is that it incorporates chemical equilibrium constants to ascertain the remaining bioactive form of a metal in any environment and from this derives the likely level of toxicity. For such nano-BLM and –BDMs to advance we need to establish if the relationships presented here (i.e. uptake vs. toxicity) are dependent on water chemistry and how to account for this. Furthermore much like the traditional BLM accounts for water chemistry and speciation of the metal thereafter, nano-BLMs will have to account for coating type, and other physicochemical characteristics and their contributions to the degree of toxicity. The degree of toxicity here was best explained by particle coating, but it is likely to be a function of many physicochemical characteristics, not one in isolation (i.e. size and aggregation).

5.6 Conclusion

The study showed it is possible to define traditional biodynamic and biotic ligand model parameters in the context of Ag NP unidirectional flow and toxicity to the organism, using already defined principles. This study also made one of the first attempts to relate toxicity to body burdens – a key modelling and toxicological principle (i.e. body

burdens are correlated with toxicity; Luoma and Rainbow, 2005 and Croteau and Luoma 2009). Despite strong relationships between these parameters and the EC_{50} of Ag NPs the study showed that these relationships may differ from what is usually observed in trace metal accumulation kinetics and toxicological response, particularly in the case of Log *K* and LA_{50} values versus EC_{50} value relationships. These parameters show correlations opposite to what is expected when looking at trace metal literature. However the research also showed that using uptake as the predictor of toxicity across all Ag forms may hold great promise to simplify and ease risk assessment. However this relationship may not hold true across several metal NP types in tandem and such relationships need to be further explored. Oliver *et al.* (2014) showed uptake of NPs is unaffected by water chemistry, but how medium ligands effect uptake of ionic or nanoparticulate Ag needs to be established in more species and waters, these parameters may then be used with chemical equilibrium constants to predict species uptake and thus toxicity in several waters and species, such relationships need to be further established. Such an approach is already well established for trace metal toxicity but here biological ligand interaction is used to define eventual toxicity and the competition this has with medium ligands changes the susceptibility of the organism. This gives us a reasonable stance to be able to start to create predictive models based on Ag uptake alone. The study also showed using BDM principles that dietary transfer of Ag NPs may be of greater importance than waterborne exposures. This highlights the most important environmental partition and may go some way in simplifying predictive models. For example should the contribution of waterborne uptake to overall body burdens be shown to be consistently low, and biologically unimportant at the levels accumulated, it may allow refinement of models based on dietary uptake. These models would focus on foodborne Ag concentrations as these would cause the most Ag burden to the organism and biological perturbations.

Due to some of the differences seen, such as those in AE and the positive relationship of Ag NP LA_{50} with Ag NP EC_{50} there may be different biological fates for Ag dependent on Ag form (i.e. $AgNO_3$ or Ag NP). Based on the observations here (e.g. higher AE than dissolved Ag) Ag NPs are more likely to be ingested and trapped within the gut and/ or organism than dissolved Ag which acts at the epipodite. This could cause toxicity through Trojan-horse mechanisms or toxic responses from Ag NP interactions thereafter. However due to the low number of sample point's further research is required in order to pool a large body of evidence. Due to the relatively high AE and

the LA_{50}'s should Ag NPs be able to affect the organism after uptake via such mechanisms (i.e. Trojan-horse) one would expect them to elicit greater cellular response as toxicity would not simply be down to epipodite binding and Ag^{+} would be facilitated across the cell membrane. Further research is required on cellular response and load as well as particle physicochemical characteristics within physiologically relevant medium.

Currently traditional biodynamic and biotic ligand principles may be more reliable than using particle physicochemical characteristics in predicting toxicological outcome when looking for rapid tests *in vivo,* which can then be applied to *in silico* scenarios and models. However as our knowledge of physicochemical characteristics expands applying these to predictive models will aid in purely *in silico* frameworks. As such these should be the focus of future research until a large pool of data can be used to solidify such relationships. The research also highlighted that Ag^{+} and Ag NPs may not be of major concern, but these concerns may rise with increased use of nanotechnology and the chronic effects of these burdens. Furthermore chronic nano-BLM constructs currently represent a knowledge gap that needs to be addressed to fully estimate the impact of NP release into the environment.

Chapter 6.

Molecular mechanisms of silver nanoparticle and silver nitrate toxicity

6.1 Introduction

Recently nano(eco)toxicological research has focused on the development, optimisation and validation of biomarker tests to allow modes of action (MOA) to be established as well as create sensitive, cheaper and more rapid screening tests for potential contaminants (Barata *et al.*, 2005, De Coen and Janssen, 2003 and Diamantino *et al.*, 2001). In the nano-field this is of particular importance where quick screening and/ or *in silico* models must be implemented to allow rapid and practical methods to test the plethora of core/ material types, sizes, shapes and coatings which have all been shown to potentially affect the biodynamics and level of toxicity of the NP (Khan *et al*. 2015, Newton *et al*., 2013 and Fan *et al.*, 2012). The establishment of such tests should allow appropriate regulation and risk mitigation based on good science (NanoBEE 2010, De Coen and Janssen, 2003 and Diamantino *et al.*, 2001).

All life has some form of homeostatic control in order to maintain the stability of their internal environment and to allow optimal conditions for survival and function (Newsholme, Challis and Crabtree, 1984). For example energy metabolism, ionoregulation, and antioxidant defences all require homeostatic control. Most pathways which rely on homeostatic control work on a negative feedback loop allowing a fine balance as well as rapid response. Perturbations of homeostasis within any organism eventually manifest into observable physiological responses (De Coen, Janssen and Segner, 2001) such as mortality, deformation, effects on behaviour, fecundity and growth, which may then lead to population level changes and effects therein (i.e. reduction in biodiversity and impacts on the food chain). Understanding and assessing the impact of these higher level effects is indeed the purpose of ecotoxicology, however, if we are able to predict these effects prior to whole body manifestations through more sensitive screening that would allow an improved understanding and protection of the environment from xenobiotics (De Coen and Janssen, 2003 and Diamantino *et al.*, 2001). Moreover, disturbances in genes or biochemical regulation processes can often be seen at lower doses or on shorter time scales, thus may be detected sooner than such endpoints as mortality or immobility (Poynton and Vulpe, 2009 and Forbes, Palmqvist and Bach 2006). Therefore it

becomes pertinent to standardise and optimise tests which may highlight homeostatic disturbances, in particular cellular and subcellular mechanisms and pathways. These can be used to establish the MOA, and adverse outcome pathways (AOP; Ankley *et al.*, 2010), for a contaminant predicting eventual physiological response. Many biochemical pathways and methods for detoxification are similar across phyla (i.e. antioxidant mechanisms), therefore similar tests can often be used on different species. When effects of a contaminant are seen to be consistent across phyla this may enable the achievement of the 3 Rs (reduction, refinement and replacement) of toxicology and lower phyla data, such as invertebrate data, could be extrapolated and used as a predictor for higher phyla toxicity, such as vertebrates, fishes, rats or humans. Knowing such adverse outcome pathways allows better ability to protect against, and predict potential toxicity of, chemicals and toxicants. However, such pathways for NPs are comparatively less well established, although, the generation of reactive oxygen species is generally accepted as a major route of toxicity for many NP types (Oberdörster, Stone, and Donaldson 2007, Stone and Donaldson 2006). The problem here of course is that such a response can be caused by multiple cellular events, that is, it is quite a generalised response. Assessment of an organism's biochemical pathways to deal with specific chemicals and modes of detoxification can never be based on the measurement of a single enzyme, protein or signaller (De Coen, Janssen and Segner, 2001). This is due to the cells' and organisms' complex nature. Therefore assessment should be made on a suite of carefully selected endpoints to allow specific MOA to be identified or dismissed.

The ensuing chapter considers a suite of biochemical endpoints, most relevant to Cladocera as they pertain to Ag NP toxicity. In particular, energy metabolism, antioxidant defence and ionoregulation are discussed and analysed. The data will allow common themes to be established, if any, between Ag NPs and their MOA, or highlight the differences that can occur despite similar core size and material. It may establish biochemical responses specific to Ag NP exposure highlighting the type of exposure certain populations are subject to i.e. Ag^{+} or Ag NP. This becomes especially advantageous when separating Ag NP and Ag^{+} in environmental samples is not possible as the organism can then become a bioindicator highlighting which contaminant may predominate and to which the organism is subject to without using more expensive experimental techniques, or when such techniques are unavailable (e.g. separating dissolved Ag concentrations from nanoparticulate form, since standard techniques such

as ICP-MS are not able to separate clearly Ag species, and so additional techniques need to be deployed). Should common themes be derived, such data can be used to establish common MOA and bioindicators contributing to further understanding of effects of different NPs and forms, and providing information and data to regulatory, risk assessment and modelling efforts (NanoBEE, 2010 and Gerhardt, 1999).

6.1.1 Ionoregulation in response to silver nanoparticle and silver nitrate exposure.

The MOA of Ag^+ in some aquatic species has been explored and elucidated. In both fish and *Daphnia magna* (and likely other Cladocera) the toxicity of Ag^+ is mainly caused by ionoregulatory disturbance. Based on Coulomb's law the epipodite of the daphnid is a negatively charged surface to which Ag^+ or other cations can bind (Bianchini and Wood, 2003). The epipodites are a major site of Na^+ and Cl^- transport from the water-column into the extracellular fluid of the organism, in large part by the energy dependent enzyme Na^+, K^+ -dependent adenosine triphosphatase (Na^+, K^+ - ATPase; Smirnov, 2013 and Bury *et al.*, 2002). In *Daphnia magna* the inhibition of Na^+, K^+ - ATPase by Ag^+ has been shown resulting in ionoregulatory failure by decreasing total body Na^+ and K^+ which leads to cardiovascular collapse and mortality (Bianchini and Wood, 2003 and Bury *et al*., 2002).

In a risk assessment context for Ag NPs ionoregulation may be one of the most important factors to consider. However to date, and our knowledge, only two publications have considered this experimentally (Stensberg *et al.*, 2014 and Zhao and Wang, 2013). Many risk assessment efforts suggest that Ag^+ biotic ligand models (BLM) may be adjusted for use with Ag NPs (NanoBEE, 2010), and this is based on, as previously mentioned, the thought that Ag NP toxicity is a function of its soluble fraction released into the water-column. For the theory to hold true similar ion level disturbances in the organism from Ag^+ and Ag NP exposure should be seen at equitoxic (i.e. concentrations showing equal toxicity) exposures, thus confirming MOA and the toxic fraction of the NP as ionic Ag. If there are no MOA commonalities between Ag^+ and Ag NP toxicity then such models may be inappropriate to use in their current form for *in silico* modelling, risk-assessment and regulation of Ag NPs. Alternatively, at the very least, careful consideration is needed to focus on the most critical information to allow a working model to be created based on a BLM-like construct.

6.1.2 Energy metabolism & antioxidant defences in response to silver nanoparticle and silver nitrate exposure.

It has previously been shown that silver is able to interfere with energy production and increase oxidative stress, furthermore the two are intricately interconnected (AshaRani *et al.*, 2012, Costa *et al.*, 2010, Marambio-Jones and Hoek, 2010, Kim *et al.*, 2010, AshaRani *et al.*, 2009b, AshaRani *et al.*, 2008).

How organisms convert food source, or other energy inputs, into usable energy (i.e. energy metabolism) is key to all life on earth. At the cellular level usable energy – as adenosine triphosphate (ATP) – is integral to cell function, homeostasis and several signalling cascades. In all eukaryotes glycolysis produces ATP within the cytosol anaerobically, however mitochondria are indispensable to producing the greatest proportion of ATP (95% greater yield than glycolysis) through cellular respiration (i.e. aerobically). As such mitochondria are often referred to as the "powerhouse" of the cell. Mitochondria are also involved in many other cell functions such as, but not limited to; cellular apoptosis, necrosis, Ca^{2+} signalling and cell differentiation. Therefore studying all facets of energy production (i.e. anaerobic and aerobic) becomes important in order to derive sound conclusions on MOA and may also hold clues as to other potential cellular disturbances.

6.1.2.1 Adenosine triphosphate (ATP)

The most important tissue/ ligand at the water-organism interface of many aquatic organisms are the gills or epipodites. This is one of the first sites at which any contaminant can interact. Furthermore these sites are mitochondrial dense and have many metabolic and regulatory processes which rely on ATP, highlighting the potential importance of cellular energetics and mitochondrial analysis; notwithstanding the importance of ATP within the organism as a whole.

ATP is vital for the energy conversion and transfer of all cells and their homeostasis as many reactions, enzymes and cellular channels are ATP-dependent (Izyumov *et. al.*, 2004, Lipman, 1941, Fiske and SubbaRow, 1929 and Lohmann, 1929). ATP is also important in intra- and extra-cellular signalling, cell death (apoptosis and necrosis) and neurotransmission (Burnstock. 2006). Many diseased states have been associated with reductions in ATP (e.g. type-II diabetes, ischaemic heart disease, Parkinson's disease and Alzheimer's disease; Wallace, 1992). A reduction in ATP is characteristic of many

forms of toxic insult and this depletion can be caused by a myriad of circumstances within the cell such as: hypoxia, increased use of ATP for repair and ATP-dependent detoxification, and interference with and/ or reduced mitochondrial function, these have all been documented (Martin and McLean, 1995).

Disturbances in energy systems *in vitro* and *in vivo* caused by Ag NPs have been previously highlighted but mainly in genomics studies and vertebrate models. In cell line studies (human lung fibroblast cells (IMR-90) and human glioblastoma cells (U251)). AshaRani *et al.* (2008) hypothesised that a reduction in ATP caused by Ag NPs was caused via interference along the mitochondrial electron transport chain (ETC) by Ag^{+} released from the particles, and this reduction eventually signalled cell death through several pathways e.g. the mitochondrial activation of the JNK-mediated death pathway or release of factors such as Cytochrome C. Toxicogenomic studies of *D. magna* exposed to Ag NPs have shown increased expression of genes involved with DNA repair as well as retardation of growth and reproduction (Poynton *et al.*, 2010). These findings corroborate with cell lineage data (again, in human lung fibroblast cells (IMR-90) and human glioblastoma cells (U251)) as DNA damage was thought to be the cause for cell cycle retardation and this retardation was likely caused by reduced ATP synthesis from the ETC by the presence of NPs (AshaRani *et al.*, 2009b). However, only one toxicological nanoparticle paper was found within the literature that has directly reported ATP levels using classical biochemical techniques (Yu *et al.*, 2013). Here Yu *et al.* (2013) also showed a decrease in ATP in skin cells caused by reactive oxygen species when exposed to zinc oxide NPs thus this effect may be common across metal NPs. However, ATP coated NPs have been implicated for use in cancer therapy and some NPs have been shown to protect cells by reducing detrimental reductions in ATP (Arya *et al.*, 2014, Hosseini *et al.*, 2013 and Zhang *et al.*, 2013).

Despite much of metal cation research being focussed on Na^{+}, K^{+}-ATPase (an ATP dependent enzyme), the direct study of ATP, particularly after acute exposure periods, to elucidate MOA of metal contaminants, or as a wide-screening selective biomarker within aquatic ecotoxicology, has been scarcely used and to our knowledge has never been considered in aquatic nano(eco)toxicology. Within *Daphnia magna* should there be perturbations to the ATP dependent Na^{+}, K^{+}-ATPase, there may also be changes in ATP level. An increase in ATP may be in an attempt to upregulate the enzymes' function or a lack of ATP may equally cause its impairment. ATP may also be affected by other mechanisms such as mitochondrial dysfunction and upregulated use for

protective purposes. Should any whole body morphological or physiological differences be observed during traditional bioassays these may also be due to ATP fluctuations, either caused by environmental changes or contaminant exposure. When cellular levels of ATP are low or critical there is a shift in the cells energy budgeting, where ATP use is prioritized to the house keeping of the cell (i.e. cell structure and repair) and thus other cellular mechanisms and functions suffer (Janssens *et al.*, 1995). Thus when energy is low organism survival becomes paramount, and therefore such biological functions as reproduction and growth may be ceased or down-regulated (Kooijman, 1986). Such effects are often seen in *D. magna* chronic bioassays during exposure to varying toxicants; however whether this is caused by a reduction in energy and/ or ATP is often not explored.

During the NanoBEE project, the role of one of the partners (University of Birmingham) was to establish global gene expression changes, using omic techniques, in *D. magna* exposed to the same PVP-Ag NPs used within our work. They also established differences between gene expressions when exposed to bulk, dissolved and nano-sized silver. The results directed our work to the most specific, logical and likely biochemical pathways that may be affected following exposures, thus highlighting appropriate biochemical assays. Alex Gavin at Birmingham University found upregulation of purine metabolism in *Daphnia magna* exposed to the PVP-Ag NPs, via metabolomic techniques (data not published). However, which purines these were could not be determined. The study of varying purines via biochemical tests focusing on specific pathways may elucidate this, and therefore here the research focuses on the purine, ATP.

6.1.2.2 Lactate dehydrogenase (LDH)

Glycolysis provides energy by breaking down glycogen to lactate (anaerobically) or pyruvate (aerobically) to form ATP. Anaerobic respiration is often preferred when short intense bursts of energy are required (as glucose is converted into ATP quicker via this pathway) or during hypoxic conditions where aerobic respiration is limited. Lactate dehydrogenase (LDH) is a cytosolic enzyme which during glycolysis reversibly converts pyruvate to lactate and nicotinamide adenine dinucleotide (NADH or NAD^+) from its reduced to oxygenated forms. LDH assays are cheap, relatively easy, sensitive and quick and may enable wide-screening of contaminants. As such the LDH assay is widely used to monitor cell, tissue and organ damage, as release into the extracellular

environment may infer a decrease in cell membrane integrity and even cell death (both apoptosis and necrosis), however it is rarely used in ecotoxicology. Furthermore its importance as a glycolytic enzymatic endpoint has not been fully exploited, again, particularly in the case of ecotoxicology (Diamantino *et al.*, 2001). Analysis of such enzymes will help derive MOA of particular contaminants as well as highlight cheap methods for testing.

As an important enzyme for glycolytic ATP production LDH can increase or decrease dependent on energy demands. For example if demand is greater than production a decrease may be likely as LDH.. LDH is particularly important when additional energy is rapidly required when an organism is under stress, for evasion, repair or detoxification processes (Zeis *et al.*, 2009). Therefore under chemical stress it can also be assumed that some fluctuation of LDH may occur, this makes it not only appropriate to measure in order to understand possible MOA but also as a bio-monitoring tool for NPs. Cells under hypoxic conditions have been shown to increase LDH levels in order to sustain heightened levels of glycolysis to ensure sufficient ATP production for cellular function when aerobic respiration is limited or not possible. Using LDH as an effect criterion for *Daphnia magna* has been reported by Diamantino *et al.* (2001). The study optimized and assessed the efficacy of *in vitro* and *in vivo* LDH assays. They found that LDH was reduced during 48 hour ionic zinc exposures (0.55 mg L^{-1}) in whole body homogenates which could be used as a more sensitive parameter of aquatic toxicity than the LC_{50} (0.8 mg L^{-1}). However there was no further exploration into why this change in LDH occurred. Guilhermino *et al.* (1994) studied *Daphnia magna* LDH activity after exposure to 3,4-dichloroaniline (DCA) and sodium bromide (NaBr), again to highlight LDH for use as a more rapid and inexpensive tool to predict toxicity. In both instances LDH effects were seen around the same dose as 21-day reproduction test lowest observed effect concentrations (LOECs). However LDH assays were consistently more rapid (i.e. 24-96 hours vs. 21-day chronic tests) indicators, though not always more sensitive than traditional methods (Guilhermino *et al.*, 1994). Again the reasons for these changes were not explored. De Coen, Janssen and Segner (2001) studied a suite of enzymes in *D. magna* including LDH after exposure to mercury and lindane in order to assess their impact on carbohydrate metabolism.

Although LDH has been explored with success in Cladocera, and specifically in *Daphnia magna*, the research is limited. Differences in LDH reaction have also been shown between pollutants in whole body homogenates, therefore LDH may also be

contaminant specific (De Coen, Janssen and Segner, 2001). The use of LDH in *in vivo* nano(eco)toxicology has not yet been utilised,

6.1.2.3 Mitochondria

Whether ATP reduction is due to glycolytic or respiratory mechanism disturbances may have important repercussions when elucidating a contaminant's MOA/ AOP. Energy supply through cellular respiration occurs at the mitochondria and thus study of this organelle may be of importance. Furthermore many of the previously noted toxicological outcomes caused by a decrease in cellular ATP originate from mitochondrial perturbations.

During cellular aerobic respiration pyruvate enters the mitochondrion and produces energy via the Citric Acid Cycle (CA cycle) in the mitochondrial matrix or via the electron transport chain (ETC) in the inner mitochondrial membrane. Therefore, both LDH and ATP are related to mitochondrial energy production, LDH for the conversion of lactate to pyruvate and ATP as the end result of mitochondrial respiration. Therefore changes seen in LDH activity or ATP output, may affect, or be a direct result of, mitochondrial dysfunction.

Mitochondria have several roles within the cell such as; apoptosis, cellular differentiation, signalling cascades and cell growth (Tait and Green, 2012). Not surprisingly mitochondrial dysfunction has been implicated in many human diseased states, for instance; neurodegenerative disorders, cardiac disorders and cancer (Wallace, 1992). Mitochondrial damage has been highlighted previously in (ultra) fine particle toxicology which can lead to diseased states i.e. lung cancer (human male subjects, Hou *et al.*, 2010; review on effects of ambient airborne particles, Kappos *et al.*, 2004; and macrophages and epithelial cells, Li *et al.*, 2003). Ag NPs may preferentially localise within mitochondria after cellular uptake, thus after internalisation the interaction and effect upon this organelle may be of paramount importance to the observable whole body effects (AshaRani *et al.*, 2009b, AshaRani *et al.*, 2008). Ag^{+} is known to induce the mitochondrial permeability transition which causes a release of apoptotic proteins into the cytosol from the mitochondrial membrane space, possibly due to silver mediated pore opening (*Daphnia magna*, Stensberg *et al.*, 2014; and isolated rat liver mitochondria, Almofti *et al.*, 2003). Currently Ag NPs are believed to cause mitochondrial disturbance via several possible mechanisms: i) Ag^{+} acts upon cellular Ca^{2+} homeostasis which then causes mitochondrial membrane damage, ii) Ag^{+} from Ag

NPs causes mitochondrial permeability transition, iii) direct mitochondrial membrane damage by Ag NPs (e.g. again increased permeability), iv) disturbances on the electron gradient and/ or v) the Ag NPs act as electron donors or disturb the electron passage causing ETC malfunction (Marambio-Jones and Hoek 2010, AshaRani *et al.*, 2009b, AshaRani *et al.*, 2008, Costa *et al.*, 2010).

Dysfunction of this organelle leads to increases in cytosolic Ca^{2+}, release of apoptotic factors (e.g. cytochrome C), excess build of reactive oxygen species (ROS; namely super oxide) and perturbations in energy supply. These can all lead to eventual morphological and population changes as well as mortality.

6.1.2.4 Oxidative Stress

During normal cellular metabolism mitochondria and phagocytic cells (these cells release ROS to destroy pathogens) inevitably produce unwanted by-products, that of, superoxide anion (O_2^-) and hydroxyl radicals ($\cdot OH^-$) – collectively reactive oxygen species (ROS; Figure 6.1). Cells are able to guard against the effects of oxidative stress via antioxidant mechanisms, which either scavenge or reduce these by-products, however, only to a limited capacity. Although under normal circumstances the cell or organism is able to cope with excess ROS, when under stress (for instance; toxic, diseased states and/ or environmental changes) these coping mechanisms may suffer or be overloaded, even after antioxidant upregulation. The increased ROS directly from the contaminant or the cell organelles may lead to cell damage (Figure 6.1). The consequence of such molecular perturbations can cause: loss of cell membrane integrity, enzyme inactivation, and interference with signal transduction (e.g. Ca^{2+} signalling). These cellular disturbances can lead to acute and chronic toxic effects (Lushchak, 2011). ROS production by NPs has been shown to be a major contributor of NP toxicity for several years across many phyla (Kim and Ryu, 2012, Oberdörster, Stone, and Donaldson 2007). Transition metal NPs have been shown to produce ROS as a by-product of dissolution (Li *et al.*, 2013, Asghari *et al.*, 2012, AshaRani *et al.*, 2009b and Costa *et al.*, 2010). In this instance Ag NPs become important not only for their potential as a mitochondrial toxicant but also as a metal that may dissolve and directly produce ROS. It may be pertinent to assess the associated pathways and organelles (i.e. ATP synthesis and mitochondrial function), and the changes in antioxidant enzymes associated with such cellular stress and malfunctions.

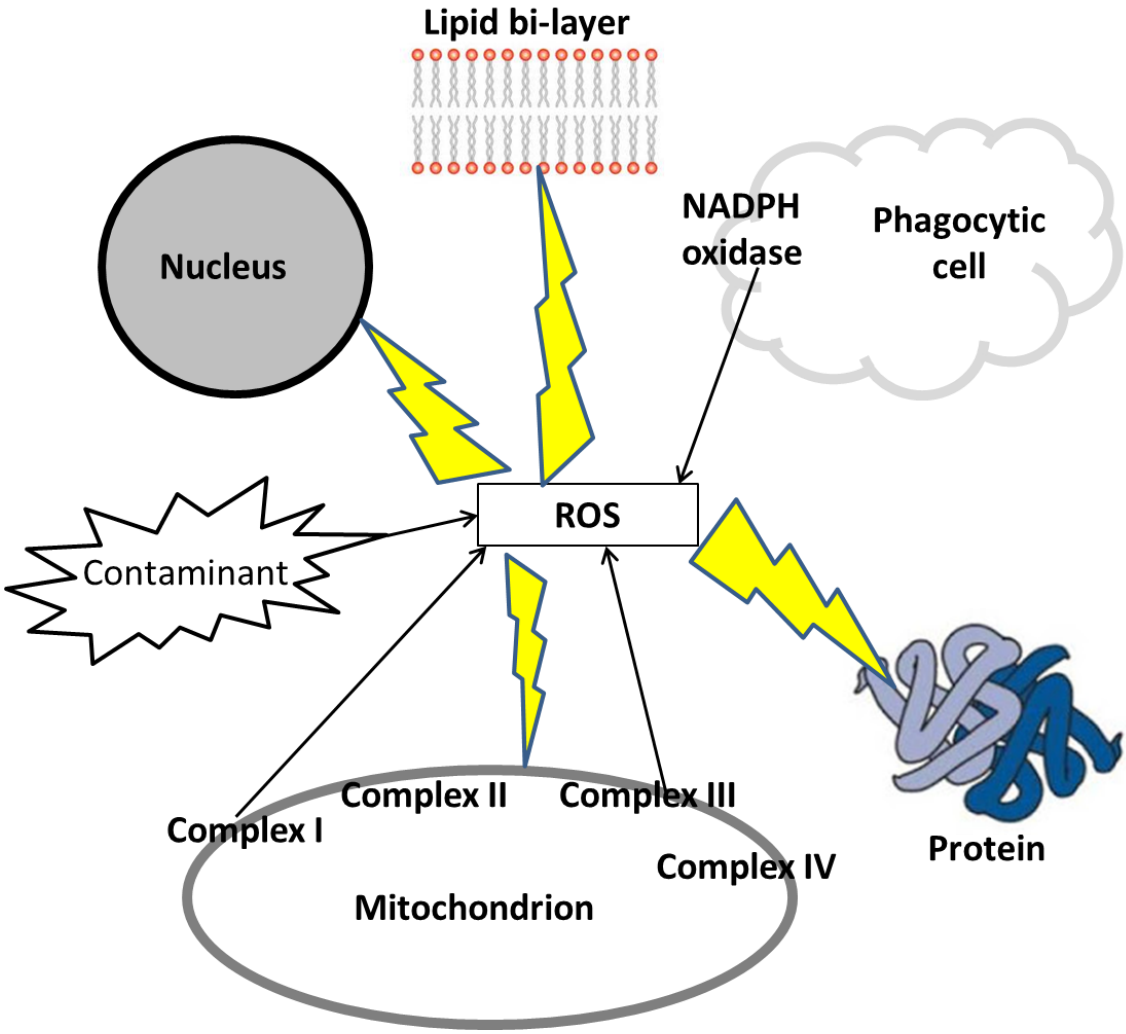

Figure 6.1. ROS production from cellular organelles (arrows) and damage to cellular structures ROS can cause (lightning bolts). ROS production from the contaminant, mitochondria and NADPH oxidase of the phagocytic cell.

NP toxicological pathways involving mitochondrial dysfunction and death linked to oxidative stress have been highlighted in rats, mice and human cell lines (e.g. macrophages, fibroblasts, skin, fibrosarcoma, liver and sperm) as well as invertebrates and fish (Kong and Zepp 2012, Foldbjerg, Dhang and Autrup, 2011, Li *et al.*, 2011, Kim *et al.*, 2010, Marambio-Jones and Hoek 2010, Li *et al.*, 2009 and Carlson *et al.*, 2008). In *Daphnia magna*,Kim *et al.* (2010) showed dose and size-dependent increases in antioxidant enzyme activities after exposure to TiO_2 for glutathione-s-transferase (GST), glutathione peroxidise (GPX) and catalase (CAT) which correlated with organism mortality. These enzymes are all involved in the detoxification of hydroxyl radicals ($^{\cdot}OH$) and hydrogen peroxide (H_2O_2) the production of which both link to ETC mitochondrial activity. Interestingly superoxide dismutase (SOD) was unchanged.

The previously noted research on Ag NPs and other NPs in cell lines and aquatic organisms highlight potential increase in ROS, but also mitochondrial disturbance and dysfunction. One major ROS from mitochondria during normal respiration and mitochondrial dysfunction is superoxide (O_2^-). Superoxide is the reduced form of dioxygen (O_2) and is produced mainly from complex I and III of the mitochondrial ETC (Costa *et al.*, 2010). Considering the literature disturbance of the mitochondria is highly likely across many phyla and as such so is the increased release of O_2^- from the organelle. Two major processes are involved in the oxidation of superoxide to rid the cellular environment of this harmful ROS. Firstly; O_2^- is oxidised by hydrogen to give rise to hydrogen peroxide and O_2 (Hancock, 2005). Although this reaction can spontaneously occur it is also catalysed by a specific enzyme, superoxide dismutase (eq. 6.1), which has been previously highlighted, this is especially important in the cellular environment where large amounts of O_2^- can be produced.

$$2\ O_2^- + 2H^+ \xrightarrow{\text{Superoxide dismutase}} H_2O_2 + O_2 \qquad \text{(eq. 6.1)}$$

Hydrogen peroxide (H_2O_2) itself however is a weak oxidizing agent which may cause cellular perturbations and must also be removed. Here H_2O_2 decomposition is achieved by breakdown to water and O_2, two harmless by-products. Again although this can be spontaneous it is also catalysed by an enzyme known as catalase (eq. 6.2).

$$H_2O_2 \xrightarrow{\text{Catalase}} H_2O + O_2 \qquad \text{(eq. 6.2)}$$

Ag^+ and nanoparticles have been shown to disrupt plasma membranes of cells (Park *et al.*, 2010, Kim *et al.*, 2009, Rungby, Hultman and Ellermann-Eriksen, 1987), in phagocytic cells which can lead to the increased release of super oxide. Furthermore if Ag NPs are able to translocate into the cell, either into the cytoplasm through passive or active processes, (e.g. via voltage-gated/ ion channels or in a vesicle e.g. clathrin) as discrete or agglomerated/ aggregated particles they may be phagocytosed and detected as pathogens also causing the increased release of O_2^-. Therefore two of the most likely up or down regulated oxidative defences (antioxidants) may be that of the enzymatic antioxidants SOD and CAT.

6.2 Aims

The similarities in response to Ag NPs between vertebrates, cell lines and invertebrates with regard to cellular respiration, ROS and mitochondrial function highlights the importance of these responses as key risk assessment criterion, or biomarker standards that may be applicable across phyla. The study therefore aimed to assess these criteria and analyse the results using varying biochemical tests. Such information may become applicable across phyla when common themes in toxicological response arise. Highlighted similarities and differences provided by these data may lead to quick wide-level screening protocols, which it is hoped will refine and replace higher level biological testing, for Ag NP, and metal NP toxicity, particularly in the case of transition metals. It is our intention that such information will ease and direct hazard assessments of Ag NPs by highlighting physiological common themes in response to these contaminants.

Due to the body of evidence, corroboration of datasets within the literature, and importance of the aforementioned organelles and enzymes this study aimed to test biochemical endpoints that will highlight their response after Ag NP and $AgNO_3$. Here the research also aimed to establish common or different MOA for each contaminant which will inevitably aid in the risk management and mitigation of Ag NPs. To achieve these aims the results from *Daphnia magna* whole body homogenate were compared, focussing on the following: cations (Na^+, K^+ and Ca^{2+}), ATP, LDH, SOD and CAT, as well as mitochondrial membrane potential in live *D. magna*

6.3 Methods

6.3.1 Organisms

Daphnia magna acquisition and husbandry has been discussed in Chapter 2. At the cessation of all tests daphnids were checked for the presence of eggs. The presence or absence of eggs ensured each daphnid was at the same developmental stage; which may also impact LDH analysis and final interpretation (De Coen, Janssen and Segner 2001). All daphnids tested had eggs in the brood chamber upon cessation of the test. Furthermore, efforts were made to select and ensure all *D. magna* were of a similar size upon collection. Before collection exposure chambers were checked for neonates, if the

D. magna had given rise to progeny they were discarded from the test as this release of young may affect enzymatic, biochemical and cation levels (De Coen, Janssen and Segner *et al.*, 2001).

6.3.2 Nanoparticle synthesis and stocks

Nanoparticle synthesis and stocks were reported in the Appendix Text A2.1, Chapter 2 and Chapter 3. NPs used were PVP-Ag NPs, PEG-Ag NPs and Cit-Ag NPs in parallel with $AgNO_3$. Concentration ranges were ~50% of the 48 hour EC_{50}, and were thus sub-lethal over the tested time, furthermore the lowest concentration was selected at a concentration lower than previous observed effects to establish if these assays were more sensitive than traditional methods, such as OECD tests 202 (2004) and 211 (2008).

6.3.3 Characterisation

Physicochemical characteristics were reported in Chapter 3.

6.3.4 Ionoregulation assessment

Ionoregulatory disturbances were assessed by measuring whole body Na^+ K^+ and Ca^{2+}. *D. magna* were all <24 hours old at the beginning of the test. A total of 20 *D. magna* were used in each exposure replicate. *D. magna* were held in 100 mL test vessels with 80 mL of medium, medium-particle suspension or medium $AgNO_3$ solution (i.e. 4 mL per *D. magna*) and fed 5 x 10^5 cells mL^{-1} day^{-1} of *Chlorella vulgaris*, in line with our previous acute and chronic toxicological assessment (Chapter 4). *Daphnia magna* were exposed for 7 days either as part of a control group or to 4 exposure concentrations. Seven day exposures were chosen due to the excessive variability in these cations at 24 hours (Figure A6.1-A6.2). Concentration ranges were 0-0.6 µg L^{-1} Ag NO_3, 0-4 µg L^{-1} PVP-Ag NPs, 0-10 µg L^{-1} PEG-Ag NPs and 0-5 µg L^{-1} Cit-Ag NPs. At the end of the exposures *Daphnia* were collected on 47 mm glass microfibre filters (GF/C Whatman™, GE Healthcare) and rinsed 3 times in Milli-Q water to remove excess cations from the daphnids surface, and subsequently brushed into 1.5 mL Eppendorf tubes. The filter was changed, and brush washed, between each exposure filtration. The Eppendorfs were pre-weighed and *D. magna* replicates were kept separate (i.e. 20 organisms per Eppendorf). The weight of the organisms and Eppendorf minus the Eppendorf weight was used to quantify the *D. magna* wet weight. The wet weight was

then multiplied by 0.08 to obtain the dry weight of the daphnids in line with previously stated procedures (Chapter 4, Smirnov, 2013 and Peterson *et al.*, 2009). *Daphnia magna* were transferred to 10 mL centrifuge tubes and digested under a fume hood in 3.6 mL of 10% analytical grade HNO_3 mixed with Milli-Q water at 100 °C for 2 hours. After digestion the mixture was diluted to 4% HNO_3 by adding 5.4 mL of Milli-Q water for analysis by ICP-MS (Varian 810, Agilent Technologies, Santa Clara, CA). Na^+, K^+ and Ca^{2+} were measured in a blank (9 mL of 4% HNO_3 in Milli-Q water), the control and each exposure replicate using a multi-element standard. The blank was subtracted from the final Na^+, K^+ and Ca^{2+} measures and these were then normalised by total dry weight of each replicate (mg(cation) . g(dry weight)$^{-1}$) and expressed as a percentage of the control mean for each cation.

6.3.5 Adenosine triphosphate (ATP), Superoxide Dismutase (SOD) and Catalase (CAT) extraction.

ATP, SOD and CAT assessments were all conducted on 7-9 day old juvenile *Daphnia magna* to ensure the organisms were at the same developmental and physiological state. Furthermore juveniles were used as this reduced the number required in each replicate to achieve measureable ATP, SOD and CAT. Between 40-50 *Daphnia magna* were exposed for 24 hours in triplicate with 4 mL of aM7 medium per *D. magna* – in line with previous toxicity tests and OECD protocols (Chapter 4, OECD 2004 and 2008). At the cessation of each test the organisms were caught on 47 mm glass microfibre filters (GF/C Whatman^{TM}, GE Healthcare) and brushed into Eppendorf tubes. The filter was changed, and brush washed, between each exposure filtration. The *Daphnia* were immediately submerged in 400 µL of potassium phosphate homogenisation buffer with EDTA (pH 7.4; 11.2 mL K_2HPO_4, 38.8 mL KH_2PO_4 and 1 mM EDTA) added. The *Daphnia* were then mechanically homogenized on ice using a hand homogenizer. The homogenates were centrifuged at 10,000 g (4 ºC) for 10 minutes. The supernatant was then removed, placed into clean Eppendorfs and frozen (-80 °C) until analysis. The *D. magna* supernatant obtained after homogenisation was thawed at room temperature (20-22°C) when required for use.

6.3.6 ATP assay

Total ATP was measured in a control group and 3 exposure concentrations. Concentration ranges for the test were 0-0.6 µg L^{-1} Ag NO_3, 0-4 µg L^{-1} PVP-Ag NPs, 0-

4 µg L^{-1} PEG-Ag NPs and 0-6 µg L^{-1} Cit-Ag NPs. ATP was analysed in a 96 well plate by measuring Luminescence on a SpectraMax M5 plate reader (Molecular Devices, LLC) plate reader using the Promega ATP detection Buffer (Promega©, Mitochondrial ToxGlo™). ATP analysis was carried out according to the supplier's guidelines with few adaptations. Briefly; the ATP detection buffer was thawed at 37 °C and then kept at room temperature. A volume 10 mL of ATP detection buffer was then transferred to ATP detection substrate to reconstitute the lyophilized enzyme/ substrate mixture. The mixture was then vortexed to obtain a homogenous solution. This resulted in a 2-times strength ATP detection reagent. The supernatant obtained after homogenisation was thawed at room temperature (20-22°C) and 50 µL from each replicate was placed into individual wells. The ATP detection reagent was then added (50 µL) to each well and the plate was then mixed by orbital shaking at 700-900 rpm for 5 minutes which was immediately followed by analysis. ATP was expressed as mean Luminescence (RLU) μg^{-1} (protein) as recorded by the plate reader and Softmax Pro 5 software package. Exposure response was assessed in relation to the control and expressed as a percentage of the relevant control mean.

6.3.7 Lactate dehydrogenase (LDH) assay

LDH assays were conducted on 3-4 day old juvenile *Daphnia magna* to ensure the organisms were at the same developmental and physiological state. Furthermore juveniles were used as this reduced the number required in each replicate to achieve measureable LDH. *Daphnia magna* were exposed in triplicate in groups of 8 with 4 mL of aM7 medium per *D. magna* – in line with our previous toxicological assessment. Total LDH was measured in a control group and 4 exposure concentrations. Concentration ranges for the test were 0-0.6 µg L^{-1} Ag NO_3, 0-4 µg L^{-1} PVP-Ag NPs, 0-10 µg L^{-1} PEG-Ag NPs and 0-5 µg L^{-1} Cit-Ag NPs. Daphnids were fed 5 x 10^5 cell mL^{-1} (≥ 0.2 mg of carbon per *D. magna*) of *C. vulgaris* only for reasons previously mentioned (Chapter 2 and 4). Medium was not changed during the test. *D. magna* were kept in their respective exposures for 96 hours before collection to ensure sufficient time for the enzyme to activity to stabilize and as changes have been found at 96 hours in energy allocation studies (De Coen and Janssen, 2003). If mortality had occurred during the test those exposure chambers which had less than 50% of the originally exposed *Daphnia magna* were discarded as this was shown to impact data due to sensitivity issues of the methods employed.

Daphnia magna were collected either before or after the 16 hour light cycle began, 7.30a.m. and 9.30a.m., respectively. After collection the *D. magna* were placed in 1.5 mL Eppendorfs and medium was removed via a 1 mL pipette. The medium was replaced by 400 µL of phosphate saline buffer (PBS) and the *D. magna* were immediately mechanically homogenized with a hand homogenizer. The homogenates were then centrifuged at 10,000 rpm for 8 minutes (Eppendorf Centrifuge 5424R) with the supernatant analysed immediately after centrifugation.

Total LDH activity was measured using methods from Bergmeyer (1974) adapted to a 96-well plate format. Standards were set at 0-2000 units mL^{-1} activity; standards were run in triplicate and each standard well contained 20 µL of PBS and 60 µL of the standard. A volume of 30 µL of supernatant from each control or exposure replicate was placed in each test well followed by the immediate addition of NADH-pyruvate mixture (1 mg mL^{-1} of NADH added to a 0.75 mM sodium pyruvate solution; Sigma Aldrich). The plate was then incubated in the dark for 30 minutes at 37 °C. After 30 minutes incubation 50 µl of 2,4-dinitrophenylhydrazine-HCl mix (0.2 mg mL^{-1} dissolved in 1M HCl; DPNH-HCl; Sigma Aldrich) was added to each well and this mixture was incubated at room temperature in the dark for 20 minutes. After this incubation period 50 µl 4 M sodium hydroxide (Sigma Aldrich) was added to each well and the plate was allowed to stand for 5 minutes. Absorbance was then measured at 540 nm on a MRX revelation plate reader (Dynex Technologies©) and test sample LDH activity was established from the standards using the Revelation Software package (v. 4.2.5).

LDH was expressed as activity per *D. magna* as protein and weight could not be quantified and shown as a percentage response relative to the control group to normalise data sets.

6.3.8 CAT assay

CAT activity was measured in a control group and 3 exposure concentrations. Concentration ranges for the test were 0-0.6 µg L^{-1} Ag NO_3, 0-4 µg L^{-1} PVP-Ag NPs, 0-4 µg L^{-1} PEG-Ag NPs and 0-6 µg L^{-1} Cit-Ag NPs. CAT specific activity was measured by the decrease in absorbance at 240 nm due to H_2O_2 consumption (e=40 M^{-1} cm^{-1}) according to Greenwald (1985). The supernatant obtained after homogenisation was thawed at room temperature (20-22°C) and 50 µL from each replicate was placed into individual wells of a UV flat bottomed microtiter® 96-well plate (Thermo Fisher

Scientific Inc.). CAT activity was then assessed by adding 180 µL of 50 mM potassium phosphate (pH 7.0) and subsequently adding 20 µL of 3% H_2O_2 to the tissue homogenate supernatant. After the addition of H_2O_2, any visible bubbles were popped. The plate was then transferred to a SpectraMax M5 plate reader (Molecular Devices, LLC) and absorbance change at 240 nm from 0-4 minutes was assessed every 20 seconds using SoftMax Pro 5 software package. CAT specific activity was quantified according to Claiborne (1985; equation (eq) 6.3) and expressed as mean units (of activity) mg^{-1} (protein). Exposure response was assessed in relation to the relevant control.

Eq. 6.3 (Claiborne, 1985)

$$\text{Specific Activity (units/mg protein)} = \frac{\Delta A \text{ x } 1000}{46.37 \text{ x mg protein/ml reaction mixture}}$$

6.3.9 SOD assay

Amount of SOD was measured in a control group and 3 exposure concentration *D. magna* homogenates using procedures similar to Marklund and Marklund (1974). Concentration ranges for the test were 0-0.6 µg L^{-1} Ag NO_3, 0-4 µg L^{-1} PVP-Ag NPs, 0-4 µg L^{-1} PEG-Ag NPs and 0-6 µg L^{-1} Cit-Ag NPs. 20 µL (or 20 µL of water for controls) from each replicate was placed into individual wells on a 96-well plate (F-sterile, VWR tissue cell culture plates). SOD activity was then assessed by the addition of 180 µL of dilute 20 mM pyrogallol 1:100 with 50 mM tris-buffer (note: dilution must occur immediately before test) to each well and then recording the change in optical density at 420 nm over 4 minutes every 20 seconds. SOD was quantified according to Greenwald (1985; eq 6.4) and expressed in ng mg^{-1} (protein). Exposure response was assessed in relation to the relevant control.

Eq. 6..4 (Greenwald, 1985)

$$\text{ng (SOD) mg}^{-1}\text{ (protein)} = \frac{\% \text{ inhibition x}}{50} \text{ x } 125 \text{ x } 3 \text{ x } \frac{1000}{\text{Sample Vol.}} \text{ x } \frac{1}{\text{Protein}}$$

6.3.10 Mitochondrial membrane potential (MMP) assessment

Mitochondrial membrane potential was assessed qualitatively using a JC-10 mitochondrial membrane dye using z-stacking on a confocal microscope. *Daphnia*

magna were <24 hours old from the 1st or 2nd brood to ensure smaller size allowing quicker z-stacks and thus analysis of the organism ensuring survival and ability to capture a whole organism with the magnifications used. *Daphnia magna* were exposed to one concentration for 24 hours. Exposure concentrations were 1 µg L^{-1} PVP-Ag NP, PEG-Ag NP and Cit-Ag NP, and 0.2 µg L^{-1} $AgNO_3$. These levels were chosen to be at or below lowest observed effect concentrations.

Immediately post-exposure the daphnids were placed in clean aM7 medium. They were then immediately transferred to 5 mL of 0.1% Pluronic® acid aM7 medium mixture for ~40 minutes to permeabilise the *Daphnia magna* cell membranes to allow uptake of the mitochondrial membrane dye. After cell permeabilisation 3.6 µL of JC-10 dye was added to the mixture and incubated in the dark at room temperature (20-22 °C). During permeabilisation and staining organisms were placed on an orbital plate shaker (100-200 rpm) to encourage *Daphnia magna* movement and uptake of the dye. The organisms were then placed on a glass microscope slide and viewed under Leica DMIRE2 confocal microscope (Leica Microsystems©). A dry 10x (0.25) objective was used and z-plane step size was set to 2 µm in order to build a 3D image. Fluorescence was observed at green and red wave lengths (525 nm and 590 nm, respectively) simultaneously, gain photomultipliers were set to 710 and 700, respectively. Detection pinhole diameter was set to 150 µm and ArHeNe (488) intensity was set at 75%. Display resolution was 1024 x 1024 pixels.

6.3.11 Protein analysis

Protein content was determined according to Bradford (1976). Protein standards were made fresh with bovine serum albumin (BSA) and serial dilutions were made between 0-1 mg ml^{-1} protein a volume of 10 µL of the standards or test samples were added to each well in 96-well plate (F-sterile, VWR tissue cell culture plates) in triplicate with 200 µL of Bradford reagent added thereafter. The 96-well plate was then immediately transferred to a MRX revelation plate reader (Dynex Technologies©) and test sample protein was established from the standards using the Revelation Software package (v. 4.2.5).

6.3.12 Statistical analysis

Ionoregulation, ATP, LDH, SOD and CAT differences were assessed in relation to the control. Mitochondrial staining was qualitatively assessed in comparison to the control

daphnids. All other methods for statistical analysis have been reported in Chapter 1. ANOVA tests when significant were followed by post-hoc Dunnett's test to establish pair-wise significance between controls and the exposure groups. Kruskall- Wallis tests, when significant were followed by pair-wise post-hoc testing between controls and exposure groups using the Mann-Whitney U test.

6.4 Results

6.4.1 Ionoregulation assessment

$AgNO_3$ significantly decreased *Daphnia magna* total body Na^+ and K^+ content in a dose dependent manner (χ^2 = -0.447, d.f. 17, $p < 0.05$, Na^+; $F = 8.571$, d.f. = 17, $p < 0.01$, K^+; Figure 6.2 A). Potassium levels were affected at $AgNO_3$ concentrations of 0.3 µg L^{-1} ($p < 0.05$) and both Na^+ and K^+ were affected significantly in the higher concentrations ($p < 0.05$), with the largest decrease seen in whole body K^+ concentrations. Sodium levels remained above 80-90% of the control which is above levels reported to lead to mortality (i.e. ~30% decrease, Paquin *et al.*, 2002). Despite the expected ~20-30% dissolution of the Ag NPs, which would lead to a similar or higher levels of dissolved Ag in Ag NP exposures in comparison to the $AgNO_3$ exposures, and despite the Ag NP exposures being at equitoxic levels to each other and $AgNO_3$, only PVP-Ag NPs significantly affected K^+ levels, seen as a decrease ($F = 7.628$, d.f. = 17, $p < 0.01$; Figure 6.2 B). No other exposures were able to affect Na^+ or K^+ ($F \leq 2.901$, d.f. = 17, $p > 0.05$; Figure 6.2 C-D). PVP-Ag NPs significantly decreased whole body K^+ content at the 2 lower exposure concentrations but this was not observed at the higher concentrations ($p < 0.01$; 1 and 2 µg L^{-1}). PEG-Ag NPs displayed a similar pattern to PVP-Ag NPs with a decrease in K^+ body content at the 2 lower exposure concentrations, followed by an increase back toward control levels, however no significant variation was found ($F = 1.814$, d.f. 17, $p = 0.186$; Figure 6.2 C).

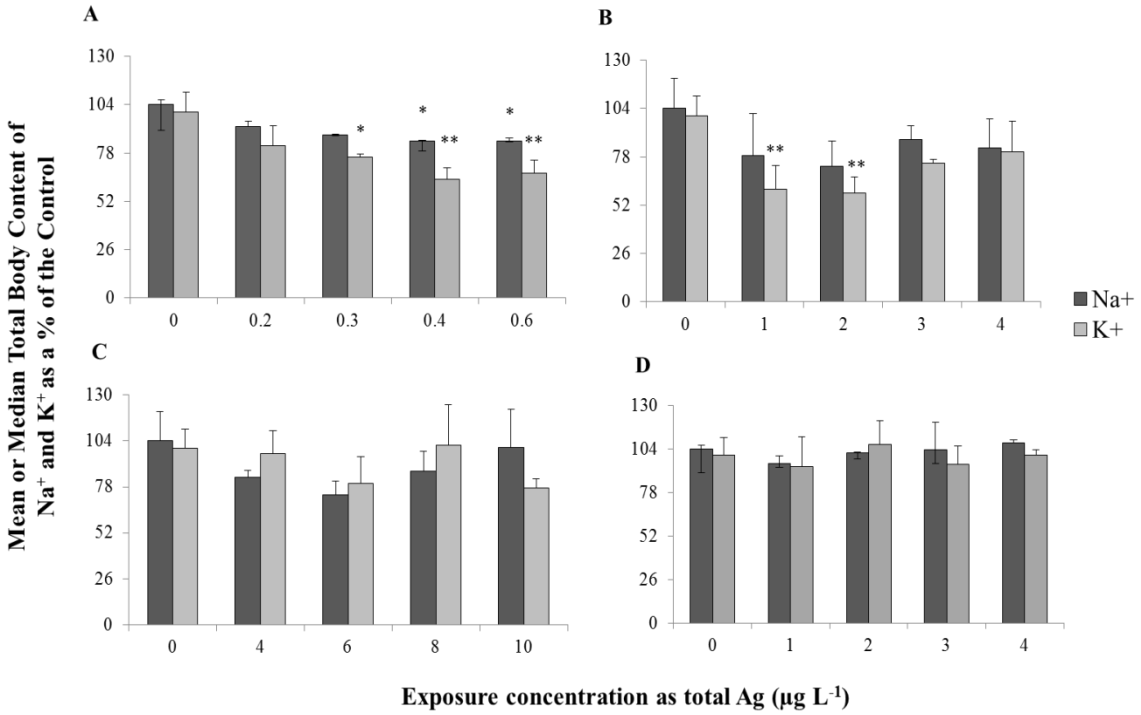

Figure 6.2 *D. magna* whole body Na^+ and K^+ content in a control group (0 µg L^{-1} Ag) and after 7 days exposure to $AgNO_3$ (A), PVP-Ag NPs (B), PEG-Ag NPs (C) and Cit-Ag NPs (D) (n = 3). Single sided error bars are 95% CI for parametric data. 2 sided error bars represent the inter-quartile range for non-parametric data. *, ** denotes significant difference from control at $p < 0.05$ and $p < 0.01$, respectively. Whole body Na^+ and K^+ content of controls ranged between 6.14-10.4 and 8.86-12.82 mg g (dry weight)$^{-1}$, respectively.

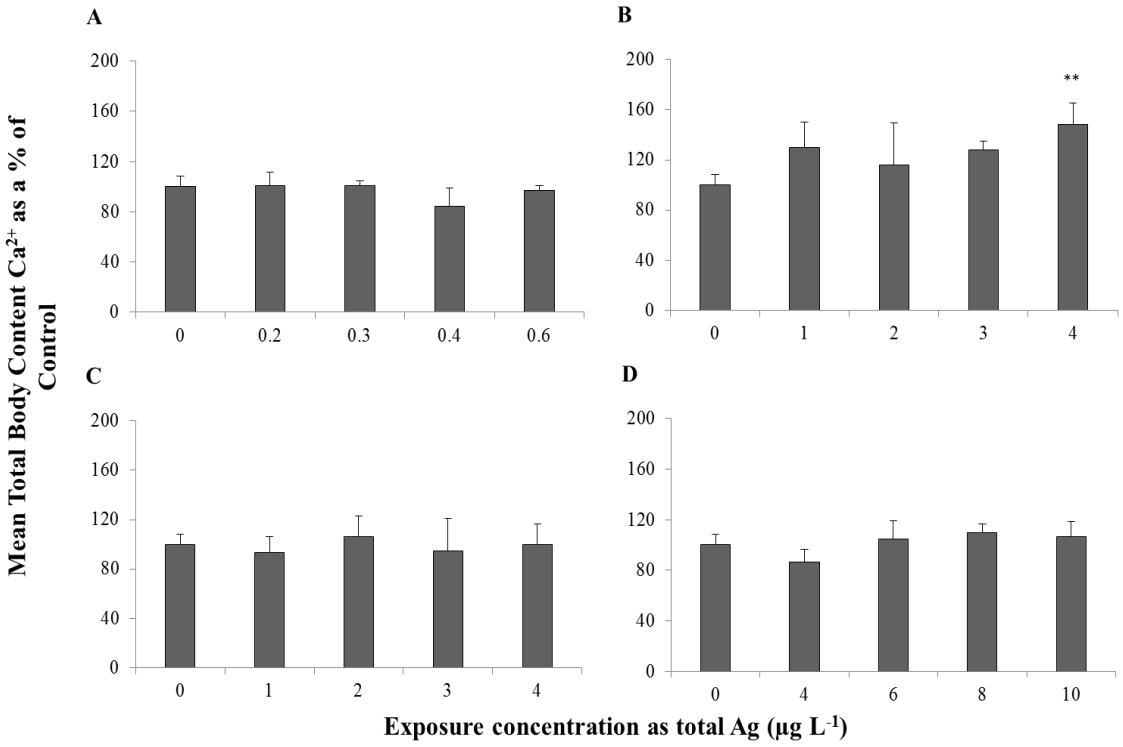

Figure 6.3 *D. magna* whole body Ca^{2+} content in a control group (0 µg L^{-1} Ag) and after 7 days exposure to $AgNO_3$ (A), PVP-Ag NPs (B), PEG-Ag NPs (C) and Cit-Ag NPs (D) (n = 3). Single sided error bars are 95% CI. ** denotes significant difference from control at $p < 0.01$. Whole body Ca^{2+} content of controls ranged between 48.58-65.51 mg g(dry weight)$^{-1}$.

PVP-Ag NP exposures at 4 µg L^{-1} significantly increased whole body Ca^{2+} levels in comparison to the control group (F = 4.978, d.f. = 17, $p < 0.05$, one-way ANOVA; $p < 0.01$, Dunnett's post-hoc test; Figure 6.3 B), no other exposures to Ag NPs or $AgNO_3$ significantly affected calcium levels in *Daphnia magna* ($F \leq 2.497$, d.f. = 17, $p > 0.05$; Figure 6.3 A, C and D).

6.4.2 Adenosine triphosphate (ATP) assay

Considering the effects upon whole body cations and the reliance of their regulation predominantly through ATP mediated mechanisms (i.e. Na^+, K^+ ATPase), and the integrity of ATP to the organism as a whole, the impact $AgNO_3$ and the 3 Ag NPs had on ATP was tested. Interestingly despite the differences seen in the level of Na^+ and K^+ in $AgNO_3$ exposures ATP levels were not significantly affected by this treatment (F = 1.829, d.f. = 11, $p < 0.05$; Figure 6.4, A). However all Ag NPs induced a dose-

dependent decrease in ATP levels ($F \geq 6.053$, d.f. = 11, $p < 0.05$, PVP-Ag NPs and PEG-Ag NPs; and $\chi^2 = 8.538$, d.f. = 11, $p < 0.05$, Cit-Ag NPs; Figure 6.4 B-D). PVP-Ag NPs appeared to be the most potent decreasing ATP content at the lowest dose tested (1 µg L^{-1}) ($p < 0.05$, 1 µg L^{-1}; Figure 6.4, B). Cit-Ag NPs showed a significant response at the 2 highest concentrations (overall; $\chi^2 = 8.538$, d.f. = 11, $p < 0.05$) again in a dose dependent manner ($Z = 1.964$, d.f. = 5, $p < 0.05$; 3 and 6 µg L^{-1}; Figure 6.4, D). PEG-Ag NPs showed a significant decrease at 4 µg L^{-1} only, however there was still a trend for decreased ATP levels with increasing Ag NP concentration ($F = 6.053$, d.f. 11, $p < 0.05$ one-way ANOVA; $p < 0.05$ Dunnett's post-hoc test; Figure 6.4, C).

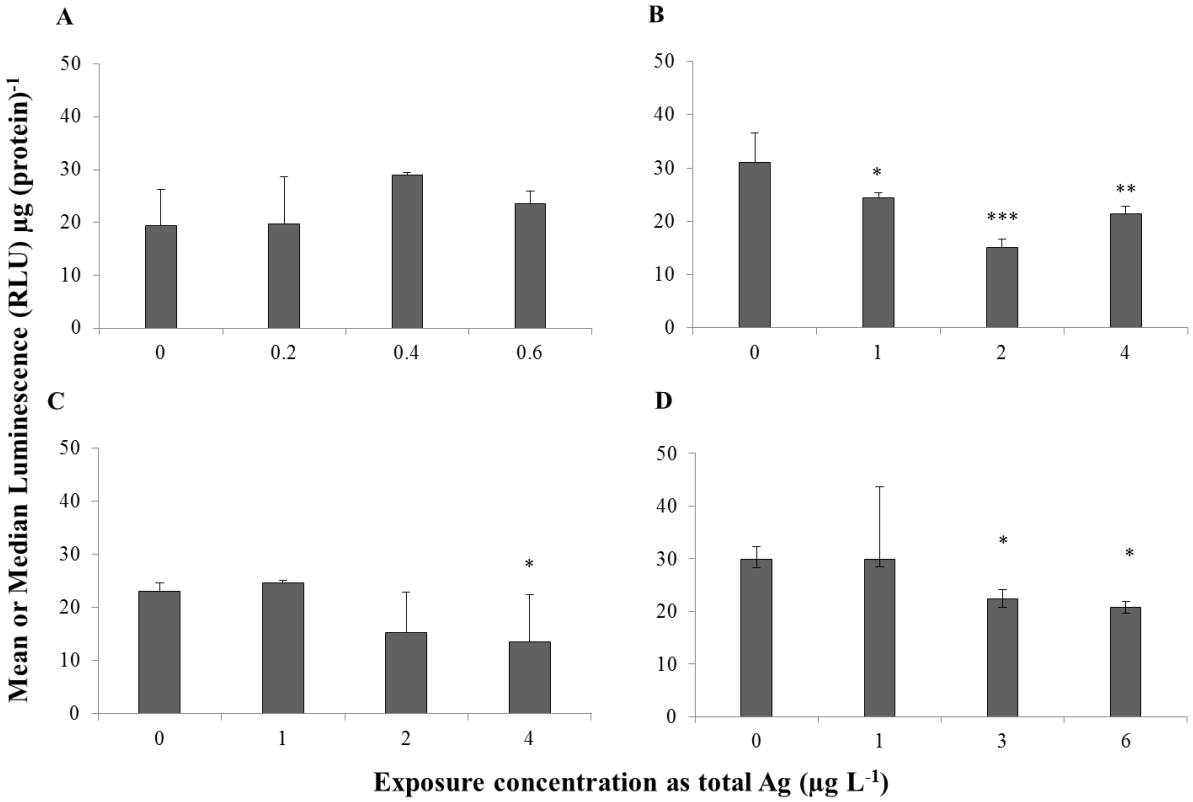

Figure 6.4 Luminescence (RLU) of *D. magna* homogenates during ATP assay, indicative of ATP content after 24 hour exposure to $AgNO_3$ (A), PVP-Ag NPs (B), PEG-Ag NPs (C) and Cit-Ag NPs (D) ($n = 3$). Single sided error bars are 95% CI for parametric data. 2 sided error bars represent the inter-quartile range for non-parametric data. *, **, *** denotes significant difference from control at $p < 0.05$, $p < 0.01$ and $p < 0.001$, respectively.

6.4.3 Lactate dehydrogenase (LDH) assay

The effects on ATP may be from either aerobic or anaerobic pathway disturbances. LDH is involved in anaerobic energy production and requirements may increase due to upregulated ATP synthesis via anaerobic pathways. Increased anaerobic metabolism can be compensatory mechanism when there are large and rapid increases in energy requirement and/ or when sufficient oxygen is not present to meet the demands of ATP production through aerobic respiration (Germann and Stanfield 2004 and Diamantino et al., 2001). The increase in requirement of LDH may be for processes such as upregulation of detoxification mechanisms and during times of stress (Zeis *et al.,* 2009, De Coen, Janssen and Segner 2001 and Diamantino *et al*., 2001) and/ or, simply more energy for movement and physiological function (Zeis *et al.,* 2009 and Germann and Stanfield 2004). When excessive or greater than normal amounts of ATP are being produced during times of rapid energy requirement (i.e. via anaerobic processes) due to stress LDH levels/ activity may increase (De Coen, Janssen and Segner 2001, Wu and Lam 1997 and Guilhermino 1994). Equally LDH activity/ levels during assays my decrease as cell function becomes compromised through damage. Therefore the reaction of such enzymes to toxicants often displays a hormetic-like affect, whereby low toxicant levels lead to increases but high levels lead to decreases (Diamantino *et al*., 2001 and Guilhermino 1994).

Here the study showed that $AgNO_3$ and Ag NP exposures were able to significantly increase and/ or decrease LDH levels/ activity in *D. magna* after 96 hour exposures (Figure 6.5). An unexpected and interesting effect was the time-dependent change in response shown in some exposures when *D. magna* were either homogenized before (7:30 a.m.) or after (9:30 a.m.) the start of the light 16 hour cycle (Figure 6.5 A-C). The time points (7:30 and 9:30 a.m.) were not chosen in order to investigate the effect of time. The initial study design simply required sampling early in the morning. Subsequent examination of the data however suggested a time dependent effect potentially linked to the light cycle timing of the incubator and hence the organism. However, some *n*-numbers were quite large and the effects were measured with more than one clutch from more than one parent animal at each time point, meaning any effect seen may be consistent across the population.

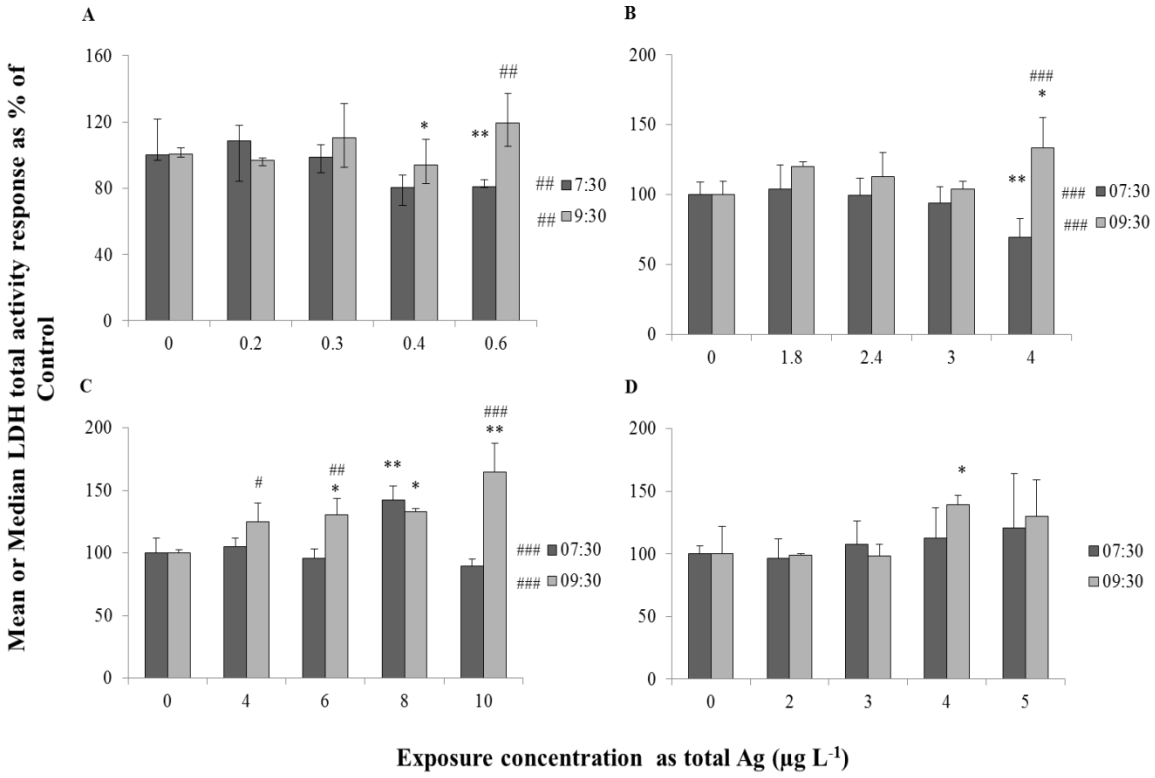

Figure 6.5 *Daphnia magna* whole body homogenate LDH activity levels taken before (7:30 a.m.) or after (9:30 a.m.) the 16 hour light cycle had begun, and the response in relation to a control group (0 µg L^{-1} Ag) when exposed to Ag NO_3 (A), PVP-Ag NPs (B), PEG-Ag NPs (C) and Cit-Ag NPs (D) for 96 hours ($n \geq 3$). 2-sided error bars are interquartile ranges (non-parametric data), 1-sided error bars are 95% CI based (parametric data). $^{\#, \#\#, \#\#\#}$ are significant differences between time points at the same concentration; significances are $p < 0.05$, < 0.01 and < 0.001 for each respective notation. *, **, *** are significant differences from the control at the same time; significances are $p < 0.05$, $p < 0.01$ and $p < 0.001$, respectively.

$AgNO_3$ response significantly differed between 7:30 and 9:30 a.m. (Z = -2.220, d.f. = 23, $p < 0.05$; 0.6 µg L^{-1}, Figure 6.5 A). Before the light cycle began LDH in $AgNO_3$ exposures showed a dose-response seen as a trend to decrease with increasing $AgNO_3$ concentrations which became significant at 0.4 and 0.6 µg L^{-1} (Z = -2.242, d.f. = 11, $p <$ 0.05, control vs. 0.4 µg L^{-1}; Z = -2.882, d.f. = 11, $p < 0.01$, control vs. 0.6 µg L^{-1}; Figure 6.5, A). However at 9:30 a.m. $AgNO_3$ showed no relationship or significant differences with increasing $AgNO_3$ concentrations (χ^2 = 4.552, d.f. = 29, $p > 0.05$; Figure 6.5, A). PVP-Ag NPs showed a similar pattern to $AgNO_3$ exposures with those homogenates taken at different times having a significantly different response in the highest PVP-Ag

NP exposure concentration (F = 15.936, d.f. = 37, $p < 0.001$; 4 µg L^{-1}; figure 6.5, B) with daphnids collected before the light cycle (7:30 a.m.) showing significant decreases in LDH levels/ activity (one-way ANOVA, F = 4.002, d.f. = 31, $p < 0.05$; Dunnett's post-hoc test, $p < 0.01$; Figure 6.5, B), and organisms collected after the light cycle began (9:30 a.m.) having significant increases in LDH levels/ activity began (one-way ANOVA F = 3.783, d.f. = 14, $p < 0.05$; $p < 0.05$, Dunnett's post-hoc test; Figure 6.5, B). For PEG-Ag NP there also appeared to be a significant difference between the 2 sampling times (F = 24.610, d.f. = 31, $p < 0.001$), however PEG-Ag NPs in both instances only significantly increased LDH levels/ activity, but at 9:30 a.m. these increases were greater (Figure 6.5, C). At 9:30 a.m. LDH was significantly increased by PEG-Ag NP exposure in *D. magna* at 6, 8 and 10 µg L^{-1} in a dose dependent manner (one-way ANOVA F = 10.832, d.f. = 13, $p < 0.01$; Dunnett's post-hoc test $p < 0.05$, 6 and 8 µg L^{-1}; $p < 0.001$, 10 µg L^{-1}; Figure 6.5, C). At 7:30 a.m. again there was an increase in LDH levels/ activity after PEG-Ag NP exposure with the effect not as pronounced only being shown at 8 µg L^{-1} (one-way ANOVA F = 11.779, d.f. = 28, $p < 0.001$; Dunnett's post-hoc test $p < 0.001$; Figure 6.5, C).

Cit-Ag NPs appear to be somewhat of an anomaly amongst this data set with no significant difference shown between times, and thus no apparent time-dependent response (F = 0.332, d.f. = 58, $p > 0.05$; Figure 6.5, D). However there was still enough disturbance (seen as an increase) at 4 µg L^{-1} to cause a significant effect on whole body LDH levels/ activity by Cit-Ag NP exposures, which was seen at homogenates taken at 9:30 a.m. (one-way ANOVA F = 5.073, d.f. = 13, $p < 0.05$; Dunnett's post-hoc test $p < 0.05$; Figure 6.5, D).

6.4.4 Superoxide dismutase (SOD) and catalase (CAT) assay

The data suggest Ag NPs and Ag^{+} are able to affect the energetic and osmoregulatory systems and are able to be accumulated within the organism causing acute toxic effect (Chapters 4 and 5), thus certain detoxification mechanisms may also be upregulated. Any disturbance in energy systems may lead to increased or decreased productions of ROS; therefore those enzymes responsible for oxidation of these harmful by-products may be affected. Firstly CAT activity was tested here no exposure caused a significant effect on CAT specific activity ($F \leq 4.172$, d.f. = 11, $p > 0.05$, Figure 6.6, A-D). SOD was also tested; here significant effects were found on SOD levels caused by PVP-Ag NP and Cit-Ag NP exposure ($\chi^2 \geq 8.744$, d.f. = 11, $p < 0.05$; Figure 6.7, B and D),

however no significant change was seen in either $AgNO_3$ or PEG-Ag NP exposures ($F \leq$ 1.389, d.f. = 11, $p < 0.05$; Figure 6.7 A and C). PVP-Ag NPs showed a dose-dependent decrease of SOD with increasing exposure concentration which was seen at the lowest concentration and thereafter (Z = -1.964, d.f. = 11, $p < 0.05$ for 1 µg L^{-1}, 2 µg L^{-1} and 4 µg L^{-1} PVP-Ag NP exposures; Figure 6.7, B). On the other hand Cit-Ag NPs showed a dose dependent increase in SOD level with increasing Ag NP exposure which was again seen at 1, 3 and 6 µg L^{-1} (Z = -1.964, d.f. = 11, $p < 0.05$; Figure 6.7, D).

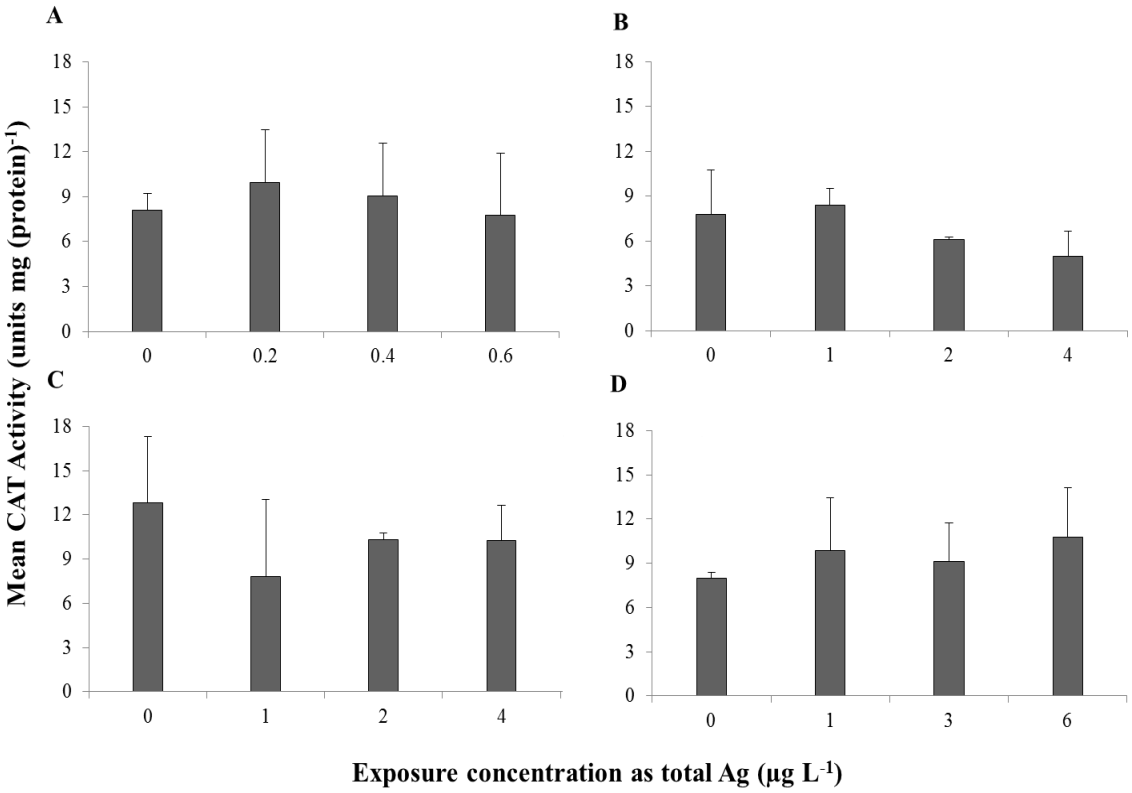

Figure 6.6 *D. magna* CAT specific activity in whole body tissue homogenates in a control group or after a 24 hour exposure to $AgNO_3$ (A), PVP-Ag NPs (B), PEG-Ag NPs (C) and Cit-Ag NPs (D) (n = 3). Error bars are 95% CI.

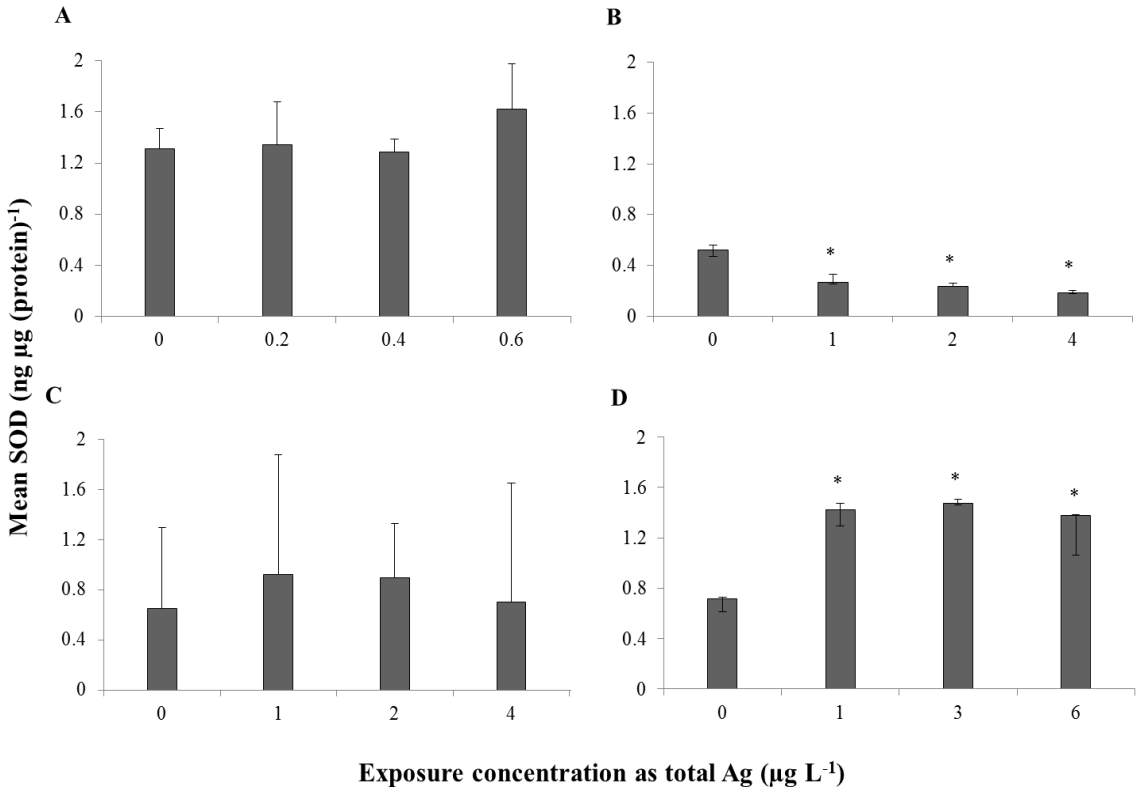

Figure 6.7 *D. magna* SOD quantity of whole body tissue homogenates in a control group or after a 24 hour exposure to $AgNO_3$ (A), PVP-Ag NPs (B), PEG-Ag NPs (C) and Cit-Ag NPs (D) (n = 3). Error bars are 95% CI. *, ** denotes significant differences from control at $p < 0.05$ and $p < 0.01$ respectively.

6.4.5 Mitochondrial Membrane potential (MMP) assessment

JC-10 staining qualitatively showed that all Ag NPs exerted an effect on mitochondrial membrane potential seen as a decrease in red fluorescence and increased green fluorescence intensity when compared to the control *Daphnia magna* images. This shows there was a drop in mitochondrial membrane potential in all exposures to Ag NP. The weakest effect was seen in Cit-Ag NPs (Figure 6.8, E) with PVP-Ag NPs (Figure 6.8, C) and PEG-Ag NPs (Figure 6.8, D) showing the strongest effect on mitochondrial membrane potential, when comparing to controls (Figure 6.8, A). $AgNO_3$ appeared to show a similar degree of red fluorescence and green fluorescence (Figure 6.8, B) when compared to the controls (Figure 6.8, A) suggesting that $AgNO_3$ exposures were unable to exhibit as strong an effect on the mitochondria as Ag NPs. *Daphnia magna* that were only exposed to either Ag NPs, Ag NO_3, or as controls showed no auto fluorescence. Furthermore mitochondrial rich physiological points of interest, such as the nuchal

organ, at the neck, and epipodite, on the filtering limbs of the *Daphnia*, can be seen (Figure 6.8, *x*-*z*).

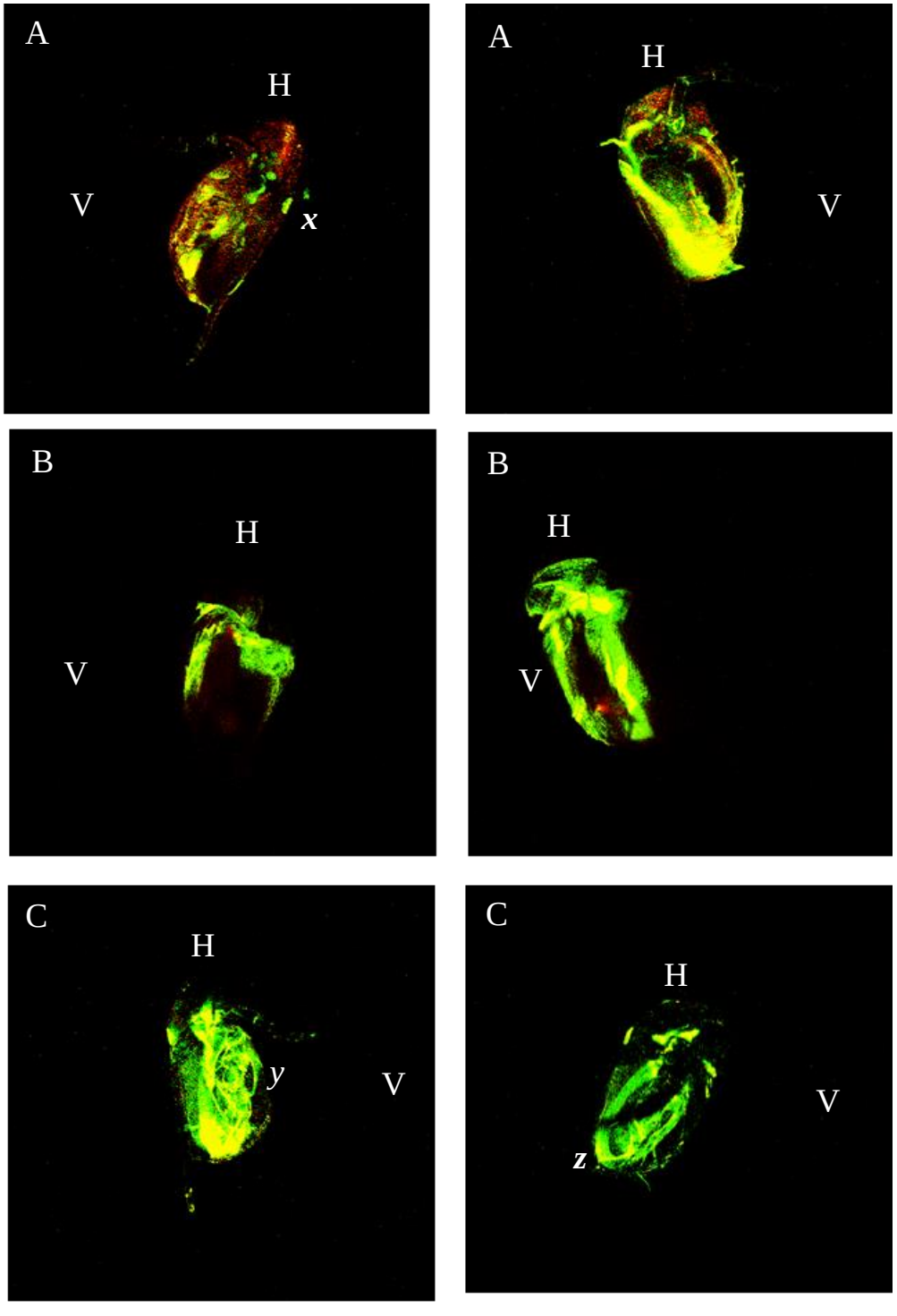

Figure 6.8 (detailed below)

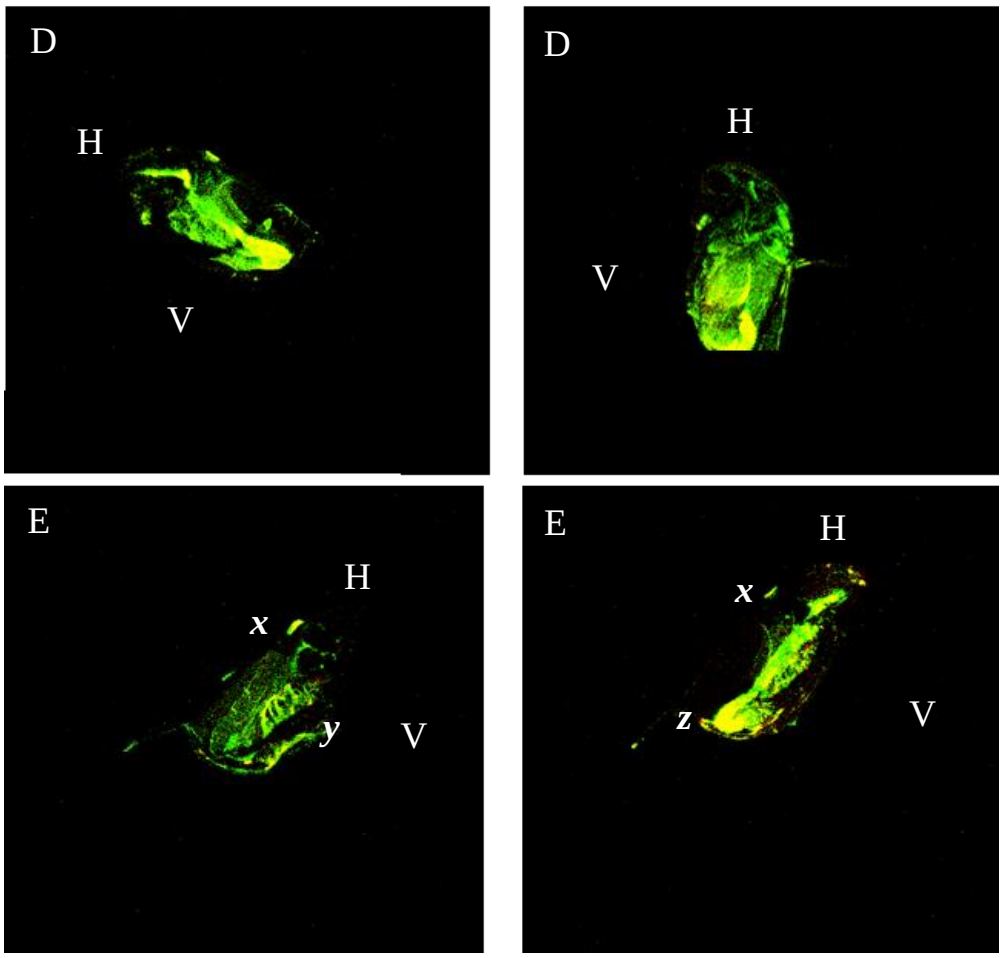

Figure 6.8 (cont.) JC-10 staining showing mitochondrial membrane potential in a control group (0 µg L^{-1} Ag; A) or after a 24 hour exposure to $AgNO_3$ (0.2 µg L^{-1}; B), PVP-Ag NPs (1 µg L^{-1}; C), PEG-Ag NPs (1 µg L^{-1}; D) and Cit-Ag NPs (1 µg L^{-1}; E). Physiological features: nuchal organ (*x*), filtering limbs and epipodite (*y*) and gut (*z*). For orientation H = head crest, V = ventral.

6.5 Discussion

6.5.1 Ionoregulation

The study showed that only $AgNO_3$ was able to significantly decrease *D. magna* Na^+ and K^+ content in a concentration dependent manner. Of the NPs, only PVP-Ag NPs were able to exert an effect on *D. magna* K^+ content, seen as a decrease at lower exposure concentrations. This effect was not present at the higher concentrations of PVP-Ag NPs. PVP-Ag NPs were the only exposure that resulted in any effect on *D. magna* calcium content, seen as a significant increase at the highest concentration

tested. The toxicological MOA of Ag^+ to aquatic organisms both acutely and chronically, including the invertebrate *Daphnia magna*, is reported to be due to ionoregulatory disturbances. This is largely caused by the inhibition of Na^+ K^+ -ATPase which leads to a reduction in whole body Na^+ and K^+ levels (Bianchini and Wood, 2003). Calcium is an integral cation in *Daphnia magna* life-history and its regulation is important for moulting processes and nerve function (Zhao and Wang, 2013). Calcium regulation also partly occurs at the epipodite, one of the main areas which can be affected by ionic silver. It has been suggested, and there is strong evidence, that Ag NPs elicit the same effects on cationic control of *Daphnia magna* and that the toxicity, and effect is due not to the Ag NP but its dissolved fraction (Newton *et al.*, 2013 and Zhao and Wang, 2013). However, it is also true that the effect of Ag NP coating on toxicological outcome has not been fully elucidated and this may not only change the degree of toxicity displayed but also how the particle interacts with the organism and thus its MOA. The current study tested the hypothesise that Ag NP toxicity is attributable to Ag^+, and ionoregulatory disturbances thereafter, by measuring Na^+, K^+ and Ca^{2+} levels in *Daphnia magna* whole body homogenates after exposure to 3 differently coated Ag NPs and $AgNO_3$ (which readily dissolves to Ag^+) as a positive control. As the Ag NP sizes remained the same but coating changed it enabled the establishment of how, and if, this factor would change the toxicological outcome.

Unlike Zhao and Wang (2013) the current study was unable to show significant decrease in Na^+ by any of the tested Ag NPs despite being at equitoxic exposures with $AgNO_3$ and despite the fact these exposures would produce higher Ag^+ exposures than the $AgNO_3$ concentrations tested. Although possible speciation with free coatings dissociated from the Ag NPs is possible and would reduce Ag^+ in the aqueous phase at equitoxic concentrations one would still expect the same physiological outcomes. This is because the same amount of free-ion would be required for the same affect. Only PVP-Ag NPs were able to affect K^+ levels but only at the lower exposure concentrations. This decrease in K^+, to our knowledge, is the first to be noted in *Daphnia magna* after Ag NP exposure.

It has been previously discussed that Ag NPs during short term exposures may affect the epipodite in the same manner as $AgNO_3$ but at higher concentrations owing to their lower affinity or, their interactions with a different organism ligand. The data here suggest that if a required critical load of Ag at the epipodite, or another external physiological feature, is the cause for toxicity in all cases then the Ag likely binds and

affects a different ligand not only between $AgNO_3$ and Ag NPs, but also between Ag NPs dependent on coating, as the effects seen are different for each NP. Although PEG-Ag NPs and PVP-Ag NPs showed a similar pattern for decrease in Na^+ and K^+ body levels only PVP-Ag NPs were significant. This may suggest that coating, steric in this instance, may be important in determining the physiological outcomes. Furthermore Cit-Ag NPs showed no such pattern and these particles were charge bound to their coating. The coating dependent pattern may be due to how the coatings are able to dissociate from the NP and interact with Ag^+ and/ or reveal more of the Ag NP surface, but further investigation would be required to elucidate such physicochemical actions. The current data only corroborates with one other study (i.e. Stensberg *et al.*, 2014) but this study is one of only 3 studies to investigate the possibility of this MOA in *Daphnia magna* exposed to Ag NPs.

Zhao and Wang (2013) are one of the only studies within the peer reviewed literature to study Ca^{2+} disturbances in *D. magna* after $AgNO_3$ and Ag NP exposure. They showed an increase in whole body Ca^{2+} after both types of exposure at 48 hours (i.e. Ag^+ and $AgNO_3$) and this was an effect they attributed solely to Ag^+ release from the Ag NP. Further to this they hypothesised the release was due to either calcium's protective role against cationic metals or due to its disturbance during cellular toxicological insult/ interactions. The authors suggested the increase due to calcium's protective role may only be short term (24-48hours) as previously demonstrated in the plasma of *Oncorhynchus mykiss* (Wood *et al.*, 1996). The short term effect would indeed suggest that it may be an initial calcium defence mechanism against increased body metal concentrations, not other processes. In corroboration with Wood *et al.* (1996) our results demonstrate that after 7 days daphnid whole body Ca^{2+} is unaffected by $AgNO_3$ exposure. However after 7 day exposures to PVP-Ag NPs (4 µg L^{-1}) Ca^{2+} is still significantly increased (148%) when compared to the controls. The effect observed may be due to a Trojan-horse mechanism whereby after uptake/ association PVP-Ag NPs are able to slowly release Ag^+ into the organism; however it may equally be due to a NP effect. It is possible that Ag exposure can interfere with Ca^{2+}-ATPase enzyme at the epipodite, leading to disturbances in this cation. Considering the Ca^{2+} regulatory control over moulting one may expect that any effect on this cation may lead to the increase, decrease or cessation of the shedding of the carapace. An effect on carapace moulting has been noted for $AgNO_3$ and PEG-Ag NPs, but also qualitatively for PVP-

Ag NPs where failure to moult led to the entrapment of a *Daphnia magna* neonate and mortality of the parent animal (Chapter 4, Figure 4.8).

Although there were strong effects on calcium (increase) and potassium (decreases) for PVP-Ag NPs, $AgNO_3$ was the only exposure that consistently effected cations in a dose dependent manner. Due to this it is suggested that each NP, dependent on particle coating, could have slightly different organism interactions (i.e. binding and uptake) but toxicity overall may be through similar processes and in most instances the major driver for NP toxicity is likely not Ag^+ release into the water column release.

6.5.2 Adenosine triphosphate (ATP)

The current study has shown Ag NPs cause a significant decrease in total ATP within *D. magna* after 24 hour exposures. The degree of the effect was coating dependent and followed the same rank order of toxicity as the acute bioassay tests (Chapter 4) with PVP-Ag NPs exerting the strongest effect, followed by Cit-Ag NPs and then PEG-Ag NPs. $AgNO_3$ was unable to affect this biochemical after 24 hour exposures. This may highlight a potential nanospecific effect.

ATP is a well-known biochemical used as cellular energy and recently its role as a cellular signaller (e.g. apoptosis and necrosis) and integrity within other systems (e.g. nervous system) has come to light (Burnstock, 2006 and Nicotera, Leist and Ferrando-May 1998). Furthermore the disturbance of cellular ATP, namely decreases, leads to cell system failure and eventual cell death (Martin and McLean 1995). Considering the toxicity displayed by Ag^+ and Ag NPs on mitochondrial function and the integral role this organelle has in ATP production both of these contaminants may cause a disturbance in cellular ATP levels which are detrimental to the cell and organism (Stensberg *et al.*, 2014 and Almofti *et al.*, 2003). Also, the previously seen effects in *D. magna* chronic bioassays, such as decrease in length, may indicate disturbance in these systems (Chapter 4). At low levels ATP may indeed cause cell death but it also cannot be overlooked that this may affect feeding ability of the daphnids as they will have less energy to graze through the water column. In order to separate these effects to some degree food was not given during acute bioassays and the ATP tests were also conducted in short term experiments with no food (24 hours). If mortality is observed during these exposures over 48 hours or effects on ATP during 24 hours with no food they are not likely to be through feeding inhibition.

Interestingly, the research showed the only exposures able to consistently affect cellular ATP levels were the Ag NPs. After uptake/ association there could be a differing fate for Ag NPs compared to Ag^+ which may have more selective MOA at the epipodite. NPs have been shown to be caught in the midgut microvilli and associate with the peritrophic membrane, likely leading to their higher AE in comparison to their bulk or ionic counterparts (Khan *et al.*, 2014, Heinlaan *et al.*, 2011 and Zhao and Wang, 2010). After organism association the Ag NPs may act as a Trojan-horse releasing Ag^+ within the organism allowing Ag^+ to interact with, and penetrate, the cell membrane. The effect would be further enhanced by Ag NPs ability to increase plasma membrane permeability which has been seen at doses as low as 10 µg L^{-1} similar to the doses used here (Bradley-Stolle *et al*., 2010 and Bradley-Stolle *et al*., 2005). This could equally happen at the surface of cellular structures or if the Ag NP penetrated the cell releasing Ag^+. In either case the Ag^+ or Ag NPs will then be able to interact with organelles such as mitochondria and this "delivery system" may cause greater disturbance on intracellular functioning than the ionic form alone, as seen here. Increased permeability and degeneration of *Daphnia magna* gut epithelia and loss of cellular adhesion has recently been observed after NP exposure. This may result in larger particle uptake into intercellular space and this supports such theories (Georgantzopoulou *et al.*, 2013). In the aforementioned study both translocation into oocytes and internalization into cells were shown. Equally the reduction in ATP could be from the upregulation of DNA repair and detoxification mechanisms. Both DNA breakage and upregulated detoxification have been shown in cells and organisms, however, whether this is an artefact of the decreased ATP or whether it is the cause of the decrease in ATP is not well known.

6.5.3 Lactate dehydrogenase (LDH)

This study showed that all forms of Ag, including the different Ag NP types, were able to significantly affect LDH levels/ activity after 96 hours of exposure. However these exhibited as both increases and decreases, and appeared dependent on the time of sampling in some instances (i.e. either before (7:30 a.m.) or after (9:30 a.m.) the incubator's 16 hour light cycle had begun). Although a lot of research has highlighted mitochondrial dysfunction caused by silver in many forms in cell line systems this is less well established in the organism as a whole, particularly in *Daphnia magna*. Furthermore during a reduction of mitochondrial function, leading to decreased ATP levels or when there is higher demand for ATP certain systems may compensate, such

as the anaerobic glycolytic system (Germann and Stanfield, 2004). The other major source of energy production is through anaerobic metabolism which occurs within the cytosol. However as the energy is produced without oxygen by-products build up which cannot be removed until i) sufficient oxygen is available and/ or ii) the increased requirements are met/ no longer present (Germann and Stanfield, 2004). The main by-product of anaerobic metabolism is lactate which builds up as a result of pyruvate being converted by LDH (Germann and Stanfield, 2004). This system allows continued energy production under anaerobic conditions. LDH is an intracellular enzyme usually used in toxicology to highlight cell death as its leakage into the external environment highlights this (Weyermann, Lochmann and Zimmer, 2005). However LDH activity/ level studied here was in whole body homogenates not in cell line assays and this was to highlight disturbances in energy systems not cell death.

In all exposures LDH was affected to some degree and were shown as increases and decreases during Ag NP and $AgNO_3$ exposures. The effects observed highlight LDH may be an effective and useful non-selective (i.e. no consistent differences between exposure types could be found) criterion to establish the degree of toxicity of any form of Ag to *Daphnia magna*, in a similar manner as it is used in cell lines (Weyermann, Lochmann and Zimmer, 2005). This is in corroboration with Diamantino *et al.* (2001). However, in the current study the assay proved no more sensitive than traditional bioassay methods (OECD 2004 and 2008). The effects on LDH were seen at similar exposure concentrations in our 48 hour immobility tests (Chapter 4) and at lower concentrations in 21-day reproduction tests (OECD 2008 Chapter 4). Carlson *et al.* (2008) showed increased LDH release from macrophage cell lines due to decreased cell viability in a dose-dependent manner after exposure to Ag NPs between 15-55 nm in diameter at doses similar to those where responses were seen here (10-75 µg). Sung *et al.* (2008) showed significant increases in LDH blood levels in female Sprague-Dawley rats after Ag NP inhalation (6.61×109 nm^2 $cm^{3\ -1}$), and Kim *et al.* (2010) saw non-significant but large decreases after oral administration in the same species after 90 days at rather high doses in the mg Kg^{-1} range.

The research here demonstrated that the differences seen may be dependent on the time of sampling. The disturbances seen here caused by Ag NPs suggest: i) LDH may be a good criterion for toxicological assessment for many contaminants for *Daphnia magna* (De Coen, Janssen and Segner 2001 and Diamantino *et al.*, 2001) and ii) increased requirement of energy production is required via anaerobic systems during times of

stress, which has been previously highlighted (Diamantino *et al.*, 2003, De Coen, Janssen and Segner 2001, and Guilhermino *et al.*, 1994). The increased requirement may be through increased need of energy for defensive and reparatory systems or dysfunction of aerobic energy production systems (Germann and Stansfield, 2004 and Diamantino *et al.*, 2003). During disturbance of aerobic metabolism there can be a build-up of NADH, with a concomitant decrease in NAD^+ due electron transport chain (ETC) overload with no oxygen or functional aerobic system to accept electrons at the end of the ETC (Germann and Stansfield, 2004). NAD^+ is essential for the production of ATP from glycolysis and the Krebs cycle, thus the conversion of NAD^+ to NADH must continue for cell or organism survival (Germann and Stansfield, 2004). The continued conversion is achieved by the breakdown of pyruvate to lactate by LDH, hence, when aerobic capabilities are compromised LDH must increase to compensate (Germann and Stansfield, 2004). The effects on LDH after toxicant exposure *in vivo* and *in vitro* are highly variable and manifest as both increases and decreases (Diamantino *et al*., 2001 and Guilhermino *et al.*, 1994).

LDH as an effect criterion in *Daphnia magna* exposed to Ag NPs has not been explored or whether similar reactions occur across phyla/ species, be it cell lines or whole organism assessment. Although some research has highlighted success for other contaminants in this arena as previously highlighted (De Coen, Janssen and Segner 2001, Diamantino *et al*., 2001 and Guilhermino *et al.*, 1994), this study is the first to explore LDH in the nano(eco)toxicological response to Ag NPs and $AgNO_3$ and show consistent perturbation of the system. Furthermore like in cell line systems and other species *D. magna* LDH levels are also shown to increase. Of course the issue is separating the LDH response for the dissolved and nanoparticulate fraction as LDH is disturbed by all exposures and therefore is a non-selective response. Furthermore sensitivity raises the question as to whether such criterion are more useful than traditional toxicological methods but it may further suggest energetic issues at the organism level which require further investigation.

6.5.4 Superoxide dismutase (SOD) and catalase (CAT)

Using the data presented here the study tried to ascertain if, after exposure to silver in any form, there was a disturbance in 2 enzymatic antioxidants, namely CAT and SOD. This was to establish if silver, in any form, could induce oxidative stress in *Daphnia magna*. The tests were also conducted to establish if there were differences in the

degree of the effect between each form and if each form could elicit an effect to highlight nano-specific or physicochemical specific effects. The study highlighted that only 2 Ag NPs were able to cause disturbance in oxidative state, and that Ag^{+} (as $AgNO_3$) showed no such effects, potentially highlighting a nano-specific effect.

There is strong evidence to suggest that one of Ag NPs main toxicological MOA is the induction of ROS subsequently leading to oxidative stress and cellular insult, both from biochemical assays and toxicogenomic assays (Kim and Ryu, 2012 and Poynton *et al.*, 2012). The induction of ROS (and oxidative stress therein) after Ag NP exposure has been shown in vertebrate cell lines and *in vivo*; including aquatic organisms (Choi *et al.*, 2010, Farkas *et al.*, 2010 and Roh *et al.*, 2009). It has also been shown to increase specific genes associated with antioxidant enzymes potentially highlighting oxidative stress. The genes that were upregulated in comparison to the control were the DNA repair gene REV1, metallothionein and heat shock protein (Poynton *et al*., 2012). However, gene upregulation may not lead to physiological perturbations.

Many studies have either measured ROS directly or disturbances in oxidative stress protection enzymes or scavengers (i.e. antioxidants). Roh *et al.* (2009) showed an increase in SOD3 expression in the nematode *Caenorhabditis elegans* after exposure to 100 µg L^{-1} of Ag NPs. Similarly Posgai *et al.* (2011) showed increased SOD activity in the fruit fly after exposure to doses as low as 30 µg L^{-1}. SOD has also been shown to increase in rat cell lines when exposed to Ag NP concentrations between 2-200 µg L^{-1}. Within the same dose range decreases in SOD activity in human cell lines have been shown. Our results corroborate with the data previously noted for SOD response to Ag NP exposures (Kim and Ryu, 2012). Here PVP-Ag NPs and Cit-Ag NPs were able to significantly decrease and increase SOD levels, respectively. These were within the dose ranges previously noted for other organisms and *in vitro* tests. An interesting point is the fact that there are 3 main forms of SOD, SOD1, 2 and 3. The effects on SOD levels, particularly when a decrease arises may be due to mitochondrial dysfunction as SOD2 is associated with this organelle. However, the only data available which discriminate between these forms suggest that the main affected isoforms are that of SOD1 and SOD3 (Kim and Ryu, 2012). These are the cytosolic and extracellular Cu/Zn SOD isoforms, not the Mn-SOD isoform associated with the mitochondrion (Hancock, 2005). This suggests that although there may be mitochondrial dysfunction and death this is not sufficient to cause significant perturbation of the SOD2 enzyme activities and that the likely cause of any up or down regulation of SOD is due to

increased activity/ production to aid in the removal of ROS or, increased saturation of the enzyme caused by excessive ROS leading to a decreased ROS clearance ability. The two SOD forms consistently shown to rise are not only able to interact with ROS but are also integral to the clearance of metal cations. The ability to bind such cations is owing to the 7 histidine and 1 asparagine site, and these are present within *Daphnia* just as they are in other species (Lyu *et al.*, 2013). Furthermore Cu/Zn SODs have been shown to be induced by Cu^{2+} a metal cation similar to that of Ag^{+} in MOA (Lyu *et al.*, 2013). Again reduction or disturbance in SOD levels, or mutations, can cause many diseased states, SOD1 mutations can cause amyotrophic lateral sclerosis (ALS; Kabashi *et al.*, 2007), SOD2 shortage leads to perinatal and neonatal death in mice (Li *et al.*, 1995), and SOD3 shortage can cause lung defects, such as chronic pulmonary disorder (Young *et al.*, 2006). These disease states all highlight the importance of each enzyme in its own right.

Although it was possible here to show a significant difference in SOD for both Cit-Ag NPs and PVP-Ag NPs, we were unable to show such effects after PEG-Ag NP exposures. SOD response after exposure to PEG-Ag NPs was extremely variable for this Ag NP within the tested exposure groups and this may have masked any SOD perturbations. $AgNO_3$ was also unable to elicit a response on this enzyme likely, however there were no issues with variability and the difference between these exposures and the Ag NPs is likely because of the more specific MOA of dissolved silver, and the likely reduced ability to enter and affect intracellular space in comparison with Ag NPs. SOD may be a nano-specific parameter when looking at low level dose responses in traditional biochemical tests but issues with variability within some data sets need to be addressed. The variation may be due to natural variation within the sampled population or, a higher amount of biological material (i.e. more daphnids) may be required to improve the assay due to sensitivity issues. In either case higher *n*-numbers may result it better quality results and tests using varying number of daphnids should be attempted to ascertain this.

SOD reduces the superoxide anion (O_2^-) to hydrogen peroxide (H_2O_2), (itself another weak oxidising agent which can inactivate some cellular enzymes), and oxygen (as O_2 a totally harmless product). As H_2O_2 can cause further damage to cellular systems or much worse react with O_2^- to create hydroxyl radicals ($OH^{\cdot}$; likely the most reactive free-radical), there are cellular mechanisms to catalytically increase its removal before damage can be done. Once SOD has catalysed the formation of H_2O_2 and O_2 from O_2^-

and hydrogen (H^+; eq. 6.1) CAT can then destroy H_2O_2 (eq. 6.2) and thus when more H_2O_2 is present this enzyme must work harder to reduce any unwanted cellular responses or damage. Therefore should there be any down- or up-regulation of SOD in response to an increased level of superoxide there will likely be some difference in CAT activity to account for the increased hydrogen peroxide. However the data here do not support this hypothesis. Both PVP-Ag NPs and Cit-Ag NPs significantly affected SOD quantity but they were unable to affect CAT in a similar manner. Exposure to any toxicant studied here was in fact unable to change this parameter significantly contrary to previously reported data in other species and cell lines (Kim and Ryu, 2012). This may be due to the natural variability within populations of the tested *Daphnia magna*. Kim *et al.* (2010) showed that TiO_2 nanoparticles were able to increase CAT and not SOD albeit at rather high concentrations unrealistic in environmental settings or even during application such as sunscreen use (i.e. 10 mg L^{-1}). The same effects have been seen in other studies, suggesting TiO_2 increases organism H_2O_2 (Costa *et al.*, 2010). The differences highlight how MOA may differ between NPs of different core materials. However, although it was not possible to show the induction or decrease of CAT activity in this study by Ag NPs, other studies both *in vivo* and *in vitro* in invertebrates and vertebrates have shown this at concentrations between 2-250 µg L^{-1}, within the range of those particle concentrations tested here (Kim and Ryu, 2012). The lack of reaction seen here may be due to population variations masking changes, but it could also be that the increased H_2O_2 production from mitochondrial disturbance was not sufficient to lead to a significant reaction to induce CAT. Furthermore other studies have also shown increased glutathione-s-transferase (GST) and glutathione peroxidase activity which are part of the glutathione cycle which also rids the cellular environments of H_2O_2. However a previous toxicogenomic study conducted on *D. magna* after Ag NP exposure showed no upregulation in GST (Poynton *et al.*, 2012) Therefore it is possible these enzymes are upregulated to such a degree that CAT does not need to significantly change or upregulate its function. There may have also been sensitivity issues with the assay, as such more *Daphnia magna* per replicate may be required in future studies.

The increased disturbance of SOD in comparison to CAT suggests 2 possibilities, either the disruption of mitochondrial respiration and/ or the plasma membrane of phagocytic cells. Superoxide comes from both complex I and III of the inner mitochondrial membrane ETC during ATP production, and NADPH oxidase part of phagocytic cell

membranes which reduces cellular oxygen in order to induce oxygen dependent apoptosis or necrosis of pathogens (Hancock, 2005). Both mitochondrial dysfunction and plasma membrane integrity have been shown to be effected by Ag^{+} and Ag NP exposures (Kim *et al.*, 2009 and Almofti *et al.*, 2003). Furthermore abnormalities to macrophages have also been seen and these phagocytic cells were able to ingest Ag NPs, thus interaction with phagocytic cells is likely (Carlson *et al.*, 2008). Although there is not likely to be isolated contribution of superoxide production from one biochemical pathway considering the effects on ATP and LDH seen within this chapter the largest proportion of O_2^{-} is likely from mitochondrial disruption.

6.5.5 Mitochondrial membrane potential (MMP)

Costa *et al.* (2010) have previously shown mitochondrial dysfunction at all four electron transport chain complexes in male adult Wistar rats exposed to Ag NPs at concentrations between 10-25 parts per million. Here at concentrations orders of magnitude lower this study showed that in comparison with controls all Ag NP exposures are able to negatively impact mitochondrial function in *D. magna*. Although the effect was not as obvious as those seen by Stensberg *et al.* (2014) it still appears to be nano-specific to some degree. In the images it is still possible to see differences in the green intensity and red intensity between $AgNO_3$ and Ag NP exposed groups suggesting mitochondrion membrane potential has been affected to a greater degree in the latter exposures. The difference between the current study and Stensberg *et al.* (2014) is that here the daphnids were exposed to a cell permeabiliser as is traditionally done with cell line experiments. This allows the rapid uptake of the dye into the cells of the organism systemically, something which is unlikely to occur within a 1 hour exposure to such dyes as seen in Stensberg *et al.* (2014). This is due to the fact the *Daphnia* first have to ingest the dye and then assimilate it before incorporation into the cells and then mitochondria. Unlike Stensberg *et al.* (2014) the current study was able to pick out specific mitochondrial rich physiological features where the dye localised such as on the epipodites. As such the protocol used here is seen as an improvement on previous literature and more representative of the dyes internal reaction within the cell and the mitochondria thereafter. The large proportion of green fluorescence within the controls may be because sufficient time was not allowed for the dye to change to its unconjugated (red/ orange) form after uptake. However although this improved with time, the dye only lasted for a maximum of 2 hours before significant degradation.

Both Stensberg *et al.* (2014) and Teodoro *et al.* (2011) have shown effects on mitochondrial membrane potential at concentrations near or below those tested here, and both attribute this to disturbance in mitochondrial membrane permeability and disturbance along the electron transport chain. Ag^{+} can form a porous mitochondrial membrane surface which is an effect likely due to the interaction Ag has with the permeability transition pathway (Stensberg *et al.*, 2014 and Teodoro *et al.*, 2011). The same can occur with Ag NPs, furthermore Ag^{+} is not usually able to easily cross the cell membrane and thus this effect can only occur if the Ag NPs act as a Trojan-horse to allow Ag^{+} -mitochondrial interaction and/ or direct interaction of the Ag NP with the mitochondria. The interaction disrupts the hydrogen gradient along the electron transport chain which is responsible for ATP generation, thus with the results seen for ATP and SOD, and those seen here for mitochondrial function, there is strong evidence, in corroboration with other studies, that mitochondrial dysfunction and effects therein are largely responsible for Ag NP toxicity (Stensberg *et al.*, 2014, Teodoro *et al.*, 2011, AshaRani *et al.*, 2008 and Almofti *et al.*, 2003) and the MOA differs from that of $AgNO_3$. Ag NPs have been shown to have similar mechanisms of disturbance in bacteria (Marambio-Jones and Hoek, 2010).

6.6 Conclusion

The study showed in a similar manner to some recent literature that the same effect on these cations was not seen after Ag NP exposures suggesting different MOA and organism interaction for each. PVP-Ag NPs were able to affect K^{+} and it was found this NP was able to affect Ca^{2+} levels likely due to compensatory mechanisms in response to the toxic events. The research was also demonstrated for the first time time-dependent LDH activity/ level responses in *D. magna*. Much like, within *in vitro* studies this may be a useful non-selective assay (i.e. does not differentiate between contaminant form) to show toxicity to many contaminants. Albeit, not more sensitive than traditional methods such as the OECD *Daphnia sp.* acute immobilisation test and the OECD *Daphnia magna* reproduction test (Chapter 4, OECD 2004 and OECD 2008). The current study also provides evidence that Ag NPs appear to exert a stronger intracellular disturbance than $AgNO_3$ and this may be due to the ability for Ag NPs to enter the cells more readily themselves with a possible release of Ag^{+} intracellulary, but Ag exposed as $AgNO_3$ which rapidly dissolves in the medium strongly binds to the epipodite surface

affecting ATP-dependent enzymes. Regardless of Ag form these effects were seen well below the current acceptable criteria for freshwater silver (USEPA water quality criteria, 3.2 μg L^{-1}; USEPA, 2009). This has been highlighted for $AgNO_3$ within previous studies but this study is the first to also show this with Ag NPs (Zhao and Wang 2011a).

Here using the results from a series of experiments it was possible to hypothesise that Ag NP toxicity is caused by decreased ATP through the disturbance of mitochondrial function which also led to increased ROS production. Furthermore this decrease in ATP may lead to cell cycle retardation, a reduced ability to repair DNA and even cell/ organism death if ATP goes below a critical threshold (Kim and Ryu, 2013, Poynton *et al.*, 2012 and Izyumov *et al.*, 2004). Further support of mitochondrial dysfunction caused by the Ag NPs was shown by the significant reduction in SOD regulation after exposure. The pathway is summarised in Figure 6.9. Ionic Ag acts through traditionally noted mechanisms causing disturbance in Na+ And K+ leading to cardiovascular collapse (Bianchini and Wood, 2003).

Currently ATP disturbances over short term exposures hold promise in being a nano-specific biochemical parameter. This may aid in detection of Ag NPs in the environment when using organisms as bioindicators and allow a simple assay to be used for regulatory and risk assessment/ management purposes. The MOAs highlighted here could be used in the detection of possible hazards on exposures to Ag NPs. The summation of the current proposed MOA for Ag NP toxicity to *Daphnia magna* and across phyla based on our research and corroborations with previously highlighted literature can be seen in the figure below (Figure 6.9). Again, the difference in the effects or degree of the effects seen could not be attributed to any particular characteristic other than surface coating, and possibly the binding type. However due to the commonalities seen between silver nanoparticles in their organism biochemical reactions this will likely ease regulatory and risk assessment/ management efforts and only the degree of effect may need to be established not a different MOA for each Ag NP type. Furthermore the differences in concentration between particles where effects occur are rather close and may be less relevant in "real life" situations.

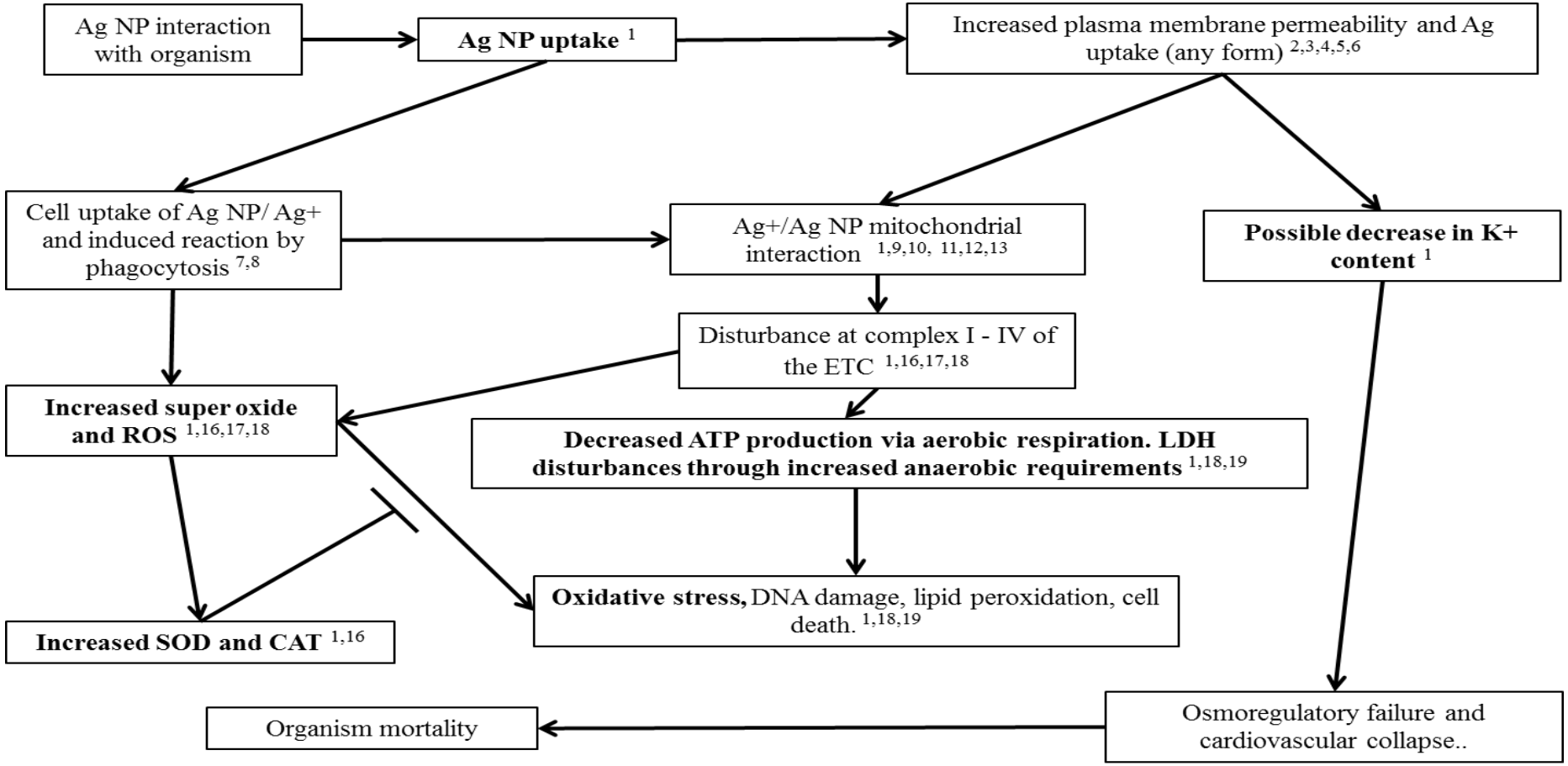

Figure 6.9 proposed MOA/ adverse outcome pathway for Ag NPs using study data (bold and superscript 1) and the literature. Superscript numbers refer to references found in Table 6.1, which also notes which cell/ organism the effect was reported for.

Table 6.1. List of references used to determine the common MOA/AOP of silver Ag NPs. Full references can be found in Chapter 8

Reference No.	Author	Cell/ organism tested
1	This thesis (Paul, 2015). Bold text in figure 6.8 highlights novel findings.	*Daphnia magna*
2	Park *et al.*, 2010	Mouse macrophage RAW264.7 cells
3	Bradley-Stolle *et al*., 2010	Spermatogonial stem cells
4	Bradley-Stolle *et al*., 2005	Mammalian germline stem cells
5	Kim *et al.*, 2009	Human hepatoma cells
6	Almofti *et al.*, 2003	Rat liver
7	Johnston *et al.*, 2015	Human cell lines
8	Carlson *et al.*, 2008	Alveolar macrophages
9	Stensberg *et al*., 2014	*Daphnia magna*
10	Almofti *et al*., 2003	Rat liver
11	Park *et al*., 2010	Mouse macrophage RAW264.7 cells
12	Costa *et al*., 2010,	brain, skeletal muscle, heart, and liver of rats
13	AshaRani *et al*., 2008	*Danio rerio* models
14	AshaRani *et al*., 2009b	Human cell line
15	Piao *et al*., 2011	Human liver cells
16	Roh *et al*., 2009	*Caenorhabditis elegans*
17	Posgai *et al*., 2011	*Drosophila melanogaster*
18	Poynton *et al*., 2012	*Daphnia magna*
19	AshaRani *et al.*, 2009	Human cell line

Chapter 7.

Overall Discussion

7.1 Overall discussion, current literature and advancements in NP toxicology

The work presented in this thesis has highlighted that $AgNO_3$ and three differently coated Ag NPs were toxic to the freshwater water flea *Daphnia magna*, at the concentrations tested, corroborating with literature observations. These results demonstrate that the degree of the effect (i.e. the concentration at which the material becomes toxic) was not only dependent on Ag form (Ag^+ vs Ag NPs) but also Ag NP coating. The research here was able to show the physical entanglement of Ag NP agglomerates/ aggregates within the filtering apparatus of *Daphnia magna* and subsequently demonstrated its accumulation and accumulation kinetics using biodynamic and biotic ligand modelling principles. Using these models the study also defined that current environmental concentrations may be unable to cause a steady state body burden in *D. magna* which would lead to acute toxicity as defined by the OECD *Daphnia* sp. immobilisation test (2004). These studies were unable to establish consistent relationships between NP toxicity, and accumulation, with their physicochemical characteristics. Most importantly contrary to some of the previous literature the toxicity presented by these NPs could not be accounted for by their dissolved fraction and thus there is some nano-specific toxicity. These results provide strong evidence that $AgNO_3$ and Ag NPs have different toxicological MOA and, that the Ag NPs MOA may be similar despite some of the differences in the level of toxicity between these NPs. In all instances $AgNO_3$ was the most toxic form of silver. The results of the thesis are summarised below (Table 7.1). Finally, irrespective of form, silver was able to exert chronic and cellular level effects well below the current USEPA (2009) acceptable levels set for silver in the freshwater environment (3.2 µg L^{-1}). The major novel findings of the thesis and corroborating/ supporting and opposing studies can be seen in Table 7.2, which will be further discussed in this chapter.

Table 7.1 A summary of the significant impacts in toxicological response caused by $AgNO_3$ and the three differently coated Ag NPs, and their accumulation, in *D. magna*. Increases in the tested parameter are shown by cells highlighted in purple, decreases are shown by grey shading and no effects by blue. Yellow blocks show EC_{50} and body residue concentrations (µg L^{-1}). Within each cell is the exposure concentration at which significant effects, or accumulation, were observed (µg L^{-1} or µg g^{-1}, respectively). A colour key can be found at the foot of the table.

	$AgNO_3$	PVP-Ag NP	PEG-Ag NP	Cit-Ag NP
EC_{50}	0.9	6.8	22.2	11.7
Predicted C_{ss}	0.0032-0.029	0.0016-0.026	0.0012-0.027	0.0008-0.012
LA_{50}	1.3	6.87	1.61	2.49
Growth	0.6	1.5		1.2
No. of Moults	0.1		1.5 | 5.0	
Neonates/ Adult	0.3			0.8
No. Of Broods				
Neonates/ Brood	0.15		2.0	
Total Body Na^+	0.4			
Total Body K^+	0.3	1.0		
Total Body Ca^{2+}		4.0		
LDH 7:30	0.4	4.0	8.0	
LDH 9:30	0.6	4.0	6.0	4.0
ATP		1.0	4.0	3.0
Catalase				
SOD		1.0		1

Key:

EC_{50}/ body residue	x
Increase	x
No Effect	x
Decrease	x
Increase to Decrease	x | x

x = concentration where significant effect, or accumulation, was observed (µg L^{-1} or µg g^{-1}, respectively). 50 % Effective concentration, EC_{50}; Steady state tissue concentrations, C_{ss}; 50% lethal accumulation concentration, LA_{50}; lactate dehydrogenase, LDH; adenosine triphosphate, ATP; super oxide dismutase, SOD.

Table 7.2 Major novel findings from the thesis research and studies in support or opposition of the conclusions or observations made.

Thesis main novel findings	Supporting Studies[1]	Opposing Studies
First study to show Cytoviva (hyperspectral imaging) may be used to study aggregation and agglomeration of Ag NPs, based on visual analysis and UV/Vis absorption spectra.	None	None
First study to show toxicological rank order of the 3 tested NPs changes between acute and chronic exposures. Acute:chronic ratios may not be appropriate for use.	Seitz et al., 2015, Asghari et al., 2012	None
First SEM images to show *D. magna* filtering apparatus is able to catch Ag NPs	Zhao and Wang, 2010, Völker *et al.*, 2013	None
First full BDM of Ag NPs in *D. magna* showed trophic transfer is possible for Ag NPs.	None	None
First full BDM of Ag NPs in *D. magna*, showed at current concentrations steady state accumulation would not lead to acute toxicity.	None	None
First full Ag NP *D. magna* BLM, showed the only reliable biokinetic parameter that consistently related to toxicity was uptake.	None	None
BLM showed short term accumulation and Log *K* were poor predictors of toxicity of Ag NPs to *D. magna*.	None	None
Biokinetics were dependent on Ag form and dependent on Ag NP coating in *D. magna*	Zhao and Wang, 2010.	None
First analysis of LDH after Ag NP exposure in *D. magna* showed variable perturbations compared to the control	None	None
First analysis of ATP after Ag NP exposure to *D. magna*. Ag NP exposure led to concentration-dependent decreases in ATP.	Stensberg *et al.*, 2014.	None
First to study a suite of biochemical endpoints to elucidate a mode of action/ adverse outcome pathway for Ag NPs as nanospecific and not driven by Ag^+ release.	Stensberg *et al.*, 2014, Poynton et al., 2012. Please note the AOP is further supported by studies conducted in other test systems (e.g. cell lines; Table 6.X).	Newton et al. 2013, Zhao and Wang, 2011a, Zhao and Wang 2011b, Zhao and Wang 2013.

[1] supporting did not fully elucidate the conclusions of this thesis, but suggested qualitatively or to a certain to degree the conclusions made. Therefore the work is still novel and fills data gaps left by these studies. Only studies conducted on *D. magna* were included within the table.

Background

Currently Ag NPs are one the most toxic and used NPs (Golovina and Kustov, 2013 and Kim and Ryu 2012). It is important, however, to weigh the risks versus the benefits before dismissing a new technology as well as exploring possible risk mitigation measures before concluding the chemical presents unacceptable risk. The results presented here show Ag NPs cause acute and chronic effects to *D. magna* and that significant effect concentrations were in fact similar across species and testing methods (i.e. *in vivo* and *in vitro*; Mackevica *et al.*, 2015, Asghari *et al.*, 2012, Kim and Ryu, 2012, Poynton *et al.*, 2012, Fabrega et al., 2011, AshaRani *et al.*, 2009a-b, Arora *et al.*, 2008, AshaRani *et al.*, 2008 and Carlson *et al.*, 2008). These values range between 1-400000 µg L^{-1} and the results reported here ranged between ~1-25 µg L^{-1} (Kim and Ryu, 2012). The higher noted doses are usually found within *in vitro* cell line studies and, in corroboration with the results here, the lower effect doses are found within studies *in vivo* on environmental model species such as fish and invertebrates (~1-50000 µg L^{-1}; Bone *et al.*, 2015, Mackevica *et al.*, 2015, Seitz *et al.*, 2015, Stensberg *et al*., 2014, Golovina and Kustov, 2013, Kim and Ryu, 2012). These ranges are rather wide and are Ag NP particle, organism, tested endpoint and environment dependent. Similarly, the range reported for the studies within this thesis for toxicological effect concentrations were determined by tested endpoint and particle coating.

Ag NP Physicochemical characteristics and their relationship with* D. magna *toxicity

The NPs which dissolved least (PVP-Ag NP) and most (PEG-Ag NPs) were the most and least toxic, respectively, opposite to what would be expected if Ag^{+} release was playing a major role and in opposition with some literature (Seitz *et al.*, 2015, Newton *et al.*, 2013, Levard *et al.*, 2012 and Zhao and Wang, 2011b). Cit-Ag NPs appeared to be an intermediary in terms of uptake, however PVP-Ag NP and Cit-Ag NP dissolution was similar. There appeared to be negative relationship between uptake and dissolution, with the more dissolved particles having the slowest uptake rates. This is unexpected as Ag^{+} uptake is reported to be the most rapid of all Ag forms and one would expect a higher rate of dissolution to lead to higher rates of uptake (Khan et al., 2014 and Lam and Wang, 2006).

Mean HDD also did not correlate with toxicity unlike previous findings for *Daphnia magna* Ag NP exposure (Zhao and Wang, 2012). PVP-Ag NPs and PEG-Ag NPs had similar and smaller HDD than Cit-Ag NPs, however both PEG-Ag NPs and PVP-Ag

NPs were consistently the least and most toxic throughout, with Cit-Ag NPs being an intermediate for toxic response, apart from in chronic exposures. There was no correlation between HDD and uptake rates, with PVP-Ag NPs being the most rapid particle to be taken up by the organism, and PEG-Ag NPs the slowest, despite similar HDD. Also despite similar core size and size range within the aM7 medium (5-5000 nm) all Ag NPs had varying degrees of toxicity, accumulation and ligand binding dynamics. This is in direct contrast to some *in vivo* and *in vitro* data, which show smaller size often results in more rapid uptake and stronger toxic response (Zhao and Wang, 2012, Hirn *et al.*, 2011 and Carlson *et al.*, 2008), as our results show that even with similar sized NPs uptake and toxicity may change significantly.

Depuration constants did not change between NP forms and therefore only have reliance on organism physiology not particle or metal form type, which has been demonstrated previously (Khan *et al.*, 2015, Croteau *et al.*, 2014 and Khan *et al.*, 2012). Again accumulation showed no pattern in relation with any physicochemical characteristics.

ζ-Potential did not correlate with any measured outcome, as PVP-Ag NPs and Cit-Ag NPs showed consistently different levels of toxicity and, accumulation and ligand binding dynamics, despite similar surface charge. However the particle with the ζ-potential closest to zero appeared to be least toxic and had the slowest uptake rates. The slower uptake rate of neutral particles may be due to the fact biological ligands often have a negative or positive charge dependent receptor types so, therefore, particle charges further away from neutral may be more likely to interact at the biological site of uptake.

Although few clear relationships between particle physicochemical properties were found and their measured parameters they are likely still of importance. Only a limited number of particles were tested and this likely limited interpretation. NPs physicochemical characteristics thereafter may be of importance in determining behaviour, within the gut, uptake across the gut into cells and their behaviour within the organism; characterisation within physiologically relevant mediums and environments may aid in this area (Khan *et al.*, 2014, Carreira *et al.*, 2013, Heinlaan *et al.*, 2011, Asati *et al.*, 2010, AshaRani *et al.*, 2009b, AshaRani *et al.*, 2008). Adsorption of molecules to the NP surface from the environment and organism have been suggested to modify uptake and biodistributions (Kumar *et al.*, 2014, Levard *et al.*, 2012, McLaughlin and Bonzongo, 2012 and Lundqvist *et al.*, 2008). In acidic environments, such as the

lysosome or the *Daphnia* gut, dissolution dynamics may differ and be increased to varying degrees dependent on particle coating. Characterisation techniques require refinement when dealing with poly-dispersed NPs within complex matrices. Therefore as new and improved characterisation techniques and information of characteristics after internalisation become available, the relationship between physicochemical characteristics of NPs and toxicity will become more apparent.

***Acute and Chronic Toxicity of Ag NPs to* Daphnia magna**

Acute toxicity can significantly vary between all Ag NP types and $AgNO_3$ with a rank of toxicity from most to least shown as $AgNO_3$ > PVP-Ag NPs > Cit-Ag NPs > PEG-Ag NPs. Interestingly although differences were presented in chronic effects between exposure types, the thesis is the first to show that these did not directly reflect the ranking in the acute Ag NP studies. In the chronic studies, again, $AgNO_3$ was seen as the most toxic. Rank order of chronic toxicity from most to least toxic was; $AgNO_3$ > Cit-Ag NPs > PEG-Ag NPs > PVP-Ag NPs. The observed differences have implications for regulatory and risk assessment frameworks as simple acute data extrapolations may not be possible in the prediction of chronic effects. Due to these changes in toxicological rank order and, differences in some of the observed effects chronically (i.e. PEG-Ag NPs were able to cause hormesis), it was assumed toxicological MOA and/ or MOA contributions may vary between acute and chronic exposures for Ag NPs and these MOA may again be coating specific, which is not the case for Ag^+ (i.e. the acute and chronic MOA of silver are the same; Adams *et al.*, 2011). Furthermore detoxification mechanisms may also play a role in the eventual chronic toxicity and these chronic effect concentrations are considerably more similar (~1 µg L^{-1}) than those seen during acute exposures. This may mean during long term exposure that Ag NP toxicity is less dependent on coating, and only concerns the core material.

This thesis showed all Ag forms were able to affect life-history traits. Ag NO_3 appeared to reduce the number of neonates per brood but, Cit-Ag NPs reduced progeny through the early cessation of their production. These differences in the reduction of progeny shown between $AgNO_3$ and Cit-Ag NP exposures are likely indicative of different MOA. However both $AgNO_3$ and the 3 Ag NPs were able to cause retardation in growth and effects on moulting. These effects to *D. magna* noted within this thesis could not be fully attributed to the release of Ag^+ from the Ag NPs, and thus different

MOA may be present or the same MOA at a varying degree caused by direct Ag NP binding at the site of action. However such concepts and assumptions required further investigation and validation.

It was shown here that $AgNO_3$ had morphological impact on offspring often making them unviable and that Ag NPs were able to significantly affect growth and may also cause neonate entrapment (Chapter 4, Figure 4.9). The studies within this thesis showed for the first time Ag NP agglomerates/ aggregates caught in the filtering apparatus of the organism; proof that organism uptake and NP interaction is possible, particularly via ingestion.

Biodynamic and Biotic Ligand Modelling

From the aforementioned findings it became apparent that the assessment of steady state body burdens, critical body burdens and modelling of the interactions of the different Ag forms at the ligand would begin to decipher differences in interactions and accumulative processes between $AgNO_3$ and the Ag NPs, if any. In a regulatory and risk assessment context such models have already been successfully used for trace metal assessment and similar models are thought to have their place in nanotechnology regulation, risk assessment and risk mitigation strategies. The research presented here is the first to take an in depth look at the accumulation and ligand kinetics of Ag NPs in *D. magna*. Although, some advancements have been made in aquatic nano(eco)toxicology research, most notably in benthic invertebrates and with other metal NPs (Croteau *et al.*, 2014, Khan *et al.*, 2012 and Croteau *et al.*, 2011). In particular the research is the first to use the biodynamic model to assess Ag NP toxic potential within the environment, studying both waterborne and foodborne exposures (Chapter 6).

By using, and combining, both biodynamic and biotic ligand principles with predicted Ag environmental concentrations and acute toxicity results (i.e. EC_{50}) the thesis was able to determine steady state tissue concentrations and critical body burdens, respectively. Here using the BDM it was found that all Ag forms were able to cause Ag body burdens at both low and high exposure scenarios. However, no Ag exposure was able to cause body burdens high enough that would result in acute toxicity (as mortality) (Table 7.1). Environmental concentrations would need to rise by 40-400 and 60-4000 fold in order for there to be acute effects caused by either Ag or its nano counterpart and concerns to occur. However these concentrations, although high, may occur in polluted

areas or as Ag NP use and release rise. The research found that the importance of waterborne and foodborne Ag accumulation to eventual body burdens was environmental scenario dependent for Ag^+ only. At low concentrations waterborne exposures dominate the proportion responsible for the largest body burdens, yet at the higher environmental scenarios foodborne exposures may be the dominant form of uptake. For Ag NPs body burdens were caused by a greater proportion from foodborne exposures, independent of exposures scenario, with 74-99% of the body burden coming from this phase (i.e. minimum and maximum measured environmental Ag concentrations from a representative environment). Zhao and Wang (2010) have also previously reported that foodborne exposures were the most important route of uptake for Ag NPs and accounted for 70% of the accumulation within *D. magna* however they only used one Ag NP type. Similarly to the studies here, these authors showed higher AE of Ag NPs in comparison to Ag^+. This result is currently attributed to physical entrapment after ingestion with such structures as the gut microvilli, and the ability Ag NPs have to affect the permeability of the plasma membrane allowing more cellular uptake of Ag in any form and/ or its Trojan-horse ability; which has previously been shown (Khan *et al.*, 2014, Kim and Ryu 2012, Heinlaan *et al.*, 2011, Park *et al.*, 2010, Peterson *et al.*, 2009 and Hwang *et al.*, 2008). Based on the results presented here and the current literature Ag NPs trophic transfer and bioaccumulation from food, such as algae, may be important routes of uptake.

The LA_{50} values for all Ag NPs were higher than for $AgNO_3$. Therefore Ag NPs are not as effective as dissolved Ag at causing a toxicological response after uptake. The thesis research also found an opposite pattern to what would be expected when looking at a single metal when isolating LA_{50} for Ag NPs (that is, the higher the LA_{50} the higher the toxicity). Here the expected pattern would be higher body burdens are less toxic as seen between $AgNO_3$ and the Ag NPs. This is because when dealing with a single toxicant the higher the burden the organism is able to cope with the less potent the effect. It was hypothesised this may be due to Ag NPs accumulation kinetics being more reliant on Ag NP filtering/ ingestion rate than upon interaction with a specific ligand, this was supported by the SEM imagery and efflux patterns of Ag NPs. Also Ag NPs may act as a Trojan-horse for Ag^+ release in the organism or into the cells. Here the higher the burden the higher the release of Ag^+ within the organism/ cell thus leading to a greater adverse effect. Here one would also expect greater cellular perturbations than shown by Ag^+ alone as studies have shown that Ag^+ less able to penetrate the cell. Furthermore

there may likely be more interaction at the organism ligand interface after uptake as Ag NPs have higher assimilation efficiencies than Ag^{+}, thus burden would be expected to last longer. The higher AE is likely due to their size and the ability of aggregates to be mechanically caught and persist within the gut.

Khan *et al.* (2012) studied ligand binding of Ag NPs in the estuarine and freshwater benthic invertebrates *Lymnaea stagnalis* and *Peringia ulvae*, respectively. The uptake and efflux rate of Cit-Ag NPs by *L. stagnalis* were considerably higher than that of its marine water counterpart. This was likely due to the complexing with medium ligands, particularly chloride in salt water environments. *P. ulvae* had higher maximal saturation constants meaning they were able to cope with more silver at the ligand-water interface; this is due to the reduced bioactivity caused by chloro-complexation. Such effects have been previously noted within the transition metal literature (i.e. less bioactive the more accumulation is possible before effects). The authors reported B_{max} values of 62 and 18 nmol g^{-1} and Log *K* values of 6.3 and 7.4, for the marine and freshwater species, respectively. This corroborates with previous transition metal literature in that lower Log *K* values are indicative of less toxicity as was found between these species. Croteau *et al.* (2014b) showed lower uptake rates of CuO NPs (0.31 L g^{-1} d^{-1}) compared with Cu^{2+} (0.74 L g^{-1} d^{-1}) a similar finding to Khan *et al.* (2012) who found lower uptake for nanoparticulate Ag in comparison to its dissolved counterpart in 2 benthic species (0.15-1.1 Ag^{+} vs. 0.074-0.35 Ag NPs). Croteau *et al.* (2014b) reported lower Log *K* values and higher B_{max} values of the NP form in comparison to the ionic form of the metal. Again this suggests the NP form was less toxic as the animal was able to cope with higher body burdens. Despite these differences in uptake kinetics and ligand binding constants most authors have noted similar depuration rates for NP and ionic forms of metals, suggesting they may be subject to the same sequestering and depurative processes and that both of these metal forms may have similar physiological fates as it pertains to the ligand to which they bind (Croteau *et al.*, 2014b, Khan *et al.*, 2012 and Zhao and Wang 2010). In *D. magna* the most notable work has been reported (other than ourselves; Khan *et al.*, 2015) by Zhao and Wang (2010, 2011a, 2011b, and 2012) with Ag NPs. However, these authors do not report ligand binding constants. Again in corroboration with other data sets they found that Ag^{+} uptake (6.20 L g^{-1} d^{-1}) was higher than that of Ag NPs (1.44 L g^{-1} d^{-1}) studied (Zhao and Wang, 2010). Zhao and Wang (2011b) also studied the influence of particle coating had on toxicity and accumulation after 48 hours, however these 48 hour accumulation values were not

modelled in relation to the LC_{50} and are therefore more indicative of short term uptake than any critical bioaccumulative concentration. Here, again, those Ag NPs with the most rapid uptake levels were the most toxic.

Using the BLM here it was possible to determine that Ag NP Log *K* (7.1-7.7) values varied from that of previously noted Ag^+ Log *K* (8.9) values in similar medium, as did K_d (1.25 vs 20-76 nmol L^{-1}) and B_{max} (200 vs. 108-186 nmol g^{-1}). In corroboration with aforementioned literature Ag^+, the most toxic Ag form had the highest Log K value. These ligand binding constants suggest i) Ag NPs are less toxic than Ag^+ and ii) that biological ligand or binding site affinity and strength vary between Ag NPs and Ag^+. Interestingly Log *K* of the Ag NPs did not follow the expected pattern when correlated with toxicity. This could be due to i) the interaction of the Ag NP at more than one site rendering single-site saturation kinetics as used within the BLM inappropriate and ii) ingestion via the gut does not rely on ligand interaction. Should there simply be differing affinities for the same biological ligand toxicological MOA of both Ag NP and Ag^+ should be the same and at equitoxic exposures would lead to similar biological perturbations.

Biodynamic and Biotic Ligand Model value Relationships with Toxicity

The research presented here corroborates with the previous research in that the Ag NPs had similar efflux rate constants between each particle and $AgNO_3$, and that uptake rates were positively correlated with the toxicity of the particles. However what was unexpected was the fact that critical accumulation levels at the EC_{50} (i.e. LA_{50}) did not show the expected relationship as the least accumulated Ag NP was the least toxic. Furthermore this was a poor predictor of toxicity when trying to predict the toxicity of all Ag forms. If such patterns continue it may be possible to treat Ag NPs as separate toxicants in comparison to $AgNO_3$, however little research has currently been conducted to establish critical accumulation factors in aquatic species, and as such, these correlations remain elusive.

The Ag NPs data reported here show an opposite relationship with Log *K* and toxicity than would be expected (i.e. higher Log *K* with lower toxicity). It is not possible to conclude with certainty such a relationship exists due to the limited number of Ag NP types tested and the fact that current studies reporting Log *K* values have only dealt with one NP coating type and the NPs ionic counterpart. If we look at the Ag^+ Log *K* in comparison to the Ag NP Log *K* values we see the expected pattern documented within

the afromentioned literature (Croteau *et al.*, 2014b and Khan *et al.*, 2012). Therefore when determining relationships between such parameters it is likely wise to do so with several varying NPs (i.e. same core material but different sizes or coatings) as well as the ionic form. The reason for the differences displayed in the relationships in LA_{50} and Log *K* values with EC_{50} values in the data set here is likely due to i) more than one ligand accounts for the accumulation of Ag NPs skewing single-ligand saturation kinetics used in the BLM, ii) Trojan-horse mechanisms may be at play, and when higher accumulation occurs so does higher release of the toxic fraction (i.e. Ag^{+}) internally leading to higher toxicity at higher LA_{50}, iii) for non-selective filter feeders Ag NPs act like food and ingestion becomes a major route of interaction which does not rely on ligand binding kinetics but ingestion and filtering rates of the species. Currently from the obtained data uptake rates are the simplest and most reliable biodynamic constant for which to base NP predictive models and further research. Collation of further research and review should pursue to establish such relationships for regulatory and risk assessment purposes. The research highlights a lack of fully informative studies, and efforts should be made when studying these new potential contaminants to report all possible modelling values, as some research reports ligand binding constants but fail to report accumulation and vice versa. To establish possible nano-specific relationships with such models for *in silico* model development a wider range of NP types should be focused on within each study rather than simply a comparison with the ionic or bulk form of the metal in question. These relationships may also be species specific dependent on feeding behaviour, thus relationships between species also need to be established.

Previously Croteau and Luoma (2009) highlighted that dietary toxicity of metals was better predicted via influx than accumulation and should ingestion be a major route for some species as it concerns with NPs then this parameter may consistently show the same relationship as seen above; with uptake being consistently higher for the more toxic form of each metal irrespective of species and metal studied. The biodynamic model should be applied in several species, scenarios and with several NP types to better understand the effects each has on the toxic potential currently in real life situations and the most important phase. Highlighting whether the dietary or water phase is more important will allow the simplification of such models which deal with the most important fraction (Croteau and Luoma, 2009). However currently limiting our ability is the assessment to accurately measure Ag NP concentrations within the

environment and separate anthropogenic/ man made forms from their incidental counterparts.

Mode of action of Ag NPs vs. dissolved silver

It has been reported that Ag^+ causes significant perturbations to sodium and potassium influx and efflux, respectively, and these effects are due to the competitive inhibition Ag^+ has on the Na^+, K^+ ATPase transporter (Bianchini and Wood, 2003). Therefore should toxicological MOA be the same for Ag NPs then they will also cause disturbances in these body cations. Therefore the research was directed to explore MOA of each Ag form, and Ag NP type, by studying organism and subcellular perturbations.

AshaRani *et al.* (2009b) and AshaRani *et al.* (2008) showed that Ag NPs may localise in the mitochondria of different human cell lines *in vitro*. They also showed this may impact cellular health. Similarly Costa *et al.* (2010) showed effects on mitochondrial ETC complexes I-IV in the rat brain, skeletal muscle, heart, and liver. In a review of the literature of the antimicrobial effects of Ag NPs it was also stated that Ag NPs may affect proton motive force, which is similar in function to the mitochondrial ETC. Finally Stensberg *et al.* (2014) showed reduced mitochondrial membrane potential in *Daphnia magna* neonates after embryonic exposure to Ag NPs. AshaRani *et al.* (2008) showed reductions in ATP *in vitro* to human lung fibroblast cells and glioblastoma cells, likely caused by disturbance along the mitochondrial ETC), an effect thought to be a direct result of Ag^+ released from the particles. Lok *et al.* (2006) also found depletion in ATP in bacterial cells caused by dissipation in bacterial proton motive force. Furthermore others have noted DNA damage and cell cycle retardation caused by Ag NPs in human cell lines which is likely linked to ATP reduction and mitochondrial dysfunction (AshaRani *et al.*, 2009b and Bradyich-Stolle *et al.*, 2005). Choi *et al.* (2010) showed Ag NPs had DNA damaging potential in zebra fish. Poynton *et al.* (2012) showed cell cycle retardation and DNA damage in *D. magna* during toxicogenomic studies.

Studies across species and phyla have also shown increases in reactive oxygen species and disturbed antioxidant defences (Kim and Ryu 2012). Roh *et al.* (2009) showed an increase in SOD in the invertebrate *Caenorhabditis elegans* exposed to Ag NPs. The increase in oxidative defences has also been shown in cell line studies as well as other vertebrates (Arora *et al.*, 2009 and Jain *et al.*, 2009). Furthermore other antioxidant

enzyme responses have been highlighted (Kim and Ryu, 2012). Looking at the corroboration in data sets between species and test types highlights there is likely a common Ag NP toxicological MOA for all forms of life. A common theme therefore begins to rise between species and phyla from human, to lower vertebrates, invertebrates and bacteria. However, the mitochondria are responsible for many cellular events and those which are affected by Ag NP need to be highlighted. Mitochondrial disturbance may lead to increases in ROS, reductions in ATP and cellular apoptosis.

The thesis is one of the first to fully explore the MOA of Ag NPs within *Daphnia magna*. The importance of studying MOA across phyla is that should common MOA occur the same strategies and risks will be applicable to all life and this will ease regulatory and risk assessment efforts. In corroboration with the literature this study showed disturbances to mitochondrial membrane potential, reductions in ATP and changes in SOD quantity.

In studying biological MOA the organism can become a biological indicator of the toxicant it is exposed to. However this is only the case when there are distinct, well defined and different MOA between the studied xenobiotics.

It was hypothesised from the research presented in the thesis that MOA would be distinct for Ag^+ and Ag NPs and possibly between Ag NP types. The thesis shows strong evidence for a nano-specific effect. In corroboration with previous literature it was found here that $AgNO_3$ exposures were able to adversely affect regulation of both sodium and potassium; the research here showed no similar effect for the Ag NPs (Bianchini and Wood, 2003). This suggested a different MOA for Ag NPs than Ag^+.. These studies were directed by the previous studies within this thesis, the literature, and by omics results obtained within the NanoBEE consortium from University of Birmingham. The selected biochemical factors were ATP, LDH, SOD and CAT as well as mitochondrial membrane potential assessment. Again, differences in MOA between Ag^+ and Ag NPs were highlighted. Although all Ag forms caused disturbances in LDH quantity/ activity only Ag NPs were able to significantly affect SOD and ATP; and this was in a dose-dependent manner. This somewhat supports the notion of some form of cellular uptake or Trojan-horse mechanism as there are greater intracellular perturbations caused by the Ag NPs than Ag^+ which act at the water-organism interface. Ag NPs were able to exert an effect on mitochondrial membrane potential and the mitochondrial health implicated by this assay was different between Ag NPs and both

the controls and $AgNO_3$ (from least healthy to most was; Ag NPs < $AgNO_3$ < controls). Therefore a schematic is suggested for Ag^+ and Ag NP toxicity (Figure 6.9), and how this can be used to determine organism exposure. The thesis showed that ATP and SOD were the most sensitive and nano-specific biochemical perturbation and using simple 96-well plate assays this could aid in wide screening of Ag NP toxicity and be used as a bioindicator in environmental situations where it is costly and hard to determine between Ag forms causing contamination i.e. often cheaper than applying analytical chemistry.

The corroboration of data sets between phyla and species, *D. magna* may be used to refine, reduce and replace testing methods. Using an invertebrate which could be indicative of a response to many species and phyla can negate issues with i) using higher organisms such as mice (replacement), ii) means that the toxicant in question is subject to a dynamic model more indicative of exposure than *in vitro* methods (refinement), iii) avoids *in vitro* carcinoma cell line testing which may behave differently from primary cells lines (refinement; Asati *et al.*, 2010), iv) reduces cost of using expensive primary cell lines for *in vitro* testing (reduction of cost) v) reduce the number of animals needed to be used to highlight potential risk, and could be a tiered approach (reduction of types of animals used and higher level organisms) vi) allows rapid testing and assumptions to be made about the toxicity of the contaminant, again which may create a tiered approach to hazard testing. A caveat to this of course is that in many instances will not provide the entire testing strategy or completely replace previous methods, but it may be used as part of a tiered testing approach.

7.2 Final conclusions from this thesis and future research

The work described in this thesis has found acute and chronic toxicity of Ag NPs may not be related and that these can significantly vary between Ag form and Ag NP type. The research showed accumulation dynamics and ligand binding constants can also change between Ag form and Ag NP type and that the relationships these modelled parameters may have with toxicity may differ from their ionic counterpart. Currently, uptake provides the most likely applicable parameter across Ag forms and Ag NP types for which to base predictions and *in silico* regulatory and risk assessment models of toxicity. Additionally, the data demonstrated foodborne Ag NP contributions are the predominant accumulation route for Ag NPs. Future studies should focus on accumulation and ligand binding constants to better establish modelled relationships. Future studies should make an effort to incorporate all possible accumulation and ligand binding constants for several NP types of the same core material and the ionic/ bulk counterpart.

The thesis research demonstrated different MOA between Ag^{+} and Ag NPs through several biochemical tests and that ATP or SOD may be used a nano-specific parameter, and *D. magna* remains a useful bio-indicator. Future work should continue to elucidate MOA/AOP of Ag NPs to further cement our understanding and to confirm results presented here.

It is acknowledged that there is a need to further investigate any possible relationships between NP physicochemical characteristics and toxicity as well as organism interaction as this research was unable to find any consistent relationships with these and the measured endpoints. Future research should focus on the relationship between a combination of physicochemical characteristics and their relationship with the observed biological effects. For instance, uptake occurs via ingestion and there are possible Trojan-horse mechanisms of Ag NPs, the characteristics of these NPs within physiological environments may change and better explain, and relate to, the eventual observed toxicity. Unfortunately we are rather limited by the complex nature of NP behaviour and the current equipment used to assess it; furthermore we are limited in our ability to measure such characteristics *in situ* and for the field to advance, so must these analytical technologies. Future research should also focus on unused and new technologies and there possible application in NP physicochemical analysis, such as cytoviva (hyperspectral imaging). For instance, the cytoviva work within this thesis

highlights new and exciting opportunities for particle physicochemical characterisation and should be explored further.

The results presented in this thesis will go some way in informing the scientific community, industry, regulators and, risk assessment and mitigation strategies. Furthermore although the current acceptable levels of silver in the freshwater environment are relatively low, set at 3.2 µg L^{-1} (USEPA, 2009), that regardless of form when using more sensitive endpoints (biochemical or chronic) this level is likely under-protective with effects seen at 0.1 and 1 µg L^{-1} for $AgNO_3$ and Ag NPs, respectively.

The research presented here has provided important data and information towards improved understanding of Ag NP exposure, uptake and effects, including MOA/ AOP.

Appendix

Appendix Text

Text A1 Nanoparticle Synthesis

Briefly; Cit-Ag NPs were taken and converted to PEG-SH coated Ag NPs by adding thiolated PEG (Mw 5000, purchased from Sigma Aldrich) under vigorous stirring overnight, the resulting NPs were PEG-Ag NPs. PVP-Ag NPs were prepared by reducing 60 mL of 1 mM silver nitrate with 180 mL of 2 mM sodium borohydride (>99% purity, Sigma Aldrich) in a PVP10 containing mixture (Mw 10000, Sigma Aldrich). Citrate Ag NPs were prepared by a reduction of $AgNO_3$ in sodium citrate. Solutions of 100 mL sodium citrate (0.31mM), 100 mL $AgNO_3$ (0.25mM) and sodium borohydride (0.25mM) were prepared in pure water and kept at 4 °C in the dark for 30min. The silver nitrate and sodium citrate solutions were then mixed. Subsequently 6 mL of the solution of the reducing agent, sodium borohydride ($NaBH_4$), was added in one batch. After 10min of stirring, the solution was heated slowly to boiling and then left to boil for 90min, left overnight and then cooled (4 °C, in the dark). Ag NPs were cleaned to remove the excess reagents.

Appendix A

Tables:

Preparation of aM7 Medium for *Daphnia magna* culturing

Preparation of aM7 Trace element Stock:

Separate stock solutions (I) of individual trace elements are first prepared in Milli-Q grade water. From these different stock solutions (I) a second single stock solution (II) is prepared, which contains all trace elements (combined solution), i.e.: (OECD 2004)

Table A2.1(1): Preparation of aM7 Trace element stock adapted from OECD 202 Guideline for testing of Chemicals (*Daphnia sp*., Acute Immobilisation Test)

Stock solution(s) I (single substance)	**Amount added to Milli-Q grade water** **mg L^{-1}**	**To prepare the combined stock solution II add the following amount of stock solution I to Milli-Q grade water** **mL L^{-1}**
		(x2strength)
H_3BO_3	**57 190**	**0.5**
$MnCl_2$.$4H_2O$	**7 210**	**0.5**
LiCl	**6 120**	**0.5**
RbCl	**1 420**	**0.5**
$SrCl_2$.$6H_2O$	**3 040**	**0.5**
NaBr	**320**	**0.5**
Na_2MoO_4 .$2H_2$	**1 230**	**0.5**
$CuCl_2$.$2H_2O$	**335**	**0.5**
$ZnCl_2$	**260**	**2.0**
$CoCl_2$.$2H_2O$	**200**	**2.0**
KI	**65**	**2.0**
Na_2SeO_3	**43.8**	**2.0**
NH_4VO_3	**11.5**	**2.0**
$Na_2EDTA.2H_2O$ **$FeSO_4$.$7H_2O$**	**5 000** **1991**	
Both Na_2EDTA and FeSO4 solutions are prepared singly, poured together and autoclaved immediately. This gives:		
Fe-EDTA		**10**
For EDTA-free medium: **$FeSO_4$.$7H_2O$**	**1991**	**5**

All stock solutions should be autoclaved for 15 minutes at 121°C, apart from $FeSO_4$ when not combined with EDTA. During autoclaving, $FeSO_4$ in solution oxidizes and precipitates out as Fe_2O_3OH; to avoid this $FeSO_4$ solution should be filter sterilized not autoclaved.

Highlighted values are double the strength suggested by the OECD.

Preparation of complete medium:

aM7 medium is prepared using stock solution II, the macro-nutrients and vitamins. These are added to Milli-Q grade water as follows:

Table A2.1(2): aM7 medium and combined vitamin stock solution preparation, adapted from OECD 202 Guideline for the testing of Chemicals (*Daphnia sp*., Acute Immobilisation Test)

	Amount added to Milli-Q grade water	**Amount of stock solution II added to prepare medium**
	mg L^{-1}	**mL L^{-1}**
		aM7
Stock Solution II (combined trace elements)		**25 (using x2 strength stock)**
Macro nutrient stock		
$CaCl_2$ $2H_2O$	**293 800**	
$MgSO_4.7H_2O$ double strength	**493 200**	**1.0**
KCl		**0.25**
$NaHCO_3$ double strength	**58 000**	
Na_2SiO_3. $5H_2O$	**129 600**	**0.1**
$NaNO_3$	**37 322**	**0.5**
KH_2PO_4	**2 740**	**0.2**
K_2HPO_4	**1 430**	**0.1**
	1 840	**0.1**
Combined vitamin stock		**0.1**
		0.1
The combined vitamin stock is prepared by adding the 3 vitamins to 1 litre of water as shown below:	**mg L^{-1}**	
Thiamine hydrochloride	**750**	
Cyanocobalamin_B_{12}	**10**	
Biotin	**7.5**	

The combined vitamin stock is stored frozen in small aliquots. Vitamins are added to the media shortly before use.

Preparation of Jaworski's Medium (JM) for *Chlorella vulgaris* stock cultures

Table 2.2: JM medium composition

Chemicals used:	**g/ 200 mL Milli-Q water**	**Amount of stock chemicals need to make 1 L of culturing medium** **mL L^{-1}**
$Ca(NO_3)_2.4H_2O$	4.0	1.0
KH_2PO_4	2.48	1.0
$MgSO_4.7H_2O$	10.0	1.0
$NaHCO_3$	3.18	1.0
EDTAFeNa	0.45	1.0
$EDTANa_2$	0.45	1.0
H_3BO_3	0.496	1.0
$MnCl_2.4H_2O$	0.278	1.0
$(NH_4)_6Mo_7O_{24}.4H_2O$	0.20	1.0
Cyanocobalamin	0.008	1.0
Thiamine HCl	0.008	1.0
Biotin	0.008	1.0
$NaNO_3$	16.0	1.0
$Na_2HPO_4.12H_2O$	7.2	1.0

Recovery of silver from Ag NP stocks:

Standard Reference Material for oyster tissue (SRM1566b): 91.3 ± 4.9% recovery of expected silver (n = 3).

Table A2.3 Analysis of stocks on AAS.

Ag form:	**Expected silver mg L^{-1}**	**Retrieved silver mg L^{-1}**	**% of expected retrieved**
$AgNO_3$	N/A	0.89 ± 0.05	89 ± 5
PVP-Ag NP	19	19.56 ± 0.53	102 ± 3
PEG-Ag NP	10	9.52 ± 0.84	95 ± 8
Cit-Ag NP	10	9.50 ± 0.06	95 ± 6

Appendix A Figures:

HWU algal stocks were previously assessed for dry weight in relation to OD, with carbon content of alga being 50% of dry weight (Lee *et al.*, 1996, Ketchum, 1954, Spoehr and Milner 1949 and Myers and Johnston 1949). A range of ODs were measured followed by catchment of the algae on pre-weighed filters, these were then weighed and a dry weight for algae only was derived and plotted against the respective OD for that filter. A strong relationship between HWU Chlorella vulgaris culture stock OD and Chlorella vulgaris dry weight (R 2 > 0.9) was shown (Figure A2.1); therefore quantity of feed required was worked out from stock OD as follows:

i. Total carbon content (CC) of stock (mg) = ((OD / 0.1761) + 0.0699 /2) /25) * volume of stock (mL)

ii. CC (mg/ mL) = Total CC of stock (mg) / Volume of Stock (mL)

iii. Amount to feed Daphnia magna (mL/ animal) = (CC (mg/mL) / 0.2)* Number of *Daphnia*

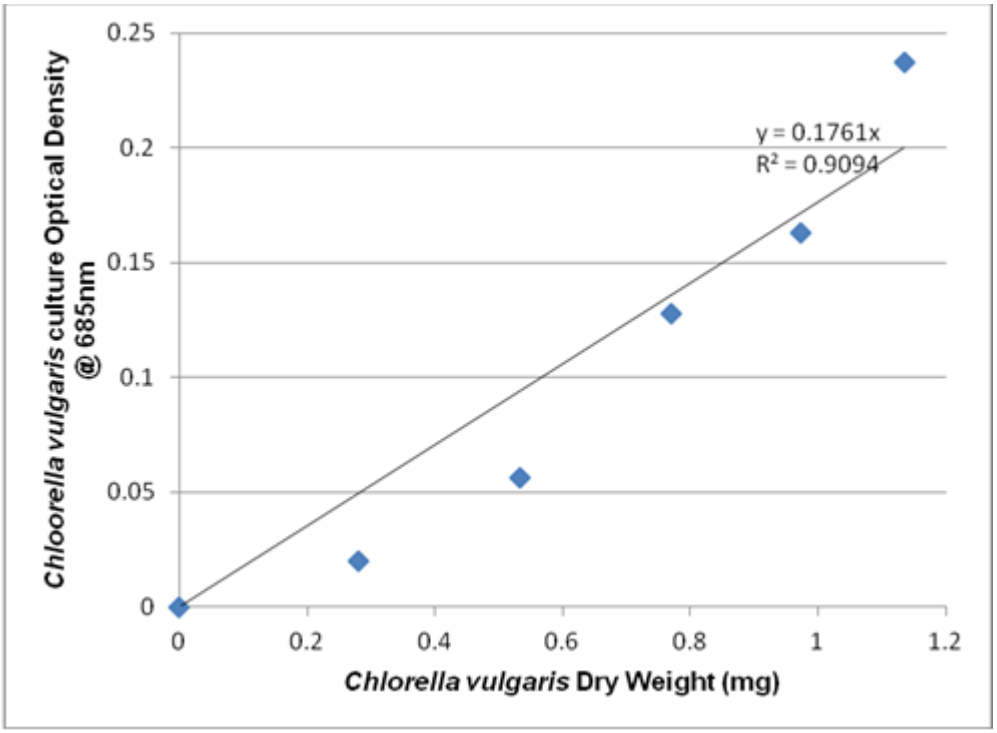

Figure A2.1: Linear relationship of *Chlorella vulgaris* Dry weight and Optical Density of *Chlorella vulgaris* culture stock.

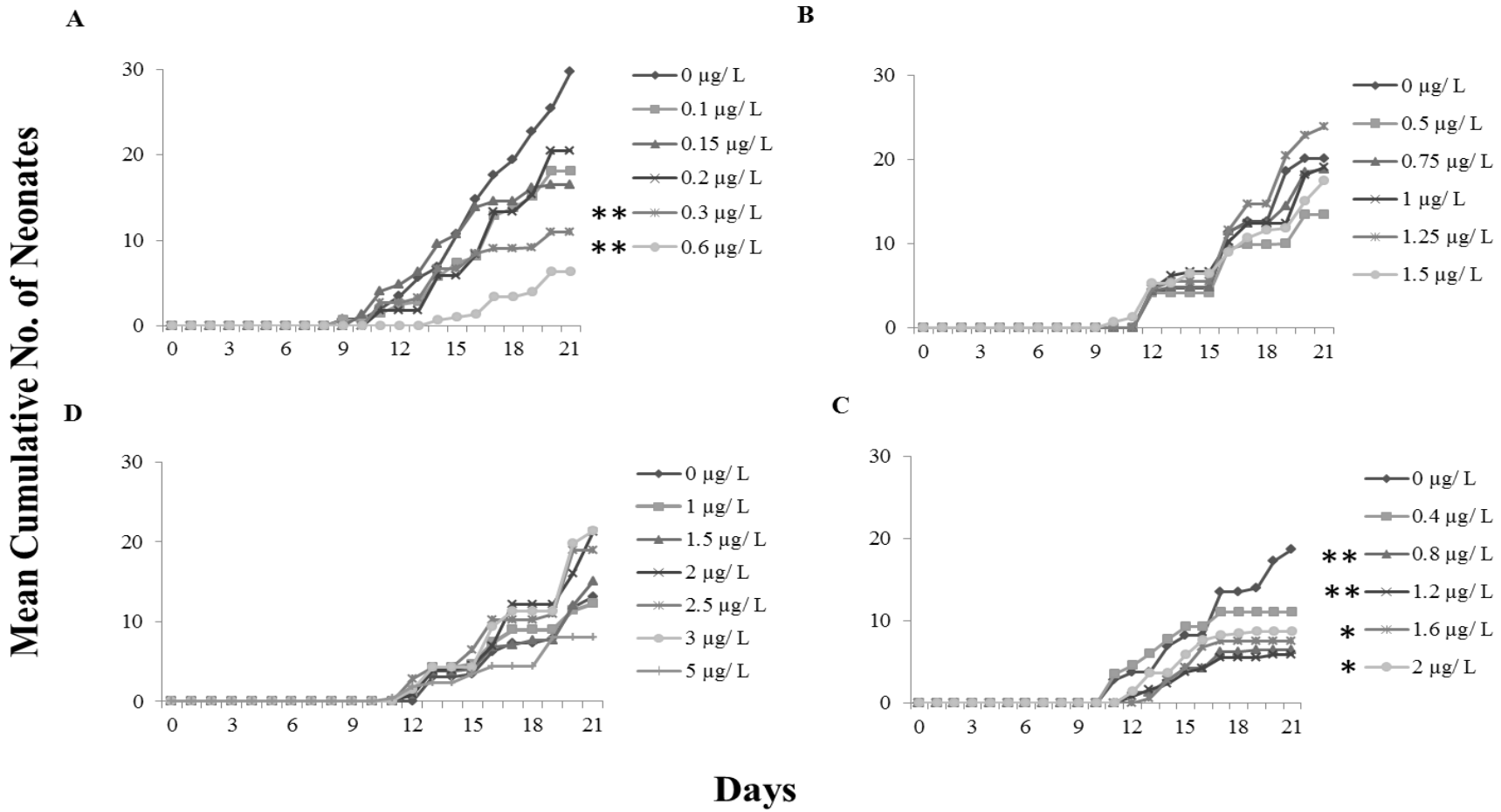

Figure A4.1: Mean cumulative number of neonates produced per day at differing Ag concentrations (shown on figure legends as total Ag in µg L^{-1}) when D. magna are exposed to Ag+ (A), PVP-Ag NP (B), PEG-Ag NP (C) and Cit-Ag NPs (D) (n = 3-10). *, ** denote significance from control at $p < 0.05$ and $p < 0.01$, respectively.

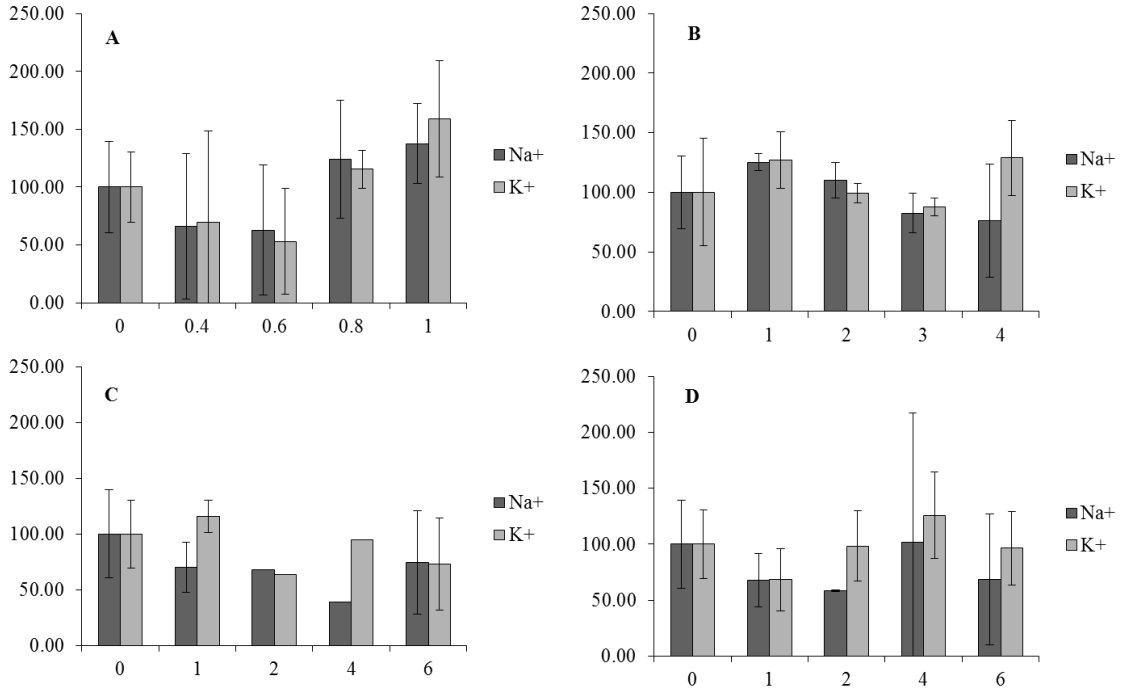

Figure A6.1. Sodium and potassium levels in *Daphnia magna* after 24 hour exposures to $AgNO_3$ (A), PVP-Ag NP (B), PEG-Ag NP (C) and Cit-Ag NP (D), showing excessive variability not allowing interpretation. Error bars: 95 % confidence intervals.

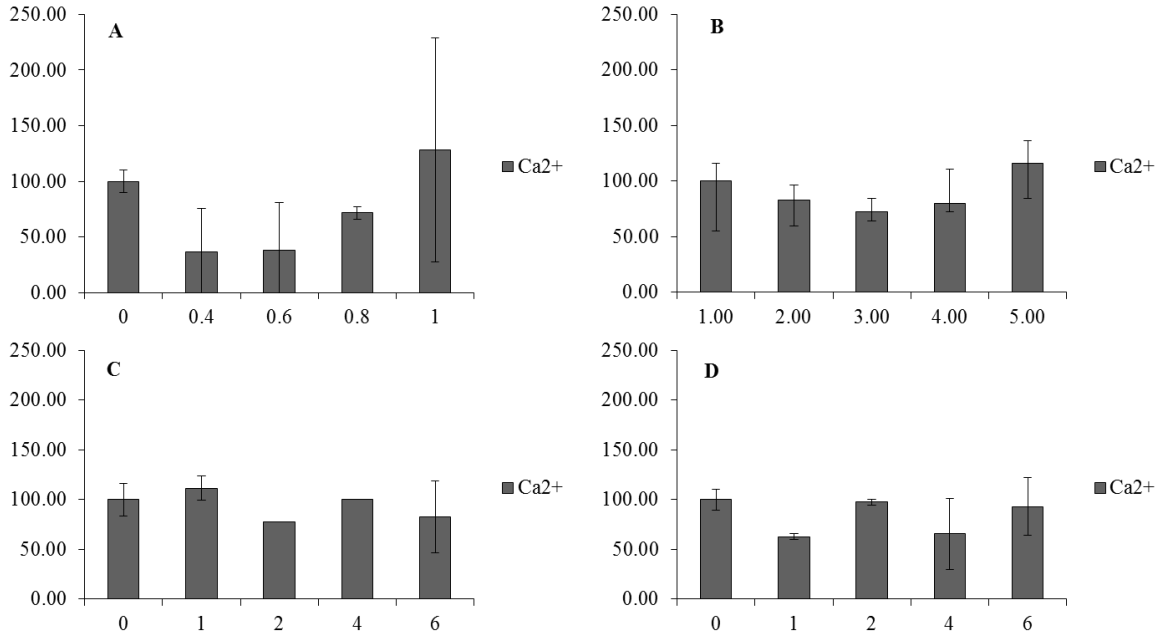

Figure A6.2. Calcium levels in *Daphnia magna* after 24 hour exposures to $AgNO_3$ (A), PVP-Ag NP (B), PEG-Ag NP (C) and Cit-Ag NP (D), showing excessive variability not allowing interpretation. Error bars: 95 % confidence intervals.

Published manuscripts

Please note Kai B. Paul was joint first author of both publications. Publication formatting and the appearance of figures have been kept in line with the official manucsripts. In particular references appear at the foot of each manuscript and a numbering system has been used throughout the text which, refer to the numbers associsted with the references in the reference list, this is also due to introduction of two more organisms not within the thesis. Thesis references appear separately directly after the published papers.

Published manuscript A

Accumulation Dynamics and Acute Toxicity of Silver Nanoparticles to *Daphnia magna* and *Lumbriculus variegatus*: Implications for Metal Modeling Approaches

Farhan R. Khan,*[,†,⊥] Kai B. Paul,[†] Agnieszka D. Dybowska,[‡] Eugenia Valsami-Jones,[§] Jamie R. Lead,[∥] Vicki Stone,[†] and Teresa F. Fernandes*[,†]

[†]School of Life Sciences, Heriot-Watt University, Edinburgh, EH14 4AS, United Kingdom

[‡]Earth Sciences, Natural History Museum, Cromwell Road, London SW7 5BD, England

§School of Geography, Earth and Environmental Sciences, University of Birmingham, Edgbaston, Birmingham, B15 2TT, England

[∥]SmartState Center for Environmental Nanoscience and Risk (CENR), Arnold School of Public Health, University of South Carolina, Columbia, South Carolina 29088, United States

Paper A: Abstract

Frameworks commonly used in trace metal ecotoxicology (e.g., biotic ligand model (BLM) and tissue residue approach (TRA)) are based on the established link between uptake, accumulation and toxicity, but similar relationships remain unverified for metal-containing nanoparticles (NPs). The present study aimed to (i) characterize the bioaccumulation dynamics of PVP-, PEG-, and citrate-AgNPs, in comparison to dissolved Ag, in *Daphnia magna* and *Lumbriculus variegatus*; and (ii) investigate whether parameters of bioavailability and accumulation predict acute toxicity. In both species, uptake rate constants for AgNPs were ∼2−10 times less than for dissolved Ag and showed significant rank order concordance with acute toxicity. Ag elimination by *L. variegatus* fitted a 1-compartment loss model, whereas elimination in *D. magna* was biphasic. The latter showed consistency with studies that reported daphnids ingesting NPs, whereas *L. variegatus* biodynamic parameters indicated that uptake and efflux were primarily determined by the bioavailability of dissolved Ag released by the AgNPs. Thus, principles of BLM and TRA frameworks are confounded by the feeding behavior of *D. magna* where the ingestion of AgNPs perturbs the relationship between tissue concentrations and acute toxicity, but such approaches are applicable when accumulation and acute toxicity are linked to dissolved concentrations. The uptake rate constant, as a parameter of bioavailability inclusive of all available pathways, could be a successful predictor of acute toxicity.

Paper A: Introduction

Silver nanoparticles (Ag NPs) are commonly used owing to their broad spectrum biocidal and antimicrobial properties. Demonstrations of environmental release[1,2] have prioritized the focus of nanoecotoxicologists and the regulatory community on NP risk assessment. Approaches that have been successfully used to address the impact of trace metals to aquatic organisms are being considered for metal-containing NPs (Me NPs).[3] For trace metals it is understood that toxicity is proportional to uptake rate above a threshold rate[4,5] − uptake being equivalent to short-term accumulation at the biotic ligand[6,7] or body tissue burdens of the metabolically available metal form in the case of the tissue residue approach (TRA).[4,5,8,9] Both biotic ligand model (BLM) and tissue residue (TR) approaches use selected accumulated trace metal tissue burdens as

predictors of toxicity, but a similar relationship between uptake, accumulation and toxicity has not been fully investigated for MeNPs. Studies have demonstrated the toxicity of Ag NPs[10−12] or their bioaccumulation dynamics,[13−15] but few have studied both together. Therefore, this knowledge gap persists. If models such as the BLM and TRA are to aid the risk assessment and regulation of Me NPs, then it is important that this relationship is verified.

BLM and TRA frameworks are founded on the principle that metal accumulation is a predictor of acute toxicity. Using water chemistry and ligand binding constants, the BLM relates shortterm accumulation (the LA_{50}, the lethal accumulation of metal on the biotic ligand that results in 50% mortality in short-term acute toxicity scenarios) at the site of uptake (the "biotic ligand", fish gill or whole body accumulation in the case of invertebrate models) to acute toxicity (48 or 96 h LC_{50}, the exposure concentration that results in 50% mortality).[6,7] Uptake and consequently short-term accumulation from solution are influenced by water chemistry, which affects the bioavailability of the metal ion to the biotic ligand. Moreover, the strength of binding between the biotic ligand and the metal of interest (the log K value) is correlated to acute toxicity.[16] Alternatively, the TRA predicts toxicity as a function of the organism's internal "metabolically available" metal concentration, that is, metal that is not detoxified.[17] In acute toxicity scenarios, the uptake rate may be so high as to swamp rates of physiological metal detoxification,[4,5] and the total accumulated tissue concentration may be used as the dose metric.[8,18] Thus, the TRA is based on the premise that, when a particular tissue concentration exceeds a defined critical body residue, adverse toxicological effects result.[9] The TRA integrates all available routes of entry (food and water), whereas the BLM only focuses on metal uptake from solution.[19] There is little research linking metal burdens resulting from NP exposure to toxic end points, but investigating the processes of short-term accumulation offers valuable insights into the bioavailability of nanoparticulate metals. The biodynamic model[20] allows the unidirectional uptake and elimination (efflux) rate constants, from food and water, to be independently characterized. Biodynamic (biokinetic) approaches have been utilized in Me NP research to demonstrate that in general aqueous Ag uptake is faster than the uptake of Ag in NP form,[13−15] that the ingestion of Me NPs from food or sediment is a key uptake route,[14,21] and in some cases the bioavailability of the metal constituent of an Me NP is due to its solubility.[22] Other studies have linked adverse effects to MeNP dissolution, most notably with ZnO NPs,[23,24] and also for Ag NPs under some exposure

scenarios.[25,26] If dissolved metal (particularly ions) released from the NP represents the sole bioavailable form of metal in the exposure, then existing biotic ligand models could, in theory, be calibrated to account for the dissolved portion.

In the present study, we investigate the waterborne toxicity and accumulation dynamics of three differently coated Ag NPs (citrate, polyvinylpyrrolidone (PVP) and polyethylene glycol (PEG)) in comparison to aqueous Ag (added as $AgNO_3$) in two model invertebrate organisms, *Daphnia magna* and *Lumbriculus variegatus*. Accumulation dynamics were determined in accordance with the biodynamic model.[20] Experimentally derived rate constants of uptake and efflux can be used to model accumulated tissue burdens for given time points and exposure concentrations. In our model scenarios, exposure concentration was set to the LC_{50}. The relationship between experimentally derived and modeled parameters of short-term accumulation (uptake rate constant (k_u), binding site affinity (log K), and short-term tissue burdens (LA_{50} or TR)) and toxicity were assessed through the BLM and TRA frameworks.

Paper A: Materials and Methods

Synthesis and Characterization of Ag NPs. The synthesis and characterization of the three Ag NPs used in this study is available elsewhere.[27] For this study, the zeta potential and hydrodynamic diameter of the NPs were determined in both organisms' media. Dissolution was determined by centrifugal ultrafiltration method.[25,28] See Supporting Information for details.

Waterborne Exposures.

D. magna and *L. variegatus* were maintained in adapted Elendt M7 medium (aM7, based on OECD 202[29]) and OECD 225[30] medium, respectively (see Supporting Information for details on the experimental animals). All laboratory glassware was soaked in 10% HCl, rinsed several time in ultrapure water and air-dried prior to use. In all exposures dissolved Ag (added as $AgNO_3$) and the three Ag NPs were added at equivalent Ag concentrations. Ag NP stock suspensions were made in the same manner as characterization suspensions (Supporting Information) and dissolved Ag solution was prepared in Milli-Q water with $AgNO_3$ salt (Sigma-Aldrich, UK). *D. magna* and *L. variegatus* toxicity assays were conducted as static nonrenewal tests for 48 and 96 h, respectively[29,30] (see Supporting Information for detailed description and concentration ranges used). Uptake and elimination experiments were based on established

methods.[14,15,31]. Based on the concentration ranges determined by the toxicity tests, *L. variegatus* were exposed for 24 h to 9.3−232 nmol L^{-1} (1−25 μg L^{-1}) dissolved Ag, 371−835 (40−90 μg L^{-1}) PVP-Ag NPs, 557−1484 (60−160 μg L^{-1}) PEG-Ag NPs and 928−3711 (100−400 μg L^{-1}) citrateAg NPs to derive unidirectional uptake rate constants for the different Ag forms. *L. variegatus* were individually exposed in 20 mL of exposure medium with 15 individuals exposed at each treatment. Similarly, *D. magna* were exposed for 24 h at 0−51 nmol L^{-1} (0−5.5 μg L^{-1}) as PVP-Ag NPs, 0−167 nmol L^{-1} (0− 18 μg L^{-1}) as PEG-Ag NPs, and 0−69 nmol L^{-1} as (0−7.5 μg L^{-1}) citrate-Ag NPs. Postexposure organisms (of both species) were rinsed with Milli-Q water to remove externally bound Ag and blotted dry.[14,15] The 15 *L. variegatus* exposed to each treatment were divided into three samples consisting of five worms each. Daphnids were exposed in groups of 20 individuals per exposure with three replicates at each exposure. Each analytical Ag sample was derived from one group of 20. Pooled samples were collected into preweighed 1.5 mL Eppendorf tubes and sacrificed by freezing.

To determine the efflux rate constants, *D. magna* and *L. variegatus* were exposed to a single Ag concentration (added as Ag NP or dissolved Ag) for 24 h and then depurated in clean media for 5 and 10 days, respectively. Exposure concentrations used for *L. variegatus* were 232 nmol L^{-1} (25 μg L^{-1}) for dissolved Ag, 464 (50 μg L^{-1}) PVP-Ag NPs, 928 (100 μg L^{-1}) PEG-Ag NPs, and 1392 (150 μg L^{-1}) citrate-Ag NPs. *D. magna* exposure concentrations were 37 nmol L^{-1} (4 μg L^{-1}) PVPAg NPs, 162 nmol L^{-1} (17.5 μg L^{-1}) PEG-Ag NPs, 70 (7.5 μg L^{-1}) citrate-Ag NPs. These concentrations were chosen so that the tissue concentrations resulting in the organisms postexposure was sufficiently elevated to remain above background for the duration of the elimination period, following 1 day exposures, organisms were rinsed in medium and transferred to new exposure chambers containing clean medium for depuration. Per Ag treatment, 15 individual *L. variegatus* were collected on each sampling day (t = 0, 1, 2, 4, 6, 8, and 10 day post exposure). Triplicate groups of 20 individual *D. magna* were collected at each sampling time-point (t = 0, 0.33 (8 h), 1, 2, 3, 4, and 5 day postexposure). As with the uptake studies, organisms were rinsed, blotted dry and sacrificed as three pools of five worms or 20 daphnids, respectively. During the depuration period worms were allowed to feed on flaked fish food for 2 h prior to water changes, and depurating daphnids were fed a diet of *C. vulgaris* at ≥0.2 mg of carbon $individual^{-1}$ day^{-1}. Complete water renewal occurred at the sampling time points

Alongside all dissolved Ag and Ag NP experiments a control set of exposures was conducted with no added Ag to ensure that there was no inadvertent contamination from experimental conditions. In addition a sample of organisms was sacrificed to measure the initial background Ag burden. The background concentration was subtracted from the measured Ag concentration in each experimental sample. Tissue samples were prepared for ICP-MS analysis by HNO_3 digestion[15] (See SI).

Table 1. Biodynamic Parameters (± 95% C.I.), Metal Binding Characteristics (± S.E.), Lethality Measurements (± 95% C.I.) and Calculated Tissue Burdens for *D. magna* and *L. variegatus* Exposed to Dissolved Ag, and PVP-, PEG- and Citrate Coated Ag NPs. LC_{50} Values Were Determined at 48 h for *D. magna* and 96 h for *L. variegatus*[a]

	Daphnia Magna				*Lumbriculus variegatus*			
	Dissolved Ag	PVP-Ag NPs	PEG-Ag NPs	Cit-Ag NPs	Dissolved Ag	PVP-Ag NPs	PEG Ag NPs	Cit-Ag NPs
Biodynamic parameters								
k_u (L g^{-1} d^{-1})	6.20 ± 0.07[a]	1.65 ± 0.56	0.26 ± 0.09	0.87 ± 0.31	1.27 ± 0.30	0.60 ± 0.08	0.24 ± 0.07	0.13 ± 0.03
k_e (d^{-1})					0.13 ± 0.06	0.042 ± 0.02	0.064 ± 0.035	0.0045 ± 0.03
k_{e1} (d^{-1})	4.27 ± 0.83[b]	2.48 ± 0.78	2.28 ± 0.11	2.40 ± 0.64				
k_{e2} (d^{-1})	0.61 ± 0.26[b]	0.27 ± 0.35	0.46 ± 0.28	0.51 ± 0.20				
Metal binding characteristics								
B_{max} (nmol g^{-1})		186 ± 67	108 ± 9	111 ± 26	338 ± 35	440 ± 88	398 ± 67	535 ± 92
K_{metal} (nmol L^{-1})		76 ± 41	20 ± 8	54 ± 24	14 ± 9	240 ± 190	877 ± 378	2630 ± 1019
Log *K*	8.9[c]	7.1 ± 0.2	7.7 ± 0.2	7.3 ± 0.2	7.9 ± 0.3	6.6 ± 0.5	6.1 ± 0.2	5.6 ± 0.2
Lethality								
LC_{50} (nmol L^{-1})	10 ± 1	55 ± 16	124 ± 14	79 ± 10	41 ± 7	599 ± 21	1180 ± 38	3040 ± 69
Calculated tissue burdens								
LA_{50} (nmol g^{-1})	7.9	11.2	4.0	8.6	6.5	359	283	395
TR at LC_{50} (nmol g^{-1})[d]	12.3	63.7	14.9	23.1	181	1377	1060	1574

[a]Derived tissue burdens LA_{50} (short-term (3 h) accumulation) and tissue residue (TR, accumulation at the LC_{50}) were calculated as described in the methods. [b]The uptake rate constant (k_u in L g^{-1} d^{-1}) was derived from the hourly rate constant of 0.256−0.264 L g^{-1} h^{-1} by Lam and Wang (2006)[35] for *D. magna* adults exposed to Ag^+ in U.S. EPA reconstituted moderately hard freshwater. [c]Fast (k_{e1}) and slow (k_{e2}) efflux rate constants were calculated from the data presented by Glover and Wood (2005)[33] for *D. magna* adults eliminating Ag in the absence of Aldrich humic acid. [d]Log K value from Bury *et al.*, 2002.[36]

Metal binding characteristics

Biodynamic models deconstruct bioaccumulation into singular unidirectional processes of uptake and loss from diet and food (and growth where appropriate) which can be experimentally derived (described in detail by Luoma and Rainbow[20]). In the present study we determined uptake (k_u) and efflux (k_e) rate constants for both species following waterborne exposure. Rate constants were used to model toxicologically relevant accumulated tissue concentrations that relate to the LC_{50}, namely, the LA_{50} and the whole body tissue concentration (i.e., tissue residue (TR)). In the biodynamic model, the influx (uptake) of Ag from solution is expressed as a function of the unidirectional uptake rate constant k_u (in nmol g tissue^{-1} d^{-1} per nmol L^{-1}, or L g^{-1} d^{-1}), the nominal exposure concentration (C_w in nmol L^{-1}) and exposure duration (t in d, eq 1). The k_u is determined from the slope of the linear portion of the relationship between the organism's uptake rate and the exposure concentration.

$$Ag_{influx} = Cw \times ku \times t \quad (1)$$

The efflux rate constant, k_e, was calculated from the change in Ag tissue concentration over the depuration period following exposure (eq 2), where $[C]_{org}$ is the bioaccumulated Ag concentration (nmol g^{-1}) at time points during efflux, $[C]^0_{org}$ is the bioaccumulated Ag concentration (nmol g^{-1}) at the start of the efflux period (i.e., t = 0 days), k_e is the rate constant of loss (d^{-1}), and t is depuration time (d). The slope formed by the points of $[C]_{org}$ and $[C]^0_{org}$ represents the rate constant for loss (k_e in d^{-1}).

$$[C]org = [C]^0_{org}e^{-kt} \quad (2)$$

To calculate the $LA_{50,}$ the short-term (3 h) tissue concentration, used within the BLM as a predictor of the LC_{50}, we used eq 1 where k_u, was the derived uptake rate constant for each Ag form, C_w was the LC_{50} of each form, and t was set to 3 h. Such short-term accumulation does not include the elimination of Ag, but to model the accumulated tissue concentration or tissue residue (i.e., the Ag concentration in the organism at the LC_{50}, 48 h for D. magna and 96 h for L. variegatus) it was necessary to account for loss. The physiological loss of accumulated Ag in L. variegatus fitted a one-component loss model (i.e., constant rate of loss over the entire efflux period). To calculate accumulation of Ag over 96 h following exposure at the LC_{50}, a loss term ($1 - k_e$) was added to eq 1 (eq 3):

$$\text{tissue residue at } LC_{50} = C_w \times k_u \times (1\ k_e) \times t \quad (3)$$

In many instances, including those involving D. magna, the loss of metal forms is biphasic[32−34] which is defined by fast (higher rate of efflux over a short period of time) and slow (lower efflux rate over a greater time period) elimination phases. To predict the Ag accumulation in daphnids exposed to dissolved Ag and AgNPs, the single efflux component in eq 3 was separated into "fast" and "slow" phases, where k_{e1} is the fast efflux rate constant for the proportional duration of the fast elimination phase (t_1), k_{e2} is the slow efflux rate constant for the proportional duration of the slow elimination phase (t_2). In this scenario t is the total exposure time, and C_w and k_u remain as the LC_{50} and uptake rate constant, respectively (eq 4).

$$\text{tissue residue at } LC_{50} = C_w \times k_u \times t \times (1((k_{e1} \times t_1) + (k_{e2} \times t_2))) \quad (4)$$

Metal influx ($influx_{organism}$ in nmol g^{-1} d^{-1}) at the site of uptake (i.e., fish gill or invertebrate whole body) following waterborne exposure can also be interpreted in terms of membrane transporter characteristics (eq 5), using Michaelis−Menten kinetics, where B_{max} is the binding site density (in nmol g^{-1}), K_{metal} is the transporter affinity of each biding site (in nmol g^{-1}) from which the log K is derived as an affinity constant, and $[M]_{exposure}$ is the exposure concentration (nmol L^{-1}).[16]

$$influx_{organism} = Bmax \times [M]exposure/Kmetal + [M]exposure \quad (5)$$

Statistical Analysis. See Supporting Information.

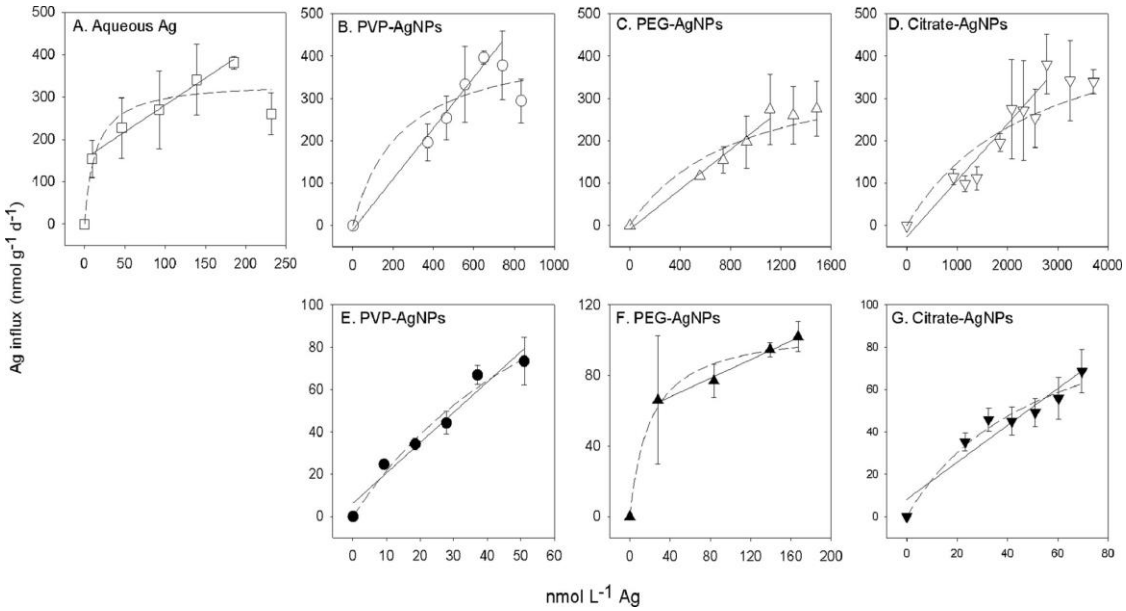

Figure 1. Ag influx into L. variegatus (A-D, open symbols) and D. magna (E-G, closed symbols) following 1 day waterborne exposures to dissolved Ag (A) and PVP (B, E), PEG (C, F), and citrate (D, G) coated Ag NPs (x-axis shows nominal exposure concentrations of total Ag (nmol L^{-1} Ag)). Mean tissue concentrations (nmol g^{-1} (dw) d^{-1}) ± S.D., n = 3) are shown following the subtraction of the background Ag concentration. Best fit linear regression (solid line) was used to estimate the uptake rate constants (k_u, L g^{-1} d^{-1}) and nonlinear regression (Michaelis−Menten) fits were used to derive metal binding characteristics.

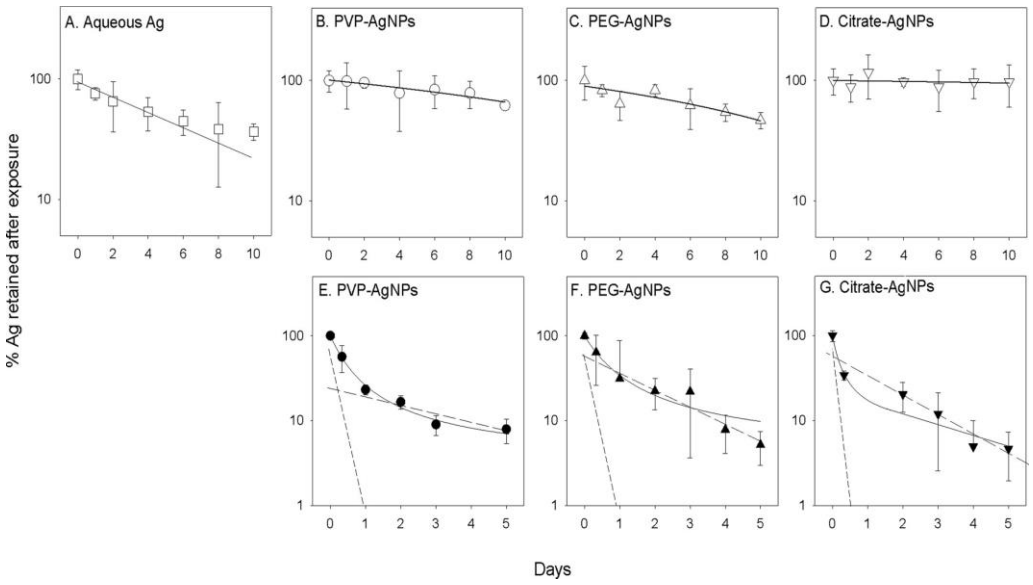

Figure 2. Proportional loss of Ag over time from *L. variegatus* (A−D, open symbols) and *D. magna* (E−G, closed symbols) following 1 day waterborne exposures. For *L. variegatus* 1 day exposures were conducted at nominal Ag concentrations of 232, 464, 928, and 1392 nmol L^{-1} for dissolved Ag and suspensions of PVP, PEG and citrate coated AgNPs, respectively, and for *D. magna* were exposed to 37, 162, and 70 nmol L^{-1} for PVP, PEG and citrate coated Ag NPs, respectively. Each symbol represents the Ag tissue concentration (with background concentration subtracted) as a percentage of the tissue concentration at day 0 (mean value ± SD, n = 3). In L. variegatus, the loss of Ag over a 10 days efflux period was described linearly (solid line, A− D). For D. magna (E−G) the loss of Ag over 5 days is described by a two-component efflux model in which the long-dashed lines represent the slow elimination phase and the short-dashed lines the fast elimination phase as determined by mathematical stripping (see text). The sum of these two terms is represented by the solid line.

Paper A: Results

Characterization of AgNPs

Characteristics of the three pristine Ag NPs are described by Tejamaya et al., (2012).[27] Hydrodynamic diameter and zeta-potential characterizations in experimental media are described within the Supporting Information (also Figure S1). Dissolution studies demonstrated that near-equilibrium was generally established within 24 h of dispersion (Supporting Information Figure S1). Comparing % dissolution between AgNPs at 72 h (used as a time point representative of equilibrium), it was shown that in OECD 225 medium, the order of dissolution was PVP-AgNPs (35.8 ± 0.3%) > citrate- AgNP (24.2 ±0.8%) > PEG-AgNP (16.7 ± 0.5%) (significant differences between each NP, $p < 0.05$, one-way ANOVA with posthoc Tukey's HSD). In aM7 medium, the order of solubility was PEG-AgNPs (28.7 ± 0.1%) > citrate-AgNPs (20.7 ± 1.0%) = PVP-AgNPs (19.7 ± 0.5%) with PEG-AgNPs releasing significantly more Ag ions than the other NPs.

Toxicity of Dissolved Ag and AgNPs

The rank order of toxicity to *D. magna* was dissolved Ag > PVP-Ag NPs > citrate-Ag NPs > PEG-Ag NPs. For *L. variegatus* the order was: dissolved Ag > PVP-Ag NP > PEG-Ag NPs > citrate-Ag NPs (Table 1, Figure S2, description in the Supporting Information).

Ag Uptake by L. variegatus *and* D. magna.

The background Ag concentrations in laboratory cultured *L. variegatus* and *D. magna* were 25.9 ± 3.4 nmol g^{-1} (dw) (2.7 ± 0.4 μg Ag g^{-1} (dw)), n = 6 pools of 5 individuals) and 4.4 ± 0.95 nmol g^{-1} (dw) (0.48 ± 0.1 μg Ag g^{-1} (dw)), n = 3 pools of 20 individuals), respectively. The uptake rate constant from solution (k_u ± 95% C.I.) for each Ag form was determined by the slope of the linear relationship between unidirectional (1 d) Ag influx into the organisms and the exposure concentration (Figure 1). For *L. variegatus*, dissolved Ag exposure resulted in the highest influx rate (k_u 1.27 ± 0.30 L g^{-1} d^{-1}), which was approximately 2 times faster than that PVP-Ag NPs (k_u 0.60 ± 0.08 L g^{-1} d^{-1}), 5 times faster than PEG-Ag NPs (k_u 0.24 ± 0.07 L g^{-1} d^{-1}) and 10 times faster than citrate-Ag NPs (k_u 0.13 ± 0.03 L g^{-1} d^{-1}) (Figure 1A− D, Table 1). PVP-Ag NP exposure also resulted in the highest uptake rate constant of the three NPs with *D. magna* (k_u 1.65 ± 0.56 L g^{-1} d^{-1}), which was approximately 2 and 6 faster than citrate- (k_u 0.87 ± 0.31 L

g^{-1} d^{-1}) and PEG-AgNPs (k_u 0.26 ± 0.09 L g^{-1} d^{-1}), respectively (Figure 1E−G, Table 1). A k_u value of 6.20 ± 0.07 L g^{-1} d^{-1} for dissolved Ag exposure (derived from Lam and Wang (2006)[35]) indicated that, as with *L. variegatus*, dissolved Ag was the most bioavailable form.

Ag uptake from all forms generally demonstrated saturation at the higher exposure concentrations (Figure 1). Nonlinear (Michaelis−Menten) regressions were used to determine the binding site density (B_{max}) and transporter affinity (K_{metal}) from which the binding site affinity constants (log K) were derived (Table 1). Rank orders of log K values were as follows for *L. variegatus*: dissolved Ag (7.9 ± 0.3) > PVP-AgNPs (6.6 ± 0.5) > PEG-AgNP (6.1 ± 0.2) > citrate-AgNPs (5.6 ± 0.2), and for *D. magna*: dissolved Ag (8.9[36])) > PEG-AgNPs (7.7 ± 0.2) > citrate-AgNPs (7.3 ± 0.2) > PVP-AgNP (7.1 ± 0.2) (Table 1).

Ag Elimination by L. variegatus *and* D. magna

Ag elimination by *L. variegatus* following exposure to all forms fitted a one-compartment loss model (Figure 2A−D). Accordingly, k_e values (efflux rate constants) were determined from the linear relationship between time (over 10 days depuration) and tissue concentration when expressed as the natural logarithm (ln) of the retained proportion (%) of the initial accumulated Ag concentration at t = 0 (i.e., immediately after exposure).[20] The k_e (±95% C.I.) value for dissolved Ag was 0.13 ± 0.06 d^{-1}, meaning that the accumulated Ag tissue concentration decreased by 13% per day. In comparison, the elimination of Ag from Ag NP exposures was slower; PEG-Ag NPs (0.064 ± 0.035 d^{-1}), PVPAg NPs (0.042 ± 0.02 d^{-1}) and citrate-Ag NPs (0.0045 ± 0.03 d^{-1}) (Table 1).

Ag elimination in *D. magna* was biphasic, comprising a slow elimination loss phase (k_{e2}) which was calculated as described above, and a fast elimination loss phase (k_{e1}) determined by mathematical stripping.[32,37] Briefly, the difference between those data points at the start of the depuration period, where considerable losses occurred, and the value predicted by the slow elimination slope, were plotted against time and a linear regression fitted (Figure 2E−G, short-dashed line). The combination of k_{e1} and k_{e2} describes the overall loss dynamics of Ag accumulated from the different Ag forms (Figure 2E−G, solid line). For each of the different Ag NPs, k_{e1} lasted for ∼8 h, and the rate of loss was relatively consistent; PVP-Ag NPs (2.48 ± 0.78 d^{-1}), citrate-Ag NPs

(2.40 ± 0.64 d^{-1}) and PEG-Ag NPs (2.28 ± 0.11 d^{-1}) (Table 1). The slow phases for the remaining portion of the 5 day depuration were not significantly different between the three Ag NPs with k_{e2} values of 0.27 ± 0.35 d^{-1}, 0.46 ± 0.28 d^{-1} and 0.51 ± 0.20 d^{-1} for PVP-, PEG- and citrateAg NPs, respectively (Table 1). For comparison, a biodynamic interpretation was made of the *D. magna* Ag elimination data presented by Glover and Wood, (2005).[33] k_{e1} and k_{e2} values of 4.27 ± 0.83 d^{-1} and 0.61 ± 0.26 d^{-1} were derived from the exposure and subsequent elimination of Ag (added as radiolabeled $^{110m}AgNO_3$), with the duration of the fast elimination phase estimated to be 6 h.

Relationship between the Modeled Parameters and Acute Toxicity of the Different Ag forms

Pearson's correlation was initially used to investigate which of the modeled or derived parameters (tissue residue, LA_{50}, k_u and log K) best explained acute toxicity. Analysis showed that all parameters significantly correlated with acute toxicity ($p < 0.01$, Pearson's correlation), but strength of the linear relationship was ordered as log K (r^2 = 0.90) > k_u (r^2 = 0.80) > LA_{50} (r^2 = 0.76) > tissue residue (r^2 = 0.70) (Supporting Information Figure S3). However, the scatter of data points indicated that significant relationships resulted from clusters of data points rather than consistent correlations. For example, the relationship between LC_{50} and LA_{50} values (Supporting Information Figure S3B), which underpins the BLM, is significant based on two clusters of data the three Ag NPs *L. variegatus* exposures, which exhibit high short-term tissue burden and high LC_{50}, and the second cluster primarily consisting of the three AgNPs *D. magna* exposures. Importantly, the regression formed by points within each cluster is not reflective of the overall correlation, and therefore the overall regression model overestimates fit. This can occur when a data set is composed of nested subsets.[38] To overcome this effect, a second analysis was undertaken in which the rank orders of each parameter were correlated to the rank order of toxicity. Kendall's tau analyses were made for each species individually and for the overall data set with both species. Kendall's tau coefficients for the correspondence of rank orders of TR (tissue concentration at the LC_{50}) and LA_{50} (3 h tissue concentration) to acute toxicity were not significant (Supporting Information Table S1). This was the case when considering each species individually and both species together. The correspondence of log K to acute toxicity was highly significant for *L. variegatus* ($p < 0.001$), and was presented as a perfect inverse relationship (τ coefficient of −1, that is, increasing binding site affinity

with decreasing LC_{50}). However, this relationship was not demonstrated for *D. magna* exposures although the most toxic form (dissolved Ag with the lowest LC_{50}) also had the highest log K value, the AgNP exposures did not conform to this pattern (Supporting Information Table S1, shown on Supporting Information Figure S3D). The rank orders for experimentally derived uptake rate constants for *L. varieagatus* (dissolved Ag> PVP-AgNPs > PEG-AgNPs > citrate-AgNPs) and *D. magna* (dissolved Ag> PVP-AgNPs > citrate-AgNPs > PEG-AgNPs) were inversely correlated to the rank order of acute toxicity in both species (τ coefficient of −1, $p < 0.001$, Supporting Information Table S1, shown on Supporting Information Figure S3C). This relationship was maintained when considering both species together (τ coefficient of −0.857, $p < 0.001$). In other words, the Ag form with the highest influx rate was the most toxic.

Paper A: Discussion

D. magna and *L. variegatus* both accumulated Ag following exposure to the various Ag NPs and dissolved Ag, but uptake and efflux rate constants differed between treatments. Dissolved Ag exposures resulted in the highest k_u values in both species, while of the Ag NPs, PVP-Ag NP exposure resulted in the fastest rate of Ag influx. Dissolved Ag and PVP-Ag NPs were also the most toxic form and NP, respectively. For both species, the uptake rate constant for dissolved Ag, was ∼2−10 times greater than for each NP except for $k_{uPEG\ AgNPs}$ in daphnids which was approximately 24 times less than $k_{uAg.}$ This is largely consistent with studies reporting waterborne uptake and when metal concentrations in dissolved and NP forms were equal.[39] Differences in bioavailability may represent the extent of dissolution within each exposure scenario, but cellular internalization of the NPs through different pathways cannot be discounted,[40] as the endocytotic entry of NPs has been demonstrated both in vitro[40,41] and in vivo.[42,43]

Studies have shown that *D. magna* readily consumes NPs suspended in the water column.[44,45] Efflux patterns are typically biphasic and describe the passage of NPs through the alimentary canal, with k_{e1} likely corresponding to the rapid defecation of nonassimilated NPs and k_{e2} to the slow excretion of NP constituent material.[34] The fate of NPs retained in the digestive tract during k_{e2}, quantified at ∼20% for Au NPs[34] and 20−45% for AgNPs,[13] is not conclusive, but many studies observe intact NPs within the gut lumen which are not assimilated into the tissue.[34,44,45] In the present study, fast and

slow phases were comparable between the three Ag NPs with k_{e1} and k_{e2} values of 2.28 ± 0.11−2.48 d^{-1} ± 0.78 and 0.27 ± 0.35−0.51 ± 0.2 d^{-1}, respectively, which conform to patterns describing elimination after NP ingestion.

Studies also describe the incidental ingestion of NPs by *L. variegatus* when exposures are conducted via spiked sediments, but, as with daphnids, there is little conclusive evidence that intake via the gut leads to the presence of NPs in the tissue.[46,47] Sediment exposures of *L. variegatus* are likely more realistic, but when wishing to maintain simplicity without the complications associated with sediment matrices[48] or aiming to contextualize biotic ligand or critical body residue frameworks,[49,50] it may be more advantageous to conduct water-only experiments. Without sediment, NP ingestion by L. variegatus appears limited. Despite showing that Cd adsorbs to TiO_2 NPs, the addition of TiO_2 NPs to Cd in aqueous exposures did not alter the bioaccumulation and toxicity of Cd to *L. variegatus*.[48] However, through the ingestion of TiO_2NPs, the uptake of Cd was facilitated in *D. magna* increasing the Cd tissue concentration without affecting toxicity.[48] These authors provide evidence that the ingestion of NPs disturbs the relationship between accumulated tissue concentrations and toxicity (i.e., *D. magna*), but in the absence of ingestion this relationship remains unaffected (i.e., *L. variegatus*).

Assuming that Ag NP ingestion by *L. variegatus* is minimal in the present study, then the uptake of Ag in either dissolved or NP form would primarily occur over the respiratory body surface (specifically in the tail portion[51]). While internalization of intact NPs through the body surface cannot be completely dismissed, it may be more logical to consider that Ag uptake is related to the presence of dissolved Ag in the water. Thus, the most straightforward scenario would be that AgNPs release labile Ag which is taken up and results in toxicity. Thus, the NP that releases the most Ag would result in the greatest Ag influx and be the most (acutely) toxic. Toxicity would correlate to parameters that quantify bioavailability (k_u) and predict toxicity based on short-term accumulated tissue burdens (LA_{50}; 3 h accumulation) and tissue residue (accumulation at LC_{50}). When considering the potential role of dissolution in these scenarios, it must be remembered that when solubility studies are conducted at higher total Ag concentrations compared to those of the exposure, the results cannot be directly extrapolated to the lower exposure concentrations.[52] Furthermore, the speciation of the resultant dissolved fraction in the test media should also be accounted for. In freshwaters (artificial or natural), dissolved Ag is subject to chlorocomplexation which

may reduce its bioavailability. However, some Ag-chlorocomplexes are bioavailable and such complexation of the dissolved Ag ion does not abolish uptake.[16] Similarly, increased aggregation of AgNPs in high ionic strength waters may reduce uptake, but not eliminate it completely.[15]

For *L. variegatus* there is significant rank concordance between acute toxicity and k_u (highest to lowest; dissolved Ag > PVPAg NPs > PEG-Ag NPs > citrate-Ag NPs), but this is not reflective of solubility at equilibrium. PVP-Ag NPs were the most soluble, but citrate-Ag NPs were more soluble than PEG-AgNPs. Citrate-Ag NP exposure results in a slower k_u and less acute toxicity than would be expected based on solubility alone. Citrate is bound to the Ag NP via van der Waals forces, as opposed to the covalently bound PVP and PEG coatings, and is more unstable owing to its weaker chemical interaction.[27] Citrate may desorb from the NP into the media[2] and bind solubilized Ag, reducing its bioavailability.[53] Free citrate was shown to complex a large portion of dissolved Ag, thereby reducing its toxicity to *C. elegans*.[53] Thus, it is not necessarily the absolute solubility of the NP that determines uptake and toxicity, but the bioavailability of the released Ag which may be affected by ligands introduced into the test system by the NP. For *D. magna*, NP ingestion appears to be the main source of the Ag tissue concentration. However, although retention occurs (during k_{e2}), based on previous research[34,44,45] it is not evident that internalization of the NPs into the tissue takes place. While Ag NPs in the gut would contribute to the body concentration, they may not be responsible for the observed toxicity. This would have significant implications for the relationship between tissue concentrations and acute toxicity.

Four parameters of accumulation and bioavailability (k_u, LA_{50}, TR and log K) were assessed as predictors of acute toxicity. Only k_u showed significant concordance to acute toxicity in both species, demonstrating that the Ag treatment that results in the greatest influx Ag into the organism is the most toxic. Although technically an uptake rate constant from solution, the ingestion of Ag NPs by *D. magna* meant that the k_u was in reality a broader influx rate that incorporated both routes of uptake (food and water). Metal influx has been shown to be a better predictor of dietborne toxicity than either tissue concentrations or concentrations of the food source.[54] This also appears to be the case with daphnids feeding on Ag NPs as there was no significant concordance between the LA_{50}, TR or log K and acute toxicity. Acute toxicity in earthworms exposed to Ag NP-spiked sediments was found to be primarily related to Ag NP oxidation and dissolution, but, owing to the ingestion of NPs, there was an increase in tissue

concentrations that did not appreciably contribute to toxicity.[55] A comparable scenario is likely with *D. magna* with toxicity related to factors other than the tissue concentration (LA_{50} or TR), potentially including, feeding inhibition,[56] physical impairment[57] or free ion activity.[26] Thus, the prediction of toxicity based on short-term BLM or TRA approaches may not be suitable for organisms that ingest NPs. Moreover, as water chemistry has been shown not to influence the dietary uptake of NPs,[58] the benefit of the BLM's incorporation of speciation modeling to derive metal bioavailable to the organism's site of uptake may be limited.[39]

When Ag uptake is predominantly due to the bioavailability of dissolved Ag released by NP, as is likely the case with *L. variegatus*, there is significant concordance between k_u and acute toxicity, and also between log K and acute toxicity. The correspondence of LC_{50} values with modeled tissue residues or LA_{50} values was not significant, but there was a trend to suggest that higher tissue burdens (3 h LA_{50}, or 48 or 96 h TR) were found in organisms experiencing less toxicity, as would be expected, and the lack of significance may be due to the low n (i.e., only 4 different Ag treatments). Where NPs are concerned, the meaning of the log K is not as straightforward as the assumption is that the toxicity is derived from labile Ag in all Ag NP exposures, and it is the bioavailability of dissolved (particularly free) Ag in the media that determines uptake and toxicity. Thus, the log K can be viewed as a representation of the proportion of dissolved Ag availability to the site of uptake. However, as our *L. variegatus* data show, in waterborne exposures the relationship between log K and acute toxicity still holds true; the most toxic form was the one with the greatest binding site affinity.

Metal-induced toxicity results when the rate of uptake exceeds the rate of efflux and detoxification.[4,59] If this relationship is consistent for Ag NPs (and Me NPs in general), then approaches based on a predictable link between short-term accumulation and toxicity, such as the TRA and BLM, could be extended to account for acutely toxic Ag NP exposures. Our study implies that this is plausible in the case of *L. variegatus*, as uptake and toxicity appeared related to the bioavailability of Ag. However, NP dissolution alone does not determine Ag bioavailability, and approaches, particularly those that employ speciation models, need to account for additional ligands, such as citrate, that are introduced into the water by the NP. For *D. magna*, principles that underpin BLM and TRA frameworks are confounded by NP ingestion. TRA and BLM approaches may be credible when accumulation and acute toxicity are related to ionic

concentrations, but they appear limited when diet is the primary route of uptake. The broad use of the biodynamic model parameter k_u to include all available pathways could be a successful predictor of acute toxicity across aquatic species.

Paper A: Associated content

* Supporting Information

Synthesis and characterization of AgNPs. Experimental animals. Toxicity assays. Sample analysis. Statistical analysis. Characterization of AgNPs. Toxicity of dissolved Ag and AgNPs. Environmental characterization of AgNPs (Figure S1). Dose-response relationships (Figure S2). Correlation of model parameters to toxicity (Figure S3). Kendall tau analyses (Table S1). This material is available free of charge via the Internet at http://pubs.acs.org.

Paper A: Acknowledgements

Funding provided by US-UK Research Program, NanoBEE (EPA-G2008-STAR-R1). John Kinross (Heriot Watt) is thanked for technical assistance. Philip S. Rainbow (Natural History Museum, London) is thanked for ICP-MS access and critically reading the manuscript.

Paper A: References

(1) Benn, T. M.; Westerhoff, P. Nanoparticle silver released into water from commercially available sock fabrics. Environ. Sci. Technol. 2008, 42, 4133−4139.

(2) Farkas, J.; Peter, H.; Christian, P.; Gallego-Urrea, J. A.; Hassellöv, M.; Tuoriniemi, J.; Gustafsson, S.; Olsson, E.; Hylland, K.; Thomas, K. V. Characterization of the effluent from a nanosilver producing washing machine. Environ. Int. 2011, 37, 1057−1062.

(3) Fabrega, J.; Luoma, S. N.; Tyler, C. R.; Galloway, T. S.; Lead, J. R. Silver nanoparticles: Behaviour and effects in the aquatic environment. Environ. Int. 2011, 37, 517−531.

(4) Luoma, S. N.; Rainbow, P. S. Metal Contamination in Aquatic Environments: Science and Lateral Management; Cambridge University Press: Cambridge, 2008.

(5) Rainbow, P. S.; Luoma, S. N.; Wang, W.-X. Trophically available metal□A variable feast. Environ. Pollut. 2011, 159, 2347−2349.

(6) Di Toro, D. M.; Allen, H. E.; Bergman, H. L.; Meyer, J. S.; Paquin, P. R.; Santore, R. C. Biotic ligand model of the acute toxicity of metals. 1. Technical basis. Environ. Toxicol. Chem. 2001, 10, 2383−2396.

(7) Paquin, P. R.; Gorsuch, J. W.; Apte, S.; Batley, G. E.; Bowles, K. C.; Campbell, P. G. C.; Delos, C. G.; Di Toro, D. M.; Dwyer, R. I.; Galvez, F.; Gensemer, R. W.; Goss, G. G.; Hogstrand, C.; Janssen, C. R.; McGeer, J. C.; Naddy, R. B.; Playle, R. C.; Santore, R. C.; Schneider, U.; Stubblefield, W. A.; Wood, C. M.; Wu, K. B. The biotic ligand model: A historical overview. Comp. Biochem. Physiol., C: Comp. Pharmacol 2002, 133, 3−36.

(8) Meador, J. P.; McCarty, L. S.; Escher, B. I.; Adams, W. J. 10th Anniversary Critical Review: The tissue-residue approach for toxicity assessment: Concepts, issues, application, and recommendations. J. Environ. Monit. 2008, 10, 1486−1498.

(9) Adams, W. J.; Blust, R.; Borgmann, U.; Brix, K. V.; DeForest, D. K.; Green, A. S.; Meyer, J. S.; McGeer, J. C.; Paquin, P. R.; Rainbow, P. S.; Wood, C. M. Utility of tissue residues for predicting effects of metals on aquatic organisms. Integr. Environ. Assess. Manage. 2011, 7, 75−98.

(10) Gaiser, B. K.; Fernandes, T. F.; Jepson, M.; Lead, J. R.; Tyler, C. R.; Stone, V. Assessing exposure, uptake and toxicity of silver and cerium dioxide nanoparticles from contaminated environments. Environ. Health 2009, 8 (Suppl 1), S2.

(11) Laban, G.; Nies, L. F.; Turco, R. F.; Bickham, J. W.; Sepulveda, Ḿ. S. The effects of silver nanoparticles on fathead minnow (Pimephales promelas) embryos. Ecotoxicology 2010, 19, 185−195.

(12) Li, T.; Albee, B.; Alemayehu, M.; Diaz, R.; Ingham, L.; Kamal, S.; Rodriguez, M.; Bishnoi, S. W. Comparative toxicity study of Ag, Au, and Ag-Au bimetallic nanoparticles on Daphnia magna. Anal. Bioanal. Chem. 2010, 398, 689−700.

(13) Zhao, C.-M.; Wang, W.-X. Biokinetic uptake and efflux of silver nanoparticles in Daphnia magna. Environ. Sci. Technol. 2010, 44, 7699− 7705.

(14) Croteau, M.-N.; Misra, S. K.; Luoma, S. N.; Valsami-Jones, E. Silver bioaccumulation dynamics in a freshwater invertebrate after aqueous and dietary exposures to nanosized and ionic Ag. Environ. Sci. Technol. 2011, 45, 6600−6607.

(15) Khan, F. R.; Misra, S. K.; García-Alonso, J.; Smith, B. D.; Strekopytov, S.; Rainbow, P. S.; Luoma, S. N.; Valsami-Jones, E. Bioaccumulation dynamics and

modeling in an estuarine invertebrate following aqueous exposure to nanosized and dissolved silver. Environ. Sci. Technol. 2012, 46, 7621−7628.

(16) Niyogi, S.; Wood, C. M. Biotic ligand model, a flexible tool for developing site-specific water quality guidelines for metals. Environ. Sci. Technol. 2004, 38, 6177−6192.

(17) Rainbow, P. S.; Luoma, S. N. Trace metals in aquatic invertebrates. In Environmental Contaminants in Biota: Interpreting Tissue Concentrations; Beyer, W. N., Meador, J. P., Eds.; Taylor and Francis Books: Boca Raton, FL, 2011; pp 231−252.

(18) Sappington, K. G.; Bridges, T. S.; Bradbury, S. P.; Erickson, R. J.; Hendriks, A. J.; Lanno, R. P.; Meador, J. P.; Mount, D. R.; Salazar, M. H.; Spry, D. J. Application of the tissue residue approach in ecological risk assessment. Integr. Environ. Assess. Manage. 2011, 7, 116−140.

(19) Luoma, S. N.; Cain, D. J.; Rainbow, P. S. Calibrating biomonitors to ecological disturbance: A new technique for explaining metal effects in natural waters. Integr. Environ. Assess. Manage. 2009, 6, 199−209.

(20) Luoma, S. N.; Rainbow, P. S. Why is metal bioaccumulation so variable? Biodynamics as a unifying concept. Environ. Sci. Technol. 2005, 39, 1921−1931.

(21) Khan, F. R.; Schmuecking, K.; Krishnadasan, S.; Berhanu, D.; Smith, B. D.; de Mello, J.; Rainbow, P. S.; Luoma, S. N.; Valsami-Jones, E. Dietary bioavailability of cadmium-containing quantum fots to the gastropod Peringia ulvae. Environ. Toxicol. Chem. 2013, 32, 2621−2629. (22) Khan, F. R.; Laycock, A. L.; Dybowska, A.; Larner, F.; Smith, B. D.; Rainbow, P. S.; Luoma, S. N.; Rehkamper, M.; Valsami-Jones, E. Ä stable isotope tracer to determine uptake and efflux dynamics of ZnO nano- and bulk particles, and dissolved Zn to an estuarine snail. Environ. Sci. Technol. 2013, 47, 8532−8539.

(23) Franklin, N. M.; Rogers, N. J.; Apte, S. C.; Batley, G. E.; Gadd, G. E.; Casey, P. S. Comparative toxicity of nanoparticulate ZnO, bulk ZnO and ZnCl2 to a freshwater microalga (Pseudokirchneriella subcapitata): The importance of particle solubility. Environ. Sci. Technol. 2007, 41, 8484−8490.

(24) Ma, H.; Williams, P. L.; Diamond, S. A. Ecotoxicity of manufactured ZnO nanoparticles A review. Environ. Pollut. 2013, 172, 78−85.

(25) Navarro, E.; Piccapietra, F.; Wagner, B.; Marconi, F.; Kaegi, R.; Odzak, N.; Sigg, L.; Behra, R. Toxicity of silver nanoparticles to Chlamydomonas reinhardtii. Environ. Sci. Technol. 2008, 42, 8959−8964.

(26) Newton, K. M.; Puppala, H. L.; Kitches, C. L.; Colvin, V. L.; Klaine, S. J. Silver nanoparticle toxicity to Daphnia magna is a function of dissolved silver concentration. Environ. Toxicol. Chem. 2013, 32, 2356− 2364.

(27) Tejamaya, M.; Romer, I.; Merrifield, R. C.; Lead, J. R. Stability of citrate, PVP, and PEG coated silver nanoparticles in ecotoxicology media. Environ. Sci. Technol. 2012, 46, 7011−7017.

(28) Croteau, M. N.; Dybowska, A. D.; Luoma, S. N.; Misra, S. K.; Valsami-Jones, E. Isotopically modified silver nanoparticles to assess nanosilver bioavailability and toxicity at environmentally relevant exposures. Environ. Chem. 2014, 11, 247−256.

(29) Daphnia sp., Acute Immobilisation test. Guidelines for the Testing of Chemicals No. 202; Organization for Economic Cooperation and Development: Paris, France, 2004.

(30) Sediment-Water Lumbriculus Toxicity Test Using Spiked Sediment No 225; Organization for Economic Cooperation and Development: Paris, France, 2007.

(31) Rainbow, P. S.; Smith, B. D.; Luoma, S. N. Biodynamic modelling and the prediction of Ag, Cd and Zn accumulation from solution and sediment by the polychaete Nereis diversicolor. Mar. Ecol.: Prog. Ser. 2009, 390, 145−155.

(32) Croteau, M.-N.; Luoma, S. N.; Topping, B. R.; Lopez, C. B. Stable metal isotopes reveal copper accumulation and loss dynamics in the freshwater bivalve Corbicula. Environ. Sci. Technol. 2004, 38, 5002−5009. (33) Glover, C. N.; Wood, C. M. Accumulation and elimination of silver in Daphnia magna and the effect of natural organic matter. Aquat. Toxicol. 2005, 73, 406−417.

(34) Khan, F. R.; Kennaway, G. M.; Croteau, M.-N.; Dybowska, A.; Smith, B. D.; Nogueira, A. J. A.; Rainbow, P. S.; Luoma, S. N.; ValsamiJones, E. In vivo retention of ingested Au NPs by Daphnia magna: No evidence for trans-epithelial alimentary uptake. Chemosphere 2014, 100, 97−104.

(35) Lam, I. K.; Wang, W. X. Accumulation and elimination of aqueous and dietary silver in Daphnia magna. Chemosphere 2006, 64, 26−35.

(36) Bury, N. R.; Shaw, J.; Glover, C.; Hogstrand, C. Derivation of a toxicity-based model to predict how water chemistry influences silver toxicity to invertebrates. Comp. Biochem. Physiol., C: Comp. Pharmacol. 2002, 133, 259−270.

(37) Riggs, D. S. In The Mathematical Approach to Physiological Problems; Williams & Williams: Baltimore, 1963; pp 120−167.

(38) Schielzeth, H.; Forstmeier, W. Conclusions beyond support: Overconfident estimates in mixed models. Behav. Ecol. 2008, 20, 416− 420.

(39) Luoma, S. N.; Khan, F. R.; Croteau, M.-N. Bioavailability and bioaccumulation of metal-based engineered nanomaterials in aquatic environments: Concepts and processes. In Frontiers of Nanoscience Volume 7: Nanoscience and the Environment; Valsami-Jones, E., Lead, J. R., Eds.; Elservier: Amsterdam, Netherlands, 2014; pp 157−193.

(40) Gratton, S. E.; Ropp, P. A.; Pohlhaus, P. D.; Luft, J. C.; Madden, V. J.; Napier, M. E.; DeSimone, J. M. The effect of particle design on cellular internalization pathways. Proc. Natl. Acad. Sci. U. S. A. 2008, 105, 11613−11618.

(41) Nan, A.; Bai, X.; Son, S. J.; Lee, S. B.; Ghandehari, H. Cellular uptake and cytotoxicity of silica nanotubes. Nano Lett. 2008, 8, 2150−4.

(42) Marchesano, V.; Hernandez, Y.; Salvenmoser, W.; Ambrosone, A.; Tino, A.; Hobmayer, B.; de la Fuente, J. M.; Tortiglione, C. Imaging inwards and outwards trafficking of gold nanoparticles in whole animals. ACS Nano 2013, 7, 2431−2442.

(43) Khan, F. R.; Misra, S. K.; Bury, N. R.; Smith, B. D.; Rainbow, P. S.; Luoma, S. N.; Valsami-Jones, E. Inhibition of potential uptake pathways for silver nanoparticles in the estuarine snail Peringia ulvae. Nanotoxicology, 2014; DOI: 10.3109/17435390.2014.948519.

(44) Peterson, E. J.; Akkanen, J.; Kukkonen, J. K.; Weber, W. J., Jr. Biological uptake and depuration of carbon nanotubes by Daphnia magna. Environ. Sci. Technol. 2009, 43, 2969−2975.

(45) Heinlaan, M.; Kahru, A.; Kasemets, K.; Arbielle, B.; Prensier, G.; Dubourquier, H.-C. Changes in the Daphnia magna midgut upon ingestion of copper oxide nanoparticles: A transmission electron microscopy study. Water Res. 2011, 45, 179−190.

(46) Petersen, E. J.; Huang, Q.; Weber, W. J. Ecological uptake and depuration of carbon nanotubes by Lumbriculus variegatus. Environ. Health. Perspect. 2008, 116, 496−500.

(47) Coleman, J. G.; Kennedy, A. J.; Bednar, A. J.; Ranville, J. F.; Laird, J. G.; Harmon, A. R.; Hayes, C. A.; Gray, E. P.; Higgins, C. P.; Steevens, J. A. Comparing the effects of nano silver size and coating variations on bioavailability, internalization, and elimination, using Lumbriculus variegatus. Environ. Toxicol. Chem. 2013, 32, 2069−2077.

(48) Hartmann, N. B.; Legros, S.; Von der Kammer, F.; Hofmann, T.; Baun, A. The potential of TiO_2 nanoparticles as carriers for cadmium uptake in Lumbriculus variegatus and Daphnia magna. Aquat. Toxicol. 2012, 118, 1−8.

(49) Ng, T. Y.; Pais, N. M.; Dhaliwal, T.; Wood, C. M. Use of wholebody and subcellular Cu residues of Lumbriculus variegatus to predict waterborne Cu toxicity to both L. variegatus and Chironomus riparius in fresh water. Chemosphere 2012, 87, 1208−1214.

(50) Leonard, E. M.; Wood, C. M. Acute toxicity, critical body residues, Michaelis−Menten analysis of bioaccumulation, and ionoregulatory disturbance in response to waterborne nickel in four invertebrates: Chironomus riparius, Lymnaea stagnalis, Lumbriculus variegatus and Daphnia pulex. Comp. Biochem. Physiol., C: Comp. Pharmacol. 2013, 158, 10−21.

(51) Penttinen, O. P.; Kukkonen, J.; Pellinen, J. Preliminary study to compare body residues and sublethal energetic responses in benthic invertebrates exposed to sediment-bound 2, 4, 5-trichlorophenol. Environ. Toxicol. Chem. 1996, 15, 160−166.

(52) Kittler, S.; Greulich, C.; Diendorf, J.; Koller, M.; Epple, M. Toxicity of silver nanoparticles increases during storage because of slow dissolution under release of silver ions. Chem. Mater. 2010, 22, 4548− 4554.

(53) Yang, X.; Gondikas, A. P.; Marinakos, S. M.; Auffan, M.; Liu, J.; Hsu-Kim, H.; Meyer, J. N. Mechanism of silver nanoparticle toxicity is dependent on dissolved silver and surface coating in Caenorhabditis elegans. Environ. Sci. Technol. 2011, 46, 1119−1127.

(54) Croteau, M.-N.; Luoma, S. N. Predicting dietborne metal toxicity from metal influxes. Environ. Sci. Technol. 2009, 43, 4915−4921.

(55) Shoults-Wilson, W. A.; Zhurbich, O. I.; McNear, D. H.; Tsyusko, O. V.; Bertsch, P. M.; Unrine, J. M. Evidence for avoidance of Ag nanoparticles by earthworms (Eisenia fetida). Ecotoxicology 2011, 20, 385−396.

(56) Taylor, G.; Baird, D. J.; Soares, A.M. V. M Surface binding of contaminants by algae: Consequences for lethal toxicity and feeding to Daphnia magna Straus. Environ. Toxicol. Chem. 1998, 17, 412−419.

(57) Hou, W.-C.; Westerhoff, P.; Posner, J. D. Biological accumulation of engineered nanomaterials: A review of current knowledge. Environ. Sci.: Processes Impacts 2013, 15, 103−122.

(58) Oliver, A. L.-S.; Croteau, M.-N.; Stoiber, T. L.; Tejamaya, M.; Römer, I.; Lead, J. R.; Luoma, S. N. Does water chemistry affect the dietary uptake and toxicity of silver nanoparticles by the frehwater snail Lymneaa stagnalis? Environ. Pollut. 2014, 189, 87−91.

(59) Rainbow, P. S. Trace metal concentrations in aquatic invertebrates: Why and so what? Environ. Pollut. 2002, 120, 497−507.

Published Paper B

Characterisation of bioaccumulation dynamics othree differently coated silver nanoparticles and aqueous silver in a simple freshwater food chain

Judit Kalman,[A,D] Kai B. Paul,[A,B] Farhan R. Khan,[C] Vicki Stone[A] and Teresa F. Fernandes[A,D]

[A] School of Life Sciences, Heriot-Watt University, Edinburgh, EH14 4AS, UK.

[B] Blue Frog Scientific, Scott House, South St Andrews Street, Edinburgh, EH2 2AZ, UK.

[C] Department of Environmental, Social and Spatial Change (ENSPAC), Roskilde University, Universitetsvej 1, PO Box 260, DK-4000 Roskilde, Denmark.

[D] Corresponding authors. Emails: judit.kalman@uca.es; t.fernandes@hw.ac.uk

Paper B: Environmental context

Nanoparticlesmaybepassedfromprimaryproducerstopredatorshigherupthefood chain, but little is currently known about this transfer. We studied the accumulation dynamics of silver nanoparticles by algae, and then from algae to zooplankton.Usingthebiodynamicapproach, were constructed the accumulation process to show that diet is the primary route of uptake for silver nanoparticles.

Paper B: Abstract

This study investigated the bioaccumulation dynamics of silver nanoparticles (Ag NPs) with different coatings (polyvinyl pyrrolidone, polyethylene glycol and citrate), in comparison with aqueous Ag (added as $AgNO_3$), in a simplified freshwater food chain comprising the green alga *Chlorella vulgaris* and the crustacean *Daphnia magna*. Algal uptake rate constants (k_u) and membrane transport characteristics (binding site density, transporter affinity and strength of binding) were determined after exposing algae to a range of either aqueous Ag or Ag NP concentrations. In general, higher k_u values were related to higher toxicity in the algae. Transmission electron microscopy images were used to investigate the internalisation of Ag NPs in algal cells following exposure to low concentrations for 72 h (mimicking inhibition tests) or high concentrations for 4 h (mimicking preparation for daphnia dietary exposure). Ag NPs were only visualised in

algal cells exposed to high Ag NP concentrations. To establish *D. magna* biodynamic model constants, organisms were fed Ag-contaminated algae and depurated for 96 h. Assimilation efficiencies ranged from 10 to 25% and the elimination of accumulated Ag followed a two-compartmental model, indicating lower loss rate constants for poly vinyl pyrrolidone-, and polyethylene glycol-coated Ag NPs. Biodynamic model results revealed that in most cases, food is the dominant pathway of Ag uptake in *D. magna*. Despite the predicted low steady-state body burdens in *D. magna*, dietary uptake of Ag was possible from aqueous and particulate forms of Ag.

Additional keywords: *Chlorella vulgaris*, *Daphnia magna*, dietary uptake, internalization.

Paper B: Introduction

Silver nanoparticles (Ag NPs) pose a potentially significant environmental problem owing to their increased use and release.[1] As such, nanoecotoxicology has received increasing attention from government, regulatory bodies and academics.[2,3] In order to set environmental quality standards or perform risk assessment for these materials, it is essential to determine their bioavailability, which is considered a prerequisite for toxicity.[4] The biodynamic model (BDM) deconstructs trace metal accumulation into a unidirectional process of uptake and efflux from food and water respectively.[5] In doing so, metal body burdens can be predicted under a variety of environmental conditions. Moreover, the BDM suggests that toxicity occurs when the metal influx rates exceed combined rates of loss and detoxification.[6] Thus, factors that affect the bioavailability of the metal species will also affect the uptake rate constant (k_u) and likely toxicity. Indeed, under some circumstances, k_u has been found to be a successful predictor of acute toxicity.[7] The BDM has been successfully applied to a wide range of trace metals and aquatic organisms[5] and the suitability of this approach for metalcontaining NPs has now been tested for a range of invertebrate species.[8–11] It is assumed metals must associate with receptor sites at a biological membrane in order for uptake to occur. The binding affinity and the binding capacity at this site, when accounting for the environmental conditions, may correlate to toxicity as has been shown for trace metals.[12–14] This relationship was recently studied on zooplankton in relation to metal

NPs[15] using the biotic ligand model, but there is still little research on the application of these models for metal-containing NPs to freshwater algae.

The importance of alga as a primary producer of energy and a food source highlights its priority in risk assessment, because impact at this level may affect the higher trophic levels. Thus, it is not surprising that there have been a few studies on he toxic effect of Ag NPs on freshwater microalgae.[16–19] Furthermore, as an important food source, algae may facilitate the uptake of NPs as organisms incidentally ingest NPs during feeding,[9,20] which may result in biomagnification and accumulation, with potentially deleterious effects.

In principle, if an Ag NP is taken up by the organism, it can be accumulated (in metabolically available or detoxified forms) or excreted. As mentioned previously, toxicity of Ag NP would occur if the rate of Ag NP uptake exceeded the combined rates of excretion and detoxification. Whether the toxicity is caused by the novel properties of the NP or its dissolved fraction is uncertain. It has been documented that dissolved Ag will associate with waterborne ligands[12] and debris, including algae, an important source of nutrition for the cladoceran *Daphnia magna*, and Ag NPs are no different.[21–24] For trace metals, including aqueous Ag, the diet is an important route of metal uptake and bioaccumulation.[25] Croteau and Luoma[6] and Zhao and Wang[8] both showed diet to be the most important route of uptake during both dissolved Ag and Ag NP exposures respectively, with over 70% of accumulated tissue burdens attributed to dietary intake. Despite this, little work has been done on the dietary uptake of Ag NPs in *D. magna* and the proportional contribution they will have to total Ag body burdens in comparison with waterborne Ag NPs.

In the present study, we use a simple food web comprising *Chlorella vulgaris* and *D.magna* to explore the dietary uptake of Ag NPs and use previously reported waterborne biodynamic parameters[7] to assess the importance of each route of uptake. Such questions are integral to the current risk assessment of Ag NPs and the future prediction of their risks, because they allow us to differentiate the importance of the different available exposure routes (food and water). Furthermore, we can assess whether the current Ag NP levels in the environment are likely to significantly accumulate and cause toxicity. It has also been suggested if one route of uptake is predominant (food or water), then this may aid in the simplification of such predictions because only the major uptake route need to be accounted for.[6] Thus, the main objectives of the present study were to (i) investigate the toxicity of aqueous Ag (added

as $AgNO_3$) and Ag NPs coated with polyvinyl pyrrolidone (PVP-Ag NPs), polyethylene glycol (PEG-Ag NPs) and citrate (Cit-Ag NPs) to *C. vulgaris*; (ii) investigate the uptake of Ag NPs by the algae, define metal-binding characteristics where appropriate; (iii) determine dietary uptake and assimilation efficiencies of Ag in *D. magna* fed *C. vulgaris* that were previously exposed to Ag as either NP or in aqueous form; and (iv) simulate a basic food we band determine the potential for Ag NPs to move between the trophic levels.

Paper B: Experimental methods

Test chemicals and nanoparticle characterisation

Stock suspensions of Ag NPs coated with PVP, PEG and citrate (nominal particle core size 10 nm) were synthesised and provided by the University of Birmingham (UK) (within the nanoBEE consortium). $AgNO_3$ (analytical reagent grade) was purchased from Fisher Scientific (Loughborough, UK) and the stock solution was prepared by dissolving the appropriate amount of silver nitrate in Milli-Q water (Millipore, Livingston, UK) with a grade of 18.2 MO cm. All $AgNO_3$ solutions and silver NP suspensions were made immediately before use.

Dynamic light scattering (DLS, Zetasizer Nano Series, Malvern Instruments, Malvern, UK) was used to monitor particle size and zeta-potentials in algal medium (Jaworski's medium, JM[26]) at 4 mg $L^{!1}$. Hydrodynamic diameters and surface-related charge of the Ag NPs were determined in triplicate after 0, 24, 48 and 72-h incubation.

For transmission electron microscopy (TEM) images, Ag NPs were incubated in algal medium at 4 mg L^{-1} for 72 h. A drop of the suspensions was deposited on carbon-coated copper TEM grids, then allowed to evaporate at room temperature overnight before analysis. NPs were viewed in a Philips CM120 TEM (Philips Electron Optics, Eindhoven, Netherlands) or FEI Tecnai F20 FEGTEM (Hillsboro, OR, USA) fitted with a Gatan Orius Charge Couple Device camera.TEM energy dispersive X-ray spectroscopy (EDX) analysis was performed using an Oxford Instruments 80 mm^2 X-Max SDD fitted to the microscope and running *INCA* software (Oxford, UK).

Dissolution of the Ag NPs was measured using ultracentrifugation methods.[27] Briefly, Ag NPs at 2 mg L^{-1} were suspended in algal medium for 4 h and then centrifuged at 51 200*g*, 20 ºC,for 1 h. After centrifugation, the supernatant was separated from the pellet.

The supernatant represented the dissolved fraction released from the NPs, and the pellet, the particulate Ag. Both fractions were acidified (2% HNO_3), and total Ag was measured using flame atomic absorption spectrophotometry (AAS, Perkin Elmer, AAnalyst 200 atomic absorption spectrometer, Beaconsfield, UK). Dissolution studies were conducted at a higher concentration than those used in the waterborne exposures to ensure accurate measurement of the dissolved fraction.[28]

Test organisms

Chlorella vulgaris (Culture Collection of Algae and Protozoa 211/12, Scottish Marine Institute, Oban, UK) culture was grown in JM in 250-mL Erlenmeyer flasks (Scientific Laboratory Supplies, Coatbridge, UK) under constant rotary agitation (225 rpm), illumination (120 mmol m^{-2} s^{-1}) and temperature (23 ºC). When the cell density reached, 10^6 cells mL^{-1}, the stock culture was maintained under static conditions (illumination of 50 mmol m^{-2} s^{-1}) in a 16:8 h light:dark photoperiod at 20 ºC. Cultures were regularly maintained by transferring a small aliquot into fresh sterile medium and were periodically checked for bacterial contamination by plating on nutrient agar (Oxoid Ltd, Basingstoke, UK).

Daphnia magna used within the current study were from an established laboratory culture originally purchased from Blades Biological (Edenbridge, UK). *D. magna* were maintained in aerated aquaria with Elendt M7 media,[29] which was adapted by the removal of ethylene diaminetetraacetic acid (EDTA) to reduce the effect of dissolved Ag or Ag NP chelation, hereafter called aM7 (adapted M7) media. Cultures were maintained with a 16:8 h light:dark photoperiod at 20 ºC. Dissolved oxygen (8 mg L^{-1}) and pH (8) remained within the range recommended by standard Organization for Economic Co-operation and Development (OECD) test protocols.[29] Daphnids were maintained on an algal diet of *C. vulgaris*[29] at 5×10^5 cells day^{-1} and medium was changed every 2–3 days. *D. magna* used in the present study were 5–10 days old to ensure peak growth rate had been reached, but that no neonate release had occurred. After exposure, daphnids were 9–10 days old, which ensured that individuals used in the study were in the same developmental and physiological state.

Algal growth inhibition test

Algal growth inhibition assays were performed according to the OECD test guideline 201[30] using *C. vulgaris* in the exponential growth phase. Temperature and light

conditions for the toxicity test were identical to those used for culture growth. Experiments were carried out in triplicates using five concentrations for each Ag form. The concentration range chosen allowed us to construct the logistic curve from which IC_{50} values (the concentration required to cause a 50% inhibition in growth after 72 h compared with the controls) were calculated. The exposure concentrations ranged between 1 and 7 mg L^{-1} or 9 and 65 nmol L^{-1} (aqueous Ag), 3 and 10 mg L^{-1} or 28 and 93 nmol L^{-1} (PVP-Ag NPs), 3 and 100 mg L^{-1} or 28 and 935 nmol L^{-1} (PEG-Ag NPs) and 1 and 15 mg L^{-1} or 9 and 140 nmol L^{-1} (Cit-Ag NPs). The initial concentration of the inoculum was 10^4 cells $mL^{!1}$, which was required to ensure exponential growth. At 24, 48 and 72 h, 1 mL of sample was taken and chlorophyll was extracted from the cells in 4 mL of pure acetone (High Performance Liquid Chromatography grade, Fisher Scientific) along with 0.1 mL of 1.5 mg mL^{-1} locust bean gum (Sigma–Aldrich, Gillingham, UK) to aid in the precipitation of particles. After 72 h, cell density was determined in the supernatant by measuring in vitro fluorescence of acetone-extracted chlorophyll (Trilogy laboratory fluorometer, Chlorophyll-*a* Non-Acidification module). IC_{50} values were calculated using *Sigma Plot 10.0* (Systat Software, Inc., San Jose, CA, USA).

Ag accumulation in C. vulgaris

To study the relationship between Ag uptake and toxicity in *C. vulgaris*, algae were exposed to ranges of concentrations (below IC_{50} values) of aqueous Ag (0.1–2.0 mg L^{-1} or 0.9–18.6 nmol L^{-1}), PVP-Ag (0.5–5.0 mg L^{-1} or 4.6– 46.4 nmol L^{-1}), PEG-Ag (0.5–10.0 mg L^{-1} or 4.6–92.8 nmol L^{-1}) and Cit-Ag (0.5–4.0 mg L^{-1} or 4.6–37.1 nmol L^{-1}) for 72 h under the test conditions described for the growth inhibition assays. Speciation modelling (using Visual MINTEQ ver. 3.0, KTH Royal Institute of Technology, Stockholm, Sweden) estimated that 93% of the total Ag added as $AgNO_3$ occurred as Ag^+. Post-exposure, algal cells were harvested by centrifugation (2230 *g* at 20 ºC for 30 min) and resuspended in Milli-Q water three times to remove weakly bound Ag or Ag NPs.The final pellet was dried to constant weight at 60 ºC, and then digested in 60 mL of concentrated HNO_3 at 90 ºC. Each digest was made up to 3 mL with Milli-Q water and analysed for Ag by inductively coupled plasma mass spectrophotometry (ICP-MS, 7500ce, Agilent Technologies, Santa Clara, CA) with rhodium as an internal standard. Standard Reference Material (SRM 1566b Oyster tissue, National Institute of Standards and Technology, Gaithersburg, MD, USA) and blanks were processed and analysed

alongside experimental samples for quality assurance. Recovery of reference material was 91.3 ± 4.9% (n = 3).

TEM was used to investigate possible internalisation of the NPs in algal cells. Two different treatments were carried out. First, algae were exposed to Ag NPs at 2 mg L^{-1} for 4 h (mimicking the preparation for daphnia dietary exposure; see below). Second, algae were exposed to lower Ag concentrations, e.g. 7 mg L^{-1} for PVP-Ag and Cit-Ag NPs, and 10 mg L^{-1} for PEG-Ag NP for 72 h (mimicking the toxicity tests). After the exposures, cells were centrifuged (2230 g at 20 ºC for 30 min) and washed three times with Milli-Q water. Algal cells were fixed using 3% glutaraldehyde in 0.1 M sodium cacodylate buffer (pH 7.3) for 2 h. Post-fixation was carried out in 1% osmium tetroxide in 0.1M sodium cacodylate for 45 min, followed by dehydration in graded acetones, then embedded in Araldite resin. Ultrathin sections were stained in uranyl acetate and lead citrate.

Dietary Ag uptake and elimination in D. magna

To study the dietary uptake of Ag by *D. magna*, daphnids were fed algae that had been previously exposed to the different Ag forms. Algal cells in exponential growth phase were exposed to either $AgNO_3$ (0.25 mg L^{-1}) or Ag NPs (2 mg L^{-1}) for 4 h. These exposure concentrations were chosen to ensure a sufficiently high tissue concentration was achieved in the daphnids without causing any mortality. After exposure, algae were centrifuged and rinsed as previously described. The algal pellet was resuspended in aM7 medium and cell density was counted with a hemocytometer (Sigma–Aldrich). Prior to exposure, daphnids were depurated in clean aM7 medium for 2–4 h to empty their guts, and then they were transferred into plastic cups with 120mLclean aM7 medium.Each exposure andsubsequent elimination was performed in groups of 60 daphnids. Daphnids were exposed to Ag-contaminated food at a cell density of 5×10^5 cells mL^{-1} for either 40 min (shorter than the gut passage time for dietary Ag assimilation study) or 24 h (ensuring sufficiently high initial body concentration of Ag for Ag elimination study). To establish assimilation efficiency (AE; the measure of the amount of metal retained from a diet) and efflux rate constants (k_{ef}), daphnids were transferred to new cups with clean aM7 medium and allowed to depurate in the presence of algae (unexposed to aqueous Ag or Ag NPs). The depuration lasted 96 h. At 0, 1, 2, 4, 6, 24, 48, 72 and 96 h of depuration, three replicate groups per treatment were sampled, thoroughly rinsed with Milli-Q water and collected on filter paper. At each time point, water and food

were renewed to avoid re-uptake of Ageliminated into thewater by daphnids. Animals were dried to constant weight at 60 ºC and digested in concentrated HNO_3. Each digest was made up to 3 mL with Milli-Q water (with a final concentration of HNO_3 of 2%) and analysed for Ag on either AAS or ICP-MS.

k_{ef} was calculated from the slope of the linear regression between the natural logarithm of the percentage Ag retained in the daphnids and the depuration time during the slowelimination phase (24–96 h). AE (percentage) was estimated as the *y* intercept of the linear regression between the percentage of Ag retained in the daphnids and the time of the slowly exchanging pool.[31] The metal loss from the organisms is described as follows:

$$[C]\text{org} = [C]^0_{\text{org}} e^{-kt} \quad (1)$$

where [C] is the bioaccumulated Ag concentration (mg g^{-1}) during the physiological loss from the slow elimination phase, $[C]_0$ is the bioaccumulated Ag concentration (mg g^{-1}) at the start of the depuration, k_e is the rate of constant of loss (day^{-1}) and *t* is the depuration time (days).

Biomagnification factors (BMF) were determined by dividing the Ag concentration in the daphnids by the concentration in the diet.

Model equations

Metal influx ($Influx_{organism}$, nmol g^{-1} day^{-1}) was interpreted in terms of membrane transporter characteristics (Eqn 2) where B_{max} is the binding site density (nmol g^{-1}), K_d is the transporter affinity of each binding site (nmol g^{-1}) from which the log *K* is derived as an affinity constant (i.e. strength of binding), and $[M]_{exposure}$ is the exposure concentration (nmol L^{-1}).[32]

$$\text{influx}_{\text{organism}} = B\text{max} \times [M]\text{exposure}/K\text{metal} + [M]\text{exposure} \quad (2)$$

Biodynamic modelling assumes that net bioaccumulation of a metal at steady state (C_{ss}) in an organism can be described as:

$$C_{ss} = ((C_w \times k_u)/ k_{ew})) + ((AE \times IR \times C_f)/ (k_{ef})) \quad (3)$$

where k_{uw}, uptake rate constant from water (L g^{-1} day^{-1}); C_w, concentration in water (mg $L^{!1}$); AE, assimilation efficiency (%); IR, ingestion rate (g food g^{-1} day^{-1}); C_f, metal concentration in food (mg g^{-1}); k_{ew}, rate constant of loss after uptake from water (day^{-1}); k_{ef}, rate constant of loss after uptake from food (day^{-1}); and g, growth rate constant (day^{-1}).

Parameters were incorporated into the model to determine the relative importance of waterborne and dietary uptake routes, and predict the steady-state concentrations of Ag in daphnids. Waterborne parameters (k_{uw} and k_{ew}) were determined in a previous study by Khan et al.[7] Ranges of dissolved Ag[33] and Ag concentrations in phytoplankton[34,35] reported in the literature were considered when attempting to validate the models. Given that it is not possible to determine concentrations of Ag

NPs in the environment, we predicted the concentrations of Ag NPs in water and food using the estimation by Gottschalk et al.,[36] in which 25% of the total Ag released is in nanoparticles. The growth rate constant determined by Guan and Wang[37] and IR applied by Zhao and Wang[8] were used in the model.

Statistical analysis

All data were checked for normality of distribution (Kolmogorov-Smirnov test) and homogeneity of variances (Levene's test). Regression analyses followed by analysis of covariance (ANCOVA) were used to establish significant differences between uptake rate constants. Analysis of variance (ANOVA) was used for all other analyses. ANCOVA and ANOVA were followed by Tukey's honestly significant difference (HSD) *post hoc* tests for *a posteriori* comparisons using STATISTICA (*Statsoft*, version 4, Tulsa, OK, USA). Percentage data were arcsine-transformed before statistical analysis to ensure compliance with the tests' assumptions.

Paper B: Results

Characterisation of Ag NPs

The physicochemical characteristics of the pristine Ag NPs have been previously reported.[38] Briefly, all Ag NPs had a core size of ,10–11 nm. The hydrodynamic diameters (HDD) of nanoparticles suspended in Milli-Q water were 22.0 nm for PEG-Ag NPs and Cit-Ag NPs. and 28.3 nm for PVP-Ag NPs.[38] The mean zeta-potentials in

Milli-Q water of the Ag NPs were -31.5, -21.0 and -31.6 mV for PVP-Ag NPs, PEG-Ag NPs and Cit-Ag NPs respectively.

The hydrodynamic diameters of the Ag NPs over the course of 3 days in the algal medium as measured by DLS were in a range of 23–54, 46–97 and 15–35 nm for PVP-coated, PEG coated and Cit-coated NPs respectively. Particle size analysis showed a high polydispersity index (0.5) for each particle type, suggesting that DLS may not be suitable for particle size estimation. Qualitatively, the TEM images showed particle size ranges of ,15 to 20 nm (PVP-Ag), 10 to 50 nm (PEG-Ag) and 20 to 30 nm (Cit-Ag) after 72 h of incubation (Fig. S1). The average zeta potentials (± s.e.) of the Ag NPs in JM for up to 3 days were -11.3 ± 0.9 mV (PVP-Ag), -10.8 ± 1.1 mV (PEG-Ag) and -23.2 ± 1.0 mV (Cit-Ag), indicating moderate NP stability in the algal medium. Changes in particle sizes or zeta potentials measured by DLS over a period of 3 days did not follow any specific or significant trend (ANOVA, p = 0.05) (Fig. S2). The mean percentage of dissolved Ag in the algal medium (± s.e.) after 4 h was lowest for Cit-Ag (1.2 ± 0.0%), followed by PVP-Ag (4.3 ± 0.6%) and highest for PEG-Ag (12.4 ± 0.2%).

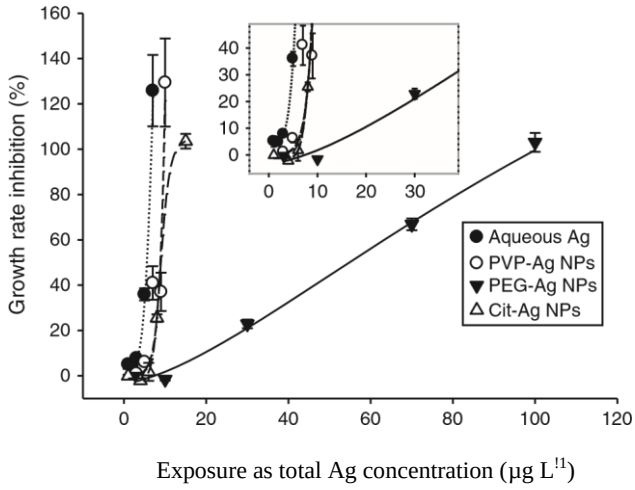

Fig. 1. Growth inhibition of *Chlorella vulgaris* after 72 h of exposure to aqueous Ag and Ag nanoparticles (NPs) (mean ± s.d., n = 3).

Toxicity of aqueous Ag and Ag NPs to Chlorella vulgaris

The acute toxicity of aqueous Ag and Ag NPs to *C. vulgaris* is shown in Fig. 1. Inhibitory effects of dissolved and nanosized silver were observed after 72 h, with higher inhibitory response in the case of dissolved silver (IC_{50} of 5.3 ± 0.5 mg L^{-1}). PVPand citrate-coated Ag NPs exhibited very similar toxicity (IC_{50} values of 9.3 ± 0.1

and 9.2 ± 1.0 mg L^{-1} respectively), whereas PEG-coated Ag NP exhibited the lowest toxicity to the algae (IC_{50} of 49.3 ± 5.2 mg L^{-1}). Exposure concentrations causing growth inhibition of more than 100% indicated lethality of the algae. Statistical comparison of the 72-h IC_{50}s revealed significant differences (ANOVA, p = 0.05) between aqueous Ag and PEG-coated Ag NP and both differed significantly from PVPand citrate-coated Ag NPs.

Uptake of Ag in C. vulgaris

A linear relationship was observed between the uptake rate of Ag by *C.vulgaris* and thelower range ofexposureconcentration after 72 h (Fig. 2). The silver uptake rate constant from solution (k_u ± s.e.) described by the slope of the best-fit regression between the uptake rate and exposure concentration was greatest for aqueous Ag (1.701 ± 0.406 L g^{-1} day^{-1}), suggesting that aqueous silver was the most bioavailable form to the algae. In the case of Ag NP exposures, the uptake rate constants were similar for PVP-Ag NP (0.233 ± 0.024 L g^{-1} day^{-1}) and Cit-Ag NP (0.246 ± 0.031 L g^{-1} day^{-1}) and higher for PEG-Ag NP (0.339 ± 0.020 L g^{-1} day^{-1}) (ANCOVA, p = 0.05).

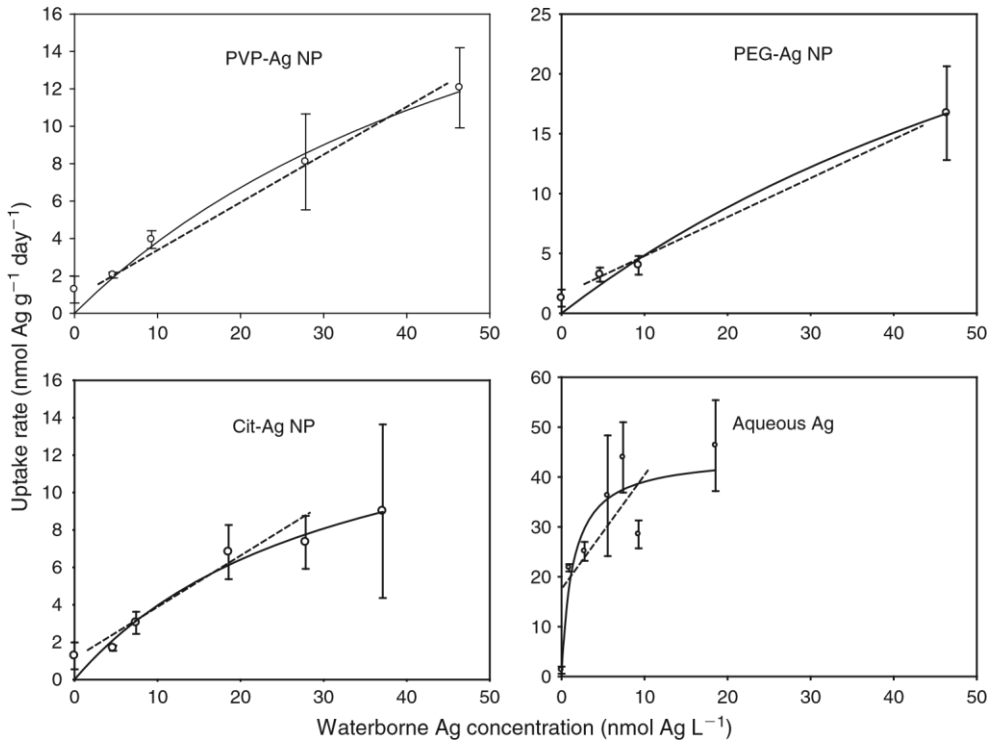

Fig. 2. Ag uptake rates (nmol $g^{-1}day^{-1}$ ± s.d.) in *Chlorella vulgaris* after waterborne exposures to aqueous Ag and Ag nanoparticles (NPs) (*n* = 3). Linear regression (dashed line) was used to determine the uptake rate constants. Non-linear regression (Michaelis–Menten) fits were used to derive membrane transport characteristics.

Ligand binding constants showed that Cit-Ag NP had the lowest binding capacity (B_{max} ± s.e.) of 17 ± 5 nmol g^{-1}, followed by PVP-Ag NP (28 ± 13 nmol g^{-1}) and aqueous Ag (44 ± 4 nmol g^{l1}) and PEG-Ag NP (51 ± 33 nmol g^{-1}). The K_d (transporter affinity) for Ag form and Ag NP were 1.4 ± 0.6, 32 ± 18, 64 ± 46 and 95 ± 89 nmol L^{-1} for aqueous Ag, Cit-Ag NP, PVP-Ag NP and PEG-Ag NP respectively. The binding site affinity constant (log *K* ± s.e.) was highest for aqueous Ag (8.86 ± 0.27), followed by Cit-Ag NP (7.49 ± 0.35), PVP-Ag NP (7.19 ± 0.55) and PEG-Ag NPs (7.02 ± 1.20).

TEM images of control and silver-exposed algal cells are shown in Fig. 3. Ag NPs were not observed in thecontrol cells or in the cells exposed to low Ag NP concentrations (,IC_{50}) for 72 h. PVP- and PEG-coated Ag NPs were, however, visualised in the algae cells exposed at 2 mg L^{-1} for 4 h. The presence of these Ag NPs in the cells was further confirmed by EDX spectrum analysis.

Dietborne Ag uptake and subsequent elimination by Daphnia magna

For dietborne exposures, the accumulated Ag concentrations in algae were 1200–3300 mg g^{-1} dry weight. The measured initial Ag body burden (102 ± 28, 128 ± 23, 124 ± 13 and 107 ± 5 mg g^{-1} for aqueous Ag, PVP-, PEG- and Cit-Ag NPs respectively) in the daphnids indicated that Ag was bioavailable to *D. magna* from the algal diet for all forms. The percentage retention of Ag (mean ± s.e.) by the daphnids feeding on algae that had been exposed to either the different Ag NPs or aqueous Ag (added as $AgNO_3$) is presented in Fig. 4. Daphnids initially eliminated ,78–88% of the total Ag depurated from dissolved or Ag NPs during the first 6 h of depuration, followed by a slow excretion thereafter with k_{ef} ranging between 0.279 and 0.591 day^{-1} (Fig. 4). *D. magna* apparently assimilated less Ag from the $AgNO_3$-exposed algae (10.3 ± 0.9%) than from the PVP-, PEG- and Cit-Ag NP-exposed diets (24.5 ± 3.6, 20.2 ± 1.9, 19.6 ± 1.1% for PVP-, PEG- and Cit-Ag NPs respectively).

Ag assimilated from algae exposed to PEG- and PVP-Ag NP was eliminated by daphnids with efflux rate constants (k_{ef}, mean ± s.e.) of 0.279 ± 0.022 and 0.321 ± 0.074 day^{-1}, corresponding to biological half-lives of 2.5 and 2.2 days respectively. Retention of Ag after uptake from diet containing $AgNO_3$ or Cit-Ag NP was significantly lower, with k_{ef} values of 0.529 ± 0.109 and 0.591 ± 0.043 day^{-1} respectively, and corresponded to retention half-lives of 1.3 and 1.1 days. BMF were calculated as 0.0013 (PVP-Ag NP), 0.0016 (PEG-Ag NP), 0.0004 (Cit-Ag NP) and 0.0005 (aqueous Ag).

Determining the importance of dietary and waterborne uptake

Model-predicted Ag concentrations in *D. magna* are presented in Table 1. Different scenarios were tested by applying ranges of dissolved Ag (C_w) and Ag concentrations in algae (C_f), in other words, varying one parameter (C_w or C_f) while all others are kept constant to see how the chosen ranges modify the relative contribution of water and food to the total Ag accumulation as well as the prediction. Incorporating the mean and ranges of biodynamic parameters developed for *D. magna*, the model shows that food is the dominant pathway of Ag uptake in the cases of Ag NPs (56–99%). For aqueous Ag (i.e. added as $AgNO_3$), water becomes the major source in the overall accumulation (60–85%) when Ag concentration in food decreases from 1.5 to 0.075 mg g^{-1}. The choices of growth rate constant and ingestion rate were based on previous studies for the same species under similar conditions. The effects of change in these constants over a range typically found in the literature on the predicted Ag concentrations in *D. magna*

are shown in Fig. S3 for completeness and shows the robustness of the biodynamic model as conclusions remain the same.

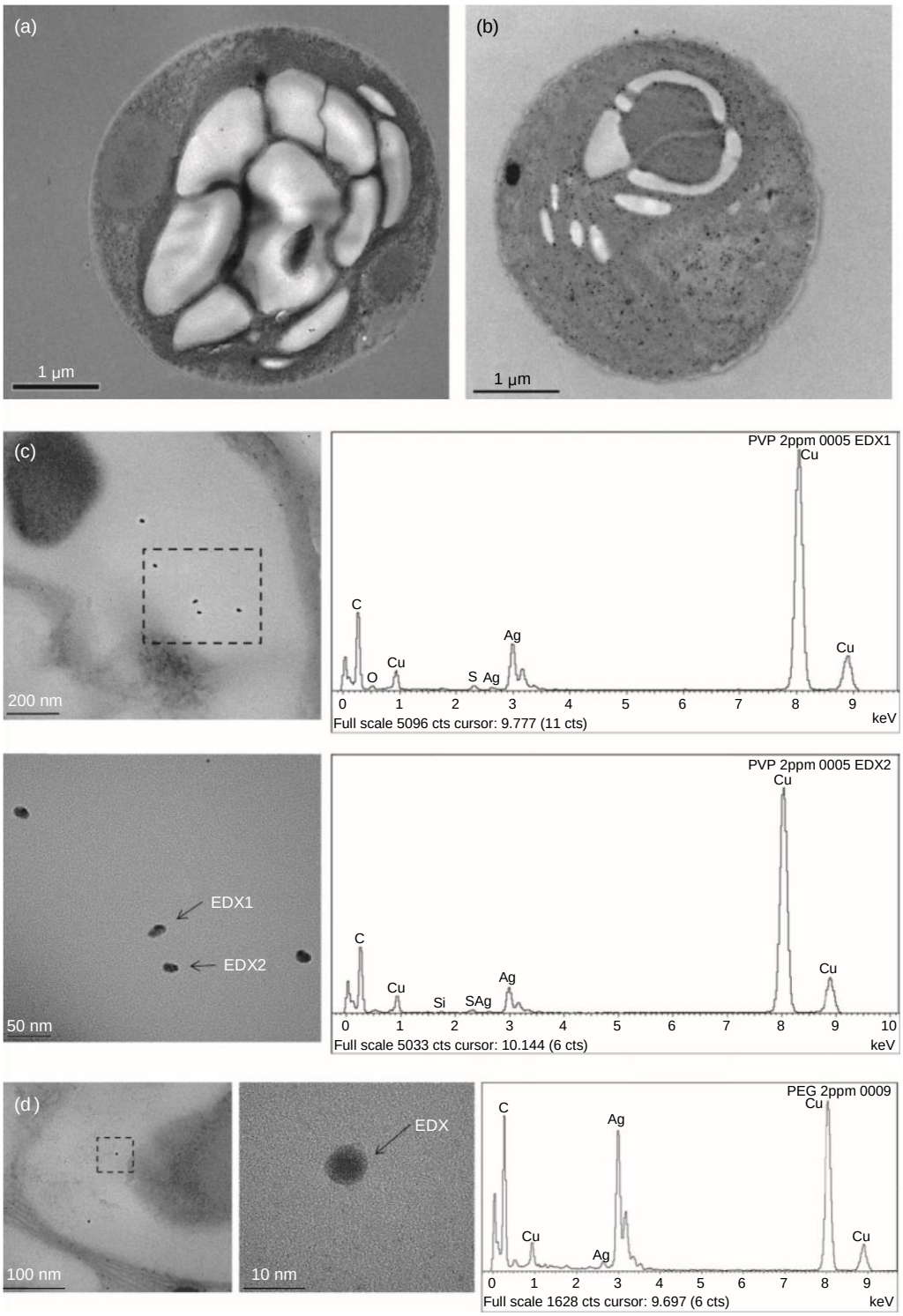

Fig. 3. Transmission electron microscopy (TEM) observations of ultrathin slices of *Chlorella vulgaris* after exposure to Ag nanoparticles (NPs): (a) control; (b) exposed to 0.007 mg L^{-1} Cit-AgNP for 72 h; (c) exposed to 2 mg L^{-1} PVP-Ag NP for 4 h; (d) exposed to 2 mg L^{-1} PEG-Ag NP for 4 h. Energy-dispersive X-ray (EDX) spectra show Ag peaks for PVP-Ag NP (c), and PEG-Ag NP (d) exposed algae, which are seen as electron-dense dark spots (arrows).

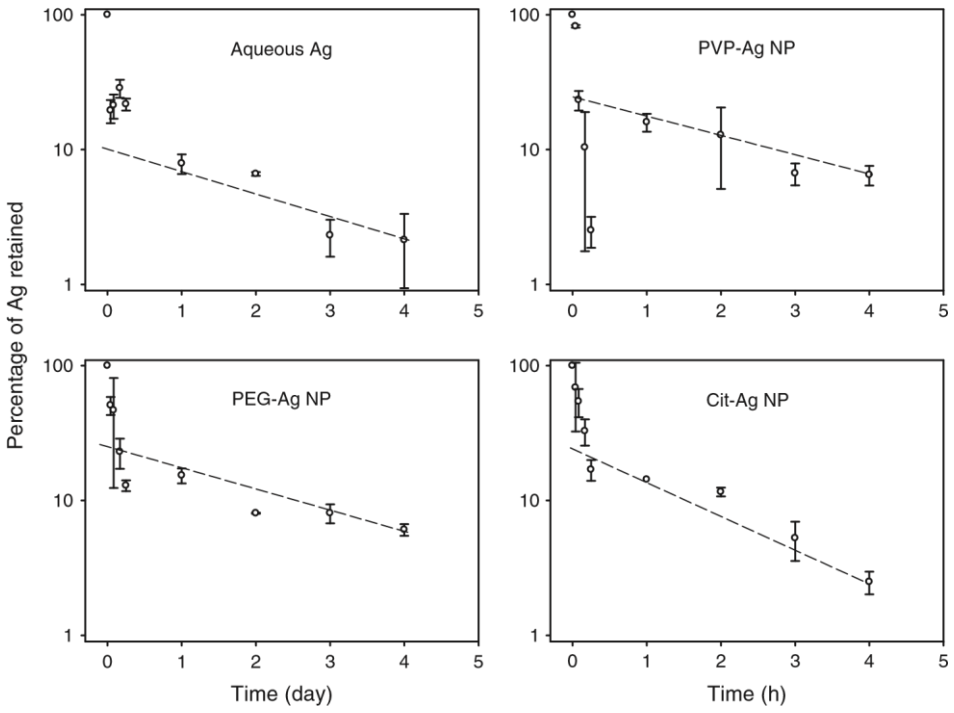

Fig. 4. Percentage of Ag retained in *Daphnia magna* after uptake from ingested Ag-contaminated algae. Data are mean ± s.e.

Table 1. Selected model-predicted silver concentrations in Daphnia magna (C_{ss} predicted) k_{uw} (6.240, 1.653, 0.264 and 0.871 L $g^{-1}day^{-1}$ for aqueous Ag, PVP-, PEG- and Cit-Ag NPs respectively) and K_{ew} (0.607, 0.274, 0.464 and 0.505 day^{-1} for aqueous Ag, PVP-, PEG- and Cit-Ag NPs respectively) from Khan et al.,[32] 0.08 day^{-1},[39] IR = 0.91 g $g^{-1}day^{-1}$.[7] AE (10.3, 24.5, 20.2 and 19.6% for aqueous Ag, PVP-, PEG- and Cit-Ag NPs respectively) and K_{ef} (0.529,0.321,0.279 and 0.591 day^{-1} for aqueous Ag, PVP-, PEG- and Cit-Ag NPs respectively) from the present study. Ranges of dissolved Ag (C_w) and Ag concentrations in food (C_f) were used to estimate the relative contribution of water (C_{ss} water) and food (C_{ss} food) to the overall Ag accumulation at steady state (C_{ss} predicted). See *Experimental methods* for more details

C_w (mg L^{-1})	C_f (mg g^{-1})	C_{ss} water (%)	C_{ss} food (%)	C_{ss} predicted (mg g^{-1})
Aqueous Ag				
0.0020	0.075	60.3	39.7	0.03
0.0020	1.5	7.0	93.9	0.25
0.0072	0.075	84.8	15.2	0.08
0.0072	1.5	21.9	78.1	0.30
PVP-Ag NP				
0.0007	0.025	18.1	81.9	0.02
0.0007	0.5	1.1	98.9	0.29
0.0024	0.025	44.9	55.1	0.03
0.0024	0.5	3.9	96.1	0.30
PEG-Ag NP				
0.0007	0.025	2.4	97.6	0.01
0.0007	0.5	0.1	99.9	0.27
0.0024	0.025	8.2	91.8	0.01
0.0024	0.5	0.4	99.6	0.27
Cit-Ag NP				
0.0007	0.025	12.6	87.4	0.01
0.0007	0.5	0.7	99.3	0.14
0.0024	0.025	34.8	65.2	0.01
0.0024	0.5	2.6	97.4	0.14

Paper B: Discussion

In the present study, we modelled transfer of different Ag NPs and aqueous Ag in a simple freshwater food chain. The biodynamic approach was used to determine the accumulation dynamics of each Ag form to the algal food source and then used to investigate the dietary transfer of Ag to *D. magna*. By parameterising the model with the results in the present study and those that previously determined the waterborne accumulation dynamics for the same set of NPs in *D.magna*,[7] we were able to assess the relative importance of both uptake routes.

Ag uptake and toxicity to C. vulgaris

The intracellular uptake of Ag NPs has been observed in the freshwater alga *Ochromonas danica* by Miao et al.[39]; however, it is unclear whether growth was inhibited by Ag NPs inside the cells directly or indirectly (by the release of Ag^{+} internally).

Table2. *Chlorella vulgaris*. Summary of biodynamic parameters (ku, uptake rate constant; mean ± s.e.),metal binding characteristics (Bmax, binding site density; Kd transporter affinity; log K, strength of binding; mean ± s.e.), growth inhibition (IC50, concentration required to cause a 50% inhibition; mean ± s.d.) and particle dissolution (mean ± s.e.) PVP, polyvinyl pyrrolidone; PEG, polyethylene glycol; cit, citrate; NP, nanoparticle

	Aqueous Ag	PVP-Ag NP	PEG-Ag NP	Cit-Ag NP
*k*u (L g^{-1} day^{-1})	1.701 ± 0.406	0.233 ± 0.024	0.339 ± 0.020	0.246 ± 0.031
Bmax (nmol g^{-1})	44 ± 4	28 ± 13	51 ± 33	17 ± 5
K_d (nmol L^{-1})	1.4 ± 0.6	64 ± 46	95 ± 89	32 ± 18
log *K*	8.86$0 ±.27	7.19 ± 0.55	7.02 ± 1.20	7.49 ± 0.35
IC50 (mg L^{-1})	5.3 ± 0.5	9.3 ± 0.1	49.3 ± 5.2	9.2 ± 1.0
Dissolution (%)	–	4.3 ± 0.6	12.4 ± 0.2	1.2 ± 0.0

Internalisation of NPs in *O. danica* was observed by TEM in cells from treatments with no obvious toxic effects. Despite carrying out specific membrane permeability assessments, the authors excluded the possibility that the increase of cell membrane permeability resulted in a passive uptake of NPs. However, polymer-coated CuO NPs (with an average size of 65 nm) were able to penetrate the cell of *Chlamydomonas reinhardtii* in particulate form after 6 h of exposure as observed by Perreault et al.[40] Internalisation of CuO NPs (~5 nm) was also revealed in the prokaryotic alga *Microcystis aeruginosa* by Wang et al.,[41] with no increase in membrane permeability observed during 24-h exposure, the time during which internalisation could have taken place. However, given that algal cell walls are often porous in their structure (usually between 5 and 20 nm), and their permeability changes during mitosis, NPs less than 20 nm in size may pass freely through the cell wall. Moreover, NPs may induce the formation of larger new pores permeable to bigger NPs,[42] which could be the case in the present study. It is important to note that no NPs were revealed by TEM in *Chlorella vulgaris* after 72 h at low exposure concentrations (IC_{50}). When cells were exposed to 200 or 285 times higher concentrations of Ag NPs, intracellular uptake was observed after 4 h of exposure. Thus, there is a possibility that such a high concentration of Ag NPs may lead to an increase in membrane permeability and subsequent internalisation of NPs. Increases in cell membrane permeability have been shown across many phyla. [43–47]

Inthepresentstudy, Ag NPs werelocalised in starch granules within the chloroplast of *C. vulgaris* as shown by TEM images, suggesting that granules may act as a storage site for NPs in this alga. Zhou et al.[48] found an increased number of starch granules in *Chlorella pyrenoidosa* after exposure to dissolved zinc and copper; this is likely a defence mechanism against such ionic metals and is likely used to sequester these toxicants. Another possible mechanism that can protect microorganisms against metal toxicity is the secretion of exopolymeric substances (EPS). The external surface of *C. vulgaris* contains EPS, proteins and carbohydrates, which facilitate the binding of metal ions.[49] Miao et al.,[50] for instance, found a higher $Ag^{þ}$ tolerance due to the secretion of EPS by the marine diatom *Thalassiosira weissflogii*, suggesting that EPS may provide binding ligands for toxicants released from NPs.

In regards to uptake, dissolved Ag exposures resulted in the highest k_u values. In comparison with the Ag NPs, the aqueous Ag uptake rate constant was, 4–7 times higher and aqueous Ag toxicity was 2–10 times greater. Higher uptake rate constants of

aqueous Ag in comparison with Ag NPs corroborates the current literature.[7,51] Thus, it can be concluded that dissolved Ag is the most bioavailable form to the algae. For the Ag NPs, both PVP-Ag NPs and Cit-Ag NPs showed similar uptake rates, which corresponded to the similar toxicity and bioavailability of these Ag NPs. In other aquatic species, it has been shown that the Ag uptake rate constant of particulate (i.e. Ag NP and food-bound Ag)[6,7] and dissolved Ag can be directly linked to toxicity. These studies show that uptake rate constants may be used to reliably predict organism toxicity across many aquatic species. A further advantage of this approach (i.e. using uptake rate constantsto predict toxicity)is that uptake rate constantsare not biased towards the route of uptake. Therefore, the burden of the toxicant from ingested food and through a biological ligand as is the case with dissolved metal, is accounted for. However, although PVP-Ag NPs and Cit-Ag NPs conformed to such a relationship, PEG-Ag NPs showed the most rapid uptake rate constant of all Ag NPs, yet the lowest toxicity. PEG- and PVPcoated Ag NPs did not reach maximal Ag saturation at any studied concentration; thus, it is likely inappropriate to determine any relationships between the derived membrane transport parameters (B_{max}, K_d and log K) and toxicity. Cit-Ag NP dissolution was more than four times lower than that of PVP-Ag NPs and PEG-AgNPs, suggesting that dissolved Ag from Ag NPs is not the only Ag form that may interact with or be bioavailable to the algae (Table 2). Therefore, toxicity does not seem to relate entirely to the dissolved Ag NP fraction but more likely the specific interactions between both dissolved Ag (from the Ag NPs) and the Ag NPs (and inherent physicochemical characteristics in the medium) themselves. However, given that solubility studies were carried out at higher total Ag concentration compared with those of the exposure, results cannot be directly extrapolated to the lower exposure concentrations.[7,52]

D. magna *biodynamic modelling*

D. magna assimilated Ag (presented to the daphnids in the form of Ag-exposed algae) from ingested dietary Ag NPs more efficiency than aqueous Ag ($AgNO_3$). These results are similar to other studies using the same species.[8,31] However, this is in opposition to Croteau et al.,[9] who showed higher assimilation of foodborne $AgNO_3$ in *Lymnaea stagnalis* fed Ag-spiked diatoms. Several factors have been shown to influence the assimilation efficiency of contaminants from ingested food, including the food quantity and quality, digestive physiology of the animals and behaviour of the contaminants in the animal's gut.[53] Although the AE of Ag is highly dependent on the algal cell density

and Ag concentration in the diet,[31] our data are comparable with those reported in the literature.[2] Significant differences between efflux rate constants in the present study indicate possible different metabolic pathways for the different types of particle coatings. Complete depuration of Ag NPs from daphnids was not obtained within 96 h indicating that Ag NPs can be passed on through trophic transfer. If Ag NPs were to reside within the gut for extended periods of time, this might result in feeding depression, which has been shown to be caused by Ag NPs.[54] The impairment of feeding can directly affect growth and reproduction of the individual, which may have consequences at the population level.[55,56]

Biodynamic modelling was applied to determine the routes of aqueous Ag and Ag NPs uptake in *D. magna* (i.e. food and water), and to predict the accumulated concentrations of Ag in the daphnids. Different scenarios tested show that food is the major source of accumulated Ag in *D. magna* in the cases of Ag NPs. This is consistent with results previously recorded for *D. magna*[8] and for *L. stagnalis*.[9] Predominance of a dissolved source of Ag in daphnids reported by Lam and Wang[31] was explained by the quite low dietary AE accompanied by high k_u; however, the authors noted a strong dependency of AE on food concentration. Taking into account the relevant pathways of metal uptake can improve predictions of metal bioaccumulation in an organism. Nevertheless, defining the relative contribution of metals to the overall steady-state body burden may allow simplification of model, particularly when one uptake route prevails.[6] Our model-predicted accumulated steady-state concentrations of Ag ranged from 0.01 to 0.30 mg g^{-1} (dry weight). These levels are below levels of Ag NP accumulation reported to cause acute toxicity for other species. For example, Zhao and Wang[57] using the same species investigated 48-h 50% lethal concentrations and 48-h bioaccumulation of Ag NPs. The authors noted that at high exposure concentration (200 mg L^{-1}) and despite the high accumulated Ag concentrations in daphnids (475–6618 mg g^{-1} dry weight), no signs of toxicity were observed. Thus, current levels of Ag within the environment may not lead to adverse effect on *D. magna*, a highly sensitive organism within freshwater aquatic biota. However, using parameters such as body burdens to predict toxicity may be ill-advised for those species that ingest a large portion of Ag NPs, such as *D. magna*.[7] In the present study, there was no appreciable Ag biomagnification by the daphnids (BMF,1); however, this route of exposure is still important within the environment.

Paper B: Conclusions

Aqueous Ag was more toxic than Ag NPs to *Chlorella vulgaris*. The internalisation of PVP- and PEG-Ag NPs into the algal cells seemed to occur only at high exposure concentration, probably owing to increased membrane permeability. In general, the uptake rate constants (k_u) derived for the algae correlated well with toxicity. According to the dissolution studies, Ag released by the Ag NPs did not wholly account for toxicity. When Ag-exposed algae were fed to the next trophic level, *Daphnia magna* assimilated Ag from ingested algae for all forms of Ag. However, Ag NPs were assimilated more efficiently than aqueous Ag. Moreover, Ag NPs were not eliminated completely from daphnids over the depuration period, which may lead to further possible transport of Ag NPs along the food chain. Testing different scenarios (minimum and maximum Ag concentrations in the water and food), the model showed that for Ag NPs, food is the dominant pathway of Ag uptake in *D. magna*. When the concentration of Ag in food is low, water becomes the major route of Ag uptake in the case of aqueous Ag.

Paper B: Author contributions

J. Kalman and K. B. Paul are joint first authors and conducted the experiments. All authors contributed to the design of the experiment, discussed the results and commented on the manuscript.

Paper B: Acknowledgements

This study was financially supported by the US Environmental Protection Agency–UK Natural Environment Research Council nanoBEE project. The authors thank Birmingham University for the Ag NPs, Steve Mitchell (University of Edinburgh) for TEM sample preparation and Dr Mike Ward (University of Leeds) for the TEM images and EDX analysis (sponsored by a Biotechnology and Biological Sciences Research Council grant).

Paper B: References

[1] T. M. Benn, P. Westerhoff, Nanoparticle silver released into water from commercially available sock fabrics. *Environ. Sci. Technol.* **2008**, *42*, 4133. doi:10.1021/ES7032718

[2] C. M. Zhao, W. X. Wang, Comparisonof acute and chronic toxicity of silver nanoparticles and silver nitrate to *Daphnia magna*. *Environ. Toxicol. Chem.* **2011**, *30*, 885. doi:10.1002/ETC.451

[3] S. W. P. Wijnhoven, W. J. G. M. Peijnenburg, C. A. Herberts, W. I. Hagens, A. G. Oomen, E. H. W. Heugens, B. Roszek, J. Bisschops, I. Gosens, D. Van de Meent, S. Dekkers, W. H. De Jong, M. Van Zijverden, A. J. A. M. Sips, R. E. Geertsma, Nanosilver – a review of available data and knowledge gaps in human and environmental risk assessment. *Nanotoxicology* **2009**, *3*, 109. doi:10.1080/17435390902725914

[4] A. Tessier, D. R. Turner, *Metal Speciation and Bioavailability in Aquatic Systems* **1995** (Wiley: Chichester, UK).

[5] S. N. Luoma, P. S. Rainbow, Why is metal bioaccumulation so variable? Biodynamics as a unifying concept. *Environ. Sci. Technol.* **2005**, *39*, 1921. doi:10.1021/ES048947E

[6] M. N. Croteau, S. N. Luoma, Predicting dietborne metal toxicity from metal influxes. *Environ. Sci. Technol.* **2009**, *43*, 4915. doi:10.1021/ ES9007454

[7] F.R.Khan,K.B.Paul, A.D.Dyboswka,E.Valsami-Jones,J. R.Lead, V. Stone, T. F. Fernandes, Accumulation dynamics and acute toxicity ofsilvernanoparticlesto*Daphniamagna*and*Lumbriculusvariegatus*: implications for metal modelling approaches. *Environ. Sci. Technol.* **2015**, *49*, 4389. doi:10.1021/ES506124X

[8] C. M. Zhao, W. X. Wang, Biokinetic uptake and efflux of silver nanoparticles in *Daphnia magna*. *Environ. Sci. Technol.* **2010**, *44*, 7699. doi:10.1021/ES101484S

[9] M. N. Croteau, S. K. Misra, S. N. Luoma, E. Valsami-Jones, Silver bioaccumulation dynamics in a freshwater invertebrate after aqueous and dietary exposures to nanosized and ionic Ag. *Environ. Sci. Technol.* **2011**, *45*, 6600. doi:10.1021/ES200880C

[10] F. R. Khan, S. K. Misra, J. Garc´ıa-Alonso, B. D. Smith, S. Strekopytov, P. S. Rainbow, S. N. Luoma, E. Valsami-Jones, Bioaccumulation dynamicsand modelling inanestuarineinvertebratefollowing aqueous exposure to nanosized and dissolved silver. *Environ. Sci. Technol.* **2012**, *46*, 7621. doi:10.1021/ES301253S

[11] L.Dai, K.Syberg,G. T.Banta, H.Selck, V.E.Forbes, Effects,uptake, and depuration kinetics of silver oxide and copper oxide nanoparticles in a marine deposit feeder, *Macoma balthica*. *ACS Sustain. Chem.& Eng.* **2013**, *1*, 760.

[12] N.R.Bury,J. Shaw,C.Glover,C.Hogstrand, Derivationof atoxicitybased model to predict how water chemistry influences silver toxicity to invertebrates. *Comp. Biochem. Phys. C* **2002**, *133*, 259.

[13] K. A. C. de Schamphelaere, C. R. Janssen, A biotic ligand model predicting acute copper toxicity for *Daphnia magna*: the effects of calcium, magnesium, sodium, potassium, and pH. *Environ. Sci. Technol.* **2002**, *36*, 48. doi:10.1021/ES000253S

[14] E. M. Leonard, C. M. Wood, Acute toxicity, critical body residues, Michaelis–Menten analysis of bioaccumulation, and ionoregulatory disturbance in response to waterborne nickel in four invertebrates:
Chironomus riparius, *Lymnaea stagnalis*, *Lumbriculus variegatus* and *Daphnia pulex*. *Comp. Biochem. Phys. C* **2013**, *158*, 10.

[15] K. M. Newton, H. L. Puppala, C. L. Kitchens, V. L. Colvin, S. J. Klaine, Silver nanoparticle toxicity to *Daphnia magna* is a function of dissolved silver concentration. *Environ. Chem.* **2013**, *32*, 2356. doi:10.1002/ETC.2300

[16] A. Oukarroum, S. Bras, F. Perreault, R. Popovic, Inhibitory effects of silver nanoparticles in two green algae, *Chlorella vulgaris* and *Dunaliella tertiolecta*. *Ecotoxicol. Environ. Saf.* **2012**, *78*, 80. doi:10.1016/J.ECOENV.2011.11.012

[17] M.Tuominen,E.Schultz,Toxicityandstabilityofsilvernanoparticles tothegreenalga*Pseudokirchneriellasubcapitata*inborealfreshwater samples and growth media. *Nanomaterials Environ.* **2013**, *1*, 48. doi:10.2478/NANOME-2013-0004

[18] B. M. Angel, G. E. Batley, C. V. Jarolimek, N. J. Rogers, The impact of size on the fate and toxicity of nanoparticulate silver in aquatic systems.*Chemosphere***2013**,*93*,359.doi:10.1016/J.CHEMOSPHERE. 2013.04.096

[19] F. Ribeiro, J. A. Gallego-Urrea, K. Jurkschat, A. Crossley, M. Hassello¨v, C. Taylor, A. M. V. M. Soares, S. Loureiro, Silver nanoparticles and silver nitrate induce high toxicity *to Pseudokirchneriella subcapitata*, *Daphnia magna* and *Danio rerio*. *Sci. Total Environ.* **2014**, *466–467*, 232. doi:10.1016/J.SCITOTENV.2013.06.101 [20] F. R. Khan, K. Schmuecking, S. H. Krishnadasan, D. Berhanu, B. D. Smith, J. C. DeMello, P. S. Rainbow, S. N. Luoma, E. Valsami-Jones, Dietary bioavailability of cadmium presented to the gastropod *Peringia ulvae* as quantum dots and in ionic form.*Environ.Toxicol.Chem.* **2013**, *32*, 2629.

[21] C. M. Levard, B. C. Reinsch, F. M. Michel, C. Oumahi, G. V. Lowry, G.E.Brown,Sulfidation processes of PVP-coated silver nanoparticles in aqueous solution: impact on dissolution rate. *Environ. Sci. Technol.* **2011**, *45*, 5260. doi:10.1021/ES2007758

[22] C. Levard, E. M. Hotze, G. V. Lowry, G. E. Brown, Environmental transformations of silver nanoparticles: impact on stability and toxicity. *Environ. Sci. Technol.* **2012**, *46*, 6900. doi:10.1021/ ES2037405

[23] G. V. Lowry, K. B. Gregory, S. C. Apte, J. R. Lead, Transformations of nanomaterials in the environment. *Environ. Sci. Technol.* **2012**, *46*, 6893. doi:10.1021/ES300839E

[24] N.von Moos, P.Bowen,V.I. Slaveykova, Bioavailability of inorganic nanoparticles to planktonic bacteria and aquatic microalgae in freshwater. *Environ. Sci. Nano* **2014**, *1*, 214. doi:10.1039/C3EN00054K

[25] S. N. Luoma, P. S. Rainbow, *Metal Contamination in Aquatic Environments: Science and Lateral management* **2008** (Cambridge University Press: Cambridge, UK).

[26] *JM (Jaworski's Medium*). *Freshwater algae* **2015** (CCAP (Culture Collection of Algae and Protozoa), Dunstaffnage Marine Laboratory: Oban, Argyll, UK) Available at http://www.ccap.ac.uk/media/ documents/JM.pdf [Verified 20 July 2015].

[27] A. J. Kennedy, M. S. Hull, A. J. Bednar, J. D. Goss, J. C. Gunter, J.L.Bouldin,P.J.Vikesland,J.A.Steevens,Fractionatingnanosilver: importance for determining toxicity to aquatic test organisms. *Environ. Sci. Technol.* **2010**, *44*, 9571. doi:10.1021/ES1025382

[28] M. N. Croteau, A. D. Dybowska, S. N., luoma, S. K., Misra, E., Valsami-Jones, Isotopically modified nanoparticles to assess nanosilver bioavailability and toxicity at environmentally relevant exposures. *Environ. Chem.* **2014**, *11*, 247. doi:10.1071/EN13141

[29] *Test number 202. OECD Guidelines for the Testing of Chemicals, Section 2* **2004** (OECD Publishing: Paris). doi:10.1787/ 9789264069947-EN

[30] *Test number 201: Freshwater Alga and Cyanobacteria, Growth Inhibition Test, OECD Guidelines for the Testing of Chemicals, Section 2* **2011** (OECD Publishing: Paris). doi:10.1787/9789264069923-EN

[31] I. K. S. Lam, W. X. Wang, Accumulation and elimination of aqueous and dietary silver in *Daphnia magna*. *Chemosphere* **2006**, *64*, 26. doi:10.1016/J.CHEMOSPHERE.2005.12.023

[32] S. Niyogi, C. Wood, Biotic ligand model, a flexible tool for developing site-specific water quality guidelines for metals. *Environ. Sci. Technol.* **2004**, *38*, 6177. doi:10.1021/ES0496524

[33] G. J. Smith, A. R. Flegal, Silver in San Francisco Bay waters. *Estuaries* **1993**, *16*, 547. doi:10.2307/1352602

[34] R. Eisler, *Silver Hazards to Fish, Wildlife and Invertebrates: A Synoptic Review. US National Biological Service, Biological Science Report 32* **1981** (US Department of the Interior: Washington, DC).

[35] J. H. Martin, G. A. Knauer, The elemental composition of plankton. *Geochim. Cosmochim. Acta* **1973**, *37*, 1639. doi:10.1016/0016-7037 (73)90154-3

[36] F. Gottschalk, T. Sonderer, B. Nowack, Modelled environmental concentrations of engineered nanomaterials (TiO_2, ZnO, Ag, CNT, fullerenes) for different regions. *Environ. Sci. Technol.* **2009**, *43*, 9216. doi:10.1021/ES9015553

[37] R. Guan, W. X. Wang, Multiphase biokinetic modelling of cadmium accumulation in *Daphnia magna* from dietary and aqueous sources. *Environ. Toxicol. Chem.* **2006**, *25*, 2840. doi:10.1897/ 06-101R.1

[38] M. Tejamaya, I. Ro¨mer, R. C. Merrifield, J. R. Lead, Stability of citrate-, PVP-, and PEG-coated silver nanoparticles in ecotoxicology media. *Environ. Sci. Technol.* **2012**, *46*, 7011. doi:10.1021/ ES2038596

[39] A. J. Miao, Z. Luo, C. S. Chen, W. C. Chin, P. H. Santschi, A. Quigg, Intracellular uptake: a possible mechanism for silver engineered nanoparticle toxicity to a freshwater alga *Ochromonas danica*. *PLoS One* **2010**, *5*, e15196. doi:10.1371/JOURNAL.PONE.0015196 [40] F. Perreault, A. Oukarroum, S. Pedroso-Melegari, W. G. Matias, R. Popovic, Polymer coating of copper oxide nanoparticles increases nanoparticles uptake and toxicity in the green alga *Chlamydomonas reinhardtii*. *Chemosphere* **2012**, *87*, 1388. doi:10.1016/J.CHEMOSPHERE.2012.02.046

[41] Z. Wang, J. Li, J. Zhao, B. Xing, Toxicity and internalization of CuO nanoparticles to prokaryotic alga *Microcystis aeruginosa* as affected by dissolved organic matter. *Environ. Sci. Technol.* **2011**, *45*, 6032. doi:10.1021/ES2010573

[42] E.Navarro, F.Piccapietra,B.Wagner,F.Marconi,R.Kaegi, N. Odzak, L. Sigg, R. Behra, Toxicity of silver nanoparticles to *Chlamydomonas reinhardtii*. *Environ. Sci. Technol.* **2008**, *42*, 8959. doi:10.1021/ ES801785M

[43] M. C. Stensberg, R. Madangopal, G. Yale, Q. Wei, H. Ochoa-Acun˜a, A. Wei, E. S. McLamore, J. Rickus, D. M. Porterfield, M. S. Sepu´lveda, Silver nanoparticle-specific mitotoxicity in *Daphnia magna*. *Nanotoxicology* **2014**, *8*, 833. doi:10.3109/17435390.2013. 832430

[44] L. K. Braydich-Stolle, S. Hussain, J. J. Schlager, M. C. Hofmann, In vitro cytotoxicity of nanoparticles in mammalian germline stem cells. *Toxicol. Sci.* **2005**, *88*, 412. doi:10.1093/TOXSCI/KFI256

[45] L. K. Braydich-Stolle, B. Lucas, A. Schrand, R. C. Murdock, T. Lee, J. J. Schlager, S. M. Hussain, M. C. Hofmann, Silver nanoparticles disrupt GDNF/Fyn kinase signalling in spermatogonial stem cells. *Toxicol. Sci.* **2010**, *116*, 577. doi:10.1093/TOXSCI/KFQ148

[46] C. Marambio-Jones, E. M. V. Hoek, A review of the antibacterial effects of silver nanomaterials and potential implications for human health and the environment. *J. Nanopart. Res.* **2010**, *12*, 1531. doi:10.1007/S11051-010-9900-Y

[47] J. S. Teodoro, A. M. Simo˜es, F. V. Duarte, A. P. Rolo, R. C. Murdoch, S. M. Hussain, C. M. Palmeira, Assessment of the toxicity of silver nanoparticles in vitro: a mitochondrial perspective. *Toxicol. In Vitro* **2011**, *25*, 664. doi:10.1016/J.TIV.2011.01.004

[48] G.J.Zhou, F.Q.Peng, L.J.Zhang, G.G.Ying, Biosorption of zinc and copper from aqueous solutions by two freshwater green microalgae *Chlorella pyrenoidosa* and *Scenedesmus obliquus*. *Environ. Sci. Pollut. Res.* **2012**, *19*, 2918. doi:10.1007/S11356-012-0800-9

[49] B. Volesky, *Bisorption of Heavy Metals* **1990** (CRC Press: Boca Raton, FL).

[50] A. J. Miao, K. A. Schwehr, C. Xu, S. J. Zhang, Z. Luo, A. Quigg, P. H. Santschi, The algal toxicity of silver engineered nanoparticles and detoxification by exopolymeric substances. *Environ. Pollut.* **2009**, *157*, 3034. doi:10.1016/J.ENVPOL.2009.05.047

[51] S. N. Luoma, F. R. Khan, M. N. Croteau, Bioavailability and bioaccumulation of metal-based engineered nanomaterials in aquatic environments: concepts and processes. *Front. Nanosci* **2014**, *7*, 157. doi:10.1016/B978-0-08-099408-6.00005-0

[52] S. Kittler, C. Greulich, J. Diendorf, M. Ko¨ller, M. Epple, Toxicity of silver nanoparticles increases during storage because of slow dissolution under release of silver ions. *Chem. Mater.* **2010**, *22*, 4548. doi:10.1021/CM100023P

[53] W. X. Wang, N. S. Fisher, Delineating metal accumulation pathways for marine invertebrates. *Sci. Total Environ.* **1999**, *237–238*, 459. doi:10.1016/S0048-9697(99)00158-8

[54] J. McTeer, A. P. Dean, K. N. White, J. K. Pittman, Bioaccumulation of silver nanoparticles into *Daphnia magna* from a freshwater algal diet and the impact of phosphate availability. *Nanotoxicology* **2014**, *8*, 305. doi:10.3109/17435390.2013.778346

[55] G. Taylor, D. J. Baird, A. M. V. M. Soares, Surface binding of contaminants by algae: consequences for lethal toxicity and feeding to *Daphnia magna* Straus. *Environ. Toxicol. Chem.* **1998**, *17*, 412. doi:10.1002/ETC.5620170310

[56] L.Maltby, T.J. Kedwards, V. E.Forbes, K. Grasman, J. E.Kammenga, W. R. Munns, Jr, A. H. Ringwood, J. S. Weis, S. N. Wood, Linking individual-level responses and population-level consequences, in *Ecological Variability: Separating Natural from Anthropogenic Causes of Ecosystem Impairment* (Eds D. J. Baird, G. A. Burton Jr) **2001**, pp. 27–82 (SETAC: Pensacola, FL).

[57] C. M. Zhao, W. X. Wang, Importance of surface coatings and soluble silver in silver nanoparticles toxicity to *Daphnia magna*. *Nanotoxicology* **2012**, *6*, 361. doi:10.3109/17435390.2011.579632

Thesis references:

Adams W.J., Blust R., Borgman U., Brix K., DeForest D., Green A.S., Meyer J.S., McGreer J.C., Paquin PR., Rainbow PS., Wood CM., 2011. Utility of Tissue Residues for Predicting Effects of Metals on Aquatic Organisms. *Integrated Environmental Assessment and Management* 7(1) 75-98.

Allen H.J., Impellitteri C.A., Macke D.A., Heckman J.L., Poynton H.C., Lazorchak J.M., Govindaswamy S., Roose D.L. and Nadagouda M.N., 2010. Effects from filtration, capping agents, and presence/absence of food on the toxicity of silver nanoparticles to *Daphnia magna*. *Environmental Toxicology and Chemistry*, 29(12), 2742-2750.

Almofti M.R., Ichikawa T., Yamashita K., Terada H. and Shinohara Y., 2003. Silver ion induces a cyclosporine a-insensitive permeability transition in rat liver mitochondria and release of apoptogenic cytochrome C. *Journal of Biochemistry* 134(1), 43–49.

Arndt DA., Chen J., Moua M. and Klaper RD (2014). Multigeneration impacts on Daphnia magna of carbon nanomaterials with differing core structures and fuctionalizations. Environmental Toxicology and Chemistry, 33(3), 541-547.

Ankley G.T., Bennet R.S., Erickson R.J., Hoff D.J., Hornung M.W., Johnson R.D., Mount D.R., Nichols J.W., Russom C.L., Schmeider P.K., Serrano J.A., Tietge J.E. and Villeneuve D.L., 2010. Adverse outcome pathways: a conceptual framework to support ecotoxicological research and risk assessment. *Environmental Toxicology & Chemistry*, 29(3), 730-741

Arora S., Jain J., Rajwade J.M., Paknikar K.M., 2008. Cellular responses induced by silver nanoparticles: *in vitro* studies. *Toxicology Letters*, 179(2), 93-100.

Arya A., Sethy N.K., Das M., Singh S.K., Das A., Ujjain S.K., Sharma R.K., Sharma M., and Bhargava K., 2014. Cerium oxide nanoparticles prevent apoptosis in primary cortical culture by stabilizing mitochondrial membrane potential. *Nanotoxicology*, 48(7), 784-793.

Asati A., Santra S., Kaittanis C. and Perez J.M. 2010. Surface-charge-dependent cell localization and cytotoxicity of cerium oxide nanoparticles. ACS Nano, 4(9), 5321-5331.

AshaRani P.V., Wu Y.L., Gong Z., Valiyaveettil S., 2008. Toxicity of silver nanoparticles in zebrafish models. *Nanotechnology*, 19(25), 255102.

AshaRani P.V., Hande M. and Valiyaveettil S., 2009a. Anti-proliferative activity of silver nanoparticles. *BMC Cell Biology*, 10(1), 1-14.

AshaRani P.V., Mun G.L.K., Hande M.P., Valiyaveettil S., 2009b. Cytotoxicity and genotoxicity of silver nanoparticles in human cells. *ACS Nano* 3(2), 279–290.

AshaRani P.V., Sethu S., Lim H.K., Balaji G., Valiyaveettil S. and Hande M.P., 2012. Differential regulation of intracellular factors mediating cell cycle, DNA repair and inflammation following exposure to silver nanoparticles in human cells. *Genome Integrity*, 3(2), 1-14.

Asghari S., Johari S., Lee J., Kim Y., Jeon Y., Cho I. H., Moon M. and Yu I., 2012. Toxicity of various silver nanoparticles compared to silver ions in *Daphnia magna*. *Journal of Nanobiotechnology*, 10(14), 1477-3155.

Atli G. and Canli M., 2013. Metals (Ag+, Cd^{2+}, Cr^{6+}) affect ATPase activity in the gill, kidney, and muscle of freshwater fish *Oreochromis niloticus* following acute and chronic exposures. *Environmental Toxicology*, 28(12), 707-717.

Baalousha M., Ju-Nam Y., Cole, P.A., Gaiser B.K., Fernandes T.F., Hriljac J.A., Jepson, M.A., Stone V., Tyler C.R. and Lead, J.R., 2012a. Characterization of cerium oxide nanoparticles—Part 1: size measurements. *Environmental Toxicology and Chemistry*, 31(5), 983-993.

Baalousha, M., Ju-Nam Y., Cole P.A., Hriljac, J.A., Jones, I.P., Tyler, C.R., Stone, V., Fernandes T.F., Jepson, M.A. and Lead, J.R., 2012b. Characterization of cerium oxide nanoparticles—Part 2: nonsize measurements', *Environmental Toxicology and Chemistry*, 31(5), 994-1003.

Baer K.N., Ziegenfuss M.C., Banks S.D. and Ling Z., 1999. Suitability of high-hardness COMBO medium for ecotoxicity testing using algae, daphnids, and fish. *Bulletin of Environmental Contamination and Toxicology*, 63(3), 289-296.

Barata C., Varo I., Navarro J.C., Arun S. and Porte C., 2005. Antioxidant enzyme activities and lipid peroxidation in the freshwater Cladoceran *Daphnia magna*

exposed to redox cycling compounds. *Comparative Biochemistry and Physiology, Part C,* 140(2), 175-186.

Baun A., Hartmann N.B., Grieger K. and Kusk K.O., 2008. Ecotoxicity of engineered nanoparticles to aquatic invertebrates: a brief review and recommendations for future toxicity testing. *Ecotoxicology,* 17(5), 387-395.

Bergmeyer H.U., 1974. *Methods of enzymatic analysis*. Verlag Chemi, USA.

Bradoford M.M., 1976. A rapid and sensitive method for the quantitation of microgram quantities of protein utilizing the principle of protein-dye binding. *Analytical Biochemistry,* 72(1-2), 248-254.

Braydich-Stolle L.K., Hussain S., Schlager J.J., Hofmann M.C., 2005. *In vitro* cytotoxicity of nanoparticles in mammalian germline stem cells. *Toxicological Sciences,* 88(2), 412-419.

Braydich-Stolle L.K., Lucas B., Schrand A., Murdock R.C., Lee T., Schlager J.J., Hussain S.M., Hofmann M.C., 2010. Silver nanoparticles disrupt GDNF/ Fyn kinase signalling in spermatogonial stem cells. *Toxicological Sciences,* 116(2), 577–589.

Broitman B.R., Mieszkowska N., Helmuth B. and Blanchette C.A., 2008. Climate and recruitment of rocky shore intertidal invertebrates in the Eastern North Atlantic. Ecology, 89(11), S81-S90.

Bianchini A. and Wood C.M., 2002. Physiological effects of chronic silver exposure in *Daphnia magna*. *Comparative Biochemistry and Physiology Part C: Toxicology & Pharmacology,* 133(1-2), 137-145.

Bianchini A. and Wood C.M., 2003. Mechanism of acute silver toxicity in *Daphnia magna*. *Environmental Toxicology and Chemistry,* 22(6), 1361-1367.

Bone A.J., Matson C.W., Colman B.P., Yang X., Meyer J.N. and Di Giulio R.T., 2015. Silver nanoparticle toxicity to Atlantic killifish (*Fundulus heteroclitus*) and Caenorhoabdits elegans: a comparison of mesocosm, microcosm and conventional laboratory studies. *Environmental Toxicology & Chemistry,* 34(2), 275-282.

Burnstock, 2006. Historical review: ATP as a neurotransmitter. *Trends in Pharmacological Sciences,* 27(3), 166-176.

Bury N.R., Galvez F., and Wood C.M., 1999. Effects of chloride, calcium, and dissolved organic carbon on silver toxicity: comparison between rainbow trout and fathead minnows. *Environmental toxicology and Chemistry*, 18(1), 56-62.

Bury N. R., Shaw J., Glover C. and Hogstrand C., 2002. Derivation of a toxicity-based model to predict how water chemistry influences silver toxicity to invertebrates. *Comparative Biochemistry and Physiology Part C: Toxicology & Pharmacology*, 133(1-2), 259-270.

Bystrzejewska-Piotrowska G., Golimowski J. and Urban P.L., 2009. Nanoparticles: their potential toxicity, waste and environmental management. *Waste Management*, 29(9), 2587-2595.

Campos B., Rivetti C., Rosenkranz P., Navas J.M., Barata C., 2013. Effects of nanoparticles of TiO_2 on food depletion and life-history responses of *Daphnia magna*. *Aquatic Toxicology,* 130(131), 174-183.

Carlson C., Hussain S.M., Schrand A.M., Braydich-Stolle L.K., Hess K.L., Jones R.L., Schlager J.J., 2008. Unique cellular interaction of silver nanoparticles: size-dependent generation of reactive oxygen species. *The Journal of Physical Chemistry B,* 112(43), 13608-13619.

Carreira S.C., Walker L., Paul K. and Saunders M., 2013. The toxicity, transport and uptake of nanoparticles in the *in vitro* BeWo b30 placental cell barrier model used within NanoTEST [pdf]. *Nanotoxicology*, early access 2013, Available at: <http://informahealthcare.com/doi/abs/10.3109/17435390.2013.833317>.

Choi O., Deng K.K., Kim N-J., Ross L.Jr., Surampallie R.Y., Hu Z., 2008. The inhibitory effects of silver nanoparticles, silver ions, and silver chloride colloids on microbial growth. *Water Research,* 42(12), 3066-3074.

Choi J.E., Kim S., Ahn J.H., Yuon P., Kang J.S., Park K., Yi J. and Ryu D.-Y., 2010. Induction of oxidative stress and apoptosis by silver nanoparticles in the liver of adult zebra fish. *Aquatic Toxicology*, 100(2),151-159.

Claiborne A., 1985. Catalase activity. In: CRC Handbook of methods for oxygen radical research, Boca Raton, ed. by R. A Greenwald. Michigan: CRC Press: 283-284.

Clare J., 2009. *Daphnia*: An Aquarists Guide [pdf]. Available at <www.caudata.org>. Last accessed 13 January 2015.

Colbourne J.K., Pfrender M.E., Gilbert D., Thomas W.K., Tucker A., Oakley T.H., Tokishita S., Aerts A., Arnold G.J., Basu M.K., Bauer D.J., Cáceres C.E., Carmel L., Casola C., Choi J.-H., Detter J.C., Dong Q., Dusheyko S., Eads B.D., Fröhlich T., Geiler-Samerotte K.A., Gerlach D., Hatcher P., Jogdeo S., Krijgsveld J., Kriventseva E.V., Kültz D., Laforsch C., Lindquist E., Lopez J., Manak J.R., Muller J., Pangilinan J., Patwardhan R.P., Pitluck S., Pritham E.J., Rechtsteiner A., Rho M., Rogozin I.B., Sakarya O., Salamov A., Schaack S., Shapiro H., Shiga Y., Skalitzky C., Smith Z., Souvorov A., Sung W., Tang Z., Tsuchiya D., Tu H., Vos H., Wang M., Wolf Y.I., Yamagata H., Yamada T., Ye Y., Shaw J.R., Andrews J., Crease T.J., Tang H., Lucas S.M., Robertson H.M., Bork P., Koonin E.V., Zdobnov E.M., Grigoriev I.V., Lynch M. and Boore J.L., 2011. The Ecoresponsive Genome of *Daphnia pulex*. *Science,* 331(6017), 555-561.

Costa C.S., Ronconi J.V.V., Daufenbach J.F., Gonc¸alves C.L., Rezin G.T., Emilio Luiz Streck E.L. and da Silva Paula M.M., 2010. *In vitro* effects of silver nanoparticles on the mitochondrial respiratory chain. *Molecular and Cellular Biochemistry*, 342(1-2), 51-56.

Croteau M.-N. and Luoma S.N., 2007. Cahracterizing dissolved Cu and Cd uptake in terms of the biotic ligand and biodynamics using enriched stable isotopes. *Environmental Science and Technology,* 41(9), 3140-3145.

Croteau M.-N. and Luoma S.N., 2009. Predicting diet-borne toxicity from metal influxes. *Environmental Science and Technology,* 43(13), 4915-4921.

Croteau M.-N., Misra S., Luoma S.N. and Valsami-Jones E., 2011. Silver bioaccumulation dynamics in a freshwater invertebrate after aqueos and dietary exposures to nanosized and ionic Ag. *Environmental Science and Technology,* 45(11), 6600-6607.

Croteau M.N., Dybowska A.D., Luoma S.N., Misra S.K. and Valsami-Jones, E., 2014a. Isotopically modified silver nanoparticles to assess nanosilver bioavailability and toxicity at environmentally relevant exposures. *Environmental Chemistry,* 11(3), 247−256.

Croteau M.-N., Misra S., Luoma S.N. and Valsami-Jones E., 2014b. Bioaccumulation and toxicity of CuO nanoparticles by a freshwater invertebrate after waterborne and diet-borne exposures. *Environmental Science and Technology*, 48(18), 10929-10937.

Das P., Xenopoulos M.A. and Metcalfe C.D., 2013. Toxicity of silver and titanium dioxide nanoparticle suspensions to the aquatic invertebrate, *Daphnia magna. Bulletin of Environmental Contamination and Toxicology*, 91(1), 76-82.

De Coen W.M., Janssen C.R. and Segner H., 2001. The Use of Biomarkers in *Daphnia magna* Toxicity Testing V. *in vivo* Alterations in the carbohydrate metabolism of *Daphnia magna* exposed to sublethal concentrations of mercury and lindane. *Ecotoxicology and Environmental Safety*, 48(3), 223-234.

De Coen W.M. and Janssen C.R., 2003. The missing biomarker link: relationships between effects on the cellular energy allocation biomarker of toxicant-stressed *Daphnia magna* and corresponding population characteristics. *Environmental Toxicology and Chemistry*, 22(7), 1632-1641.

De Schamphelaere K.A.C. and. Janssen C.R., 2004. Development and Field Validation of a Biotic Ligand Model Predicting Chronic Copper Toxicity. *Environmental Toxicology and Chemistry*, 23(6), 1365–1375.

Demling R.H. and DeSanti L., 2001. Effects of silver on wound management. *Wounds*, 13(1 supplmetn A), 1-15.

Diamantino T.C., Almeida E., Soares A.M.V.M. and Guilhermino, L., 2001. Lactate dehydrogenase activity as an effect criterion in toxicity tests with *Daphnia magna* straus. *Chemosphere*, 45(4-5), 553-560.

Di Toro D.M., Allen H.E., Bergman H.L., Meyer J.S., Paquin P.R. and Santore R.C., 2001. Biotic ligand model of the acute toxicity of metals: 1. technical basis. *Environmental Toxicology and Chemistry*, 20(10), 2383-2396.

Domingos R.F., Baalousha M.A., Ju-Nam Y., Reid M.M., Tufenkji N., Lead J.R., Leppard G.G. and Wilkinson, K.J., 2009. Characterizing manufactured nanoparticles in the environment: multimethod determination of particle sizes. *Environmental Science and Technology*, 43(19), 7277-7284.

Editorial, 2009. ‘Plenty of room’ revisited. *Nature Nanotechnology*, 4, 781.

El Badawy A.M., Silva R.G., Morris B., Scheckel K.G., Suidan M.T., Tolaymat T.M., 2011. Surface charge-dependent toxicity of silver nanoparticles. *Environmental Science and Technology*, 45(1), 283–287.

Ebert D., 2005. *Ecology, Epidemiology, and Evolution of Parasitism in Daphnia* [online]. National Center for Biotechnology Information (US). Available at < http://www.ncbi.nlm.nih.gov/books/NBK2036/>.

Elendt B. P., 1990. Selenium deficiency in Crustacea. *Protoplasma*, 154(1), 25-33.

European Commission (EC), 2011. Commission recommendations of XXX on the definition of nanomaterial [pdf]. Available at: <http://ec.europa.eu/environment/chemicals/nanotech/pdf/commission_recommendareco.pdf>, Accessed 20 January 2012.

Fabrega J., Fawcett S.R., Renshaw J.C. and Lead J.R., 2009. Silver nanoparticle impact on bacterial growth: effect of pH, concentration, and organic matter. *Environmental Science and Technology*, 43(19), 7285-7290.

Fabrega J., Luoma S.N., Tyler C.R., Galloway T.S. and Lead J.R., 2011. Silver nanoparticles: Behaviour and effects in the aquatic environment. *Environment International*, 37(2), 517-531.

Fan W., Wang X., Cui M., Zhang D., Zhang Y., Yu T. and Guo L., 2012. Differential Oxidative Stress of Octahedral and Cubic Cu2O Micro/ Nanocrystals to *Daphnia magna*. *Environmental Science and Technology*, 46(18), 10255-10262.

Farkas J., Christian P., Gallego-Urrea J.A., Roos N., Hassellöv M., Tollefsen K.E. and Thomas K.V., 2011. Uptake and effects of manufactured silver nanoparticles in rainbow trout (*Oncorhynchus mykiss*) gill cells. Aquatic Toxicology, 101(1), 117-125.

Farré M., Gajda-Schrantz K., Kantiani L. and Barceló D., 2008. Ecotoxicity and analysis of nanomaterials in the aquatic environment. *Analytical and Bioanalytical Chemistry*, 393(1), 81-95.

Feynman R.P., 1960. There’s plenty of room at the bottom. Engineering and Science, 23(5), 22-36.

Field A., 2009. Discovering Statistics using SPSS, 3rd Edition, London: Sage Publications Limited.

Fiske C.H. and SubbaRow Y., 1929. Phosphocreatine. *Journal of Biological Chemistry*, 81, 629-679.

Foldbjerg R., Dhang D.A. and Autrup H., 2011. Cytotoxicity and genotoxicity of silver nanoparticles in the human lung cancer cell line, A549. *Archives of Toxicology*, 85(7), 743-750.

Forbes V.E., Palmqvist A. and Bach L., 2006. The use and misuse of biomarkers in ecotoxicology. *Environmental Toxicology and Chemistry*, 25(1), 272-280.

Gaiser B.K., Biswas A., Rosenkranz P., Jepson M.A., Lead J.R., Stone V., Tyler C.R. and Fernandes, T.F., 2011. Effects of silver and cerium dioxide micro- and nano-sized particles on *Daphnia magna*. *Journal of Environmental Monitoring*, 13(5), 1227-1235.

Gao J., Yuon S., Hovsepyan A., Llaneza V.L., Wang Y., Bitton G. and Bonzongo J.-C.J., 2009. Dispersion and toxicity of selected manufactured nanomaterials in natural river water samples: effects of water chemical composition. *Envrionmental Science and Technology*, 43(9), 3322-3328.

Georgantzopoulou A., Balachandran Y.L., Rosenkranz P., Dusinka M., Lankoff A., Wojewodzka M., Kruszewski M., Guignard C., Audinot J.-N., Girija S., Hoffman L. and Gutleb A.C., 2013. Ag nanoparticles: size- and surface-dependent effects on model aquatic organisms and uptake evaluation with NanoSIMS. *Nanotoxicology*, 7(7), 1168-1178.

Geranio L., Heuberger M. and Nowack B., 2009. The behavior of silver nanotextiles during washing. *Envrionmental Science and Technology*, 43(21), 8113-8118.

Gerhardt A., 1999. Recent trends in online biomonitoring for water quality control." Biomonitoring of polluted water. Reviews on actual topics. *Environmental Research Forum*, 9, 95-118.

Germann W.J. and Stanfield C.L, 2004. *Principles of human physiology*. International 2nd Edition, Pearson Benjamin Cummings, USA.

Golovina N.B. and Kustov L.M., 2013. Toxicity of metal nanoparticles with a focus on silver. *Mendeleev Communications*, 23(2), 59-65.

Glover, C.N. and Wood, C.M., 2005. Accumulation and elimination of silver in Daphnia magna and the effect of natural organic matter. *Aquatic Toxicolicology*, 73(4), 406−417.

Goodman C.M., McCusker C.D., Yilmaz T., Rotello V.M., 2004. Toxicity of gold nanoparticles functionalized with cationic and anionic side chains. *Bioconjugate Chemistry*, 15(4), 897–900.

Gottschalk F., Sonderer T., Scholz R.W., Nowack B., 2009. Modeled environmental concentrations of engineered nanomaterials (TiO2, ZnO, Ag, CNT, Fullerenes) for different regions. *Environmental Sciences and Technology*, 43(24), 9216–9222.

Gottschalk F., Scholz R.W. and Nowack B., 2010. Probabilistic material flow modeling for assessing the environmental exposure to compounds: Methodology and an application to engineered nano-TiO_2 particles. *Environmental Modelling and Software*, 25(3), 320-332.

Greenwald R.A., 1985. *CRC Handbook of methods for oxygen radical research*, Michigan: CRC Press.

Griffitt R.J., Brown-Peterson N.J., Savin D.A., Manning C.S., Boube I., Ryan R.A. and Brouwer M., 2012. Effects of chronic nanoparticulate silver exposure to adult and juvenile sheepshead minnows (*Cyprinodon variegatus*). *Environmental Toxicology and Chemistry*, 31(1), 160-167.

Griscom S.B., Fisher N.S. and Luoma S.N., 2002. Kinetic modeling of Ag, Cd and Co bioaccumulation in the clam *Macoma balthica*: quantifying dietary and dissolved sources. *Marine Ecology: Progress Series*, 240, 127-141.

Guilhermino L., Lopes M.C., Donato A.M., Silveira L., Carvalho A.P. and Soares A. M. V.M., 1994. Comparative study between the toxicity of 3,4-dichloroaniline and sodium bromide with 21-days chronic test and using lactate dehydrogenase activity of *Daphnia magna* straus. *Chemosphere*, 28(11), 2021-2027.

Hadioui M., Leclerc S. and Wilkinson K. J., 2013. Multimethod quantification of Ag+ release from nanosilver. *Talanta*, 105(15), 15-19.

Hancock J.T., 2005. *Cell signalling*, 2nd edition, Oxford: Oxford University Press.

Handy R., Owen R. and Valsami-Jones, E., 2008. The ecotoxicology of nanoparticles and nanomaterials: current status, knowledge gaps, challenges, and future needs. *Ecotoxicology*, 17(5), 315-325.

Handy R.D., Cornelis G., Fernandes T., Tsyusko O., Decho A., Sabo-Attwood T., Metcalfe C., Steevens J.A., Klaine S.J., Koelmans A.A. and Horne N., 2012. Ecotoxicity test methods for engineered nanomaterials: Practical experiences and recommendations from the bench. *Environmental Toxicology and Chemistry*, 31(1), 15-31.

Heijerick D.G., De Schamphelaere K.A., van Sprang P.A. and Janssen C.R., 2005. Development of a chronic zinc biotic ligand model for *Daphnia magna*. *Ecotoxicology and Environmental Safety*, 62(1), 1-10.

Heinlaan M., Kahru A., Kasemets K., Arbeille B., Prensier G., and Dubourguier H.C., 2011. Changes in the Daphnia magna midgut upon ingestion of copper oxide nanoparticles: a transmission electron microscopy study. *Water Research*, 45(1), 179-190.

Hessen D.O., Alstad N.E.W. and Skardal L., 2000. Calcium limitation in *Daphnia magna*. *Journal of Plankton Research*, 22(3), 553-568.

Heyworth P.G., Cross A.R. and Curnette, 2003. Chronic granulomatous disease. *Current Opinion in Immunology*, 15(5), 578-584.

Hirn S., Semmler-Behnke M., Schleh C., Wenk A., Lipka J., Schäffler M., Takenaka S., Möller W., Schmid G., Simon U. and Kreyling W.G., 2011. Particle size-dependent and surface charge-dependent biodistribution of gold nanoparticles after intravenous administration. *European Journal of Pharmaceutics and Biopharmaceutics*, 77(3), 407-416.

Hoff D., Lehmann W., Pease A., Raimondo S., Russom C. and Steeger T. (2010). Predicting the Toxicities of Chemicals to Aquatic Animal Species [pdf]. US Environmental protection agency. Available at:

<http://owpubauthor.epa.gov/scitech/swguidance/standards/criteria/aqlife/upload/whitepaper_effects.pdf.>

Hosseini A., Baeeri M., Rahimifard M., Navaei-Nigjeh M., Mohammadirad A., Pourkhalili N., Hassani S., Kamali M. and Abdollahi M., 2013. Antiapoptotic effects of cerium oxide and yttrium oxide nanoparticles in isolated rat pancreatic islets. *Human and Experimnetal Toxicology*, 32(5), 544-553.

Hou L., Zhu Z.-Z., Zhang X., Nordio F., Bonzini M., Schwartz Joel., Hoxha M., Dioni L., Marinelli B., Pegoraro V., Apostoli P., Bertazzi P.A. and Baccarelli A., 2010. Airborne particulate matter and mitochondrial damage: a cross-sectional study [pdf]. *Environmental Health*, 9(48), Available at: <http://www.ehjournal.net/content/pdf/1476-069X-9-48.pdf>.

Hou W.-C., Westerhoff P. and Posner J.D., 2013. Biological accumulation of engineered nanomaterials: a review of current knowledge. *Environmental Science: Processes and Impacts*, 15(1), 103-122.

Hunter R.J., 1981. *Zeta Potential in Colloid Science: Principles and Applications*. London: Academic Press Limited.

Hussain S.M., Hess K.L., Gearhart J.M., Geiss K.T. and Schlager J.J., 2005. *In vitro* toxicity of nanoparticles in BRL 3A rat liver cells. *Toxicology in Vitro*, 19(7), 975-983.

Hwang E.T., Lee J.H., Chae Y.J., Kim Y.S., Kim B.C., Byoung-In Sang B.-I. and Gu M.B., 2008. Analysis of the toxic mode of action of silver nanoparticles using stress-specific bioluminescent bacteria. *Small*, 4(6), 746-750.

Izyumov D.S., Avetisyan A.V., Pletjushkina O.Y., Shakharov D.V., Writz K.W., Chernyak B. and Skulachev V.P., 2004. "Wages of Fear": transient threefold decrease in intracellular ATP level imposes apoptosis. *Biochimica et Biophysica Acta – Bioenergetics*, 1658(1-2), 141-147.

Jain J., Arora S., Rajwade J.M., Omray P., Khandelwal S. and Paknikar K.M., 2009. Silver nanoparticles in therapeutics: development of an antimicrobial gel formulation for topical use. *Molecular Pharmaceutics*, 6(5), 1388–1401.

Janssens D., Michiels C., Delaive E., Eliaers F., Drieu K. and Remacle J., 1995. Protection of hypoxia-induced ATP decrease in endothelial cells by ginkgo beloba extract and bilobalide. Biochemical Pharmacology, 50(7), 991-999.

Johnston H., Pojana G., Zuin S., Jacobsen N. R., Moller P., Loft S., Semmler-Behnke M., McGuiness C., Balharry D., Marcomini A., Wallin H., Kreyling W., Donaldson K., Tran L., and Stone V., 2012. Engineered nanomaterial risk. Lessons learnt from completed nanotoxicology studies: potential solutions to current and future challenges. *Critical Reveiws in Toxicology*, 43(1), 1-20.

Jillavenkatesa A., Dapkunas S.J. and Lum L.-S.H., 2001. *Particle size characterisation.* Nathional Institute of Standards and Technology, Special Publication 960-1. Available at < http://www.ceramics.nist.gov/ftproot/PracticeGuides/960-1/SP960-1.pdf> [accessed 20 January 2015].

Kabashi E., Valdmanis P.N., Dion P. and Rouleau G.A., 2007. Oxidized/misfolded superoxide dismutase-1: the cause of all amyotrophic lateral sclerosis? *Annals of Neurology*, 62(6), 553-559.

Kaegi R., Voegelin A., Sinnet B., Zuleeg S., Hagendorfer H., Burkhardt M. and Siegrist H., 2011. Behavior of metallic silver nanoparticles in a pilot wastewater treatment plant. *Environmental Sciences and Technology*, 45(9), 3902-3908.

Kalman J., Smith B.D., Riba I., Blasco J. and Rainbow P.S., 2010. Biodynamic modelling of the accumulation of Ag, Cd and Zn by deposit-feeding polychaete *Nereis diversicolor*. Inter population variability and a generalised predictive model. *Marine Environmental Research*, 69(5), 363-373.

Kappos A.D., Bruckmann P., Eikmann T., Englertd N., Heinriche U., Höppef P., Kochg E, Krauseb G.H.M, Kreylingh W.G., Rauchfussb K., Rombouti P., Schulz-Klempj V., Thielk W.R. and Wichmannl H.E., 2004. Health effects of particles in ambient air. *International Journal of Hygiene and Environmental Health*, 207(4), 399-407.

Ketchum, B. H. (1954) 'Mineral Nutrition of Phytoplankton', Annual Review of Plant Physiology, 5(1), 55-74.

Khan F.R., Misra S. K., Garcia-Alonso J., Smith B. D., Strekopytov S., Rainbow P. S., Luoma S. N. and Valsami-Jones E., 2012. Bioaccumulation dynamics and modelling in an estuarine invertebrate following aqueous exposure to nanosized and dissolved silver. *Environmental Science & Technology*, 46(14), 7621-7628.

Khan F.R., Kennaway G.M., Croteau M.-N., Dybowska A., Smith B.D., Nogueira A.J.A., Rainbow P.S., Luoma S.N. and Valsami-Jones E., 2014. *In vivo* retention of ingested Au NPs by *Daphnia magna*: No evidence for trans-epithelial alimentary uptake. *Chemosphere*, 100, 97-104.

Khan F.R. Paul K.B., Dybowska A., Valsami-Jones E., Lead J.R., Stone V. and Fernandes T.F., 2015. Accumulation dynamics and acute toxicity of silver nanoparticles to *Daphnia magna* and *Lumbriculus variegatus*: Implications for metal modelling approaches. *Environmental Science & Technology*, ahead of press.

Kim S., Choi J.E., Choi J., Chung K.-H., Park K., Yi J. and Ryu D.-Y., 2009. Oxidative stress-dependent toxicity of silver nanoparticles in human hepatoma cells. *Toxicology in Vitro*, 23(6), 1076-1084

Kim K.-J., Sung W.S., Suh B.K., Moon S.-K., Choi J.-S., Kim J G, Lee D.G., 2009. Antifungal activity and mode of action of silver nano-particles on *Candida albicans*. *BioMetals*, 22(2), 235-242.

Kim K.T., Klaine S.J., Cho J., Kim S.-H. and Kim S.D., 2010. Oxidative stress responses of *Daphnia magna* exposed to TiO_2 nanoparticles according to size fraction. *Science of The Total Environment*, 408(10), 2268-2272.

Kim S. and Ryu D.-Y., 2012. Silver nanoparticle-induced oxidative stress, genotoxicity and apoptosis in cultured cells and animal tissues. *Journal of Applied Toxicology*, 33(2), 78-89.

Kittler S., Greulich C., Diendorf J., Köller M. and Epple M., 2010. Toxicity of silver nanoparticles increases during storage because of slow dissolution under release of silver ions. *Chemistry of Materials*, 22(16), 4548-4554.

Kong L. and Zepp R.G., 2012. Production and consumption of reactive oxygen species by fullerenes. *Environmental Toxicology and Chemistry*, 31(1), 136-143.

Kooijman S.A.L.M., 1986. Energy budgets can explain body size. *Journal of Theoretical Biology*, 121(3), 269-282.

Kumar A., Kumar P., Anandan A., Fernandes T.F., Ayoko G.A. and Biskos G., 2014. Engineered Nanomaterials: Knowledge Gaps in Fate, Exposure, Toxicity, and Future Directions [pdf]. *Journal of Nanomaterials*, 2014. Available at: <http://www.hindawi.com/journals/jnm/2014/130198/abs/>.

Kurshid S., Saridakis E., Govada L. and Chayen N.E., 2014. Porous nucleating agents for protein crystallization. *Nature Protocols*, 9, 1621-1633.

Kvitek L., Panáček A., Soukupová J., Kolář M., Večeřová R., Prucek R., Holecová M, and Radek Zbořil, 2008. Effect of Surfactants and Polymers on Stability and Antibacterial Activity of Silver Nanoparticles (NPs). *The Journal of Physical Chemistry C*, 112(15), 5825-5834.

Laforsch C. and Tollrian R., 2000. A new preparation technique of daphnids for scanning electron microscopy using hexamethyldisilazane. *Archiv fur Hydrobiologie*, 149(4), 587-596.

Lam I.K.S. and Wang W.-X., 2006. Accumulation and elimination of aqueous and dietary silver in *Daphnia magna*. *Chemosphere*, 64(1), 26-35.

Lamkemeyer T., Zeis B. and Paul R.J., 2003. Temperature acclimation influences temperature-related behaviour as well as oxygen-transport physiology and biochemistry in the water flea *Daphnia magna*. Canadian Journal of Zoology, 81(2), 237-249.

Lampert W., 2011. *Daphnia development of a model organism in ecology and evolution.* Oldendorf/Luhe: International Ecology Institute.

Leanord E.M. and Wood C.M., 2013. Acute toxicity, critical body residues, Michaelis–Menten analysis of bioaccumulation, and ionoregulatory disturbance in response to waterborne nickel in four invertebrates: *Chironomus riparius*, *Lymnaea stagnalis*, *Lumbriculus variegatus* and *Daphnia pulex*. *Comparative Biochemistry and Physiology*: *Part C*, 158(1); 10-21.

Lee, Y.-K., Ding, S.-Y., Hoe, C.-H. and Low, C.-S. (1996) 'Mixotrophic growth of *Chlorella sorokiniana* in outdoor enclosed photobioreactor', Journal of Applied Phycology, 8(2), 163-169.

Lee C.-H., Cheng S.-H., Huang I-P., Souris, J.S., Yang C.-S., Mou C.-Y. and Lo L.-W., 2010. Intracellular pH-responsive mesoporous silica nanoparticles for the controlled release of anticancer chemotherapeutics. *Angewandte Chemie*, 122(44), 8390-8395.

Levard C.M., Reinsch B.C., Michel F.M., Oumahi C., Lowry G.V. and Brown G.E., 2011. Sulfidation processes of PVP-Coated silver nanoparticles in aqueous solution: impact on dissolution rate. *Environmental Science and Technology*, 45(12), 5260-5266.

Levard C., Hotze E. M., Lowry G. V. and Brown, G. E., 2012. Environmental transformations of silver nanoparticles: impact on stability and toxicity. *Environmental Science & Technology*, 46(13), 6900-6914.

Li K.G., Chen J.T., Bai S.S., Wen X., Song S.Y., BufrYua Q., Li J. and Wang Y.Q., 2009. Intracellular oxidative stress and cadmium ions release induce cytotoxicity of unmodified cadmium sulfide quantum dots. *Toxicology in Vitro*, 23(6), 1007-1013.

Li N., Sioutas C., Cho A., Schitz D., Misra C., Sempf J., Wang M., Oberley T., Froines J. and Nel A., 2003. Ultrafine particulate pollutants induce oxidative stress and mitochondrial damage. Environmental Health Perspectives, 111(4), 455-460.

Li Y., Huang T.-T., Carlson E.J., Melov S., Ursell P.C., Olson J.L., Noble L.J., Yoshimura M.P., Berger C., Chan P.H., Wallace D.C. and Epstein C.J., 1995. Dilated cardiomyopathy and neonatal lethality in mutant mice lacking manganese superoxide dismutase. *Nature Genetics*, 11, 376-381.

Li Y., Wu Y. and Ong B.S., 2005. Facile Synthesis of Silver Nanoparticles Useful for Fabrication of High-Conductivity Elements for Printed Electronics. Journal of the American Chemical Society, 127(10), 3266-3267.

Li Y., Sun L., Jin M., Du Z., Liu X., Guo C., Li Y., Huang P. and Sun Z., 2011. Size-dependent cytotoxicity of amorphous silica nanoparticles in human hepatoma HepG2 cells. *Toxicology in Vitro*, 25(7), 1343-1352.

Li Y., Zhang W., Niu J. and Chen Y., 2013. Surface-Coating-Dependent Dissolution, Aggregation, and Reactive Oxygen Species (ROS) Generation of Silver Nanoparticles under Different Irradiation Conditions. Environmental Science and Technology, 47(18), 10293-10301.

Liong M., Lu J., Kovochich M., Xia T., Ruehm S.G., Nel A.E., Tamanoi F. and Zink J.I., 2008. Multifunctional Inorganic Nanoparticles for Imaging, Targeting, and Drug Delivery. *ACS Nano*, 2(5), 889-886.

Lipmann F., 1941. Metabolic generation and utilization of phosphate bond energy. *Advances in Enzymology and Related Areas of Molecular Biology*, 1(1941), 99-162.

Liu J., Pennell K.G. and Hurt R.H., 2011. Kinetics and Mechanisms of Nanosilver Oxysulfidation. *Environmental Science & Technology*, 45(17), 7345-7353.

Liu Z., Qi X.-L. and Wang H., 2012. Synthesis and characterization of spherical and mono-disperse micro-silver powder used for silicon solar cell electronic paste. Advanced Powder Technology, 23(2), 250-255.

Lockman P.R., Koziara J.M., Mumper R.J. and Allen D.D., 2004. Nanoparticles surface charges alter blood-brain barrier integrity and permiability. *Nanotoxicology*, 12(9-10), 635-641.

Lohmann K., 1929. Über die Pyrophosphatfraktion im Muskel. *Naturwissenschaften*, 17(31), 624–625.

Lok C.-N., Ho C.-M., Chen R., He Q.-Y., Yu W.-Y., Sun H., Tam P.K.-H., Chiu J.-F. and Che C.-M., 2006. Proteomic analysis of the mode of antibacterial action of silver nanoparticles. *Journal of Proteome Research*, 5(4), 916-924.

Lorenz C., Windler L., von Goetz N., Lehmann R.P., Schuppler M., Hungerbühler K., Heuberger M. and Nowack B., 2012. Characterization of silver release from commercially available functional (nano)textiles. *Chemosphere*, 89(7), 817-824.

Lowry G.V., Grogory K.B., Apte S.C. and Lead J.R., 2012. Transformations of nanomaterials in the environment. *Environmental Science and Technology*, 46(13), 6893-6899.

Lundqvist M., Stigler J., Elia G., Lynch I., Cedervall T. and Dawson K.A., 2008. Nanoparticle size and surface properties determine the protein corona with possible

implications for biological impacts. *Proceedings of the National Academy of Sciences of the United States of America*, 105(38), 14265-14270.

Luoma, S.N. and Rainbow P.S., 2005. Why is metal bioaccumulation so variable? Biodynamics as a unifying concept. *Environmental Science and Technolology*, 39(7), 1921-1931.

Lushchak V., 2011. Environmentally induced oxidative stress in aquatic animals, *Aquatic Toxicology*, 101(1), 13 – 30.

Lyu K., Zhu X., Wang Q., Chen Y. and Yang Z., 2013. Copper/Zinc Superoxide Dismutase from the Cladoceran *Daphnia magna*: molecular cloning and expression in response to different acute environmental stressors. *Environmental Science and Technology*, 8887-8893.

Mackevica A., Skjolding L.M., Gergs A., Palmqvist A. and Baun A. 2015. Chronic toxicity of silver nanoparticles to *Daphnia magna* under different feeding conditions. *Aquatic Toxicology*, 161, 10-16.

Marambio-Jones C. and Hoek E.M.V., 2010. A review of the antibacterial effects of silver nanomaterials and potential implications for human health and the environment. *Journal of Nanoparticle Research*, 12(5), 1531-1551.

Marklund S. and Markland G., 1974. Involvement of the superoxide anion radical in the autoxidation of pyrogallol and a convenient assay for superoxide dismutase. *European Journal of Biochemistry*, 47(3), 469-474.

Martin F.L. and Andre E.M. McLean A.E.M., 1995. Adenosine triphosphate (ATP) levels in paracetamol-induced cell injury in the rat *in vivo* and *in vitro*. *Toxicology*, 104(1-3), 91-97.

McLaughlin J. and Bonzongo J-C.J., 2012. Effects of natural water chemistry on nanosilver behaviour and toxicity to *Ceriodaphnia dubia* and *Pseudokirchneriella subcapitata*. *Environmental Toxicology and Chemistry* 31(1), 168-175.

Misra S.K., Dybowska A., Berhanu D., Luoma S.N. and Valsami-Jones E., 2012. The complexity of nanoparticle dissolution and its importance in nanotoxicological studies. *Science of the Total Environment*, 438, 225-232.

Moore, 2006. Do nanoparticles present ecotoxicological risks for the health of the aquatic environment? *Environment International*, 32(8), 967-976.

Myers, J. and Johnston, J. A. (1949. Carbon and nitrogen balanace of Chlorella during growth. *Plant Physiology*, 24(1), 111-119.

Naddy R.B., Gorsuch J.W., Rehner A.B., McNerney G.R., Bell R.A. and Kramer J.R., 2007. Chronic toxicity of silver nitrate to *Ceriodaphnia dubia* and *Daphnia magna*, and potential mitigating factors. *Aquatic Toxicology*, 84(1), 1-10.

Nanotechproject.org, 2014. *The Project on Emerging Nanotechnologies* [online]. Available from <http://www.nanotechproject.org/>.

Navarro E., Piccapietra F., Wagner B., Marconi F., Kaegi R., Odzak N., Sigg L., Behra R., 2008. Toxicity of silver nanoparticles to *Chlamydomonas reinhardtii*. *Environmental Science and Technology*, 42(23), 8959–8964.

Neal A.L., 2008. What can be inferred from bacterium–nanoparticle interactions about the potential consequences of environmental exposure to nanoparticles? *Ecotoxicology*, 17(5), 362-371.

Nel A., Xia T., Mädler L. and Li N., 2006. Toxic Potential of Materials at the Nanolevel. *Science*, 311(5761), 622-627.

NERC (Natural Environment Research Council); Consortium for Manufactured Nanomaterial Bioavailability and Environmental Exposure (NanoBEE), 2010. *Core Project Description.* Outline available at <http://cfpub.epa.gov/ncer_abstracts/index.cfm/fuseaction/display.highlight/abstract/9271> [accessed November 2011].

Newsholme E.A., Challiss R.A., and Crabtree B., 1984. Substrate cycles: their role in improving sensitivity in metabolic control. *Trends in Biochemical Science*, 9(6), 277-280.

Newton K.M., Puppala H.L., Kitchens C.L., Colvin V.L., and Klaine S.J., 2013. Silver nanoparticle toxicity to *Daphnia magna* is a function of dissolved silver concentration. *Environmental Toxicology and Chemistry*, 32(10), 2356-2364.

Nicotera P., Leist M. and Ferrando-May E., 1998. Intracellular ATP, a switch in the decision between apoptosis and necrosis. *Toxicology Letters*, 102-103, 139-142.

Nisbet R.M., McCauley E., Johnson L.R., 2010. Dynamic energy budget theory and population ecology: lessons from *Daphnia*. *Philosophical Transactions of the Royal Society B: Biological Sciences*, 365(1557), 3541-3552.

Niyogi and Wood, 2004. Biotic ligand model, a flexible tool for developing site-specific water quality guidelines for metals. *Environmental Sceince and Technology*, 38(23), 6177-6192.

Nowack B. and Bucheli T. D., 2007. Occurrence, behavior and effects of nanoparticles in the environment. *Environmental Pollution*, 150(1), 5-22.

Oberdörster G., Stone V., and Donaldson K., 2007. Toxicology of nanoparticles: a historical perspective. *Nanotoxicology*, 1(1), 2-25.

OECD Guidelines for the Testing of Chemicals, Section 2 Effects on Biotic Systems: Daphnia sp., Acute Immobilisation Test., 2004. [pdf] (Test No. 202) Organisation for Economic Co-operation and Development (OECD). Available at: <http://www.oecd-ilibrary.org/environment/test-no-202-daphnia-sp-acute-immobilisation-test_9789264069947-en> [Accessed 12 January 2012].

OECD Guidelines for the Testing of Chemicals, Section 2 Effects on Biotic Systems: Daphnia magna Reproduction Test, 2008. [pdf] (Test No. 211) Organisation for Economic Co-operation and Development (OECD). Available at: <http://www.oecd-ilibrary.org/environment/test-no-211-daphnia-magna-reproduction-test_9789264070127-en> [Accessed 12 January 2012].

Oliver A.L., Croteau M.-N., Stoiber T.L., Tejamaya M., Römer I., Lead J.R., Luoma S.N., 2014. Does water chemistry affect the dietary uptake and toxicity of silver nanoparticles by the freshwater snail Lymnaea stagnalis? *Environmental Pollution*, 189, 87-91.

O'Rourke S., Stone V., Stolpe B and Fernandes T.F., 2015. Assessing the acute hazard of zinc oxide nanomaterials to *Lumbriculus variegatus*. *Ecotoxicology*, 24(6), 1372-1384.

Park E.J., Yi J., Kim Y., Choi K., Park K., 2010. Silver nanoparticles induce cytotoxicity by a Trojan-horse type mechanism. *Toxicology in Vitro*, 24(3) 872–878.

Parker W.J., Jenkins R.J., Butler C.P. and Abbott G.L., 1961. Flash Method of Determining Thermal Diffusivity, Heat Capacity, and Thermal Conductivity. *Journal of Applied Physics*, 32(9), 1679-1684.

Paquin P.R., Gorsuchb J.W., Apte S., Batley G.E., Bowles K.C., Campbell P.G.C., Delos C.G., Di Toro D.M., Dwyer R.L., Galvez F., Gensemer R.W., Goss G.G., Hogstrand C, Janssen C.R., McGeer J.C., Naddy R.B., Playle R.C., Santore R.C., Schneider U., Stubblefield W.A., Wood C.M. and Wu K.B., 2002. The biotic ligand model: a historical overview. *Comparative Biochemistry and Physiology Part C: Toxicology & Pharmacology*, 133 (1-2), 3-35.

Persoone, G., Baudo, R., Cotman, M., Blaise, C., Thompson, K., Cl., Moreira-Santos, M., Vollat, B., Törökne, A. and Han, T. (2009). Review on the acute *Daphnia magna* toxicity test – evaluation of the sensitivity and the precision of assays performed with organisms from laboratory cultures or hatched from dormant eggs. *Knowledge Management and of Aquatic Ecosystems*, 393(1), 1-29.

Peterson E.J., Akkanen J., Kukkonen J.V.K. and Weber W.J. Jnr., 2009. Biological uptake and depuration of carbon nanotubes by *Daphnia magna*. *Environmental Science and Technology*, 43(8), 2969-2975.

Piao M.J., Kang K.A., Lee I.K., Kim H.S., Kim S., Choi J.Y., Choi J. and Hyun J.W., 2011. Silver nanoparticles induce oxidative cell damage in human liver cells through inhibition of reduced glutathione and induction of mitochondria-involved apoptosis. *Toxicology Letters*, 201(1), 92-100.

Posgai R., Cipolla-McCulloch C.B., Murphy K.R., Hussain S.M., Rowe J.J. AND Nielsen M.G., 2011. Differential toxicity of silver and titanium dioxide nanoparticles on *Drosophila melanogaster* development, reproductive effort, and viability: size, coatings and antioxidants matter. *Chemosphere*, 85(1), 34-42.

Poynton H.C., Lazorchak J.M., Impellitteri C.A., Smith M.E., Rogers K., Patra M., Hammer K.A., Allen H.J. and Vulpe C.D., 2010. Differential Gene Expression in *Daphnia magna* suggests distinct modes of action and bioavailability for ZnO nanoparticles and Zn Ions. *Environmental Science & Technology*, 45(2), 762-768.

Poyton H.C. and Vulpe C.D., 2009. Ecotoxicogenomics: emerging technologies for emerging contaminants. *Journal of the American Water Resources Association*, 45(1), 83-96.

Poynton H.C., Lazorchak J.M., Impellitteri C.A., Blalock B.J., Rogers K., Allen H. J., Loguinov A., Heckman J.L., and Govindasmawy, S., 2012. Toxicogenomic responses of nanotoxicity in *Daphnia magna* exposed to silver nitrate and coated silver nanoparticles. *Environmental Science & Technology*, 46(11), 6288-6296.

Prathna T.C., Chandrasekaran N. and Mukherjee A., 2011. Studies on aggregation behaviour of silver nanoparticles in aqueous matrices: effect of surface functionalization and matrix composition. *Colloids and Surfaces A: Physicochemical and Engineering Aspects*, 390, 216-224.

Rasband, W.S., ImageJ, U. S. National Institutes of Health, Bethesda, Maryland, USA, http://imagej.nih.gov/ij/, 1997-2014.

Reieiro F., Gallego-Urrea J.A., Jurkschat K., Crossley A., Hassellöv M., Taylor C., Soares A.M.V.M. and Loureiro S., 2014. Silver nanoparticles and silver nitrate induce high toxicity to *Pseudokirchneriella subcapitata*, *Daphnia magna* and *Danio rerio*. *Science of the Total Environment*, 466-467, pp. 232-241.

Riggs, D.S., 1963. *The Mathematical Approach to Physiological Problems*. Baltimore: Williams & Wilkins.

Roh J.Y., Sim S.J., Yi J., Park K., Chung K.H., Ryu D.Y. and Choi J., 2009. Ecotoxicity of silver nanoparticles on the soil nematode *Caenorhabditis elegans* using functional ecotoxicogenomics. *Environmental Science and Technology*, 43(10), 3933–3940.

Römer I., White T.A., Baalousha M., Chipman K., Viant M.R. and Lead J.R., 2011. Aggregation and dispersion of silver nanoparticles in exposure media for aquatic toxicity tests. *Journal of Chromatography A*, 1218(27), 4226-4233.

Rungby J., Hultman P. and Ellerman-Eriksen S., 1987. Silver affects viability and structure of cultured mouse peritoneal macrophages and peroxidative capacity of whole mouse liver. *Archives of Toxicology*, 59(6), 408-412.

Seitz F., Rosenfeldt R.R., Storm K., Metreveli G., Schaumann G.E., Schulz R. and Bundschuh M., 2015. Effects of silver nanoparticle properties, media, pH and dissolved organic matter on toxicity to *Daphnia magna*. *Ecotoxicology & Environmental Safety*, 111, 263-270.

Smirnov N.N., 2013. Physiology of the Cladocera, London: Academic Press.

Smith G.J. and Flegal A.R., 1993. Silver in San Francisco Bay waters. *Estuaries*, 16(3), 547–558.

Spoehr, H.A. and Milner, H.W., 1949. The chemical compostion of *Chlorella*; effects of environmental conditions. *Plant Physiology*, 24(1), 120-149.

Stensberg M.C., Madangopal R, Yale G, Wei Q, Ochoa-Acuña H, Wei. A, McLamore E.S., Rickus J., Porterfield D.M. and Sepúlveda M.S., 2014. Silver nanoparticle-specific mitotoxicity in *Daphnia magna*. *Nanotoxicology*, 8(8), 833-42.

Stephenson R.R. and Watts S.A., 1984. Chronic toxicity tests with *Daphnia magna*: the effects of different food and temperature regimes on survival, reproduction and growth. *Environmental Pollution Series A, Ecological and Biological*, 36(2), 95-107.

Stone V., Shaw J., Brown D.M., MacNee W., Faux S.P. and Donaldson K., 1998. The role of oxidative stress in the prolonged inhibitory effect of ultrafine carbon black on epithelial cell function. *Toxicology in Vitro*, 12(6), 649 – 659.

Stone V., Pozzi-Mucelli S., Tran L., Aschberger K., Sabella S., Vogel U., Poland C., Balharry D., Fernandes T.F., Gottardo S., Hankin S., Hartl M.G., Hartmann N., Hristozov D., Hund-Rinke K., Johnston H., Marcomini A., Panzer O., Roncato D., Saber A.T., Wallin H. and Scott-Fordsmand J.J., 2014. ITS-NANO--prioritising nanosafety research to develop a stakeholder driven intelligent testing strategy. *Particle and Fibre and Toxicology*, 11(9), 11 pages.

Sun X., Liu Z., Welsher K., Robinson J.T., Goodwin A., Zaric S. and Dai H., 2008. Nano-graphene oxide for cellular imaging and drug delivery. *Nano Research*, 1(3), 203-212.

Sung J.H., Ji J.H, Yoon J.U., Kim D.S., Moon Yong Song M.S., Jeong J., Han B.S., Jeong Hee Han J.H., Chung Y.H., Kim J., Kim T.S., Chang H.K., Lee E.J., Lee J.H., and Yu I.J., 2008. Lung function changes in Sprague-Dawley Rats after prolonged inhalation exposure to silver nanoparticles. *Inhalation Toxicology*, 20(6), 567-574.

Tait S.W.G. and Green D.R., 2012. Mitochondria and cell signalling. *Journal of Cell Science*, 128(1), 807-815.

Tejamaya M., Römer I., Merrifield R. C. and Lead J. R., 2012. Stability of Citrate, PVP, and PEG coated silver nanoparticles in ecotoxicology media. *Environmental Science & Technology*, 46(13), 7011-7017.

Teodoro J.S., Simões A.M, Duarte F.V., Rolo A.P., Murdoch R.C., Hussain S.M. and Palmeira C.M., 2011. Assessment of the toxicity of silver nanoparticles in vitro: a mitochondrial perspective. *Toxicology in Vitro*, 25(3), 664-670.

Terminology for Nanomaterials [pdf]. British Standards Institute (BSI), 2007. Available at: < http://shop.bsigroup.com/en/Browse-by-Subject/Nanotechnology/>. [Accessed January 2012].

Tiede K., Boxall A.B.A., Tear S.P., Lewis J., David H. and Hassellöv M., 2008. Detection and characterization of engineered nanoparticles in food and the environment. *Food Additives & Contaminants: Part A*, 25(7), 795-821.

Tolaymat T.M., El Badawy A.M., Genaidy A., Scheckel K.G., Luxton T.P. and Suidan M., 2010. An evidence-based environmental perspective of manufactured silver nanoparticle in syntheses and applications: a systematic review and critical appraisal of peer-reviewed scientific papers. *Science of The Total Environment*, 408(5), 999-1006.

Trop M., Novak M, Rodl S., Hellbom B., Kroell W., Goessler W., 2006. Silver-Coated Dressing acticoat caused raised liver enzymes and argyria-like symptoms in burn patient. *Journal of Trauma-Injury Infection & Critical Care*, 60(3), 648-652.

Tzeng Y., Holt A., and Ely R., 1988. High performance silver ohmic contacts to $YBa_2Cu_3O_{6+x}$ superconductors. *Applied Physics Letters*, 52(2), 155-156.

USEPA Methods for Measuring the Acute Toxicity of Effluents and Receiving Waters to Freshwater and Marine Organisms [pdf] U.S. ENVIRONMENTAL

PROTECTION AGENCY (USEPA) EPA-821-R-02-012. Fifth Edition ed. Washington, DC, U.S. Environmental Protection Agency, 2002. Available at: <http://www.epa.gov/region6/water/npdes/wet/wet_methods_manuals/atx.pdf> [Accessed 01 January 2012].

U.S. Environmental Protection Agency. 2009. *National Recommended Water Quality Criteria*. EPA/822/H-04/001, EPA/822F-04/010. Washington, DC.

van der Oost R., Beyer J. and Vermeulen N. P. E., 2003. Fish bioaccumulation and biomarkers in environmental risk assessment: a review. *Environmental Toxicology and Pharmacology,* 13(2), 57-149.

Veronese F.M. and Gianfranco P., 2005. PEGylation, successful approach to drug delivery. *Drug Discovery Today*, 10(21), 1451-1458.

Völker C., Boedicker C., Daubenthaler J., Oetken M. and Oehlmann J., 2013. Comparative toxicity assessment of nanosilver on three *Daphnia* species in acute, chronic and multi-generation Experiments. *Public Library of Science One*, 8(10), e75026.

von der Kammer F., Ferguson P.L., Holden P.A., Masion A., Rogers K.R., Klaine S.J., Koelmans A.A., Horne N. and Unrine J.M., 2012. Analysis of engineered nanomaterials in complex matrices (environment and biota): general considerations and conceptual case studies. *Environmental Toxicology and Chemistry*, 31(1), 32-49.

Wallace D.C., 1992. Mitochondrial genetics: a paradigm for aging and degenerative diseases? *Science*, 256(5057), 628-632.

Wang W.-X., 2013. Dietary toxicity of metals in aquatic animals: recent studies and perspectives. Chinese Science Bulletin, 58(2), 203-213.

Weyermann J,, Lochmann D. and Zimmer A., 2005. A practical note on cytotoxicity assays. *International Journal of Pharmaceutics*, 288(2), 369-376.

Wijnhoven S.W.P., Peijnenburg, W.J.G.M., Herberts C.A., Hagens W.I., Oomen A.G., Heugens E.H.W., Roszek B., Bisschops J., Gosens I., Van De Meent D., Dekkers S., De Jong W.H., Van Zijverden M., Sips A.J.A.M., Geertsma R.E., 2009.

Nano-silver - a review of available data and knowledge gaps in human and environmental risk assessment. *Nanotoxicology*, 3(2), 109–138.

Wood C.M., Hogstrand C., Galvez F. and Munger R.S., 1996. The physiology of waterborne silver toxicity in freshwater rainbow trout (*Oncorhynchus mykiss*) 1. The effects of ionic Ag^{+}. *Aquatic Toxicology*, 35(2), 93–109.

Wu R.S.S. and Lam P.K.S, 1997. Glucose-6-phosphate dehydrogenase and lactate dehydrogenase in the green-lipped mussel (*Perna viridis*): Possible biomarkers for hypoxia in the marine environment. *Water Research*, 31(11), 2797-2801.

Yang X., Gondikas A.P., Marinakos S.M., Auffan M., Liu J., Hsu-Kim H. and Meyer J.N., 2012. Mechanism of silver nanoparticle toxicity is dependent on dissolved silver and surface coating in *Caenorhabditis elegans*. *Environmental Science and Technology*, 46(2), 1119-1127.

Young R.P, Hopkins R., Black P.N., Eddy C., Wu L., Gamble G.D., Mills G.D., Garrett J.E., Eaton T.E., and Rees M.I., 2006. Functional variants of antioxidant genes in smokers with COPD and in those with normal lung function. *Thorax*, 61(5), 394-399.F

Yu K.-N., Yoon T.-J., Minai-Tehrani A., Kim J.-E., Park S.J., Jeong M.S., Ha S.-W., Lee J.-K. Kim J.S. and Cho M.-H., 2013. Zinc oxide nanoparticle induced autophagic cell death and mitochondrial damage via reactive oxygen species generation. *Toxicology in Vitro*, 27(4), 1187-1195.

Yu S.-J., Yin Y.-G. and Liu J.-F., 2013. Silver nanoparticles in the environment. *Environmental Science: Processes & Impacts*, 15(1), 78-92

Zeis B., Buers I., Morawe T. and Paul R.J., 2009. The role of the lactate dehydrogenase of *Daphnia magna* and *Daphnia pulex* for the tolerance of elevated temperatures. *Comparative Biochemistry and Physiology, Part A*, 154(1), S7-S9.

Zhang W.-X., 2003. Nanoscale iron particles for environmental remediation: an overview. *Journal of Nanoparticle Research*, 5(3-4), 323-332.

Zhang Y., Chen Y., Westerhoff P. and Crittenden J., 2009. Impact of natural organic matter and divalent cations on the stability of aqueous nanoparticles. *Water Research*, 43(17), 4249-4257.

Zhang Y., Li X., Huang Z., Zheng W., Fan C. and Chen T., 2013. Enhancement of cell permeabilization apoptosis-inducing activity of selenium nanoparticles by ATP surface decoration. *Nanomedicine: Nanotechnology, Biology and Medicine*, 9(1), 74-84.

Zhao C.-M. and Wang, W.-X., 2010. Biokinetic uptake and efflux of silver nanoparticles in *Daphnia magna.* *Environmental Science and Technology*, 44(19), 7699-7704.

Zhao C.-M. and Wang W.-X., 2011a. Comparison of acute and chronic toxicity of silver nanoparticles and silver nitrate to *Daphnia magna.* *Environmental Toxicology and Chemistry*, 30(4), 885-892.

Zhao, C.-M. and Wang, W.-X. 2011b. Importance of surface coatings and soluble silver in silver nanoparticles toxicity to *Daphnia magna.* *Nanotoxicology*, 6(4), 361-370.

Zhao C.-M. and Wang, W.-X., 2012. Size-dependent uptake of silver nanoparticles in *Daphnia magna*. *Environmental Science & Technology*, 46(20), 11345-11351.

Zhao C.-M. and Wang, W.-X., 2013. Regulation of sodium and calcium in *Daphnia magna* exposed to silver nanoparticles. *Environmental Toxicology and Chemistry*, 32(4), 913-919.

Zhu, X., Chang, Y. and Chen, Y., 2010. Toxicity and bioaccumulation of TiO_2 nanoparticle aggregates in *Daphnia magna*. *Chemosphere*, 78(3), 209-215.

Zook J., Long S., Cleveland D., Geronimo C. and MacCuspie R., 2011. Measuring silver nanoparticle dissolution in complex biological and environmental matrices using UV–visible absorbance. *Analytical and Bioanalytical Chemistry*, 401(6), 1993-2002.